

CHEMISTRY

INVESTIGATION OF GLYCOSAMINOGLYCAN SULFATION PATTERN BY HIGH PERFORMANCE CHIP ELECTROSPRAY MULTISTAGE MASS SPECTROMETRY

FLANGEA Corina^{1,2}, SISU Eugen², SERB Alina F.^{1,2}, TUDOR Sorin³, PANCAN Ioan
Bujor³, SEIDLER Daniela G.⁴, ZAMFIR Alina D.^{1,3*}

¹Mass Spectrometry Laboratory, National Institute for Research and Development in Electrochemistry and Condensed Matter, Timisoara, Romania; ²"Victor Babes" University of Medicine and Pharmacy, Timisoara, Romania; ³Department of Chemical and Biological Sciences, "Aurel Vlaicu" University of Arad, Romania; ⁴Institute for Physiological Chemistry and Pathobiochemistry, University of Münster, Germany; *Correspondence: alina.zamfir@uav.ro

Abstract

We developed here a novel strategy for identification of specific sulfation motifs in hybrid chondroitin/dermatan sulfate (CS/DS) based on enzyme cleavage and multistage mass spectrometry (MS² and MS³). CS/DS chains released from bovine aorta were digested with chondroitin AC I lyase to obtain oligosaccharides of known hexuronic acid (HexA) epimerization. Depolymerized chains were separated by gel filtration chromatography and collected tetrasaccharides were analyzed by fully automated chip-based nanoelectrospray ionization tandem mass spectrometry recently introduced in carbohydrate research by our laboratory. MS screening and MS²-MS³ sequencing allowed us to identify and structurally characterize an unusual unsulfated tetramer motif within hybrid CS/DS chain, without the need for supplementary investigation by any other analytical or biochemical methods.

Keywords: glycosaminoglycans, chip-based electrospray ionization, ion trap mass spectrometry, multistage sequencing, sulfation

Introduction

Proteoglycans (PGs) are structural components of extracellular matrix aggregates or of cell surfaces to which they are anchored by membrane-spanning domains or by inositol phospholipids. PGs contain core proteins covalently linked to linear sulfated polysaccharides, the glycosaminoglycan chains (GAGs). One type of GAGs is chondroitin sulfate (CS) consisting of repeating disaccharide units of D-glucuronate (D-GlcA) and N-acetylgalactosamine (D-GalNAc) with usually sulfated 4'- or 6'-OH groups. The glycosidic linkage stereochemistry in CS is (βD-GlcA 1'→3' βD-GalNAc1'→4'-). A part of D-GlcA in CS can be epimerized to L-iduronate (L-IdoA) giving rise to dermatan sulfate (DS). So called oversulfation occurs by generation of GalNAc-4',6'-disulfate- or sulfated uronic acid residues.

Glycosaminoglycans participate in several biological functions in the arterial wall through their specific structures. They undergo particular compositional and structural modifications during the development of vascular diseases [1]. The concentration of chondroitin sulfate/dermatan sulfate (CS/DS) is differentially affected during the progression of atherosclerosis [1, 2]. Decreased sulfation of high molecular weight CS proteoglycans in the advancing atherosclerotic lesions may predispose the lesions to thrombosis by disrupting osmotic regulation, limiting avidity for antithrombin and decreasing activation efficiency [2].

Bovine aorta is used as biological material in many studies regarding glycosaminoglycan investigations in vascular pathophysiology. For example, heparin sulfate polysaccharide chain from proteoglycans regulate thrombin-induced responses as potential target of cardiovascular disorders [3].

Because of high molecular weight and degree of glycosylation, the structural analysis of proteoglycans by mass spectrometry (MS) and related MS methods almost always requires a detachment of the GAG chains followed by their depolymerization and the separate investigation of the core protein by common proteomics methods.

Recent mass spectrometric studies investigated sulfation pattern of CS/DS oligosaccharides from bovine aorta using a combination of nanoelectrospray ionization quadrupole time-of-flight and Fourier-transform ion cyclotron resonance mass spectrometry [4]. Other methods involved high-performance capillary electrophoresis in conjunction with electrospray ionization quadrupole time-of-flight tandem mass spectrometry for structural analysis of chondroitin/dermatan sulfate hexasaccharides from bovine aorta [5].

In the present study we investigated the sulfation pattern of a hybrid chondroitin/dermatan sulfate tetrasaccharide motif isolated from bovine aorta and digested with chondroitin AC I lyase. For this analysis we applied a novel method based on fully automated chip-electrospray ionization (ESI) high capacity ion trap (HCT) MS and tandem MS, recently developed by our group and introduced in glycomics.

Experimental

Reagents and materials

Analytical grade methanol was purchased from Merck (Darmstadt, Germany) and used without further purification. All sample solutions were dried in a SpeedVac Concentrator, SPD 111V-230 from Thermo Electron Corporation, (Asheville, NC, USA), coupled to a vacuum pump PC 2002 Vario with CVC 2000 Controller from Vaccubrand (Wertheim, Germany). Prior to chip-based MS analysis, the sample/methanol solutions were centrifuged for 2 h in a SIGMA 2-16 model centrifuge from Sartorius GmbH (Göttingen, Germany).

Sample preparation

GAG chains from hybrid CS/DS proteoglycans were obtained from bovine aorta by a β -elimination reaction. For further purification, samples were applied to a Biogel TSK DEAE-5PW (Biorad) anion-exchange chromatography column and eluted by a NaCl gradient. Depolymerization of CS/DS was carried out by digesting 0.5 mg of GAGs with 1 mU chondroitin AC I lyase (Seikagaku Kogyo, Tokyo, Japan) in 200 μ l 50 mM Tris/HCl, pH 8.0, containing 60 mM sodium acetate, 60 mM NaCl, 0.01 % bovine serum albumin and 3 mM NaN₃ for 2h at 37°C. After the first hour of incubation 1 mU of enzyme was added again. The enzyme cleaves the linkages between GalNAc and D-GlcA by elimination irrespective of the sulfation pattern. Size fractionation of oligosaccharides was performed on a Superdex Peptid HR10/30 column (Amersham-Pharmacia, Freiburg, Germany) equilibrated and eluted with 0.5 M (NH₄) HCO₃ at a flow rate of 0.5 ml/min with UV detection at 232nm. Fractions of 150 μ l were collected, and the tetrasaccharide CS/DS peaks were pooled and desalted on a prepacked D-Salt column (MW 1000) (Perbio Science, Bonn, Germany).

Fully automated chip-based high capacity ion trap mass spectrometry

Mass spectrometry was conducted on a high capacity ion trap MS (HCT Ultra PTM, Bruker Daltonics, Bremen, Germany) operating in negative ion mode.

Fully automated chip-based nanoESI was performed on a NanoMate 400 robot incorporating ESI Chip technology (Advion BioSciences, Ithaca, NY) coupled to the HCT Ultra MS via an in-laboratory made mounting system. The robot was set up on three adjustable supports and connected to the HCT MS nebulizer nitrogen supply pipeline. The position of the electrospray chip was adjusted with respect to the HCT counterelectrode to ensure an optimal transfer of the ionic species into the MS. NanoMate/HCT MS system was tuned as follows: ChipESI: 1.36 kV; capillary exit: -50 V; back nitrogen pressure 0.30 p.s.i.; nitrogen nebulizer on MS at 50 p.s.i. Multistage MS was performed by collision-induced dissociation (CID) used He as collision gas and a fragmentation amplitude ramped within 0.40-0.80 V.

Results and Discussion

We have isolated a hybrid CS/DS domain and after purification and depolymerization of parent chain with chondroitin AC I lyase, Δ -4,5-GlcA-GalNAc-IdoA-GalNAc hybrid tetrasaccharide structure was obtained (Figure 1a). In the tetrasaccharide molecule, a double bond indicating the presence of the Δ -4,5-glucuronic acid building block was formed by elimination during the enzymatic cleavage (Figure 1b) of the polysaccharide chain (CS/DS) by chondroitin AC I lyase.

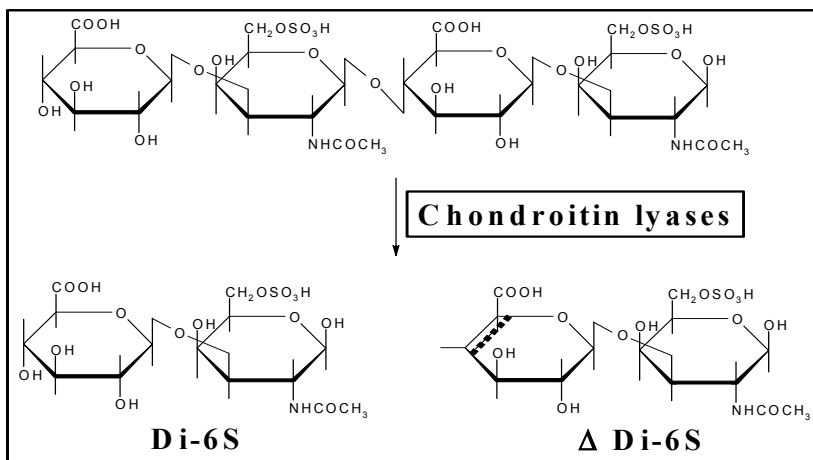


Fig. 1a

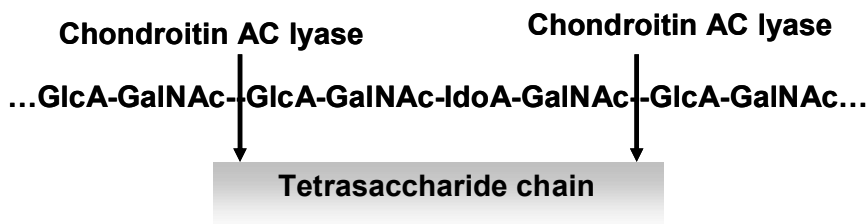


Fig. 1b

Fig. 1. Recognition specificity of chondroitin AC lyase as a tool for identification of GlcA-containing domains in CS/DS GAG chains. Mechanism of cleavage (Fig. 1a) and generated tetrasaccharide chain (Fig. 1b).

The sample was loaded onto the microtiter plate of the NanoMate robot in aliquots obtained by successive dilution of the starting material from 1:2 to 1:7 in pure methanol. Highest ionization efficiency was observed at a dilution of 1:5. For infusion and MS analysis, the samples were submitted to negative nanoESI chip MS screening by NanoMate 400 robot coupled to the HCT Ultra mass spectrometer via an in-laboratory made mounting system (Figure 2) [7].

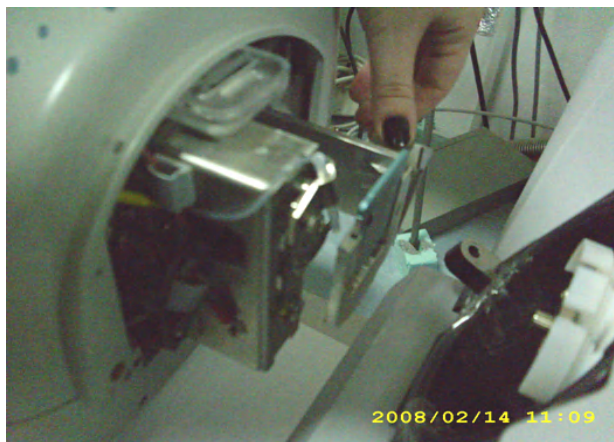


Fig. 2. Coupling of the NanoMate robot to HCT MS

Tandem mass spectrum (MS^2) of the collected CS/DS tetrasaccharide is presented in Figure 3 (a, b). As visible the spectrum is dominated by the singly charged ion at m/z 773.72 assigned to a saturated unsulfated tetrasaccharide, which is accompanied by the singly charged ion detected at m/z 757.40 attributed to an unsaturated tetrasulfated hexasaccharide. The ion at m/z 757.40 indicates the presence of the Δ -4,5-GlcA sequence at the non-reducing end within the Δ -4,5-GlcA-GalNAc-IdoA-GalNAc species. The same sugar building block composition was found for the singly charged ions at m/z 796.40 corresponding to the sodiated saturated GlcA-GalNAc-IdoA-GalNAc glycoform and the unsaturated counterpart at m/z 777.70 assigned, according to exact mass calculation to the sodiated Δ -4,5-GlcA-GalNAc-IdoA-GalNAc species. Moreover, the eight unsulfated sodiated and nonsodiated sequence ions, i.e., $B_3(3Na-3H_2O)$, $B_3(3Na-2H_2O)$, Z_3 , $Z_3(2Na)$, $Z_3(3Na)$, $C_3(3Na+H_2O)$, $Y_3(Na+H_2O)$ and $Y_3(2Na+H_2O)$, generated by cleavage of the glycosidic bonds provided evidence on non-sulfation of the molecule (Figure 3a and Figure 3b).

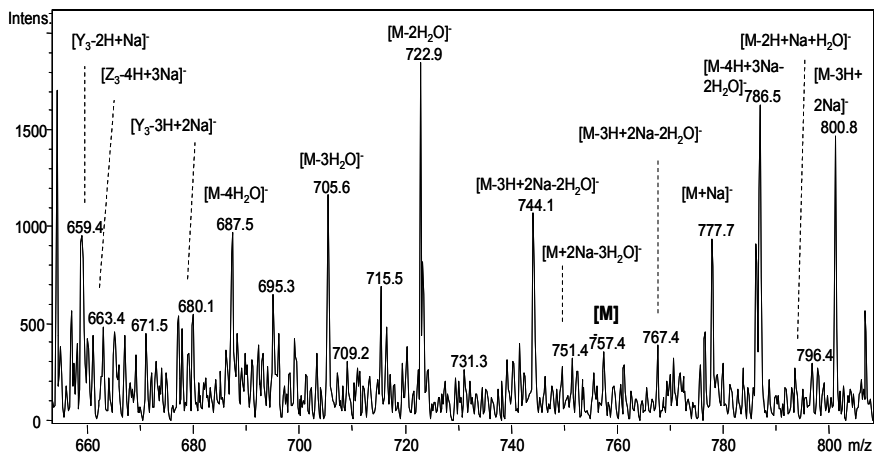


Fig. 3a

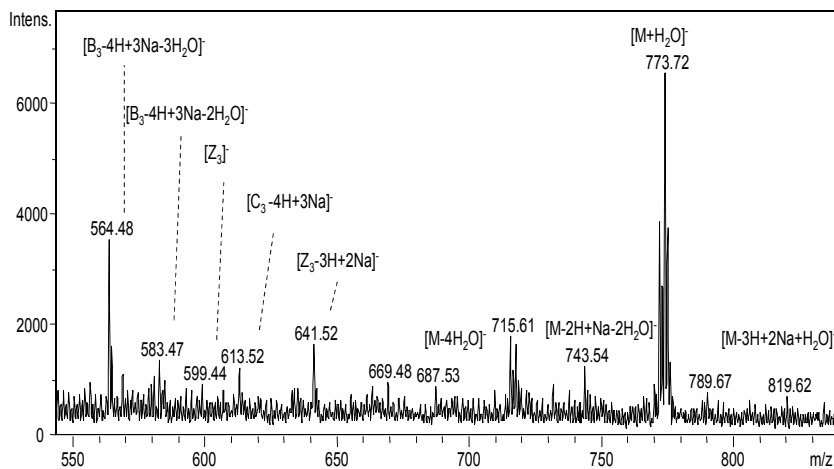


Fig. 3b

Fig. 3. Fully automated chip (-) nanoESI HCT MS² of bovine aorta tetrasaccharide obtained after depolymerization with chondroitin AC lyase and separation on GFC-Superdex peptide column: a) zoomed *m/z* area between 659.40 and 800.80; b) zoomed *m/z* area between 564.48 and 819.626. The assignment of the fragment ions followed the nomenclature introduced by Domon and Costello [10]

In superior stages of tandem MS, (MS^3), generation of distinct fragmentation pattern under controlled collision energy and gas conditions represents the prerequisite for determination of sulfation content and distribution in hybrid CS/DS molecules [8]. As reported by us previously [5-9], to obtain a high coverage of sequence ions, fingerprint for the investigated structure, CID MS^3 conditions need to be reconsidered and carefully optimized. Therefore, we have chosen to acquire scans at variable collision energy by elevating the ion fragmentation amplitude during the ongoing fragmentation process.

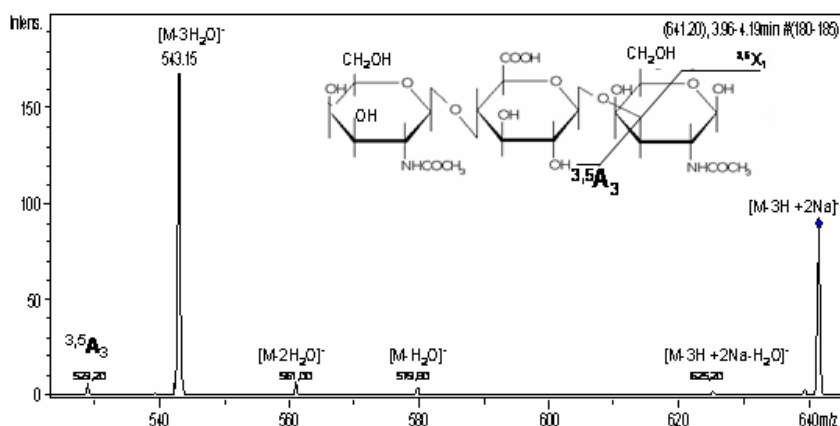


Fig. 4. Fully automated chip (-) nanoESI HCT CID MS^3 of the singly deprotonated ions at m/z 641.20 assigned according to mass calculation to the trisaccharide having a composition of disociated GalNAc-IdoA-GalNAc. The assignment of the fragment ions followed the nomenclature introduce by Domon and Costello [10]

Under these conditions, as visible in spectrum in Figure 4, multiple molecule cleavages rendering shorter chains and internal fragmentations yielding ring cleavage product ions were obtained. These fragment ions were all diagnostic for structure elucidation of the CS/DS tetrasaccharide and are consistent with the presence of a novel unsulfated structural motif (Figure 5) within CS/DS from bovine aorta.

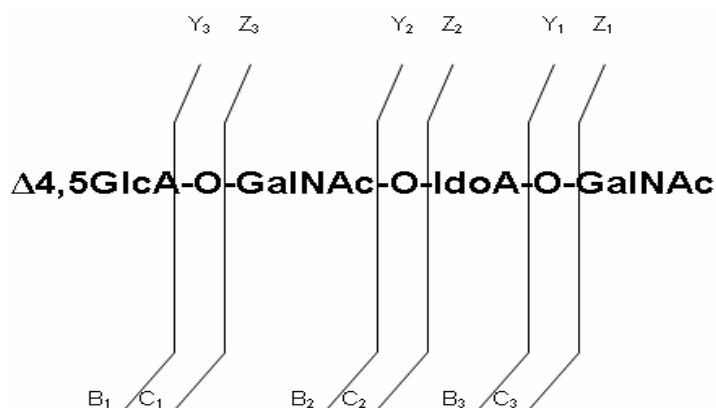


Fig.5. Structure of identified unsulfated tetrasaccharide CS/DS motif. Sequence nomenclature is according to ref. [10]

Conclusions

In this study fully automated chip-based nanoESI mass spectrometry was for the first time introduced in glycomics of glycosaminoglycans and particularly applied to a Δ -4,5-GlcA-GalNAc-IdoA-GalNAc tetrasaccharide fraction from bovine aorta proteoglycans. By developing an advanced, highly sensitive and rapid MS method based on fully automated chip (-) nanoESI HCT MS we were able to identify an unusual unsulfated tetrasaccharide motif. Sequencing in the MS² and MS³ mode of the tetrasaccharide detected at m/z 757.40 gave rise to a fragmentation pattern consistent with a non-sulfated CS/DS motif. By our method, this new structure was unequivocally identified and characterized without the need for supplementary investigation by any other analytical or biochemical methods.

Acknowledgments

This work was supported by Romanian National Authority for Scientific Research Grants: 14/2005, 98/2006, 111/2006 and PN-II- 41001/2007.

References

- [1] A.D. Theocharis, D.A. Theocharis, G. De Luca, A. Hjerpe and N.K. Karamanos. Compositional and structural alterations of chondroitin and dermatan sulfates during the progression of atherosclerosis and aneurysmal dilatation of the human abdominal aorta, *Biochimie*, **84**, 667-674 (2002).
- [2] M. McGee and W.D. Wagner. Chondroitin Sulfate Anticoagulant Activity Is Linked to Water Transfer Relevance to Proteoglycan Structure in Atherosclerosis, *Arterioscler Thromb Vasc Biol*, **23**, 1921-1927 (2003).

- [3]. C. Kimura, M. Oike Heparan sulfate proteoglycan is essential to thrombin-induced calcium transients and nitric oxide production in aortic endothelial cells. *Thromb Haemost*, 100, 483–488 (2008).
- [4]. M. Morman, A.D. Zamfir, D.G. Seidler, H. Kresse and J. Peter-Katalinić. Analysis of Oversulfation in a Chondroitin Sulfate Oligosaccharide Fraction from Bovine Aorta by Nanoelectrospray Ionization Quadrupole Time-of-Flight and Fourier-Transform Ion Cyclotron Resonance Mass Spectrometry *J Am Soc Mass Spectrom*, 18, 179-187 (2007).
- [5]. A. D. Zamfir, D. G. Seidler, H. Kresse and J. Peter-Katalinić. Structural characterization of chondroitin/dermatan sulfate oligosaccharides from bovine aorta by capillary electrophoresis and electrospray ionization quadrupole time-of-flight tandem mass spectrometry, *J. Rapid Commun. Mass Spectrom*, 16, 2015-2023 (2002).
- [6]. A.D. Zamfir, N. Lion Z. Vukelic L. Bindila J. Rossier H.H. Girault and J. Peter-Katalinic Thin chip microsyrayer system coupled to quadrupole time-of-flight mass spectrometer for glycoconjugate analysis. *Lab Chip*, 5, 298–307 (2005).
- [7] R. Almeida, C. Mosoarca, M. Chirita, V. Udrescu, N. Dinca, Ž. Vukelić, M. Allen and A.D. Zamfir. Coupling of fully automated chip-based electrospray ionization to high-capacity ion trap mass spectrometer for ganglioside analysis *Anal Biochem*, 378, 43-52 (2008).
- [8] S.Y. Vakhrushev, A. D. Zamfir and J. Peter-Katalinić. $^{0,2}A_n$ cross-ring cleavage as a general diagnostic tool for glycan assignment in glycoconjugate mixtures. *J Am Soc Mass Spectrom*, 15, 1863-1868 (2004).
- [9] I. Sisu, V. Udrescu, C. Flangea, S. Tudor, N. Dinca, A.D. Zamfir and E. Sisu, *Central Eur J Chem*, in press (2008)
- [10] B. Domon, C.E. Costello, A systematic nomenclature for carbohydrate fragmentations in FAB-MS spectra of glycoconjugates, *Glycoconjugate J* 5, 397-409 (1988).

RESEARCH ON THE ADHESION OF SiC SUBSTRATE USING ATOMIC FORCE MICROSCOPY METHOD

VOICAN Cristiana¹, STAMATIN Ioan², STANESCU Constantin D.³, ANDRONIE Adriana²

¹Electronics Technical College, e-mail: voicancristiana@yahoo.com

²University of Bucharest, Faculty of Physics, e-mail: andronie@3nanosae.unibuc.ro

³University Politehnica of Bucharest, e-mail: prof_cstanescu@yahoo.com

Abstract

Silicon carbide (SiC) based semiconductor electronic devices and circuits are presently being developed for use in high-temperature, high-power, and/or high radiation conditions under which conventional semiconductors cannot adequately perform. Silicon carbide's ability to function under such extreme conditions is expected to enable significant improvements to a far-ranging variety of applications and systems.

Keywords: silicon carbide, adhesion, AFM

Introduction

These range from greatly improved high-voltage switching [1-3] for energy savings in public electric power distribution and electric power distribution and electric motor drives to more powerful microwave electronics for radar and communications. In sensors and controls for cleaner-burning more fuel-efficient jet aircraft and automobile engines [4].

Fundamental semiconductor properties

Silicon carbide occurs in many different crystal structures, called polytypes. A comprehensive introduction to SiC crystallography and polytypism can be found in [7]. Despite the fact that all SiC polytypes chemically consist of 50% carbon atoms covalently bonded with 50% silicon atoms, each SiC polytype has its own distinct set of electrical semiconductor properties. The most common polytypes of SiC presently being developed for electronics are 3C-SiC, 4H-SiC, and 6H-SiC. 3C-SiC, also referred to as β -SiC, is the only form of SiC with a cubic crystal lattice structure. The non-cubic polytypes of SiC

are sometimes ambiguously referred to as α -SiC. Table 1 presents comparison of selected important semiconductor properties of major SiC Polytypes with Silicon and GaAs.

For comparison Table 1 also includes comparable properties of silicon, the semiconductor employed in most commercial solid-state electronics, it is the yardstick by which other semiconductor materials must be evaluated against to varying degrees. The major SiC polytypes exhibit advantages and disadvantages in basic material properties compared to silicon. The most beneficial inherent material superiorities of SiC over silicon

listed in Table 1 are its exceptionally high breakdown electric field ,wide band gap energy, high thermal conductivity, and high carrier saturation velocity.

Table 1

Property	UM	Silicon	GaAs	4H-SiC	6H-SiC	3C-SiC
Bandgap	eV	1.1	1.42	3.2	3.0	2.3
Relative Dielectric	-	11.9	13.1	9.7	9.7	9.7
Breakdown Field	MV/cm	0.6	0.6	//c : 3.0	//c: 3.2 ⊥ c: >1	>1.5
Thermal Conductivity	W/cmK	1.5	0.5	3 – 5	3 – 5	3 – 5
Concentration	cm ⁻³	10 ¹⁰	1.8 x 10 ⁶	~ 10 ⁻⁷	~ 10 ⁻⁵	~ 10
Electron Mobility	cm ² /Vs	1200	6500	//c: 800 ⊥ c: 800	//c: 60 ⊥ c: 400	750
Hole Mobility	cm ² /Vs	420	320	115	90	40
Saturated Electron Velocity	10 ⁷ cm/s	1.0	1.2	2	2	2.5
Donor Dopants& Shallowest Ionization Energy	meV	P: 45 As: 54	Si: 5.8	N : 45 P : 80	N : 85 P : 80	N : 50
Acceptor Dopants& Shallowest Ionization Energy	meV	B: 45	Be, Mg, C: 28	Al : 200 B: 300	Al : 200 B: 300	Al : 270
Wafer Diameter	cm	30	15	5	5	None

Growth of 3C-SiC on large-area silicon substrates

Despite the absence of SiC substrates, the potential benefits of SiC hostile environment electronics nevertheless drove modest research efforts aimed at obtaining SiC in a manufacturable wafer form. Towards this end, the heteroepitaxial growth of single crystal SiC layers on top of large area silicon substrates was first carried out in 1983 [5],and subsequently followed by a great many other over the years using a variety of growth techniques. Primarily due to large differences in lattice constant (20% difference between SiC and Si) and thermal expansion coefficient (8% difference), heteroepitaxy of SiC using silicon as a substrate always results in growth of 3C-SiC with a very high density of crystallographic structural defects such as stacking faults, microtwins and inversion domain boundaries [6].

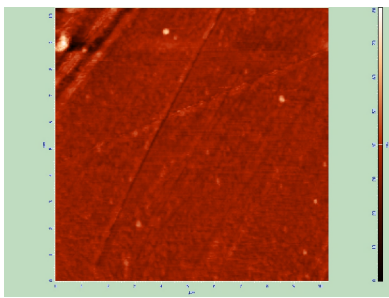
SiC RF devices

The main use of SiC RF devices appears to lie in high-frequency solid-state high-power amplification at frequencies from around 600MHz (UHF-band)to perhaps around 10 Ghz (X-band).As discussed in better detail in the high breakdown voltage and high thermal conductivity coupled with high carrier saturation velocity allow SiC RF transistors to handle much higher power densitiesthan their silicon or GaAs RF counterparts, despite SiC disadvantage in low field carrier mobility.

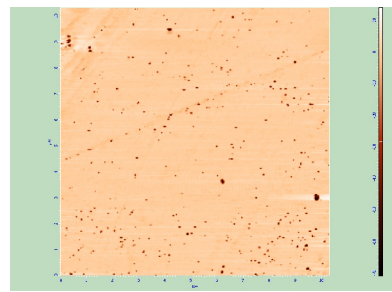
$$P_{max} = I_{dson}(V_b - V_{knee})/8 \tag{1}$$

The higher breakdown field of SiC permits higher drain breakdown voltage (V_b) allowing for RF operation at elevated drain biases. Given that there is little degradation in I_{dson} for SiC versus GaAs and silicon, the increased drain voltage directly leads to higher SiC MESFET output power densities.

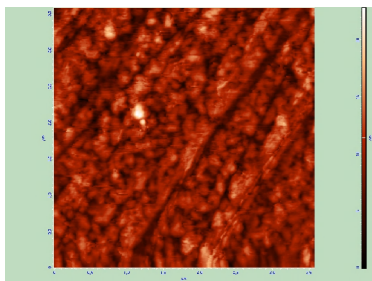
Figure 1 present the images and hystograms of the adhesion of substratum SiC using force atomic microscopy method.



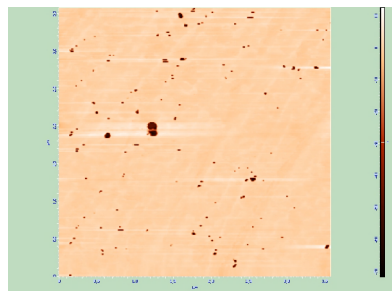
a. Topografy AFM aprox. 10x10 μ m



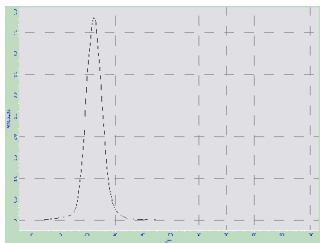
b. Contrast AFM aprox. 10x10 μ m.



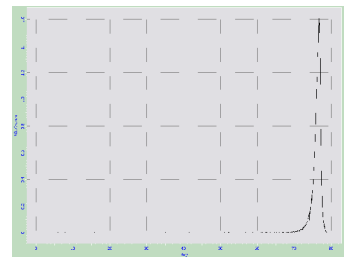
c. Topografy AFM prox. 3.5x3.5 μ m.



d. Contrast AFM ta aprox. 3.5x3.5 μ m.

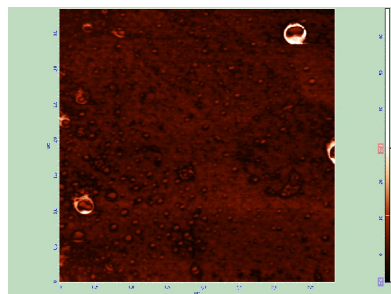
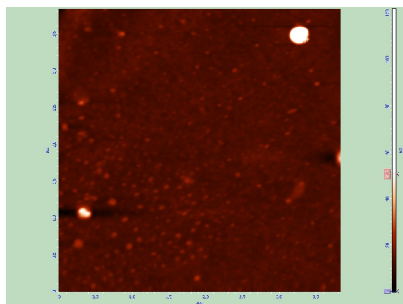


e. Hystogramm for topography image AFM



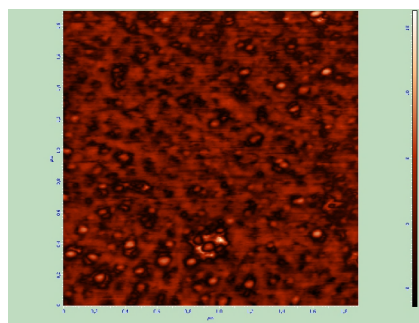
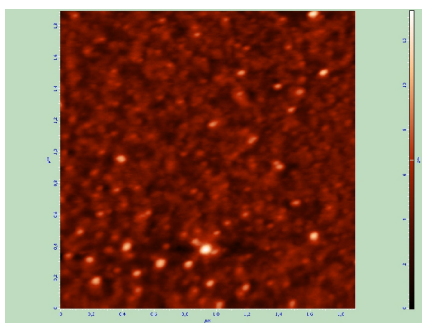
f. Hystogramm for topography image AFM

2.64625nm.



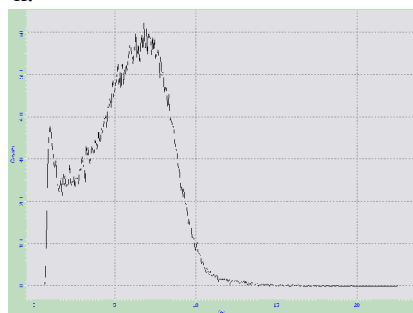
g. Topografy AFM Si S=aprox. 3.5x3.5μm.

h. Contrast AFM Si S= aprox. 3.5x3.5μm.



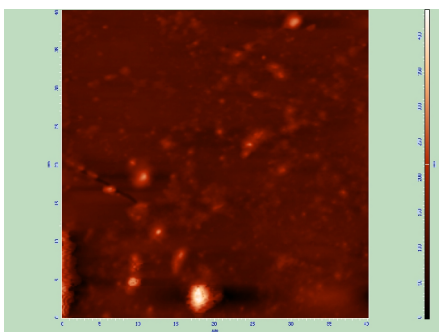
i. Topografy AFM Si S= aprox. 1.8x1.8μm.

j. Contrast AFM Si S= aprox. 1.8x1.8μm.
k.

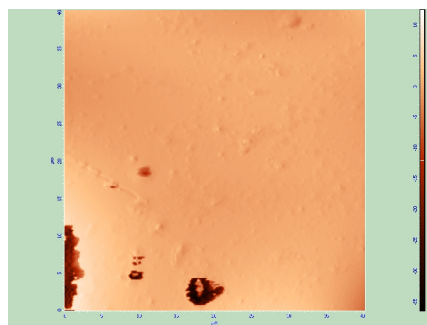


l. Histogramm for topografy image AFM Si .
21.6201nm.

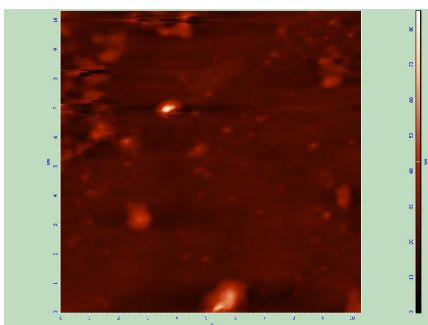
m. Histogramm for image AFM Si



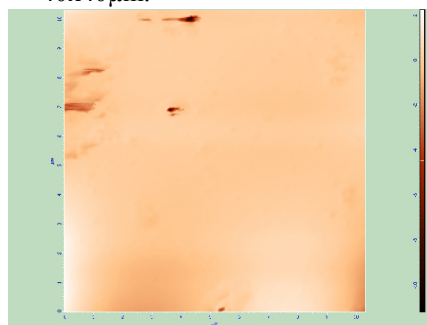
n. Topografy AFM halfcircle, S= aprox. 40x40 μ m.



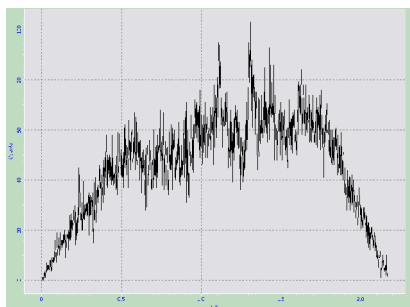
o. Contrast AFM halfcircle) , S= aprox. 40x40 μ m.



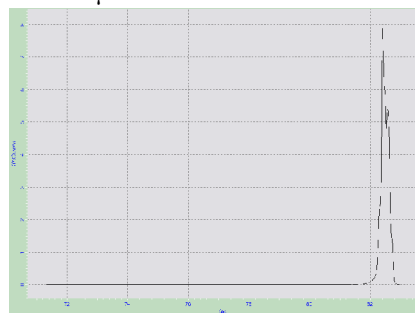
p. Topografy AFM halfcircle, S= aprox. 10x10 μ m.



q. Contrast AFM halfcircle, S= aprox. 10x10 μ m..



r. Hystogramm topografy image AFM halfcircle.



s. Hystogramm for contrast AFM half circle.

Fig.1 Images and hystogrammes of the adhesion of substratum SiC using atomic force microscopy

Conclusions

Despite the fact that SiC RF transistors are not nearly as optimized, they have still demonstrated higher power densities than silicon and GaAs RF power transistors. The commercial availability of semi-insulating SiC substrates to minimize parasitic capacitances is crucial to the high-frequency performance of SiC RF MESFET's device yield consequences arising from micropipes than vertical high-power switching devices, primarily because an e-axis micropipe can no longer short together two conducting sides of a high field junction in most areas of the lateral channel MESFET structure. In addition to micropipes, other non-idealities, such as variations in epilayer doping and thickness, surface morphological defects and slow charge trapping/detrapping phenomena causing unwanted device 1 V drift also limit the yield size and manufacturability of SiC RF transistors. However, increasingly beneficial SiC RF transistors should continue to evolve as SiC crystal quality and device processing technology continues to improve.

References

- [1] Baliga, B.J., Power Semiconductor Devices for Variable –Frequency Devices, Proceeding of the IEEE, 82, 1112, 1994
- [2] Baliga, B.J., Power ICs In The Saddle, IEEE Spectrum, 32, 34, 1995.
- [3] Baliga, B.J., Trends in Power Semiconductors Devices IEEE Transaction on Electron Devices, 43, 1717, 1996.
- [4] Blattnagar, M and Baliga, B.J., Comparison of 6h-SiC, 3D-SiC and Si for Power Devices IEEE Transaction on Electron Devices, 40, 645, 1993
- [5] Nishino, S., Powell, J.A and Will, H.A., H.A., Production of Large-Area Single Crystal Wafer of Cubic SiC for Semiconductor Devices, Applied Physics Letters, 42, 460, 1983
- [6] Pirous, P., Chorey, C.M. and Powell, J.A., Antiphase Boundaries in Epitaxially Grown Beta-SiC, Applied Physics Letters, 50, 221, 1987.
- [7] Power, J.A., Pirouz, P and Characterization of Silicon Carbide Polytypes for Electronic Applications, Semiconductor Interfaces, Microstructures and Devices : Properties and Applications, Feng, Z., C., Eds, Institutes of Physics Publishing, Bristol, United Kingdom, 1993, 257.

PROCESS-INDUCED MORPHOLOGICAL DEFCTS IN EPITAXIAL CVD SILICON CARBIDE

STANESCU Constantin D.¹, VOICAN Cristiana²

**University Politehnica of Bucharest, e-mail: prof_cstanescu@yahoo.com*

*** University Politehnica of Bucharest, e-mail: voicanristiana@yahoo.com*

Abstract

Silicon carbide (SiC) semiconductor technology has been advancing rapidly, however there are numerous crystal growth problems that need to be solved before SiC can reach its full potential. Among these problems is a need for an improvement in the surface morphology of epitaxial films that are grown to produce device structures. Various processes before and during epilayer growth lead to the formation of morphological defects observed in SiC epilayers grown on SiC substrates. In studies of both 6H and 4H-SiC epilayers, atomic force microscopy (AFM) and other techniques have been used to characterize SiC epilayer surface morphology.

Keywords: silicon carbide, epitaxial CVD, morphological defects

Introduction

The recent advances of SiC semiconductor technology have been greatly aided by the commercial availability of SiC wafers of reasonable size and quality. Bulk crystals of various SiC polytypes (e.g. 4H, 6H, and 15R) are now being grown by vapor sublimation processes at various institutions. The 4H and 6H polytypes are available commercially as polished wafers. Currently, both of these polytypes are actively being developed, but recent emphasis has shifted to the 4H polytype because of the larger electron mobility (800 versus 370 cm²/Vs) and lower donor activation energy (45 versus 90 meV) of 4H-SiC compared to 6H-SiC [1, 2]. These commercial wafers typically contain dislocations at a density greater than 10⁴ cm⁻² and a defect known as micropipes at a density of about 100 cm⁻² [3, 4]. The micropipes are tubular voids, approximately a micrometer in diameter, that extend along the crystal c-axis (the $\{0001\}$ growth direction). The micropipes propagate from the SiC substrate into the subsequently grown epitaxial films [5]. These micropipes can negatively impact devices that are fabricated from the epitaxial films [4].

Chemical vapor deposition (CVD) is currently the method of choice to produce SiC device structures consisting of thin doped epitaxial films. Step-controlled epitaxy has been used to obtain homoepitaxial growth (i.e. film and substrate are the same polytype) on SiC substrates [6]. This epitaxy takes place by the lateral growth of atomic-scale steps that are present on the substrate whose growth surface has been tilted "off-axis" from the (0001) basal plane as shown schematically in Fig. 1.

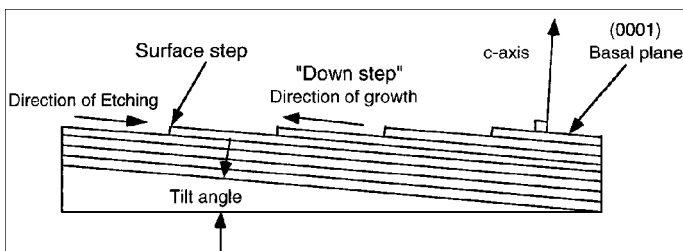


Fig. 1. Cross-sectional schematic diagram illustrating step flow growth on the surface of an "off-axis" SiC substrate

two-dimensional nucleation on atomically-flat terraces between steps or at other unwanted nucleation sites caused by defects or contamination [7]. The polished growth surface of SiC substrates used for device fabrication is typically tilted "off-axis" from the (0001) plane by approximately 3° to 8° . The term "vicinal" (0001) SiC surface is often used for surfaces that are "off-axis" by an angle of up to a few degrees. The precise definition of "vicinal" means "in the neighborhood of", so any angle from zero up to a few degrees is included. The "down-step" direction will refer to the direction of the lateral growth of the steps (refer to Fig. 1). The "up-step" direction is the opposite of "down-step".

Results and discussion

Considerations of wafers and epilayers

The crystal structure and quality of selected wafers and epilayers were determined by low temperature photoluminescence (LTPL) and transmission electron microscopy (TEM) as described previously. Topographical maps of defects in selected wafers and epilayers were produced by Synchrotron White Beam X-Ray Topography (SWBXT).

The surface morphologies of the epilayers in this study were characterized by Nomarski differential interference contrast (NDIC) optical microscopy and atomic force microscopy (AFM). The latter technique allowed the observation of features down to near atomic scale. The AFMs used were a Park Scientific Instruments Auto-Probe LS and a Digital Instruments Dimension 3000, each with a lateral scan range of up to 100 μm .

Epitaxial silicon wafer quality

SiC substrates were obtained from 6H-SiC and 4H-SiC wafers up to 35 mm in diameter that were produced by two commercial suppliers from sublimation-grown boules. In this article, the vendors will be identified as source A and source B. The wafers were sliced "on-axis" (less than 1° tilt) or "off-axis" (3° to 8° tilt) from the (0001) basal plane in the (1120) direction with the Si-face side of the wafers polished to form the growth surface. The SiC wafers were usually cut into either four equal-sized pie-shaped pieces, or into smaller $7.5 \times 6 \text{ mm}^2$ pieces to reduce the substrate cost of epilayer growth experiments.

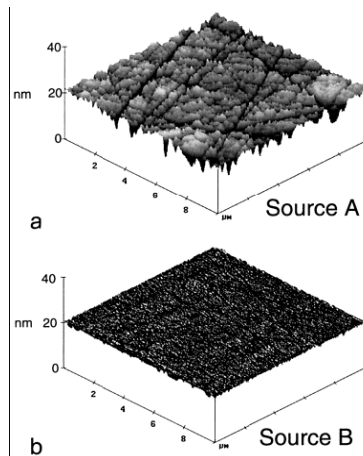


Fig. 2. AFM images of SiC wafer surfaces obtained from two different commercial sources

Occasional irregular-shaped voids of various sizes intersected the surface. Compared to 6H-SiC, 4H-SiC as-received generally had more of the larger irregularly shaped voids as revealed by optical microscopy. Fig. 2 illustrates the surface of wafers from two commercial sources. Most of the work reported in this paper was carried out on wafers from source A (Fig. 2a) because more wafers were available from this source. Only a few wafers from source B (Fig. 2b) were obtained; this was not sufficient to allow definitive conclusions regarding the impact of the better surface of source B wafers on growth morphology.

Typical epilayer growth processes

The epilayer growth experiments were carried out in a CVD system that has been described previously. The horizontal fused silica CVD chamber was water cooled with an inside diameter of 50 mm. All pregrowth etching and epitaxial growth was carried out at atmospheric pressure. The substrates were heated by an rf-heated SiC-coated graphite susceptor, 80 mm long x 30 mm wide x 10 mm thick.

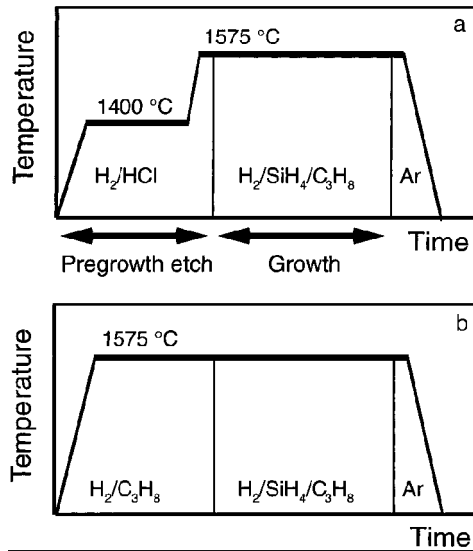


Fig.3. Two CVD processes used in growth of SiC epilayers on SiC substrates: a.) Typical pregrowth etch using H₂/HCl and b) investigated pregrowth etch using H₂/C₃H₈

During etching and growth, the H₂ carrier gas flow was maintained at 3 l/ min. Prior to growth, the substrates were typically subjected to a 4 min HCl etch (3% in H₂) at (1400 +/- 25) °C in order to remove unintentional contamination and to reduce the surface damage caused by the wafer cutting and polishing process. A pregrowth etch in H₂ was also investigated and will be discussed in Section 8. Epilayer growth was carried out at a fixed temperature in the range 1450 to 1600 °C with SiH₄ (3% in H₂) and C₃H₈ (3% in H₂) as the sources of Si and C. Two CVD process schedules that were used in the growth of the epilayers in this study are shown in Fig. 3. If, during CVD, the substrate/susceptor is heated in H₂ above the melting point of silicon (1410 °C), silicon droplets are produced on the SiC substrate. It is believed that the Si droplets contribute to the formation of morphological defects During the startup portion of the CVD process (Fig. 3a), the presence of HCl inhibits the formation of Si droplets.

Conclusions

From the above sections, it is clear that there are a sequence of processes that can impact the morphology of SiC epilayers. The first (and most important) process is the growth of the bulk crystal since micropipes and dislocations are known to propagate into SiC epilayers. The increasing number of SiC developers who use commercial wafers are at the mercy of the quality of the wafers available from the few commercial SiC bulk crystal

growers A second set of processes is that of cutting and polishing the wafer. The finding that these processes are having a major impact on morphology was somewhat surprising. It had been assumed that the defects in the bulk crystal were the dominant cause of morphological defects. Wafer users may be forced to repolish wafers to achieve scratch-free and damage-free surfaces. This problem of imperfect wafers surfaces prompted to develop an in-house polishing capability and to collaborate with others to develop new polishing processes. This leads to the development of a new SiC CMP process.

Although in an early state of development, it shows promise of being suitable for the final stage of polishing which will provide a scratch-free surface free of subsurface damage. Our characterization of commercial wafers showed that at least one supplier can produce a nearly scratch-free surface. Hopefully, commercial SiC wafer suppliers will be able to apply this new technology and provide the required polished surfaces that will yield improved SiC epilayers.

References

1. W. J. SCHAFFER, H. S. KONG, G. H. NEGLEY, J. W. PALMOUR, Silicon Carbide and Related Materials, Proc. 5th Conf. 1-3 Nov. 1993, Washington, DC, USA, Ed. M. G. Spencer et al., Institute of Physics Publishing, Bristol and Philadelphia 1994 (p. 155).
2. W. J. SCHAFFER, G. H. NEGLEY, K. G. IRVINE, J. W. PALMOUR, Mater. Res. Soc. Symp. Proc. 339, 595 (1994).
3. K. KOGA, Y. FUJIKAWA, Y. UEDA, T. YAMAGUCHI, Amorphous and Crystalline Silicon Carbide IV, Vol. 71, Eds.
4. C. Y. YANG, M. M. RAHMAN, G. L. HARRIS, Springer-Verlag, Berlin/Heidelberg 1992 (p. 96).
5. P. G. NEUDECK, J. A. POWELL, IEEE Electron Device Lett. 15, 63 (1994).
6. J. A. POWELL, D. J. LARKIN, P. G. NEUDECK, J. W. YANG, P. PIROUZ, see [1] (p. 161).
7. H. MATSUNAMI, K. SHIBARA, N. KURODA, W. YOO, S. NISHINO, Amorphous and Crystalline Silicon Carbide. Vol. 34, Eds. G. L. Harris, C. Y.-W. Yang, Springer-Verlag, Berlin/Heidelberg 1989 (p. 34).
8. J. A. POWELL, J. B. PETIT, J. H. EDGAR, I. G. JENKINS, L. G. MATUS, J. W. YANG, P. PIROUZ, W. J. CHOYKE, L. CLEMEN, M. YOGANATHAN, Appl. Phys. Lett. 59, 333 (1991).
9. S. Tyc, J. Physique I 4, 617 (1994).

COPPER ELECTRODEPOSITION ON PRINTED CIRCUITS I. KINETIC STUDY BY VOLTAMMETRIC METHODS

VĂDUVA Claudiu ¹, KELLENBERGER Andrea ¹, PANCAN Ioan Bujor ²,
VASZILCSIN Nicolae ¹

¹ University "Politehnica" from Timisoara, Faculty of Industrial Chemistry and Environmental Engineering, Piata Victoriei 2, 300006 – Timisoara, ROMANIA

² University Aurel Vlaicu Arad, Elena Drăgoi 2, 310330 – Arad, ROMANIA

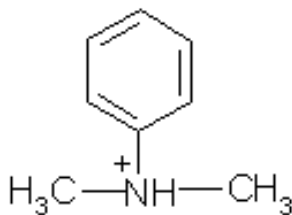
Abstract

A thickening step of the copper layer deposited by a chemical method on the insulating substrate is provided in the modern printed circuits technology. This technological stage is feasible by electrochemical deposition of a copper layer with 5 μm thickness from acid bath. In order to assure a good quality of the printed circuits an adherent and compact copper layer is necessary, as well as a high purity of the electrochemical deposited copper. An important role in achieving these requirements is performed by brightening additives. The influence of N,N-dimethylaniline on the quality of the copper deposits has been studied by linear and cyclic voltammetry. An exchange current of about 200 A m^{-2} has been calculated for copper deposition process from the acid bath in the presence of N,N-dimethylaniline.

Keywords: copper electrodeposition, kinetics, voltammetry

Introduction

It is well known that in the absence of the brightening additives, the metal deposits obtained by electrochemical way are non-adherent and spongy [1-4]. The aim of these additions, as a rule, is the increasing of the cathodic polarization, so that the nucleation rate would be large enough in order to obtain microcrystalline deposits [5-10]. N,N-dimethylaniline is one of the compounds used as a brightening agent in the copper galvanic bath. In strong acidic conditions, N,N-dimethylaniline is protonated at N atom, resulting the N,N-dimethyl-phenyl-ammonium cation, with a positive charge centre at N atom:



In the electric field of the cathode – electrolyte solution interface N,N-dimethyl-phenyl-ammonium cation is adsorbed with the nitrogen atom to metal. The adsorption of cations is achieved preferentially on the peaks of the cathodic surface, thus hydrophobic methyl groups block the access of the electrolyte solution, as well as of the Cu^{2+} cations, on the deposit tips (figure 1). This is a way that favors the copper deposition in the hollows of the metal surface. The successive adsorption-desorption of N,N-dimethyl-phenyl-ammonium cations has a brightening effect.

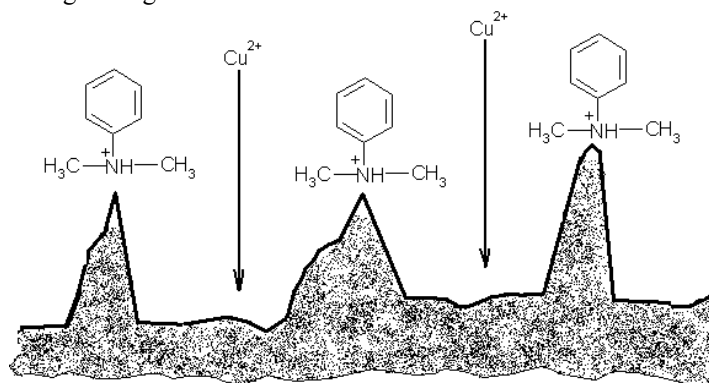


Fig. 1. Adsorption of N,N-dimethyl-phenyl-ammonium cations on peaks

In order to establish a correlation between the properties of the organic compound and the brightening effect the electrochemical behavior of the N,N-dimethylaniline was studied by voltammetric methods.

Experimental

The electrochemical measurements were performed in a conventional Princeton Applied Research corrosion cell using an Autolab 302N potentiostat. The working electrode was fixed in a teflon holder having a free surface area of 1 cm^2 . In order to minimize the ohmic drop of the electrolyte solution a Luggin capillary was used. The working electrode surface was prepared by polishing with diamond spray (Struers) with increasing finesse up to $0.25 \mu\text{m}$. Two graphite rods were used as counter electrodes and a saturated calomel electrode (SCE) as reference.

The morphology of the copper deposits has been studied using an optical microscope GUANGZHOU L2020A equipped with digital camera.

Reagents used were sulphuric acid puriss. p.a., copper (II) sulphate pentahydrate puriss. p.a., and N,N-dimethylaniline puriss. p.a. $\geq 99.5 \%$ (all from Fluka).

Results and Discussion

In order to study the electrochemical behavior of N,N-dimethylaniline, the polarization curves have been recorded on smooth platinum in 1 mol L^{-1} sulphuric acid, and then in the same solution with successive addition of N,N-dimethylaniline.

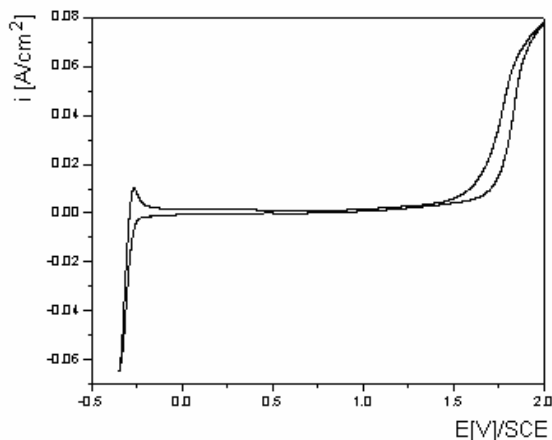


Fig. 2. Cyclic polarization curve on platinum in 1 mol L⁻¹ sulphuric acid, Temperature: 23°C, polarization rate: 50 mV s⁻¹

In the absence of N,N-dimethylaniline, the hydrogen evolution reaction occurs at cathodic polarization, and the oxygen evolution reaction at anodic one (figure 2). Also, an anodic peak due to adsorbed hydrogen oxidation process can be observed.

The addition of N,N-dimethylaniline has as a consequence a diminution of the hydrogen oxidation peak (figure 3). That means that N,N-dimethylaniline is adsorbed on the platinum surface decreasing the quantity of adsorbed hydrogen. In the same time, the anodic process is not influenced by the presence of the organic compound.

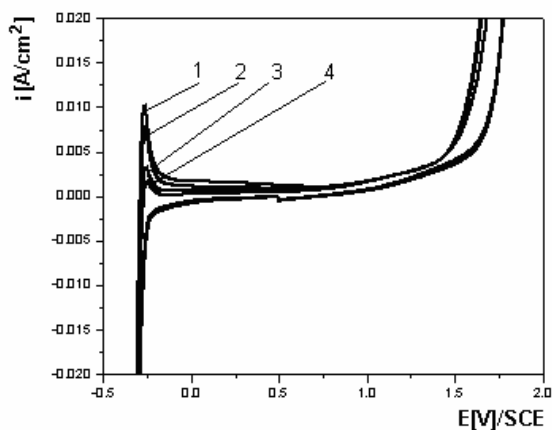


Fig. 3. Polarization curves on platinum in 1 mol L⁻¹ sulphuric acid, in the presence of N,N-dimethylaniline, scan rate: 50 mV s⁻¹, N,N-dimethylaniline concentration:

1 – without, 2 – 0.5 mmol L⁻¹, 3 – 1 mmol L⁻¹, 4 – 2 mmol L⁻¹

The process following on the cathodically polarized copper electrode, in 1 mol L⁻¹ sulphuric acid, is the hydrogen evolution reaction, proved by the presence of the gas bubbles. The hydrogen evolution reaction is as intense as the cathodic potential electrode is more negative. A limit current of Cu²⁺ reduction may be observed when copper sulphate is added to the electrolyte solution (figure 4).

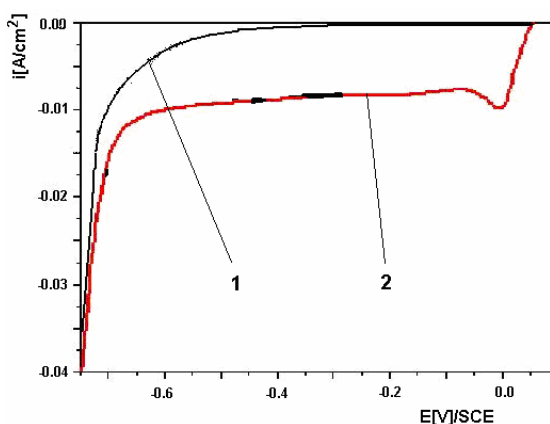


Fig. 4. Polarization curves on smooth copper: 1 - 1 mol L⁻¹ sulphuric acid; 2 - 1 mol L⁻¹ sulphuric acid + Cu²⁺ (5 g L⁻¹)

The cathodic peak of Cu²⁺ reduction appears because of the higher Cu²⁺ concentration on the metal – electrolyte interface than in the bulk of solution due to the adsorption phenomenon. The height of the cathodic peak depends on the scan rate (figure 5). The higher the scan rate, the higher peak intensity, because the amount of electricity necessary to discharge the surface excess of the Cu²⁺ is the same, but the time is smaller. At potential values more negative than -0.7 V/SCE, the current undergoes a considerable increase due to the hydrogen evolution reaction occurring concurrently with the copper deposition.

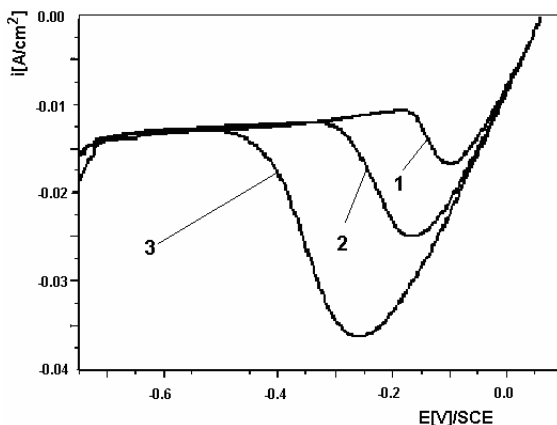


Fig. 5. The dependence of the peak height of the copper deposition on scan rate: 1 – 50 mV s⁻¹, 2 – 100 mV s⁻¹, 3 – 200 mV s⁻¹

Increasing the Cu²⁺ concentration in the electrolyte solution one can observe that the limit current increases proportionally, e.g. in 20 g L⁻¹ Cu²⁺ the limit current reaches about 400 A m⁻², that means the copper deposition process may be carried out up to 400 A m⁻² with maximum current yield. Technical limits of the current density are due to the anodic passivation of the copper anods.

In order to intensify the cathodic deposition of copper the temperature effect on polarization curves has been studied. From the polarization curves (figure 6) it follows that the limit current is enlarged by raising the temperature of the electrolyte solution.

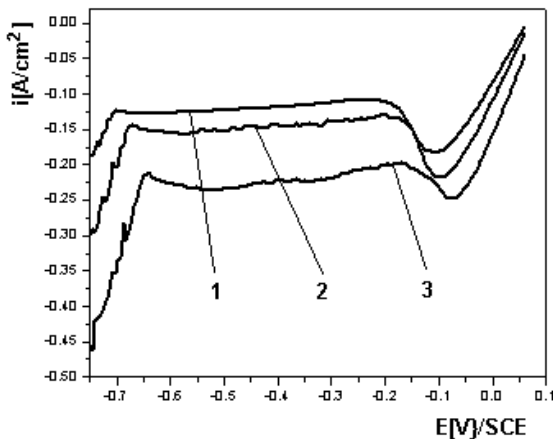


Fig.6. Influence of the temperature on the limit current of copper deposition in 1 mol L⁻¹ sulphuric acid + Cu²⁺ (5 g L⁻¹), scan rate: 50 mV s⁻¹

Unfortunately, at industrial level, the operating temperature is limited by the vaporization of the electrolyte solution and, more important, by the deterioration of the copper deposits quality. The increasing of the temperature causes a microcrystalline deposition (figure 7).

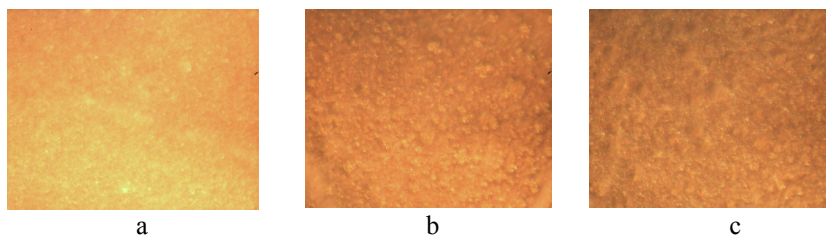


Fig. 7. Optical micrographs of the copper deposits obtained at various temperatures: a. 23°C, b. 43°C and c. 60°C

Conclusions

The study about electrochemical behavior of N,N-dimethylaniline emphasizes that, on the one hand, the organic compound used as a brightener does not influence the anodic processes. On the other hand, N,N-dimethylaniline is adsorbed on the cathode having a powerful brightening effect expressed in microcrystalline copper deposits. This behavior is due to the N,N-dimethyl-phenyl-ammonium cation arising by N,N-dimethylaniline protonation in a copper acidic bath. The diminution of the anodic peak of hydrogen oxidation is an evidence of the N,N-dimethyl-phenyl-ammonium cation adsorption.

The limit current for copper deposition depends on the Cu^{2+} concentration from the electrolyte solution. Even at small Cu^{2+} concentration, e.g. $20 \text{ g L}^{-1} \text{ Cu}^{2+}$, the limit current is considerable, about 400 A m^{-2} , that allows large operating current densities, with maximum yield. Technical limits of the current density are due to the anodic passivation of copper. As it was expected, the temperature rising intensifies the copper deposition process by the reduction of the cathodic overpotential. Also, the temperature rising decreases the resistance of the electrolytic bath. Nevertheless, this advantage can not be turn to account because of the macrocrystalline copper deposits obtained on the cathode.

References

1. L.Oniciu, E.Grünwald, *Galvanotehnica*, Editura Științifică și Enciclopedică, București, 1980, p. 366.
2. A.Strauch (Editor), *Galvanotechnisches Fachwissen*, VEB Deutscher Verlag, Leipzig, 1990, p.214.
3. E.Grünwald, L.Mureșan, G.Vermeșan, H.Vermeșan, A.Culic, *Tratat de galvanotehnică*, Editura Casa Cărții de Știință, Cluj-Napoca, 2005, p.363.
4. E.Raub, K.Müller, *Fundamentals of Metal Deposition*, Elsevier Publishing Company, Amsterdam, London, New York, 1967, p.129.
5. E.E.Farndon, F.C.Walsh, S.A.Cambell, *J.Appl.Electrochem.*, **25**, 574, 1995.

6. Healy, J.P., D.Pletcher, M.Goodenough, *J.Electroanal.Chem.*, **338**, 155, 1992.
7. W.Plieth, *Electrochim.Acta*, **37**, 2115, 1992.
8. M.A.Pasquale, L.M.Gassa, A.J.Arvia, *Electrochim.Acta*, **53**, 5891, 2008.
9. L.D.Burke, C.A.Buckley, R.Sharna, *ECS Transactions*, **2**, 197, 2007.
10. D.Stoychev, C.Tsvetanov, *J.Appl.Electrochem.*, **26**, 741, 1996.

COPPER ELECTRODEPOSITION ON PRINTED CIRCUITS II. STUDY BY ELECTROCHEMICAL IMPEDANCE SPECTROSCOPY

KELLENBERGER Andrea¹, VASZILCSIN Nicolae¹, VADUVA Claudiu¹,
Pancan Ioan BUJOR²

¹ University "Politehnica" from Timisoara, Faculty of Industrial Chemistry and Environmental Engineering, Piata Victoriei 2, 300006 – Timisoara, ROMANIA

² University Aurel Vlaicu Arad, Elena Drăgoi 2, 310330 – Arad, ROMANIA

Abstract

The influence of N,N-dimethylaniline on the copper electrodeposition process has been investigated by electrochemical impedance spectroscopy (EIS). An acid copper sulphate galvanic bath has been used with a composition similar to those used in the production of printed circuit boards. The mechanism of N,N-dimethylaniline action is explained in terms of adsorption on the surface of the cathode, as indicated by the reduction of the double layer capacitance from $2.5 \cdot 10^{-5} \text{ F cm}^{-2}$ to $1.5 \cdot 10^{-5} \text{ F cm}^{-2}$.

Keywords: copper electrodeposition, electrochemical impedance spectroscopy

Introduction

Copper electrodeposition is preferred against other processes due to several advantages such as lower cost, faster deposition rate and generally better metallurgical properties of the electrodeposited copper layer.

Significant application of the copper electrodeposition is the production of printed circuit boards (PCB) by copper deposition on the inner conducting lines. An important aspect is the thickness of the metal layer, which should be as uniform as possible, with a regular morphology to avoid dendritic growth which may result in a poor precision or even a short circuit between two neighboring tracks.

Different chemical compositions of electroplating copper baths have been in use, such as alkaline pyrophosphate baths and acid copper sulfate baths. For industrial applications sulfuric acid based compositions are widely used. A large number of studies were carried out to test the influence of additives on the properties and morphology of the deposited copper layer. It has been demonstrated that the use of organic additives such as brighteners, carriers, and levelers [1,2] has the ability to improve the throwing power, e. g. the ability to deposit a relatively uniform layer of copper on the board surface. In spite of their importance, the mechanism of additives interaction in the copper deposition is not entirely elucidated. Due to their highly polar nature the levelers are supposed to adsorb preferentially near the most negatively charged sites of the cathode (PCB). This action slows down the charge transfer of the copper ions to copper metal, thus slowing down the plating rate in those areas typically considered high current density areas.

The aim of this work is to investigate the effect of copper concentration and of leveler agents such as N,N-dimethylaniline on the copper electrodeposition in the production of printed circuit boards. The composition of the galvanic bath corresponds to a highly acid copper sulphate bath used in the production lines of PCB. Electrochemical investigations were carried out by electrochemical impedance spectroscopy in the absence and in the presence of different amounts of N,N-dimethylaniline by varying the bath composition. Electrochemical parameters such as double layer capacitance and diffusion coefficient were determined.

Experimental

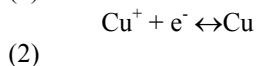
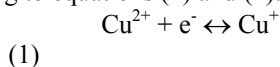
The electrochemical copper deposition was carried out from aqueous acid electrolyte solutions containing 122 mL L⁻¹ H₂SO₄ and 0.394 mol L⁻¹ CuSO₄·5H₂O which corresponds to a Cu²⁺ ions concentration of 25 mg L⁻¹, with or without the addition of N,N-dimethylaniline (DMA).

The electrochemical studies were performed with an AUTOLAB PGSTAT302N in a conventional three-electrode one-compartment electrochemical cell equipped with a copper working electrode, graphite counter electrodes and a silver-silver chloride reference electrode. The working electrode was a 15 mm copper disc (99.9% Cu) fixed in a Teflon holder, leaving exposed a geometrical surface area of 1 cm². Before each experiment the copper electrode was polished with SiO₂ paper up to 2400 grade and thoroughly washed with distilled water. The reference electrode was placed via a Luggin capillary to about 1 mm of the electrode surface to minimize the *iR* drop in the solution. All determinations were made at ambient temperature (25°C).

Impedance spectra were recorded potentiostatically in the frequency range 50 kHz to 100 mHz, with 11 measured frequencies per decade and 10 mV peak-to-peak sine wave amplitude signals using the Autolab frequency response analyzer FRA2 module. The experimental data were fitted to the equivalent electrical circuit by a complex non-linear least squares (CNLS) Levenberg-Marquardt procedure using the FRA software.

Results and Discussion

The mechanism of copper deposition is known to proceed in two steps: the reduction of copper ions to cupric ions followed by the reduction of cupric ions to metallic copper, according to equations (1) and (2):



Standard potentials E_1° and E_2° of processes (1) and (2) are 0.167 and 0.522 V/NHE respectively. From the standard potentials the disproportionation constant of the cupric ions can be estimated to be 9.62×10^{-7} mol L⁻¹.

Figure 1 shows the impedance spectra measured for the copper deposition from a solution containing $25 \text{ mg L}^{-1} \text{ Cu}^{2+}$ in the absence of additives. The electrode potential was increased in the negative direction from -0.025 V to -0.200 V in steps of 0.025 V .

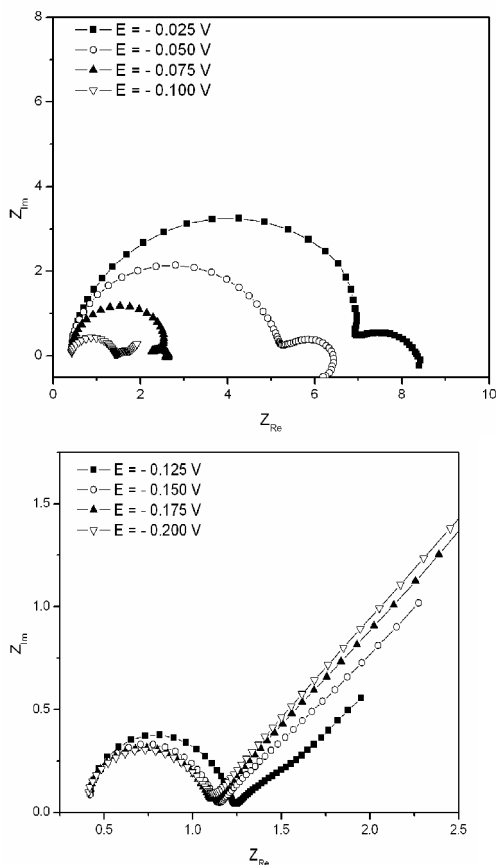


Fig.1. Impedance spectra for the copper deposition in $122 \text{ mL L}^{-1} \text{ H}_2\text{SO}_4$ solution with $25 \text{ g L}^{-1} \text{ Cu}^{2+}$ without additives. (a) potential range -0.025 to -0.100 V ; (b) potential range -0.125 to -0.200 V

The experimental impedance spectra depend strongly on the applied potential. At values situated near the open circuit potential the spectra consisted of one well resolved loop in the higher frequency domain related to the charge transfer resistance in parallel with the double layer capacity. In the low frequency region an inductive loop appears which is generally attributed to absorption-desorption process of inhibiting species on the electrode surface or to nucleation processes on the facets of the copper crystallites [3]. At more negative electrode potentials the shape of the impedance spectra in the low frequency

region changes to a classical diffusion controlled situation. In this case the straight line with slope 1 indicated the diffusion of Cu^{2+} ions from the solution towards the electrode. The impedance spectra measured at the same electrode potentials but with the addition of 1 and 2 mL respectively N,N-dimethylaniline as brightener are given in Figure 2 and 3.

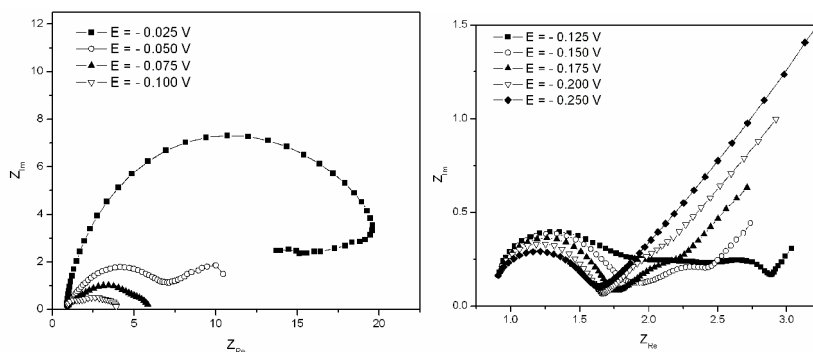


Fig. 2. Impedance spectra for the copper deposition in 122 mL L⁻¹ H₂SO₄ solution with 25 g L⁻¹ Cu²⁺ and 1 mL DMA. (a) potential range -0.025 to -0.100 V; (b) potential range -0.125 to -0.200 V

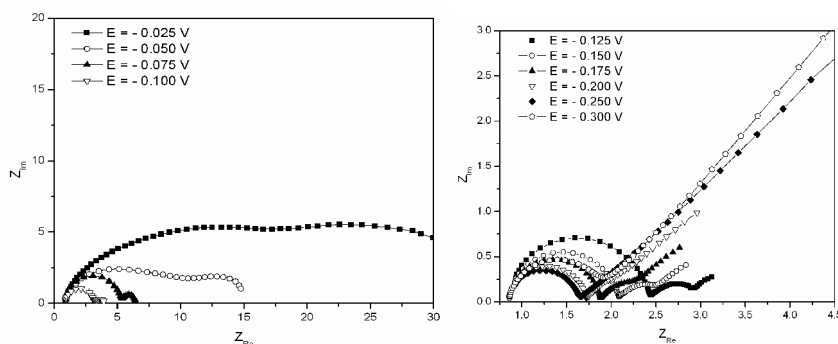


Fig.3. Impedance spectra for the copper deposition in 122 mL L⁻¹ H₂SO₄ solution with 25 g L⁻¹ Cu²⁺ and 2 mL DMA. (a) potential range -0.025 to -0.100 V; (b) potential range -0.125 to -0.200 V

As expected, the presence of DMA changes the shape of the impedance spectra. At less negative potentials two depressed semicircles can be observed in the complex plane plots. At intermediate values of the potential the charge transfer resistance decreases and the second capacitive loop is still present, followed by a tail corresponding to the diffusion of copper ions. At higher potentials the second loop completely disappears and the low frequency tail changes into a well resolved straight line.

The experimental impedance data were modelled using a classical equivalent circuit consisting from the electrolyte solution resistance R_s in series with a parallel combination between the constant phase element (CPE) and the charge transfer resistance R_{ct} with a Warburg impedance W . The results of the CNLS fitting for different potential values, in the absence and in the presence of N,N-dimethylaniline are given in Tables 1-3.

The capacitance of the electrode in an additive-free solution has a value between 1.5 and 3.0 F cm⁻², in good agreement with the literature data [4-6]. In the presence of DMA the double layer capacitance decreases due to the DMA adsorption on the electrode surface. A further increase in the concentration of DMA has a less pronounced influence on the double layer capacitance. The values of the charge transfer resistance in the absence of the additive are about 0.7 Ω cm⁻² and they tend to increase to about 40% by the addition of DMA. The value of the diffusion coefficient of the Cu²⁺ cations estimated from the impedance data is about 1.8·10⁻¹² m² s⁻¹, independently on the presence of DMA.

Table 1. Values of the equivalent circuit elements without additive.

	$E = -0.150$ V	$E = -0.175$ V	$E = -0.200$ V	$E = -0.250$ V	$E = -0.300$ V
R_s	0.41	0.39	0.38	0.37	0.37
CPE-T	2.52·10 ⁻⁵	5.00·10 ⁻⁵	7.85·10 ⁻⁵	1.90·10 ⁻⁴	3.13·10 ⁻⁴
CPE-P	1.00	0.94	0.92	0.89	0.93
R_{ct}	0.68	0.68	0.68	0.75	0.82
W-R	6.83	10.27	17.35	34.4	47.19
W-T	44.53	27.96	25.36	27.28	25.00
W-P	0.45	0.50	0.50	0.50	0.45
C_{dl}	2.52·10 ⁻⁵	2.43·10 ⁻⁵	3.05·10 ⁻⁵	5.54·10 ⁻⁵	1.54·10 ⁻⁴

Table 2. Values of the equivalent circuit elements with 1 mL N,N-dimethylaniline.

	$E = -0.150$ V	$E = -0.175$ V	$E = -0.200$ V	$E = -0.250$ V	$E = -0.300$ V
R_s	0.84	0.84	0.83	0.78	0.84
CPE-T	4.21·10 ⁻⁵	4.74·10 ⁻⁵	5.94·10 ⁻⁵	3.11·10 ⁻⁴	5.74·10 ⁻⁴
CPE-P	0.92	0.91	0.89	0.75	0.83
R_{ct}	0.64	0.79	0.77	0.83	0.95
W-R	2.418	2.016	3.28	14.78	34.11
W-T	109.2	10.07	9.82	22.58	31.48
W-P	0.15	0.28	0.38	0.49	0.52
C_{dl}	1.61·10 ⁻⁵	1.58·10 ⁻⁵	1.55·10 ⁻⁵	1.63·10 ⁻⁵	1.08·10 ⁻⁴

Table 3. Values of the equivalent circuit elements with 2 mL N,N-dimethylaniline.

	$E = -0.150\text{V}$	$E = -0.175\text{ V}$	$E = -0.200\text{ V}$	$E = -0.250\text{ V}$	$E = -0.300\text{ V}$
R_s	0.86	0.86	0.86	0.84	0.84
CPE-T	$2.05 \cdot 10^{-5}$	$2.12 \cdot 10^{-5}$	$2.27 \cdot 10^{-5}$	$3.70 \cdot 10^{-5}$	$3.126 \cdot 10^{-4}$
CPE-P	0.97	0.97	0.97	0.93	0.89
R_{ct}	1.10	0.95	0.82	0.78	1.02
W-R	2.212	2.354	7.208	15.00	38.92
W-T	42.36	13.99	59.03	19.39	31.45
W-P	0.25	0.34	0.42	0.50	0.53
C_{dl}	$1.46 \cdot 10^{-5}$	$1.48 \cdot 10^{-5}$	$1.55 \cdot 10^{-5}$	$1.58 \cdot 10^{-5}$	$1.08 \cdot 10^{-4}$

Conclusions

The results of this study show that N,N-dimethylaniline can be used as organic brightener in the copper electrodeposition for the production of printed circuit boards. In strong acid media DMA is protonated to the N,N-dimethyl-phenyl-ammonium cation which adsorbs on the surface of the cathode. The adsorption process is evidenced by the appearance of a second capacitive loop in the EIS spectra, as well as by the decrease of the double layer capacitance and the increase of the charge transfer resistance. The diffusion coefficient of the Cu^{2+} cations is not affected by the presence of the brightener.

References

- [1] L.Bonou, M.Eyraud, R.Denoyel, Y.Massiani, *Elchim. Acta*, 47 (2002) 4139-4148.
- [2] W.P.Dow, M.Y.Yen, C.W.Liu, C.C.Huang, *Elchim. Acta*, 53 (2008) 3610-3619.
- [3] C.Gabrielli, P.Mocotéguy, H.Perrot, R.Wiart, *J. Electroanalytical Chemistry*, 572 (2004) 367-375.
- [4] S.Goldbach, W.Messing, T.Daenen, F.Lapicque, *Elchim. Acta*, 44 (1998) 323-335.
- [5] L.D.Burke, R.Sharna, *J. Electrochem. Soc.*, 155 (2008) D285-D297.
- [6] M.A.Pasquale, L.M.Gassa, A.J.Arvia, *Elchim. Acta*, 53 (2008) 5891-5904.

STRUCTURE AND MORPHOLOGY OF OXIDE CRYSTALS

NICOLOV Mirela F.¹, WOENSDREGT Cornelis F.²

¹Faculty of Engineering, "Aurel Vlaicu" University of Arad, Department of Physics, Bd. Revolutiei no.77, 310130 Arad, Romania;

²Faculty of Earth Sciences, Utrecht University, P.O. Box 80.021, NL-3508 TA Utrecht, The Netherlands

Abstract

The mineral quartz (α -SiO₂) is also known as a technologically indispensable material. In this study theoretical growth forms and equilibrium forms based on several different force fields, according to the Hartman-Perdok, will be presented. Special interest will also be given to the surface topologies at atomic scale of F forms and the theoretical growth forms.

Keywords: oxide crystals, structure, morphology

Introduction

The crystal structure determines the surface structure and surface related energies, *e.g.*, specific surface energy, attachment energy and slice energy. Attachment energies are supposed to be directly proportional to the growth rates of *F* faces [1]. Calculations of attachment energies enable to construct the theoretical growth forms. Hartman [2,3] derived these forms for quartz by calculating the Coulomb interaction energies in an electrostatic point charge model. In the present paper the theoretical growth forms are presented not only including the Coulomb interaction energies, but also the dispersion (van der Waals attraction) and Born repulsion.

Hartman [2-4] investigated the structural morphology of quartz based on the space group symmetry of P322. According to this configuration the major rhombohedron (*r*) has the Bravais indices {01-11}, and the minor rhombohedron (*z*): {10-11}. This is the RHCS *z*(+)setting according to Donnay and Le Page [5]. In the present study we use atomic coordinates as determined by Glinneman *et. al.* [6]. They used the space group P3₁21 that corresponds to the RHCS *r*(+) setting with the hexagonal unit cell constants of: $a = b = 0.4921$ nm and $c = 0.5163$ nm. Hence in our paper the major rhombohedron has the Bravais indices {10-11} and the minor rhombohedron {01-11}.

Results and discussion

ENERGY CALCULATIONS

The crystal energy, E_c , is the energy released per mole, when the crystal crystallizes from the vapor. The following relation holds:

$$E_c = E_s + E_a$$

(1)

MATSUI [12] APPROXIMATES IN HIS CMAS 94 MODEL THE POTENTIAL ENERGY AS AN APPROXIMATION OF THE SUM OF PAIRWISE INTERACTIONS BETWEEN ATOMS:

$$V(r_{ij}) = -\frac{q_i q_j}{r_{ij}} - \frac{C_i C_j}{r_{ij}^6} + f(B_i + B_j) \times \exp\left[\frac{(A_i + A_j - r_{ij})}{(B_i + B_j)}\right] \tag{2}$$

where the terms represent Coulomb, van der Waals and Born repulsions, respectively. Here r_{ij} is the interatomic distance between atoms i and j , f is a standard force of $4.184 \text{ kJ A}^{-1} \text{ mol}^{-1}$, and q_i , A_i , B_i and C_i are the net charges, repulsive radii, softness parameters and van der Waals coefficients of the ion i , respectively.

Table 1. Matsui Characteristics

	$q/ e $	A/Å	B/Å	$C/[A(kJ/mol^{1/2})]$
Si	1.890	0.7204	0.023	49.30
O	-0.945	1.8215	0.138	90.61

Computations of energies using Gilbert Equation

All the results in computation depend on charges of Si and O. For these reasons we have carried out our study for the following two cases: using formal charges and Matsui Charges.

a) corrections for the energy using formal charges for

Si: $q_{Si} = +4 |e|$ and that of O : $q_O = -2 |e|$.

The attachment energies including only Coulomb interactions are listed in Table 2a. They are based on the formal charges of Si ($q_{Si} = +4 |e|$) and that of oxygen ($q_O = -2 |e|$). Instead of these formal charges the attachment energies have also been computed in a model with reduced point charges according to those published by Matsui [12]. These lower effective charges are $q_{Si} = 1.89 |e|$, $q_O = -0.945 |e|$. The thus obtained results are listed in table 4 b, second column as E_a .

All the simulations are made for the next configuration Si(1,000); Si(2,0-10); Si(2,0-10); O(1,0-10); O(2,000); O(3,-1-10); O(4,0-10); O(5,0-10); O(6,0-1-1)

Hartman [2,4] made calculations for attachment energies, but he used in his calculation only coulomb interactions and the orientation for the unit cell that he used was 60° than usual. He has the next values: for primes m 248.06 kcal/mol, for the rhombohedra r: 303.27kcal/mol and for rhombohedra z: 275.88 kcal/mol.

We can see from table 2 a in column 6 the correction for the energy using Born repulsion (column 6 in table 2a) are always positive and corrections for the attachment energy using van der Waals attraction (column 7 in table 2a) are always negative. We can obtained the attachment energy corrected with those two values using Born and van der Waals energies and we can obtain the value listed in column 8 of table 2 a.

b) corrections for the energy using Matsui charges for

Si : $q_{Si} = +1.89 |e|$ and that of O : $q_O = -0.945 |e|$.

Corrections for the attachment energies take into account the contributions Si-Si, Si-O and O-O for the total attachment energies in the case of van der Waals attractions and Born repulsions. In the case of Matsui charges in all the cases that the contribution of O-O is bigger almost 20 times the Si-Si contribution to the total attachment energy in the case of the van der Waals attractions, and the contribution to this energy of Si-O is almost 10 times higher. In the table 2 b in column 6 the correction for the energy using Born repulsion (column 6 in table 2b) are always positive and corrections for the attachment energy using van der Waals attraction (column 7 in table 2a) are always negative. We can obtain the attachment energy corrected with those two values using Born and van der Waals energies and we can obtain the value listed in column 8 of table 2b. Making comparison between final values obtained for attachment energies listed in table 2 a and b we can say that using a model with reduced point charges according to those published by Matsui the values of attachment energies are smaller than in formal charges between 4 and 5 times.

Short – range forces represented by Buckingham potentials

Short – range forces are represented by Buckingham potentials:

$$\varphi_{ij}(r) = A_{ij} \exp\left(\frac{-r_{ij}}{\rho_{ij}}\right) - \frac{C_{ij}}{r_{ij}^6}$$

(3)

with summations truncated at $r=12\text{\AA}$ in this study . In order to model dielectric properties and the long- range polarization energy for defects, a dipolar shell model may be included for most ions.

According to equation (3) we used in our calculations the following values for O-O : $A_{ij}/\text{eV} = 25.41$; $\rho_{ij}/\text{\AA} = 0.6937$; $C_{ij}/\text{eV \AA}^{-6} = 32.32$

When we make computations of the attachment energies using Buckingham potentials we take in account only the contributions of O-O bonds energy to the total value of the attachment energy .and we obtained the corrections for the energy.

Table 2

a) Normal charges

hkl	E_a	Buckingham corrections			Gilbert corrections		
		Born	vdW	Eat	Born	vdW	Eat
(10-10)	-1043	2.0	-0.3	-1041	+97.3	-88.2	-1033
(01-11)	-1279	2.0	-0.3	-1277	+101.2	-98.6	-1274
(10-11)	-1162	2.0	-0.3	-1160	+88.4	-97.7	-1171

b) Matsui charges

Hkl	E _a	Buckingham corrections			Gilbert corrections		
		Born	vdW	E _{at}	Born	vdW	E _{at}
(10-10)	-233	2.0	-0.3	-231	97.2	-88.2	-224
(01-11)	-259	2.0	-0.3	-258	101.2	-97.6	-252
(10-11)	-286	2.0	-0.3	-284	88.4	-87.3	-275

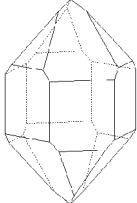
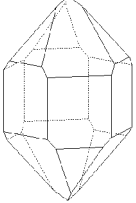
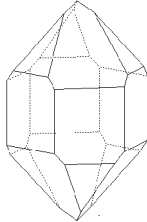
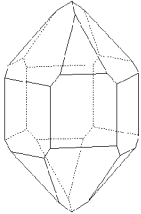
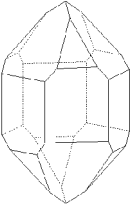
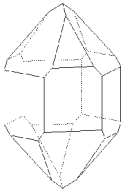
Growth forms	Coulomb interactions only	Including Born and van der Waals	Including Buckingham
Formal charges	 a	 b	 c
Matsui charges	 d	 e	 f

Figure 1 :Growth and Equilibrium form of Quartz (α -SiO₂)

The results of the corrections of energy using Born repulsions and van der Waals attraction in the considered model are the same, as we can see in column 3 and 4 from the table 4 a and 4 b. But the attachment energy corrected in those to cases are different for the formal charges ($q_{Si} = +4 |e|$ and that of O: $q_O = -2 |e|$.) and for the Matsui Charges ($q_{Si} = +1.89 |e|$ and that of O: $q_O = -0.945 |e|$) as we can see in column 5 from table 2 a and 2 b. Using Buckingham potentials in simulations of attachment energies, the final attachment energies corrected that we get are bigger values for the formal charges and are 4-5 times bigger than in Matsui case. In table 2 a in column 5 we can see all these values. Making comparison between attachment energies corrected column 5 and 8 from table 4 a and 4 b we can conclude that using Buckingham potentials the values of the attachment energies are smaller than in the case of using Gilbert equation.

Growth form of quartz

Using formal charges for the calculations for attachment energies and taking into account that the rate of growth form of the face (hkl) is direct proportional to the attachment energy, we can construct the growth form of quartz crystal. Using the values of the column 2, 5 and 8 from the table 2a and 2b we can obtain the growth form of quartz as depicted in figure 1 (a-f). All those growth forms are simulated at the same volume $V=109 \text{ \AA}^3$.

Conclusions

The presence of high index faces is attributed to a slow growth of steps of which the interaction energy becomes repulsive when they move closer. Here is stated again that F forms are $m\{10\bar{1}0\}$, $r\{10\bar{1}1\}$, $z\{\bar{1}011\}$. The absence of the basal plane and of S faces between the basal plane and the rhomboedra r and z is attributed to the fact that these faces have a K character. The absence of S faces between the prism faces is due to the fact that two neighboring faces do not contain the same PBC.

From the studies of structure we found that $\{10\cdot10\}$, $\{10\cdot11\}$, $\{-1011\}$, $\{01\cdot10\}$ and $\{01\cdot11\}$ are F faces. We can conclude that $\{01\cdot10\}$ is a new F face. We found that these forms are obtained because after studying PBC according to PBC theory, they exhibit importance as crystalline forms. However, from current mineralogy literature appears obvious that all these forms are present in the 3 zones ($\{10\cdot10\}$, $\{10\cdot11\}$ and $\{-1011\}$) [3].

References

1. P. Hartman and P. Bennema, J. Crystal Growth 49 (1980), 145
2. P. Hartman, Sur la morphologie des cristaux, Bull. Mineral., 101(1978) 195
3. P. Hartman, in *Morphology of Crystals*, ed. I. Sunagawa, Terra Scientific Publications Cy., Tokyo and Reidel Dordrecht (1988), part A, Chap 4, pp. 269
4. J. Glinnemann, H.E. King Jr, H. Schulz, Th. Hahn, SJ. LA Placa and F. Dacol, Z. Kristallogr. 198(1992) 177
5. J.D.H. Donnay and Yvon Le Page, Acta Cryst. A 34,(1978) 584
6. P. Hartman, in *Crystal Growth: an Introduction*, ed. P. Hartman, North-Holland Publishing Cy, Amsterdam, (1973), Chap 14, pp. 367-402
7. C.F. Woensdregt, Faraday Discuss., 1993, 95 (1993)
8. C. F. Woensdregt, Physics and Chemistry of Minerals, 19(1992)52
9. C. F. Woensdregt, Physics and Chemistry of Minerals, 19(1992)59
10. M. Matsui , Phys Chem Minerals, 23 (1996)345
11. T.S. Bush et. al., J. Mater. Chem., 4/6(1994) 831
12. P. Hartman , Fortschr. Miner.,57/2(1979)127.
13. P.Hartman , Zeitschrift fur Kristallographie, Bd.147(1978)S141.
14. P. Hartman and W.G. Perdok , American Mineralogist, 41(1956)449.
15. M. Kunz, T. Armbruster, Acta Cryst., B48 (1992) 609
16. R.M. Hazen,et. al. , Solid, state communications, 72/5(1989)507
17. P. Norby, J. Appl.Cryst. 30(1997)21

**THE NEW SINGLE CRYSTALS WITH ALPHA-QUARTZ STRUCTURE
OBTAINED BY HYDROTHERMAL METHOD**

MICLAU Marinela¹, GROZESCU Anamaria¹, BUCUR Raul¹, POIENAR Maria¹,
VLAZAN Paulina¹, GROZESCU Ioan¹, MICLAU Nicolae²

¹Condensed Matter Research Department, National Institute R&D Electrochemistry and
Condensed Matter, Plautius Andronescu 1, Timisoara, Romania, Phone: (0040) 256-
494413, Fax: (0040) 256- 204698, marinela.miclau@gmail.com

²“Politehnica” University of Timisoara, Bd. Vasile Parvan 2, Timisoara, Romania, Phone:
(0040) 256-403325, Fax: (0040) 256-403295, nicolae.miclau@gmail.com

Abstract

Interest of Si_{1-x}Ge_xO₂ single crystal with alpha-quartz structure is connected to improvement of electromechanical coefficients and rise of α – β phase transition of quartz one. Growth of α -Si_xGe_{1-x}O₂ crystal was realized by a hydrothermal method of temperature gradient in autoclaves, made from Cr–Ni alloys. Nutrient material was prepared from synthetic quartz as crashed crystals or rods and placed in the bottom of autoclaves. There was loaded GeO₂ powder additive in proportions to quartz nutrient. Single crystals were investigated by electron microprobe analysis, X-ray diffraction and atomic force microscopy. The most important result, obtained during the investigations, is an experimental proof of growth of Si_xGe_{1-x}O₂ solid solutions single crystals (with quartz structure) under the hydrothermal conditions. The present results thus open the possibility to tune the piezoelectric properties of these materials by varying the chemical composition.

Keywords: alpha-quartz, hydrothermal, piezoelectric

Introduction

α-Quartz type materials are of major interest due to their piezoelectric properties. In addition to α-quartz itself, this family is composed of GeO₂ and compounds with the general formula M^{III}X^VO₄ where M= Al, Ga, Fe, B, and X=P and As.

The structural distortion present can be described by two interrelated angles: the intertetrahedral bridging angle M-O-X, θ, and the tetrahedral tilt angle δ [1]. In the case of undistorted tetrahedra, the relation between these two parameters is given by:

$$\cos \theta = \frac{3}{4} - \left[\cos \delta + \frac{1}{2\sqrt{3}} \right]^2$$

For very well characterized crystals (SiO₂, AlPO₄ and GaPO₄), it proved possible to relate linearly their M-O-X values (143.7°, 142.8° and 134.6° respectively) to their piezoelectric properties [2]. The more distortion structure, the more the θ and δ values decrease and increase, respectively. One of main way to obtain a more distortion structure, it is to increase the average size of ⟨r_M⟩ of M-site cations.

Therefore, in the present paper, the Si_{1-x}Ge_xO₂ single crystal (x<0.30) were obtained by hydrothermal method and the crystal structure was determined by X-ray diffraction. These

results can be used to tune the piezoelectric properties of these materials by varying the chemical composition.

Experimental

Growth of α - $\text{Si}_x\text{Ge}_{1-x}\text{O}_2$ crystal was realized by a hydrothermal method of temperature gradient in autoclaves of 500 cm³ in volume, made from Cr–Ni alloys. A chemical of NaOH was used as mineralizer. Seeds were cut from synthetic quartz crystals in the shape of plates parallel to {c} faces and sizes of the seeds were 2 x 10 x 50 mm. Nutrient material was prepared from synthetic quartz as crashed crystals or rods and placed in the bottom of autoclaves. There was loaded GeO_2 powder additive in proportions to quartz nutrient. Temperature has a high influence on Ge-content in α - $\text{Si}_x\text{Ge}_{1-x}\text{O}_2$ crystals. With the same relation of quartz and germanium dioxide in nutrient and same crystal growth temperature 470 °C, nutrient dissolution zone temperature rises from 500 to 520 °C (pressure up to 2700 bar) leads to increasing of GeO_2 content from $x=0.1$ to 0.3.

Results and discussion

Single crystals of diameter 8mm and length 50 mm (Fig.1) were investigated by electron microprobe analysis, X-ray diffraction and atomic force microscopy (AFM).

For all the samples of $\text{Si}_{1-x}\text{Ge}_x\text{O}_2$ single crystal ($x<0.30$), a single α -quartz phase in the P3₁21 space group was determined (Fig. 2). The cell volume is found to vary continuously as a function of composition in according with ionic radius of Si^{4+} (0.26 Å), and Ge^{4+} (0.39 Å), from 112.28 Å³ ($x=0$) to 114.965 Å³ ($x=0.3$).

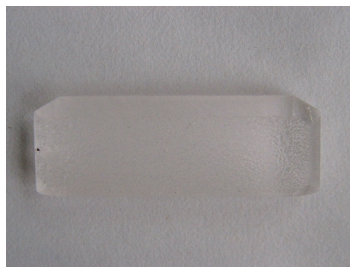


Fig.1. Photograph of grown $\text{Si}_{0.9}\text{Ge}_{0.1}\text{O}_2$ crystal obtained after 15 days, used a temperature gradient 30°C and the crystal growth temperature 500°C

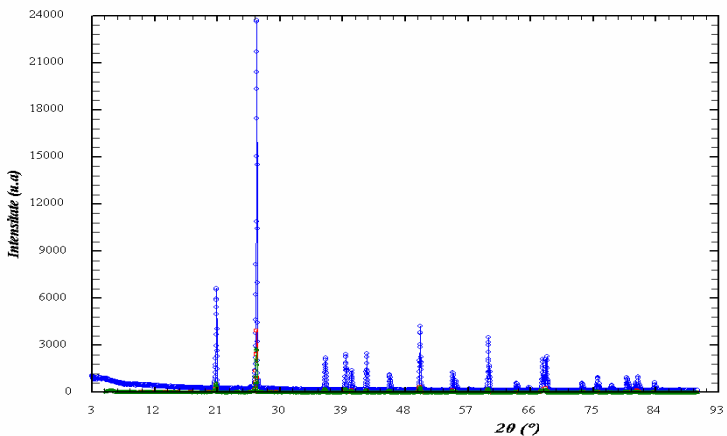


Fig.2. X-rays diffraction pattern of single crystal of $\text{Si}_{0.9}\text{Ge}_{0.1}\text{O}_2$ at the growth condition. The fine details of the crystal structures, the intertetrahedral bridging angle, was found to vary with the germanium content (Fig. 3).

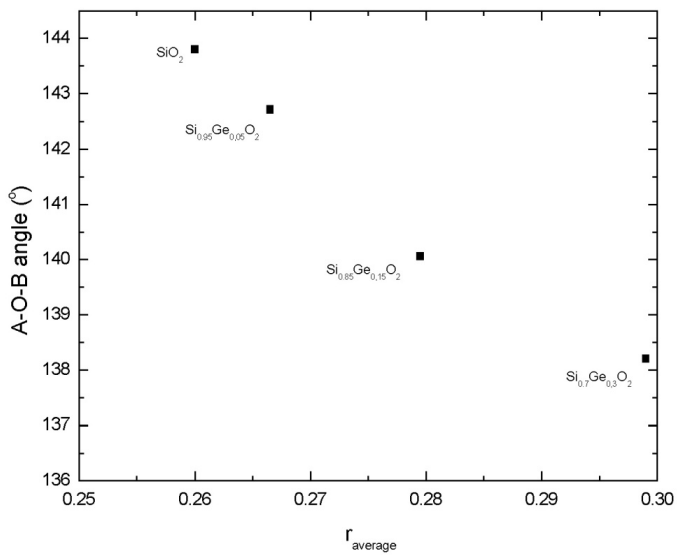


Fig. 3. Intertetrahedral angle versus average radius of A position

The electron microprobe analysis was performed at different points in the sample and was confirmed the uniformity and the closely stoichiometric composition with the precursor material (Fig. 4).

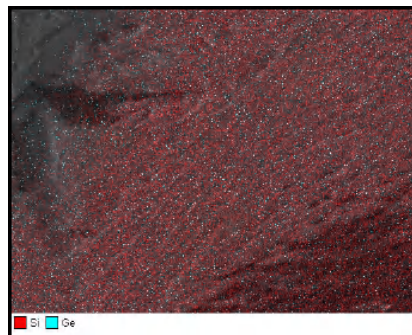


Fig.4. Map of Si-Ge distribution in α -Si_{0.9}Ge_{0.1}O₂

The crystal quality was characterized by atomic force microscopy measurements. The Si_{1-x}Ge_xO₂ single crystals were investigated for chemically polished by using H₃PO₄ acid solutions at the temperature 120 °C for 15 minutes. To characterize growth perfection of Si_{1-x}Ge_xO₂ single crystals, dislocation density was measured by the density of etch pits for prepared samples (Fig. 5).

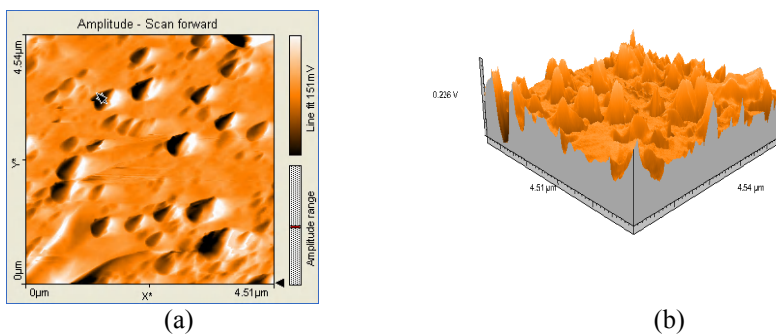


Fig.5. (a) Etch pit distribution and the shape of etch pit on the {c} face of grown Si_{0.9}Ge_{0.1}O₂ crystal; (b) 3D representation of the etch pit distribution and the shape of etch pit on the {c} face of grown Si_{0.9}Ge_{0.1}O₂ crystal.

Etch pits were found to be nonuniformly distributed over the horizontal of crystal sections. The size of etch pit is about 250 nm and assure of good quality of grown crystal

Conclusions

The most important result, which was obtained during the investigations, is an experimental proof of growth of $\text{Si}_x\text{Ge}_{1-x}\text{O}_2$ solid solutions single crystals (with quartz structure) under the hydrothermal conditions. The fine details of the crystal structures, the intertetrahedral bridging angle, was found to vary with the germanium content. The piezoelectric properties of α -quartz homeotypes are known to be correlated to this angle [1]. The present results thus open the possibility to tune the piezoelectric properties of these materials by varying the chemical composition.

References

- [1]. Phillipot E., Single-crystal X-ray diffraction study of α -quartz-type GaPO_4 , J. Solid State Chem. 1996, p.p.203-207.
- [2]. Phillipot E., Single-crystal X-ray of α -quartz-type AlPO_4 obtained by hydrothermal method, J. Solid State Chem., 1999, p.p. 153-158.

IMMUNE RESPONSE OF ANIMAL ORGANISM TREATED WITH TiO₂ NANOCRYSTALS

LAZAU Carmen¹, BURADA F.², SILOSI Isabela², SFIRLOAGA Paula¹, RATIU Cornelia¹, ORHA Corina¹, NOVACONI Stefan¹, VLAZAN Paulina¹, ROGOZ Ioan², ROGOZ Suzana², BARVINSCHI Paul³, GROZESCU Ioan¹

¹National Institute for Research and Development in Electrochemistry and Condensed Matter, Plautius Andronescu, No.1, Timisoara

²University of Medicine and Pharmacy from Craiova, Petru Rares No.2, Craiova

³West University of Timisoara, Vasile Parvan No.4, Timisoara

l_carmen@icmct.uvt.ro

Abstract

In these studies undoped and doped (Au, Ag, Pt) TiO₂ nanocrystals, synthesized through sol-gel route were investigated. The materials were characterized by XRD, SEM and EDAX analysis. TiO₂ nanocrystals present the *anatase* form crystallization, and the dimension range it was between 20-40 nm. To establish the titanium dioxide nanocrystals behavior, concerning the humoral immune response and cell-mediated immunity response we accomplished tests on white mice-*Mus Musculus*.

Keywords: immune response, TiO₂ doped, *Mus Musculus*.

Introduction

In last years, was initiated studies regarding TiO₂ activities on biological systems: bacterium [1, 2] plants (algae) [3], animals or human [4, 5]. Olmedo et al. showed that TiO₂ is transported in blood by monocyte with a role in fagocitose and deposited in some organ liver, spleen and lungs at 6 months after intraperitonean injection. To testing „in vitro” biological action of TiO₂, a different human and animal cell line was used [6-8]. Recent studies revealed that the presence of Nb and Ag ion doping in the TiO₂ nanostructure has significant effect on the transformation of anatase to rutile phase and increase photocatalytic activity [9]. Other studies prove that TiO₂ nanocrystals killed the tumoral cell in cancer culture [10].

In this paper it was study the undoped /doped TiO₂ nanocrystals influence, obtained through sol-gel method, over the immune system to organism animal (*Mus Musculus*).

Experimental

Achievement of undoped and doped TiO₂ nanocrystals.

Undoped and doped titanium dioxide nanocrystals were synthesized by the sol-gel route, using the precursors: titanium isopropoxide, isopropyl alcohol, distilled water, nitric acid, gold (III) chloride trihydrate, silver nitrate and chloroplatinic acid hexahydrate. 5 ml of titanium isopropoxide (in drops) were mixed with 30 ml of isopropyl alcohol, under continuous stirring. After a few minutes of stirring, distilled water was added,

continuously controlling the solution pH with nitric acid in order to avoid the precipitation. In the case of Au, Ag, Pt-doped TiO₂ ions, after the adjustment of the pH (2.5) the previously prepared solutions, precursors for doping were added under continuous stirring. In both cases, the gel was dried and washed in order to remove the secondary reaction products. The calcination was achieved in the oven, at a temperature of 250°C for undoped TiO₂ and 500°C for Au, Ag, Pt -doped TiO₂. The obtained materials were characterized by X-ray diffraction (XRD), scanning electron microscopy (SEM) and energy dispersive X-ray analysis (EDAX).

Immunological Methods

To establish the action of undoped and doped titanium dioxide nanocrystals obtain by the sol gel route, concerning the humoral immune response and cell-mediated immunity response we accomplished tests on white mice-*Mus Musculus*. The group contained 12 males white mice, with weight between 23-25 g. The substances were administered by intraperitoneally injection and we used three concentrations 1mg/mouse (a), 0,5mg/mouse (b) and 0,05mg/mouse (c). The first two concentrations were administered in three doses, each of them at 48 hours and respectively the last concentration 0,05mg/mice in five doses at 24 hours interval. After 24 hours from the last injection all mice were sacrificed. From the blood samples collected from the jugular vein and from the tail were determined hematological parameters and immunoglobins levels (by radial immunodiffusion method, Mancini technique) using Easy Rid kits (Liafilmchem.Bacteriology Products, Italy).

Results and Discussion

The X-ray patterns (Fig.1) present the crystallization as *anatase* form of the undoped / Au, Ag, Pt - doped TiO₂, even if the calcination temperatures for the TiO₂ doping surpass the value of 250°C. From the diffraction spectra it is noticed that the dopants did not present separate peaks, which means that they are distributed uniformly in the crystalline network.

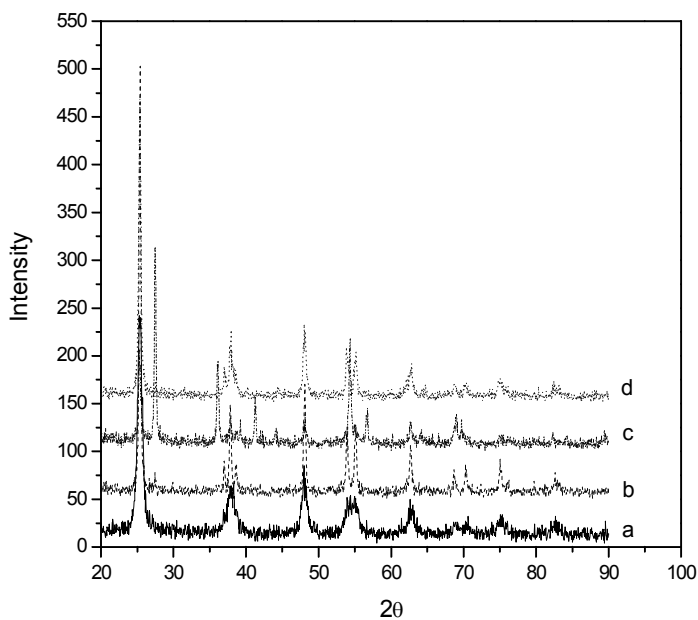
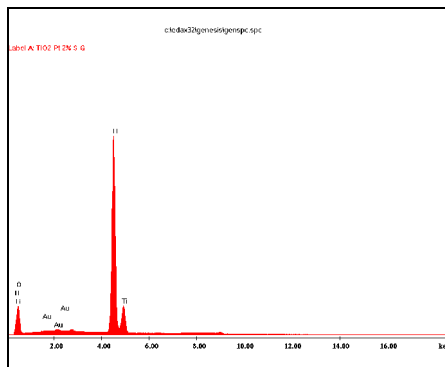
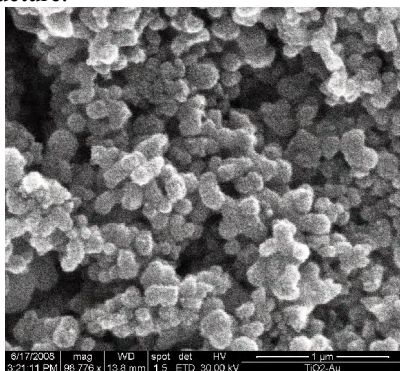


Fig.1. X-ray patterns for TiO₂ undoped (a) and doped TiO₂-Ag (b), TiO₂-Pt (c), TiO₂-Au (d)

From the surface morphology (SEM) it can be observed that the TiO₂-Au, TiO₂-Ag and TiO₂-Pt nanospheres dimensions range between 20-40 nm (Figs. 2a, 2b, 2c). EDAX analyses (Figs. 2d, 2e, 2f) confirm the presence of Au, Ag, Pt dopants in titanium dioxide structure.



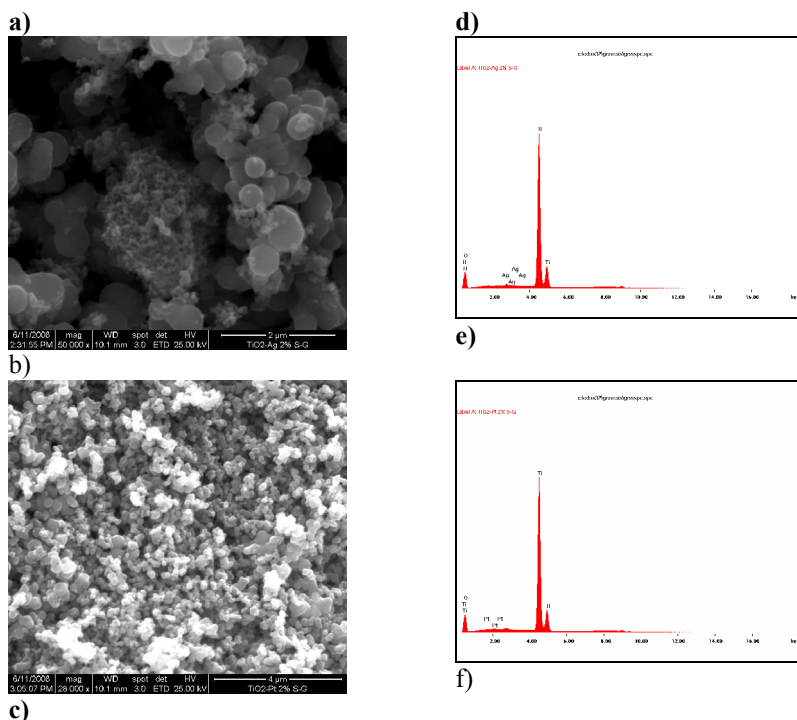


Fig.2. SEM morphology for TiO₂-Au (a), TiO₂-Ag (b), TiO₂-Pt (c) and EDAX analysis for TiO₂-Au (d), TiO₂-Ag (e), TiO₂-Pt (f)

The hematological and immunoglobins levels were compared with normal values of *Mus Musculus* parameters. The values of hemoglobin found in all mice were similar with the values of control (Table 1). The erythrocytes number was a little bit higher at the mice treated with TiO₂-Pt (2b), TiO₂-Au (4b), TiO₂-Ag (3c) and TiO₂ undoped (1a and 1b) than control. In all mice it is not recorded lysis of erythrocytes that could indicate a cytotoxic effect. The quantitative modifications of hematocrit were not important comparative with the control. The leukocytes had higher values at the mice treated with TiO₂-Au at all concentrations (4a, 4b, 4c) and also at the mice treated with 1mg/mouse (1a) and 0,5mg/mouse (1b). The increased number of PMN and lymphocytes indicated that the TiO₂ doped/undoped stimulate the immune system of the mice. The highest values of immunoglobins IgM was measured at the mice treated with TiO₂-Au at 0,5mg/mouse and 0,05mg/mouse concentrations. IgA was not detected at all mice, one of the explication is the lower concentration than identify capacity of technique and the transitory deficiency of the tested animals.

Table 1. Mice hematological parameters

Mice	Erythrocytes/mm ³	Hb g/dl	Ht%	Leukocytes/mm ³	Tromb./mmc	NS %	S %	Eo %	Ba%	Lym %	Mo %
Control	7 000 000	12,18	38	8500	1 010 000	1	57	1	0	38	3
1a* TiO ₂	9 000 000	15	46	11200	670 000	1	65	3	0	24	7
1b** TiO ₂	8 200 000	14,40	45	15000	300 000	2	73	1	0	19	5
1c*** TiO ₂	6 900 000	11,76	37	4900	1 600 000	2	41	3	0	50	4
2a TiO ₂ -Pt	7 150 000	12,64	39	5700	900 000	2	67	1	0	27	3
2b TiO ₂ -Pt	8 900 000	14,52	45	5860	850 000	1	78	2	0	15	4
3a TiO ₂ -Ag	6 800 000	12,92	40	5000	980 000	2	60	3	0	32	3
3b TiO ₂ -Ag	6.700 000	12,58	39	6500	1 000 000	1	59	4	0	30	6
3c TiO ₂ -Ag	8 400 000	12,82	40	7400	870 000	2	48	2	0	45	3
4a TiO ₂ -Au	6 000 000	12,35	38	12 000	1 009 000	2	77	2	0	16	3
4c TiO ₂ -Au	8 700 000	14,88	45	10 500	770 000	1	75	1	0	18	5
4c TiO ₂ -Au	7 900 000	12,25	39	15 000	950 000	1	52	2	0	40	5

* a -1mg/mouse, ** b - 0,5mg/mouse, *** c- 0,05 mg/mouse

Higher values of IgG was noticed at the mice treated with TiO₂-Pt (1 and 0,5mg/mouse concentrations), TiO₂-Au (0,5 and 0,05mg/mouse) and TiO₂ (0,5mg/mouse) (Table 2). These values of IgG higher than control could be the result of the immune response and prove the role of undoped and doped TiO₂ nanocrystals in the stimulation of the immune response of the animal.

Table 2. The values IgG and IgM

Mice	IgM 80-650mg%	IgG 200-1000 mg%
Control	-	200
1a TiO ₂	-	700
1b TiO ₂	-	1250
1c TiO ₂	-	250
2a TiO ₂ -Pt	-	1372
2b TiO ₂ -Pt	-	1190
3a TiO ₂ -Ag	-	700
3b TiO ₂ -Ag	-	700
3c TiO ₂ -Ag	-	211
4a TiO ₂ -Au	-	250
4c TiO ₂ -Au	160	1250
4c TiO ₂ -Au	160	700

* a - 1mg/mouse, ** b - 0,5mg/mouse, *** c- 0,05mg/mouse

Conclusions

The undoped and doped TiO₂ nanocrystals used in this experiment, present the *anatase* form crystallization, the TiO₂-Au, TiO₂-Ag and TiO₂-Pt nanospheres, present dimensions range between 20-40 nm. TiO₂-Au nanocrystals had the most immunostimulator effect on the animal system and this hypothesis is prove by the increase of leucocytes and highest levels of IgG.

The potential of the TiO₂ doped/undoped used to induce immune response is depended by dose, the nature of biological materials and the specific class of immunoglobulin produced.

References

- [1] Yaghoubi S., Schiewert C.W., McCue J.P., 2000 – Biological roles of titanium. Biol. Trace Elem. Res. 78 (1-3): 205-217;
- [2] McCue J.P., 2004 – Letter to the Editor: Management of bacterial burde in cattle by TiO₂ from Grazing. J. Dairy Sci., 87: 1579;
- [3] Hund-Rinke K., 2006 – Ecotoxic effect of photocatalytic activity nanoparticles (TiO₂) on alga. www.scientificjournals.com;
- [4] Olmedo G.D., Tasat R.D., Guglielmotti B.M., Cabrini L.R., 2005 – Effect of titanium dioxide on the oxidative metabolism of alveolar macrophages: an experimental study in rats. J. Biomed. Mat. Res., 73A (2): 142-149.
- *Chah S., Hammond R.M., Zare N.R., 2005 – Gold nanoparticles as a colorimetric sensor for protein condormational changes. Chemistry and Biology, 12: 323-328;
- [5] Kamal M., Wroblewski J., Hultenby K., Blanca Lopez S., Arvidson K., 2000 – Effects of titanium surfaces blasted with TiO₂ particles on the initial attachment of cells derived from human mandibular bone: a scanning electron microscopic and histomorphometric analysis. Clinical Oral Implants Res., 11 (2): 116-128;
- [6] Wang JJ, Sanderson BJ, Wang H. - *Cyto- and genotoxicity of ultrafine TiO₂ particles in cultured human lymphoblastoid cells*. Mutat Res. 2007 Apr 2;628 (2):99-106. Epub 2006 Dec 15.
- [7] Linnainmaa K.; Kivipensas P.; Vainio H.- *Toxicity and Cytogenetic Studies of Ultrafine Titanium Dioxide in Cultured Rat Liver Epithelial Cells* ;Toxicology in Vitro, 1997, Volume 11, Number 4pp. 329-335(7)
- [8] Türkez Hasan - *An in vitro blood culture for evaluating the genotoxicity of titanium dioxide: the responses of antioxidant enzymes*; Toxicology and Industrial Health, 2007, Vol. 23, No. 1, 19-23 .
- [9] A Ahmad, J Thiel and S Ismat Shah- *Structural effects of niobium and silver doping on titanium dioxide nanoparticles*, J. Phys.: Conf. Ser. 2007, 61 11-15.
- [10] R. Cai, Y. Kubota, T. Shuin, H. Sakai, K. Hashimoto, A. Fujishima, -*Induction of cytotoxicity by photoexcited TiO₂ particles*, Cancer Research, vol. 52, no. 8, pp. 2346–2348, 1992.

STUDY ON THE SOLUTIONS FOR IMPROVING WATERS DECONTAMINATION PROCESS WITH CHLORINE

CÎRȚÎNĂ Daniela, ȘCHIOPU Cătălin

*"Constantin Brâncuși" University, Engineering Faculty, Tg.-Jiu, Romania,
E-mail: daniela@utgjiu.ro*

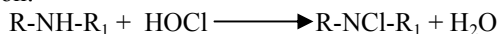
Abstract

The issue of water decontamination is of great actuality due to the limited drinkable water reserves and increasing pollution of water basins. Providing the safety from the sanitary and hygienic point of view of drinkable water connects to drawing some efficient technologies and creating great productivity devices for treating it. This paper proposes some methods for improving the process of water sterilization with chlorine applicable for decreased the lacks of water chloridization.

Keywords: water decontamination, sterilization, chlorine

Introduction

The chemical method of disinfection uses chlorine is the most frequently used because it is a simple, economical and safe method. Moreover, chlorine disinfection can be applied for great amount of water while other methods can be used only for relatively small amounts of water. The reactions occurring in the chlorine hydrolysis and its compounds allow the understanding of the chlorine bactericide action. Active of efficient chlorine is the hypochlorous acid (HOCl) or the hypochlorite ion (OCl⁻). Together with the HOCl oxidative action, it can combine with compounds of the microorganism cells according to the relation:



The resulted organo-chlorinated compounds are incompatible with the life of germs [1,2]. When chlorine is introduced into polluted water containing ammonia results - due to the reactions occurring between these two substances - a mixture of mono-chloramines, dichloramine and trichloramine (nitrogen trichloride). The more acid the pH is, the more mono-chloramine forms comparing to dichloramine, like in the case of water chlorination. The chlorine used for water disinfection is said to produce certain chlorinated organic substances that could be harmful or cancer producing [3]. Most of the authors think that three main processes can be distinguished in the water disinfection with chlorine: organic and ammonia compounds oxidation and some chlorine greedy anorganic substances. The chlorine used in this process is called absorbed chlorine. Only after carrying the oxidation the rest of chlorine acts upon microbial germs, reason why the dose of chlorine that has to add to water for an efficient disinfection is caused by this oxidation process; direct chlorination of organic substances causes some organo-chlorinated compounds which give an unpleasant taste to the water. These organo-chlorinated derivatives can be eliminated through an overdose of chlorine, and the excess of chlorine shall be removed later; the destroy of microbial germs leads to the alteration of the microbial cell membrane, when

the chlorine enters the germ and alterations of its protoplasm which is incompatible to life [4].

Experimental

The water disinfection with chlorine is influenced by the following factors:

- The biological features of microorganisms. It has been experimentally proved that in order to sterilize incremented bacteria chlorine doses 6 times higher are necessary for vegetative forms and a longer period of time [5]. The concentration of bacteria into water also influence the disinfection efficiency. (Table 1)
- .- Bactericide properties of chlorine products. Chlorine disinfecting action depends to a greater extent from the product used. Therefore, chlorine disinfecting action is stronger than of bleach and even stronger than of chloramines.

Table 1. The influence of the water bacterial contamination upon the bactericide action of chlorine.

Dose Cl ₂ (mg/dm ³)	Duration of action (min)	Content colibacili (colibacil/cm ³)	
		Before dezinfecțion	After dezinfecțion
0,5	30	3230000	20000
0,5	30	75000	64
1,0	30	3570000	5000
1,0	30	24000	10

- The type and form of available chlorine. For being able to make an efficient destroy of bacteria, we need an amount of combined chlorine 25 times bigger than the amount of free chlorine, at the same temperature, duration and pH contact.

- The chemical composition of water. This and especially the presence of suspensions, dissolved organic substances, ferrous or manganese compounds, ammonia and other chlorine consuming substances have a significant influence upon the efficiency of disinfection.

Table 2. The bactericide influence of chlorine according to the dose of chlorine an contact time.*

Dose Cl ₂ (mg/dm ³)	The number of bacteria left on 1 ml		
	After 5 minute	After 30 minute	After 120 minute
0,5	10.800	600	200
1,0	2.400	200	0
2,0	10	0	0

*The initial time of b. coli 1 630 000/ml.

- The water temperature influences the disinfectant effect of chlorine in the sense that the more temperature decreases the more the efficiency of chlorine decreases.
- pH influences the chlorine disinfectant effect, because, at different values, different forms of chlorine appear with different bactericide properties.
- The contact time of chlorine with water and chlorine concentration are essential, and the bactericide effect increases together with the increase of the dose and the contact time (Table 2).

Results and discussion

The lacks of water decontamination method with chlorine can be eliminated by increasing the anti-microbial action of the active chlorine. We shall thus follow the creation of some conditions, where the maximum amount of active chlorine be directly consumed in the decontamination process. This is made by reducing the treated water capacity of absorption by eliminating organic and mineral mixtures in water, and also by increasing the degree of using the reactive due to an intense mixture. Besides, the intensity of the anti-microbial action of the active chlorine can be increased by combining the given methods of decontamination with other methods, both physical and chemical.

Water treatment with products containing active chlorine allows to achieve a bactericide effect of 100% in few times smaller disinfectant doses, comparing to those traditionally used. Also, the combination of low power electric discharge with sodium hypochlorite causes a synergetic effect occurring in the case of chlorine doses that are below the limit concentration allowed in water (0.3-0.5 mg/l). In the water decontamination practice chlorination is used at the same time with ultrasound treatment. In this case we notice an alteration of electro-physical parameters of cellular membranes: polarization, electric conduciveness and electro-kinetic potential of cells which leads to their rapid destroy under the action of disinfectants. The use of active chlorine together with ultraviolet irradiation allows also to substantially reduce the necessary time for water decontamination. An analogous effect is noticed when combining chlorine active products with electron and gamma rays irradiation.

Among the chemical intensification methods the most used is treatment with different halogens, oxidants, alkaline metals and alkaline earthy salts, as well as variable valence metals. The researchers' attention has been lately focused on the use of variable valence metals as a catalyst in the water treatment with chlorine.

Therefore, in the chlorination of biologically treated waste waters in the presence of oxides and iron salts, the ammonia sodium oxidation reaction is accelerated as well as of the nitrate of the organic substance and the chlorine consumption reduces. The copper ions are introduced for the intensification of the manganese elimination process from underground waters using sodium hypochlorite. The waste waters treatment degree with chlorine increases by introducing cobalt and nickel salts.

For elaborating an efficient technology for water treatment with chlorine in the presence of metals ions, researches have been carried for choosing some catalysts that would lead to the increase of the decontamination speed and the decrease of the disinfectant

concentration, without worsening the physical and chemical indices of treated water. Together with NaCl, into the infected water variable valence metals salts have been introduced at the level of the maximum allowed concentration.

As experiments prove, in the presence of Cu^{2+} or Ag^+ a substantial increase of the water treatment with active chlorine occurs. The presence of Fe^{3+} and Mn^{2+} into the water does not influence the treatment quality, and the presence of Fe^{2+} , Co^{2+} and Ni^{2+} causes its worsening. Regarding the fact that the introduction of Cu or Ag ions causes the acceleration of the water decontamination with chlorine, the influence of lower concentrations than the limit concentration allowed have been studied upon the antimicrobial properties of NaCl. Researches have allowed to justify the dose of active chlorine and the concentration of metals ions established as basis for the new method of intensification the process of water treatment.

For appreciating whether the intensification of the antimicrobial action of sodium hypochlorite is the cumulated totality of bactericide effects of reactive or their actions goes beyond the additive one, after a method proposed, the coefficient of surviving have been computed both experimentally (E) and theoretically (T) of E.coli both in the case of separated reactive action and at their combined action. Calculations prove that the values of the theoretical coefficient of surviving of the coli bacilli at the reactive combined use, are beyond the experimental data. In the case of all the combinations of disinfectants greater than a unit, the theoretical and experimental coefficients T/E prove the existence of synergism in their action.

In this way, we thus propose a method of intensifying the water treatment process with active chlorine, based on the synergic action of the sodium hypochlorite with the ions of copper or argentums. The use of this method allows to obtain a safe antimicrobial effect at admitted concentrations of disinfectants for water supply. Due to the researches we show that together with water treatment, the drinkable water conservation also occurs, being conditioned by the flow of metals ions into the water, with the role of extending the conservation duration. The data are at the basis of achieving the plants for treating and conserving the water used in different systems of water supply.

Conclusions

Disinfection is the compulsory final stage of the water treatment process, leading to the complete elimination of pathogen germs from water and the decrease of the saprophytes ones to the limitations established in the water drinkability STAS. Disinfection can be made through chemical methods (chlorine treatment and chlorigene substances treatment, ozone, potassium permanganate etc.) or physical (distillation, boiling, ultraviolet radiations, ionizing radiations, ultrasounds etc). The substances used for water disinfection has to comply with certain conditions, namely: to be efficient to bacteria and viruses in a shorter time, not to alter water organoleptic qualities, not to leave harmful substances for the body into the water after exercising its effect, to be easily to apply and procured at a low price.

Chlorination, one of the most used water treatment methods, is characterized by safety, economy and technological simplicity. Among its lacks we have to mention: microorganism groups resistant to the action of chlorine; the possibility to form toxic chlorinated compounds within the chlorination process and the necessity of dechlorination. The methods proposed for improving the water sterilization process with chlorine follow to increase the antimicrobial action of active chlorine by combining decontamination with other physical or chemical methods. Among the physical methods, chlorination combined with ultraviolet water irradiation also applies, as well as water treatment with ultrasounds, combining some chlorine active products with irradiation with electrons or gamma rays, respectively. The chemical methods used successfully for accelerating the bactericide effect of chlorine consists of using variable valence metals as well as copper, argentum, iron ions as catalysts of the decontamination process. The data got from the researches on the process of sterilization of water with chlorine have allowed to draw some efficient water treatment technologies.

Also, we propose a method for intensifying the water treatment process with active chlorine, based on the synergic action of sodium hypochlorite with copper or argentums ions, method allowing an antimicrobial effect for allowed concentrations of disinfectants for water supplies.

References

1. Traista, E., Madear, G. - Environmental hygiene. Hygiene of air and water, Ed. Universitas, 1999.
2. Forster, C. F. - Biotechnology and Wastewater Treatment, New York, NY: Cambridge University Press, 1985.
3. Hites, R. A., Eisenreich, S. J. - Sources and Fates of Aquatic Pollutants, Advances in Chemistry Series 216, American Chemical Society, Washington DC, 1987.
4. Negulescu, M., Antoniu, R., Rusu, G., Cuşa, E. – Protection of water quality, Ed. Tehnică, Bucureşti, 1982.
5. Manahan, S.E., Toxicological Chemistry, Lewis Publishers, Chelsea, 1992.

ASPECTS REGARDING THE CHEMISTRY OF THE SURFACE AND UNDERGROUND WATER FROM THE TURCENI AREA

CÎRȚÎNĂ Daniela

"Constantin Brâncuși" University, Engineering Faculty, Tg.-Jiu, Romania,

E-mail: daniela@utgjiu.ro

Abstract

Satisfying the water request of the population and economy, capitalizing new water resources, rational usage of the water and protection against pollution, as well as fitting out the water courses, it must be realized in a unitary way and in conformity with social and economic development. Now numerous efforts for keeping and improving the water are made. Various technologies of water improvement were developed, which ultimately have as purpose protection of water quality. Although, water protection measures prove to be, in some situations, insufficient, they are left behind by the impurity growth rhythm. In this paper a study regarding the influence of the energy production activity by Thermal Power Station Turceni on the surface and underground water from the area is presented.

Keywords: surface and underground water, protection, purification

Introduction

The most important problem caused by the growth of the energy consumption necessary for the living level of the humanity is the ecological impact, through the reduction of the fuel reserves and rough material, as well as de pollution phenomenon, which has to be controlled. The energy is at the same time a solution and a problem for the lasting development, because it allows the progress, but it is also the major cause of pollution and other damages brought to human health and the environment.

In the technical-scientific process conditions and continuous development of industrial production, environment protection has become one of the main problems of our present days. Technical and industrial process meant sometimes a step back from ecological point of view especially when in the environment secondary effects, of toxic nature for biosphere appeared. Besides natural pollution, anthropological pollution has a special importance and it is the main cause of air contamination, water and earth [1,2].

Laws from the domain of the environment are distinguished through their complex approach. These laws regulate all meaningful human activities, which, in one way or another, have an incidence on the environment. These activities are seen, through the meaning of their negative impact on the environment, in the purpose of the elimination or at least diminution of the effect, but also from the point of view of human activities development in a healthy environment [3,4].

At the elaboration of the laws regarding the environment are taken in consideration four characteristics of its usage:

- environment is a dynamic system, within the framework of which there are occur numerous interactions, many times very complex; a substantial modification of an individual component of the system leads to the partial modification or even global of the entire system;
- damaging of the environment has in general a latent character, so that the damages are not directly and permanently observed, but, many times, they are identified when it is already too late to fix the damages
- natural resources have become rare and for this reason, it is necessary to be kept in mind the fact that not only the not-regenerable resources must be exploited in a rational way, but also the fact that some regenerable resources have become poor.
- environment protection constitutes an extremely important way for maintaining a healthy environment.

The composition of water varies depending on the regional factors, but, in general, it depends on: the salts dissolved in the rain water, the erosion of the continental material from the area, anthropogenic evacuations. Water constituents can be found under physical aspect in dissolved, colloidal or suspension form, and under chemical, ionic, complex, absorbed form. All constituents of natural water are framed on the following categories of physical-chemical indicators: chemical: pH, turbidity, conductivity, anions and cations, heavy metals, organic substances etc.

Of course that all the indicators will be found, more or less, in all running waters, dead waters, depending of the three presented forms. Through anthropogenic activities, many impurities are present in the water and in bigger concentrations [5,6].

Experimental

Physical-chemical characterization of the water in Turceni area

Auto-purification of the surface water takes place under the influence of the climate factors (precipitations, water and air temperature, wind speed, solar radiations) and hydrological (debit of the receiver, river's bed characteristics) and is possible only if those had not suffered previous pollution phenomenon. These elements must be considered to assure the necessary of water usage from downstream by steam power plant Turceni. River Jiu - main water course that crosses Turceni area has been watched in the downstream section Turceni, by carrying out physical-chemical analyses and biological-bacterial.

The evolution of the yearly average concentrations for suspension indicators, CCOMn, CBO₅ is represented in the table 1. Regarding the characterization of the water courses from biological-bacterial point of view, have been taken every four months water specimens from the downstream section by used water eviction from the activities at the steam power plant Turceni. Biological and bacterial analysis show an improvement and a decrease of the total coli form bacterium (BCT), as it can be noticed from table 2.

Table 1. Physical and chemical indicators of water.

Year	Section control	Suspension (mg/l)	CCO Mn (mg/l)	CBO ₅ (mg/l)
2004	Jiu downstream Turceni	37,25	3,65	2,45
2005		34,5	4,37	2,45
2006		30,33	3,63	2,2
2007		29	4,17	2,52

Table 2. Indicators of biological and bacteriological water.

Year	Section control	Quarter I		Quarter II		Quarter III		Quarter IV	
		C%	BCT/ 100ml	C%	BCT/ 100ml	C%	BCT/ 100ml	C%	BCT/ 100ml
2004	Jiu downstream	83,3	36000	83,3	17000	80	2780	85,7	38000
2005	Turceni	85,7	1720	83,3	2960	80	2780	83,3	900
2006		83,3	18000	83,3	9200	83,3	14000	83,3	9500
2007		75	-	87,5	-	88,8	-	88,8	-

C% - cleaning degree; BCT – total coli form bacterium

Results and discussion

By watching out the river Jiu on section from Gorj county it was noticed that in all the analyzed sections the suspensions content had a downward evolution over the years, so that in the present the process of clarifying is more obvious. This process continues on the section Tg. Jiu - Turceni because of the enlargement of the river bed and small speed of water flow. The decrease of the water suspensions in the river Jiu determines a decrease of the organic substances in the water (fig.1, fig.2).

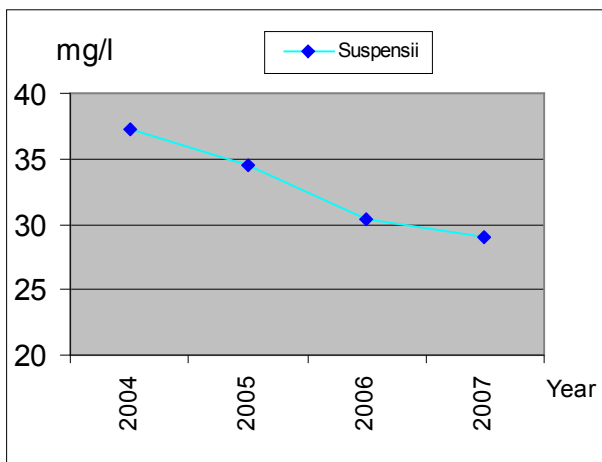


Fig.1. Evolution indicator suspension in river water -sections Gorj County.

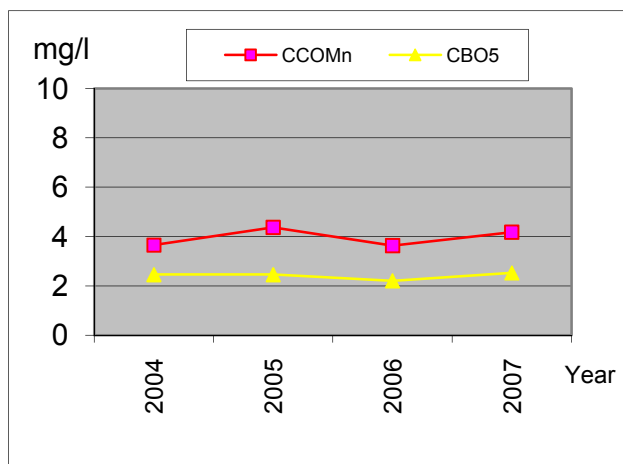


Fig.2. Evolution annual average concentrations for indicators CCOMn and CBO₅

Cleaning degree evolution of Jiu river, in downstream by TPS Turceni, on the period 2004-2007 is presented in fig. 3. The values of the cleaning degree and the saprob index registered in the period 2006-2007, frame the surface water from saprobiological point of view, specific to the water moderate polluted and in the IInd quality class according to the Order 1146/2002.

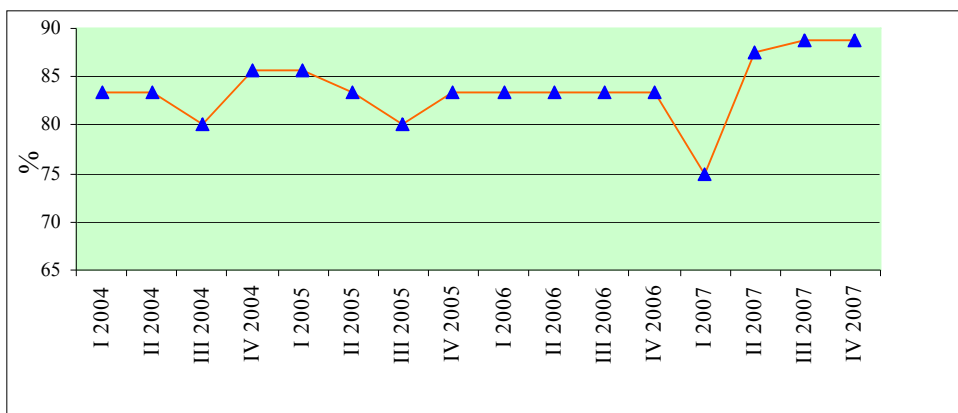


Fig. 3. Evolution of the degree of cleanliness - Jiu downstream Turceni 2004 – 2007.

State of the ground water

The Agency for Environment Protection Gorj, watched the quality of the ground water layer from physical-chemical point of view in the area Turceni affected by the activities of the steam power plant Turceni, according STAS 1342/91 Potable water. Quality conditions. There have been analyzed, samples from six fountains in the area of the locality Turceni. The results of the physical-chemical analysis at different fountains from the area Turceni in the year 2006 and the variation of the concentration of the different ions in the ground water layers represented in the graphics fig. 4 and 5. Reporting the results of the analysis to STAS 1342-91 can be taken the following conclusions:

- the concentrations of the Ca and Mg ions outrun the permitted values to all the inspected fountains;
- the ions concentrations are superior to the CMA's stipulated by STAS 1342-91 regarding the water drinkability;
- In the Turceni area, in the under water layer are found large concentrations of sulphates (between 251 – 850 mg/l), calcium and magnesium, as a follow up of the influence of the slag and ashes deposit in area Valea Ceplea of the SC Energetic Complex Turceni.

Conclusions

Economical-social development without precedent and energy production through the burning of fossils, lead to the eviction of large slag and ashes quantities that must be managed appropriately because of their pollutants content. When the measures of environment protection are not enough, the impurifying of the under water layer is inevitable. In the area of the locality Turceni, as a follow up of the extractions from the slag and ashes pond from Valea Ceplea belonging to the steam power plant Turceni, the under water layers are influenced by the used evicted water, modifying the chemistry of the under water layers from fountains or the springs at the base of the slope. So, after the analysis it was noticed a growth of the sulphate anion values in connection with the natural fond of the area, fact that indicates the presence of the extra filtrations of these in the under water layers from the area. Inhabitants of the commune Turceni are affected at the same time from point of view of the usage of non-drinkable water, but also under the aspect of rising the under water layer level, with bad repercussions on the construction and individual households.

In the water quality protection domain, the permanent knowledge of the actual status and the evolution tendencies of the water resources quality is indispensable for the adoption of fundamental decisions. In the plans of water quality management for energetically units, a determinant role has the surveillance of the quality, having as a finishing purpose the protection against the noxious effects. This implies two important stages: knowledge of the quality of the waters and protection measurements of water quality protection. The knowledge of the water quality starts with the gathering phase and analysis of the water samples, according to the structure of the quality surveillance system.

In the case of the T.P.S Turceni are imposed as main measures of pollution reduction: watching the under water layers and from the area of the slag and ashes deposits, through the

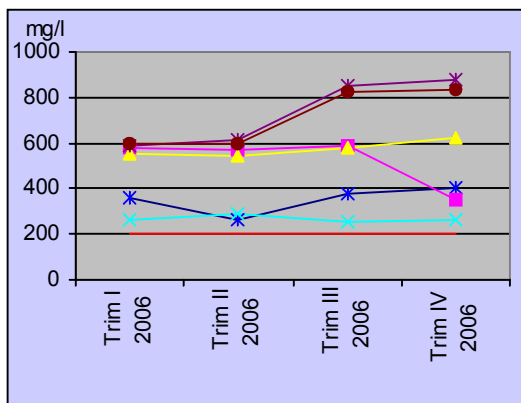


Fig. 4. Concentration of sulfate ions in groundwater in area Turceni

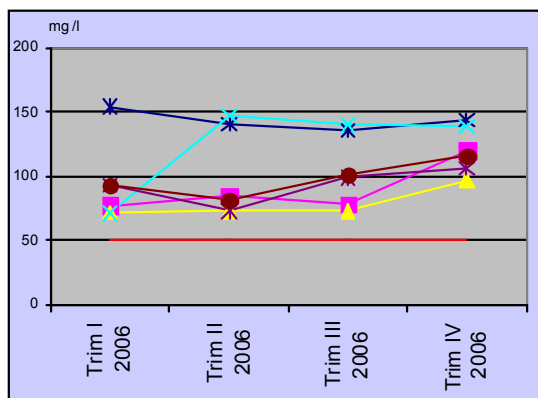


Fig.5. Concentration of magnesium ions in groundwater in area Turceni

chemical analysis as well as the watching of the quality index of the evicted used water in the slag and ashes deposits.

References

1. Lăzăroiu, Gh. - The CTE Impact upon the Environment, Ed. Politehnica Bucharest, Romania, 2005.
2. Negulescu, M., Antoniu, R., Rusu, G., Cuşa, E. - Quality water protection, Technical Publishing House, Bucharest, 1982.
3. Ianculescu, O., Ionescu, Gh., Racoviteanu, R. - Waste Water Treatment, Ed. Matrix Rom, Bucureşti, 2001.
4. Ionescu, C., Manoliu, M. - Policy and law environment, Ed. H.G.A. Bucureşti, 2000.
5. Rojanschi, V. – Engineering and Environmental Protection, Ed. Economică, Bucureşti, 1997.
6. Traistă, E., Madear, G. - Environmental hygiene. Hygiene of air and water, Ed. Universitas, 1999.

ANALYSIS OF HUMAN BRAIN GANGLIOSIDES BY ELECTROSPRAY IONIZATION FOURIER TRANSFORM ION CYCLOTRON RESONANCE MASS SPECTROMETRY

Alina D. ZAMFIR^{1,2}, Željka VUKELIĆ³

¹Department of Chemical and Biological Sciences, "Aurel Vlaicu" University of Arad, Romania; ²Mass Spectrometry Laboratory, National Institute for Research and Development in Electrochemistry and Condensed Matter, Timisoara, Romania; ³Department of Chemistry and Biochemistry, Faculty of Medicine, University of Zagreb, Croatia; *correspondence: tel: +40-257-219331; fax: +40-257-219242; e-mail: alina.zamfir@uav.ro

Abstract

As part of our ongoing effort to implement novel mass spectrometry methods into the field of complex lipid-linked carbohydrate analysis, we developed hereby a protocol based on negative ion nanoelectrospray ionization Fourier transform ion cyclotron resonance mass spectrometry, (-) nanoESI-FTICR MS, for comparative screening of ganglioside mixtures extracted and purified from normal adult cerebrum and cerebellum. Analysis conditions were thoroughly optimized to promote efficient ionization, reduce the in-source fragmentation and enhance the detection of intact molecular ganglioside species. Using this methodology a reliable and detailed compositional fingerprint of the mono- and polysialylated ganglioside species as well as of biologically relevant components modified by fucosylation could be achieved. Negative ion nanoelectrospray ionization FTICR-MS at 9.4 T is shown here to represent a method of choice for identification of single components in such complex glycomixtures due to ultra-high resolution and mass accuracy.

Keywords: gangliosides, human brain, electrospray ionization, high resolution mass spectrometry

Introduction

Sialylated glycosphingolipids known as gangliosides (GGs) are outer leaflet plasma-membrane components, expressed at the cell surface of various cell types and widely distributed in vertebrates, especially in the nervous system of mammals [1]. GGs are most abundant in the central nervous system (CNS), particularly in synapses and as members of functionally specialized membrane lipid domains (rafts) [2]. They are implicated in prominent biological processes, in particular during fetal development, maturation, differentiation, aging development, but also malignant transformation and neurodegeneration, participating primarily in cell-to-cell and/or cell-substrate

recognition/communication as well as in cell signaling through direct intermolecular non-covalent interactions (GG-GG, GG-protein etc.) and through modulation of receptors and/or other signal transducer molecules involved in transmembrane signal transduction pathways [3-9]. GGs also participate in induction or development of various diseases and are in the current focus of interest as potential diagnostic markers [10,11] and as therapeutic targets for cancer and potentially for other diseases, highlighting the need for a systematic structural characterization of their distribution pattern in tissues.

A high structural diversity of GGs structures in tissues/cells accounts for a high complexity of their tissue/cell-specific composition. To elucidate the structure of a particular GG species involved in a particular physiological or pathological process, a detailed structural analysis is of essential necessity. To define and understand the structure-to-function interrelationship for each particular GG structural entity implicated in a certain physiological/pathological process as well as to improve their valuable diagnostic and potential therapeutic significance, initially fast atom bombardment mass spectrometry (FAB-MS) strategy was introduced in ganglioside research [12]. FAB MS was the first technique able to provide reliable structural analysis at the nanomolar sensitivity. In the past years, however, novel highly sensitive and accurate MS platforms were developed and implemented in glycolipidomics. Successful strategies based on nanoESI-QTOF MS tandem MS [13,14], coupling of the capillary electrophoresis to (-)nano-ESI-QTOF MS/MS [15], fully automated chip-based nanoESI-QTOF MS [16] and high capacity ion trap multistage MS [17, 18] for detection and sequencing of different types of GG species have been established by us. These modern methods allowed not only the detection and structural characterization of individually isolated fractions but also a detailed compositional mapping of complex native mixtures isolated from tissues in very low amounts, followed by MS/MS sequencing of individual species.

Fourier transform ion cyclotron resonance (FTICR) MS has matured to become an indispensable tool in bioanalytical studies for examination of complex mixtures, such as those encountered in glycomics. The unique features of the FTICR MS in comparison to all other MS methods are the ultra-high resolution exceeding 10^6 and the mass-determination accuracy often below 5 ppm. This technique in combination with ESI-source has been introduced by us in glycomics for the analysis of glycopeptides allowing mapping of glycoforms and a detailed investigation by multiple fragmentation using nanoFTICR SORI-CID-MS³. However, for nanoESI-FTICR MS analysis of gangliosides, only initial data from our laboratory on detection (MS¹) and sequencing by SORI-CID MS² and MS³ were so far reported [19].

In this context, the aim of this study was to develop an approach based on the negative ion ESI-FTICR MS for comparative screening under identical instrumental and solution parameters of complex ganglioside mixtures extracted and purified from normal adult cerebrum and cerebellum.

In our strategy a particular attention was paid to establishing optimal instrumental conditions on one hand, to testing of different solvent systems adequate for ionization yield increase of major and minor components of native ganglioside mixtures and

reduction of the in-source fragmentation during the ionization process on the other. According to the high performance of the nanoESI-FTICR MS exhibiting high mass accuracy, resolution and sensitivity for both low and high abundant species in complex ganglioside mixtures, this approach could be proposed as a potent new tool in glycolipidomics.

Experimental

Reagents and materials

Methanol and propanol of analytical-grade were purchased from AppliChem (Darmstadt, Germany) and used without further purification. Omega glass capillaries (Hillenberg, Germany) used for nanoESI-FT-ICR MS experiments were pulled *in-house* by a vertical pipette puller model 720, David Kopf Instruments (Tujunga, CA, USA). Prior to analysis, all sample solutions were centrifuged at 7000 rpm for 2h in a Biocentrifuge 5415C (Eppendorf, Hamburg, Germany). All sample solutions were dried in a SpeedVac SPD 111V evaporator (Savant, Düsseldorf, Germany).

Ganglioside sampling

Ganglioside samples investigated in this study were: (a) a crude mixture from normal adult human cerebrum; (b) a crude mixture extracted from the gray matter of the normal adult human cerebellum.

The normal adult human brain (20 years old) without any pathological signs according to morphoanatomical and histopathological examination, originated from a healthy male subject who died in a traffic accident. The brain was obtained from the Department of Forensic Medicine, Faculty of Medicine, University of Zagreb, Croatia. Permission for experiments with human tissue for scientific purposes was obtained from The Ethical Commission of the University of Zagreb, Croatia, under project no. 108120 by the Ministry of Science and Technology of the Republic of Croatia. The cerebrum and cerebellum were carefully separated. Further on, cerebellar gray matter was separated from the white matter by dissection. Samples were weighed and stored at -20 °C until the extraction procedure. The native mixtures of gangliosides were extracted from cerebrum and cerebellum gray matter and purified in our laboratories as described in detail elsewhere [13-19].

Stock solutions of the extracted mixtures were prepared by dissolving the dried lipid material at the concentration of approximately 1 mg/ml in methanol, and were subsequently stored at -20 °C. The stock sample/methanol solutions were dried and dissolved in either methanol:propanol 7:3, v/v, to obtain the working aliquots at the concentration of 5 –15 pmol/μl calculated for an average molecular weight of 1500 g/mol. In this paper gangliosides are abbreviated according to the system of Svennerholm [20] and the recommendations of IUPAC-IUB Commission [21].

Mass Spectrometry

MS experiments were performed on a Bruker Apex II Fourier transform ion cyclotron resonance mass spectrometer (Bruker Daltonik, Bremen, Germany) equipped with a 9.4 T superconducting actively shielded magnet (Magnex Scientific Ltd., Oxford, UK) and an Infinity™ cell.

Gas-phase ions were generated from solution by nanoelectrospray ionization in the negative ion mode using an *Apollo* ion source. In this configuration the sample is introduced into the home-made non-coated glass capillaries in which a stainless steel wire kept at the ground potential is inserted. ESI parameters were optimized to allow an efficient ionization and to reduce the *in-source* fragmentation of molecular ions. The capillary exit voltage was varied within 100 – 380 V to ensure an optimal ion transfer into MS and provide a high ionic yield of the molecules. 150 V was found the optimal value as described below. The electrospray generated ions were accumulated for 1-2 s in the hexapole located after the second skimmer of the ion source and then transferred into the ion cyclotron resonance cell. All mass spectra were acquired in the broad band mode with 512 kpoints/scan and externally calibrated. For the calculation of the theoretical monoisotopic masses of ions, the values for atomic masses of the most abundant isotopes were used. The mass of electron, generating the negative charge, was included.

Results and Discussion

Screening of gangliosides by MS is a challenging task. Our previous studies upon brain GG ionization by (-) nanoESI QTOF MS [13-16] and high capacity ion trap MS [17,18] demonstrated that for efficient ionization and sequencing, elevated capillary and sampling cone voltages are required. These features are attributed to the presence of the less ionizable lipid moiety and lability of the Neu5Ac moiety. Besides, GG solubility in organic solvents or their mixtures with water is restricted, giving rise to formation of layers or micelles, both representing inhomogeneous phases incompatible with formation of a stable spray and an efficient ionization process. For these reasons in order to find an optimal solvent enabling high solubility, full miscibility, stable spray and a minimal level of in-source fragmentation, a number of solvents such as methanol, 1-propanol, 2-propanol, ammonium acetate, chloroform, and water in different combinations, volume ratios, and concentrations were tested. For nanoESI FTICR MS screening of the complex GG mixtures from human cerebrum and cerebellum the best solvent combination meeting all the above-described requirements was found to be methanol:propanol.

To enhance the ion formation from intact molecules and the detection of additional possible species at higher m/z values, as well as to prevent in-source desialylation the capillary exit voltage was set to the moderate value of 150 V. A capillary exit voltage in the range of 150 – 300 V allowed only a poor ionization level and solely signals up to 1200 m/z were detected, which indicates that at elevated values of capillary exit voltages in-source fragmentation of GG species occurs as the dominant process.

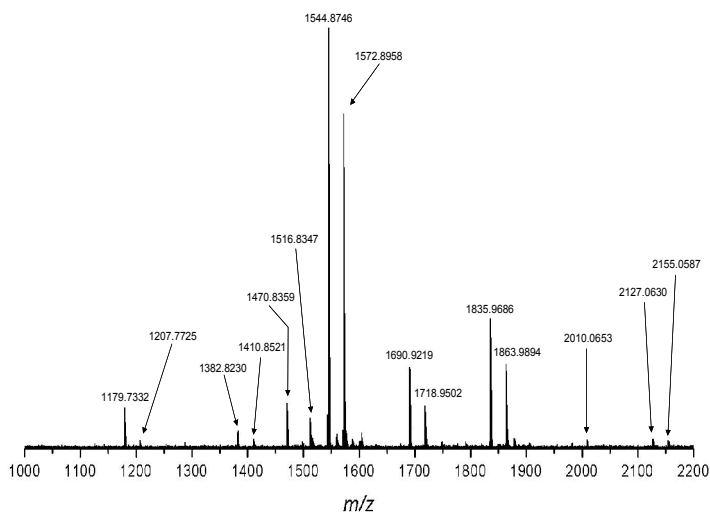


Fig. 1. (-) NanoESI FTICR MS of the native ganglioside mixture from normal adult human cerebrum. Solvent: methanol:propanol (7:3, v/v); ESI: 1100 V; Capillary exit: 150 V; Number of scans: 100

Table 1. Assignment of the major ions detected by (-) nanoESI FTICR MS in the native ganglioside mixture from normal adult cerebrum

m/z		proposed structure [M - H] ⁻
exp.	theor.	
1179.7332	1179.7372	GM3 (d18:1/18:0)
1207.7725	1207.7685	GM3 (d18:1/20:0)
1382.8230	1382.8166	GM2 (d18:1/18:0)
1410.8521	1410.8479	GM2 (d18:1/20:0)
1470.8359	1470.8326	GD3 (d18:1/18:0)
1516.8347	1516.8381	GM1 (d18:1/16:0)
1544.8746	1544.8694	GM1 (d18:1/18:0)
1572.8958	1572.9007	GM1 (d18:1/20:0)
1690.9219	1690.9273	Fuc-GM1 (d18:1/18:0)
1718.9502	1718.9586	Fuc-GM1 (d18:1/20:0)
1835.9686	1835.9648	GD1 (d18:1/18:0)
1863.9894	1863.9961	GD1 (d18:1/20:0)
2010.0653	2010.0540	Fuc-GD1 (d18:1/18:0)
2127.0630	2127.0602	GT1 (d18:1/18:0)
2155.0587	2155.0915	GT1 (d18:1/20:0)

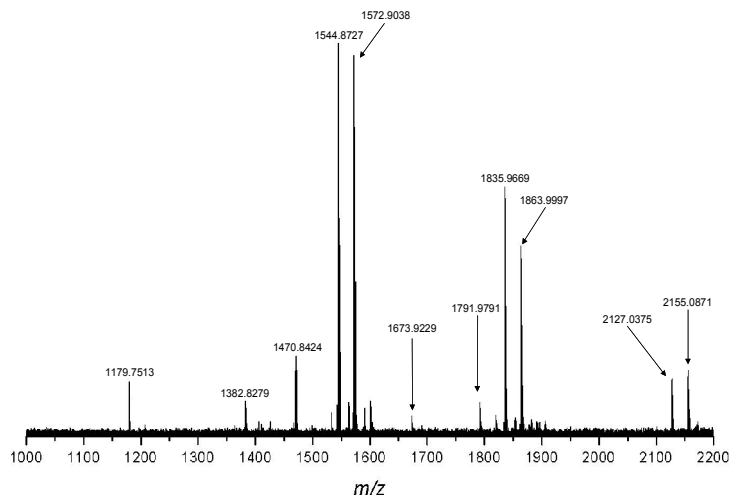


Fig. 2. (-) NanoESI FTICR MS of the native ganglioside mixture from the gray matter of normal adult human cerebellum. Solvent: methanol:propanol (7:3, v/v); ESI: 1100 V; Capillary exit: 150V; Number of scans: 100

Table 2. Assignment of the major ions detected by (-) nanoESI FTICR MS in the native ganglioside mixture from normal adult cerebellum

m/z		proposed structure
exp.	theor.	[M - H]
1179.7513	1179.7372	GM3 (d18:1/18:0)
1382.8279	1382.8166	GM2 (d18:1/18:0)
1470.8424	1470.8326	GD3 (d18:1/18:0)
1544.8727	1544.8694	GM1 (d18:1/18:0)
1572.9038	1572.9007	GM1 (d18:1/20:0)
1673.9229	1673.9120	GD2 (d18:1/18:0)
1835.9669	1835.9648	GD1 (d18:1/18:0)
1863.9997	1863.9961	GD1 (d18:1/20:0)
2127.0375	2127.0602	GT1 (d18:1/18:0)
2155.0587	2155.0915	GT1 (d18:1/20:0)

Figures 1 and 2 depict nanoESI FTICR MS analyses of complex GG mixtures extracted from human cerebrum and cerebellum using methanol:propanol (7:3, v/v) as the solvent and electrospray voltage of 1100 V and capillary exit voltage of 150V as instrumental settings. Each spectrum is a sum of 100 scans acquired over 10 min. As inferable by inspecting the spectra in Figures 1 and 2, employed solvent system and instrument conditions significantly enhanced GG ionization translated into high spray stability, generated a fair ionization level, and allowed ion detection at a substantially increased signal-to-noise ratio.

Assignment to GG structures of singly charged monodeprotonated ions detected in the spectra in Figures 1 and 2 is presented in Tables 1 and 2, respectively. The assignment of molecular ions to a certain GG composition was made on the basis of exact mass calculation under the high accuracy of FTICR MS situated between 5 and 10 ppm, while the postulation of oligosaccharide core structures was based on the previously acquired information [10-15, 17] and GG biosynthesis pathway principles.

15 different species were identified in the GG mixture extracted from human adult cerebrum, while in the spectrum corresponding to cerebellum extract only 10 signals could be assigned to GG glycoforms. As can be seen, both spectra are dominated by GM3, GM2, GM1, GD1 and GT1 species exhibiting the same two ceramide motifs: (d18:1/18:0) and (d18:1/20:0). However, judging after the relative ionic intensity, obviously in cerebellum tissue, GG species of higher sialylation degree such as GD and GT are better expressed. Another interesting aspect is that in cerebrum GG mixture three different *O*-fucosylated species namely Fuc-GM1 (d18:1/18:0), Fuc-GM1 (d18:1/20:0) and Fuc-GD1 (d18:1/18:0) were detected as [M-H]⁻ ions at *m/z* 1690.9219, 1718.9502 and 2010.0653 respectively. These components are not present in the cerebellum mixture, which indicates that GG forms exhibiting peripheral attachments such as *O*-fucosylation are prone to occur rather in cerebral than cerebellar brain region. This feature along with the observation upon GG differential sialylation status in cerebrum vs. cerebellum is of particular biological importance as it demonstrates that GG expression has a distinct regional specificity, which can be used as a marker of regional brain ailments via FTICR MS comparison of normal vs. pathological tissue.

Conclusions

As a part of our systematic studies upon implementation of mass spectrometry in the field of complex carbohydrate analysis, the purpose of this work was to develop a new method for screening of lipid-linked carbohydrates within different structural systems based on (-) nanoESI-FTICR MS at 9.4 T and to find the best suitable conditions in terms of sensitivity, ionization efficiency, resolution and mass accuracy. Instrumental set-up and solubilizing solvent systems parameters were found to play a crucial role for sialylated glycosphingolipid ion formation/detection by FTICR MS experiments. A particularly beneficial attribute of the negative ion nanoESI ionization FTICR MS in comparison with

other MS strategies is the enhancement of the relative sensitivity for the minor versus major components in mixtures which allows detection and identification of novel structures previously not identified by any other analytical methods. This aspect is of particular relevance for characterization of material from biological sources.

NanoESI FTICR MS screening indicated differences in GG expression in human cerebrum vs. cerebellum and consequently provided hard evidence upon the topospecificity of brain ganglioside expression. The newly developed methodology enabled the identification in the two investigated tissues of 16 different glycoforms, with a high degree of heterogeneity in the ceramide motifs and biologically relevant modifications such as *O*-fucosylation. Therefore, we consider FTICR MS a practical approach for large-scale investigations of highly sialylated glycoconjugates of biological origin and applications for diagnostic screening purposes.

Acknowledgements

We thank Prof. Dr. Jasna Peter-Katalinić and Prof. Dr. Franz Hillenkamp, Institute for Medical Physics and Biophysics, University of Münster, Germany for their invaluable help and support. This work was financed by Romanian National Authority for Scientific Research through the grants CE. Ex.111/2006, 98/2006 and PN-II-41001/2007 to ADZ and Croatian Ministry of Science and Technology, project no. 108120 granted to ZV.

References

1. Yu RK, Macala LJ, Taki T, Weinfeld HM and Yu FS (1988) *J Neurochem* 50:1825-1829
2. Yu RK (1994) *Prog Brain Res* 101:31-44
3. Hakomori S (2000) *Glycoconj J* 17L: 627-647
4. Ledeen RW, Wu G (2002) *Neurochem Res* 27:637-647
5. Maccioni HJ (2007) *J Neurochem* 103:81-90
6. Fish RG (1996) *Med Hypotheses* 46:140-144
7. Hakomori S (2001) *Adv Exp Med Biol* 491:369-402
8. Ariga T, McDonald MP, Yu RK (2008) *J Lipid Res* 49:1157-1175
9. Jung WR, Kim HG, Kim KL (2008) *Neurosci Lett* 439:220-225
10. Hakomori S (2002) *Proc Natl Acad Sci USA* 99:10231-10233
11. Hakomori S and Handa K (2002) *FEBS Lett* 531:88-92
12. Lavery SB (2005) *Methods Enzymol* 405:300-369
13. Zamfir AD, Vukelić Z, Bîndilă L, Peter-Katalinić J, Almeida R, Sterling A, Allen M (2004) *J Am Soc Mass Spectrom* 15: 1649-1657
14. Vukelić Z, Kalanj-Bognar S, Froesch M, Bîndilă L, Radić B, Allen M, Peter-Katalinić J, Zamfir AD *Glycobiology* (2007) 17:504-515
15. Zamfir AD, Vukelić Z, Peter-Katalinić J (2002) *Electrophoresis* 23:2894-2903
16. Zamfir AD, Lion N, Vukelić Z, Bîndilă L, Rossier J, Girault HH, Peter-Katalinić J (2005) *Lab Chip* 5: 298-307

17. Zamfir AD, Vukelić Z, Schneider A, Sisu E, Dinca N, Ingendoh A (2007) *J Biomol Tech* 18:188-193
18. Almeida R, Mosoarcă C, Chiriță M, Udrescu V, Dincă N, Vukelić Z, Allen M, Zamfir AD (2008) *Anal Biochem* 378: 43-52
19. Vukelić Z, Zamfir AD, Bîndilă L, Froesch M, Peter-Katalinić J, Usuki S, Yu RK (2005) *J Am Soc Mass Spectrom* 16:571-580
20. Svennerholm L, (1980) *Adv Exp Med Biol* 125: 125–211
21. IUPAC–IUB Joint Commission on Biochemical Nomenclature (1998) *Eur J Biochem* 257: 293–298

PROFILING OF GANGLIOSIDES EXPRESSED IN HUMAN HEMANGIOMA BY FULLY-AUTOMATED CHIP-BASED NANO-ELECTROSPRAY TANDEM MASS SPECTROMETRY

SERB Alina^{1,2}, SCHIOPU Catalin¹, FLANGEA Corina^{1,2}, SISU Eugen², TUDOR Sorin³, PANCAN Ioan Bujor³, VUKELIĆ Željka⁴, ZAMFIR Alina D.^{1,3*}

¹Mass Spectrometry Laboratory, National Institute for Research and Development in Electrochemistry and Condensed Matter, Timisoara, Romania; ²Department of Biochemistry, "Victor Babes" University of Medicine and Pharmacy Timisoara, Romania; ³Department of Chemical and Biological Sciences, "Aurel Vlaicu" University of Arad, Romania; ⁴Department of Chemistry and Biochemistry, University of Zagreb Medical School, Zagreb, Croatia; *Correspondence: alina.zamfir@uav.ro

Abstract

In the present work we carried out a systematic characterization of ganglioside composition in human hemangioma vs. normal brain tissue using our recently developed mass spectrometry (MS) methods, employing nanoelectrospray ionization (nanoESI) high capacity ion trap (HCT) MS and fully automated chip-based nanoESI-HCT MS. The ultra-high ionization efficiency, sensitivity and reproducibility of the experiments uniquely provided by the chip-ESI approach allowed for a reliable MS-based ganglioside comparative assay and enabled detection and structural assignment of 14 distinct hemangioma-associated ganglioside species, a 2.8-times lower total ganglioside content as compared to the age-matched normal brain tissue. These results indicate that the combination of fully automated chipESI with HCT MS is able to provide specific data upon ganglioside profile in human brain tumors, which might be of high value in clinical investigation and for studies related to ganglioside-based therapy of various central nervous system diseases.

Keywords: gangliosides, hemangioma, chip-based electrospray, mass spectrometry, biomarker discovery

Introduction

Hemangioma is a congenital benign tumor or vascular malformation of endothelial cells. Once thought to be strictly congenital, these vascular lesions have been found to occur *de novo* [1-4]. The disease is characterized by grossly dilated blood vessels with a single layer of endothelium and an absence of neuronal tissue within the lesions [5]. These thinly-walled vessels resemble sinusoidal cavities filled with stagnant blood. Cavernous hemangiomas (the most common type of hemangioma in the brain) vary from several millimeters to several centimeters (usually <3 cm) in diameter and commonly resemble raspberries in external structure.

Not all cavernous hemangiomas are associated with symptoms, but once patients become symptomatic, 40-50% present with seizures, 20% present with focal neurologic deficits, and 10-25% present with hemorrhage (cerebral hemorrhage, or hemorrhagic stroke), and even death. Symptoms may progress rapidly or be stable for years as in multiple sclerosis.

The nature and severity of the symptoms depend on the lesion's location in the brain. Cavernous hemangiomas can be found in any part of the brain because they can occur at any location along the vascular bed. Frontal and temporal lobes are the most common sites of occurrence, and approximately 70% of these lesions occur in the supratentorial region of the brain; the remaining 30% occur in the infratentorial region. Cavernous hemangiomas also can occur in the spinal cord, where they frequently coexist with multiple brain lesions.

Diagnosis is most commonly made accidentally by routine magnetic resonance imaging (MRI) screening, though detection is far more likely via a specific imaging technique known as a gradient-echo sequence MRI, which can unmask small or punctate lesions that may otherwise remain undetected [6]. The only practical alternative to these methods is the early detection of hemangioma at a resectable stage, which should be based on routine screening and cancer biomarker discovery before clinical symptoms arise. As known, tumorigenesis/malignant transformation is accompanied by aberrant cell surface composition, particularly due to irregularities in glycoconjugate glycosylation pathways. Various glycosyl epitopes constitute tumor-associated antigens. Some of them promote invasion, while some others suppress tumor progression. Among molecules bearing characteristic glycosyl epitopes causing such effects are: gangliosides, sialic acid containing glycosphingolipids (GSLs) incorporated into outer leaflet of the cell-membrane bilayer and particularly enriched in microdomains [7]. They consist of a hydrophobic ceramide (Cer) moiety and a hydrophilic extracellular oligosaccharide chain which protrudes from the membrane surface. Gangliosides contain one or more sialic acids in the form: *N*-acetylneuraminic acid (Neu5Ac) or *N*-glycolylneuraminic acid (Neu5Gc) or derivatives thereof which are attached to the neutral oligosaccharide moiety by an acetosidic linkage.

Ganglioside expression is particularly enriched in mammalian central nervous system (CNS) [8-10] where the expression is clearly developmentally regulated and also closely related to the differentiation state of the cell [11, 12]. They are implicated in a variety of phenomena involving: cell-cell recognition, cell-substrate interaction, cell adhesion, cell differentiation, transformation, and intracellular signaling [13-17]. Specific changes of gangliosides pattern in brain tumors correlating with tumor histopathological origin, malignancy grade, invasiveness and progression have been also observed [13-14].

In recent years, ganglioside metabolism, biosynthesis, and physiological function have been studied extensively; in the past decade fast atom bombardment (FAB) mass spectrometry (MS) strategies were applied for the first time for human brain ganglioside analysis [18].

Differences in ganglioside composition and quantity in different anatomic regions of the brain have been so far demonstrated by thin layer chromatographic (TLC) as well as

immunochemical and immunohistochemical methods [19-22]. These methods have, however, limited usefulness since they do not adequately detect the total heterogeneity of ganglioside species.

Among all available biophysical and analytical methods, modern and sophisticated mass spectrometric approaches are the most precise and sensitive ones, able to provide detailed information upon ganglioside expression and structure within a short analysis time and with a minimal sample consumption.

To elucidate the structure of ganglioside species involved in particular physiological or pathological processes our group recently implemented novel mass spectrometric methods based on nanoelectrospray ionization (nanoESI) high capacity ion trap (HCT) MS and fully automated chip-based nanoESI-HCT MS. We applied these methods for structural characterization of ganglioside fractions isolated from brain and for detailed compositional mapping of complex native ganglioside mixtures extracted from normal and pathological brain tissue [23, 24].

In the present study a systematic and detailed characterization of ganglioside expression in human brain hemangioma in comparison with ganglioside distribution in an age-matched normal brain tissue was carried out by fully automated chip-based nanoESI-HCT MS method. Comparative screening mass spectra provided hard evidence upon differential expression of gangliosides in the tumour vs. normal tissue which led to the discovery of tumour-specific ganglioside biomarkers.

Experimental

Hemangioma and Normal Brain Tissue Characterization

Brain tumour localized in frontal cortex of right hemisphere in an adult male patient, age 42, was clinically diagnosed using computerized tomography (CT) and magnetic resonance imaging (MRI) (Figure 1).

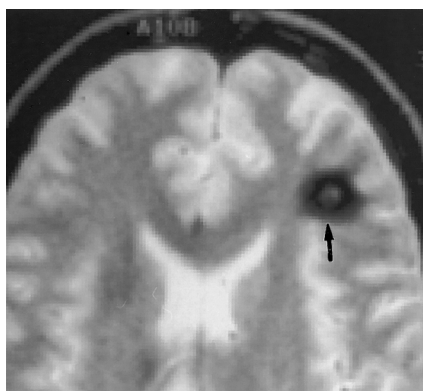


Fig. 1 MRI showing hemangioma localized in frontal cortex of right hemisphere

Brain tumour sample was obtained during surgical procedure. The histopathological diagnosis of cavernous hemangioma was confirmed using Haematoxylin & Eosin stain showing tumor tissue composed of cellular connective tissue and blood spaces with walls varying in thickness, covered with symmetrical endothelium and filled with erythrocytes. The sample of normal frontal cortical brain tissue from an age-matched male subject (deceased in a traffic accident) was dissected to serve as control; the brain was obtained from the Department of Forensic Medicine, Faculty of Medicine, Zagreb, Croatia. Tissue samples used for biochemical analysis were weighed and stored at $-20\text{ }^{\circ}\text{C}$ after careful removal of blood vessels and necrotic elements.

Ganglioside Extraction and Purification

Ganglioside extraction was performed according to the method of Svennerholm and Fredman [25] with some modifications [26]. Tissue sample was weighed and homogenized in ice-cold distilled water as to obtain the 10% homogenate. Lipids were extracted twice using solvent mixture of chloroform: methanol (1:2, by vol.), followed by partition and repartition by adding chloroform, methanol and water to a final volume ratio 1:1:0.8. The combined upper phases, containing gangliosides were collected. The rough ganglioside extract was purified in several steps: precipitation of co-extracted protein-salt complexes followed by centrifugation; low-molecular weight contaminants were removed by gel-filtration on Sephadex G-25 column and dialysis against water (overnight at $4\text{ }^{\circ}\text{C}$). Finally, the pure extract was evaporated to complete desiccation.

Sample Preparation for MS

For chip nanoESI MS analysis, the stock solution of each native ganglioside extract (approximately 0.5 mg/ml) was prepared by dissolving the dried material in pure methanol to be stored at $-27\text{ }^{\circ}\text{C}$. Working aliquots at concentration of approximately $3\text{ pmol}/\mu\text{L}$ (calculated for an average molecular weight of 2000) were obtained by dilution of the stock solution in pure methanol. Methanol was obtained from Merck (Darmstadt, Germany) and used without further purification.

Mass Spectrometry

Mass spectrometry was conducted on a High Capacity Ion Trap Ultra (HCT Ultra, PTM discovery) mass spectrometer from Bruker Daltonics, Bremen, Germany. All mass spectra were acquired in the mass range $100\text{--}3000\text{ }m/z$, with a scan speed of $8000\text{ }m/z$ per second. The m/z scale of the mass spectrum was calibrated by use of an external calibration standard G2421A electrospray "tuning mix," from Agilent Technologies (Santa Rosa, CA, USA). The reference provided in negative ion mode a spectrum with a fair ionic coverage of the m/z range scanned in MS. The obtained mass accuracy was situated within the normal range of an HCT MS instrument.

The assignment of molecular ions to a certain composition was made by exact mass calculation, while the postulation of oligosaccharide core structures and linkages was based on the previously acquired information [27] and ganglioside biosynthesis pathway principles. Ion designation followed the generally accepted nomenclature introduced by Domon, Costello [28] and revised by Costello et al [27].

Automated Chip-Based Nanoelectrospray

Fully automated chip-based nanoelectrospray was performed on a NanoMate robot incorporating ESI 400 Chip technology (Advion BioSciences, Ithaca, USA) controlled and manipulated by ChipSoft 7.1.1 software operating under Windows system. The robot was coupled to the HCT Ultra mass spectrometer via an in-laboratory made mounting system, which allows robot O-xyz positioning with respect to HCT counter electrode as described by us before [23]. 5 μL aliquots of each working sample solution were simultaneously loaded into three different wells of the NanoMate 96-microtiter plate. The robot was programmed to aspirate the whole volume of sample, followed by 2 μL of air into the pipette tip and afterwards deliver the sample to the inlet side of the 400 microchip. NanoMate HCT MS system was tuned for operating in the negative ion mode previously demonstrated [29] as the most appropriate ionization mode for underivatized acidic glycosphingolipids. Electrospray was initiated by applying a voltage of -0.85 kV on the pipette tip, and 0.60 p.s.i. nitrogen back pressure. In order to prevent possible *in-source* fragmentation, HCT capillary exit was set to -30 V. The source block was maintained at the constant temperature of 200^oC. Heating of the source block provided an optimal desolvation of the generated droplets without the need of desolvation gas. Following each infusion and MS analysis, the pipette tip was ejected and a new tip and nozzle were used for each sample, to prevent any cross-contamination or carry-over. Each chip nozzle had an internal diameter of 2.5 μm , which under the given conditions, delivered a working flow rate of approximately 50 nL/min.

The position of the electrospray chip was adjusted with respect to the sampling cone potential to give raise to an optimal transfer of the ionic species into the mass spectrometer.

Results and Discussions

High throughput chip-based nanoESI MS profiling

Purified ganglioside mixtures extracted from normal and hemangioma bearing cortical tissue of the same frontal lobe were submitted to high-throughput negative nanoESI chip MS¹ screening under identical solution and instrumental parameters.

The obtained corresponding mass spectra are presented in Figures 2 and 3 while the comparative ion assignment to ganglioside structures is listed in Tables 2 and 3. The ion assignment and postulation of structures by mass calculation was carried out based on the previously described evidences, knowledge upon this type of substrates [23, 26, 30-34] and biosynthesis pathway criteria.

The robotic chip-based nanoESI system sprayed with a flow rate of 50 nL/min so that for generating each mass spectrum in Fig. 2 and 3 only 3 pmols of ganglioside sample were consumed. General inspection of spectra shows that optimized nanoESI chip HCT MS conditions allowed for the concomitant formation of singly, doubly and triply charged ions, enhanced the ionization of long chain polysialylated GT and GQ structures, provided a fair ionization/detection of minor components and prevented the *in-source* fragmentation of labile carbohydrate or non-carbohydrate type of modifications. As visible, even under

the time-restrictive high-throughput conditions a remarkably rich molecular ion pattern, proving the presence of a large number of glycoforms and an unpredicted diversity of the ceramide chain for certain species in normal frontal cortex was observed. Moreover, the presence of 10 biologically relevant species modified by *O*-fucosylation, *O*-acetylation and GalNAc attachment could be postulated. The ceramide portion was found to contain predominantly C18:1- and C18:0-long-chain bases in both normal and tumoral tissue.

Comparative assessment of ganglioside profile in normal frontal cortex vs. hemangioma frontal cortex

Under identical solution and instrumental conditions nanoESI chip HCT MS analysis revealed a significant difference in ganglioside structural and quantitative expression in normal tissue vs. hemangioma. Thus, 40 different ganglioside species were identified in normal frontal cortex (NFC) and only 14 in hemangioma frontal cortex (HFC).

Besides this dramatic difference in the number of detected species, the abundance of the ions corresponding to mono-polysialylated GM, GD, GT, and GQ components as well as asialo species appears completely different in the two tissues.

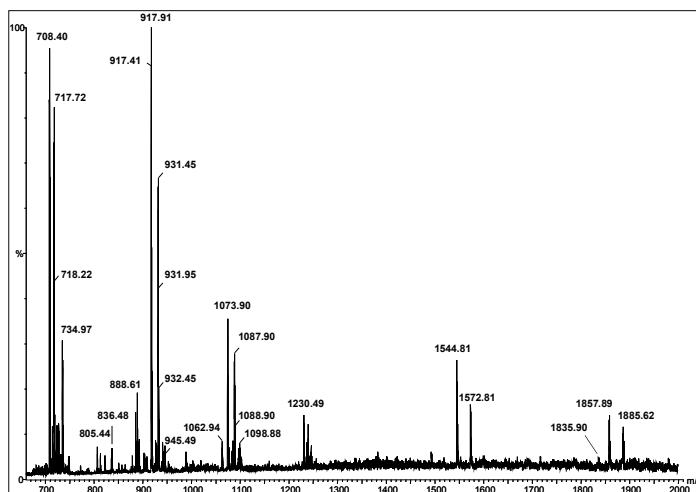


Fig.2 Fully automated (-) nanoESI chip HCT MS¹ of the native ganglioside mixture extracted from normal frontal cortical tissue. Solvent: MeOH; sample concentration 3 pmol/ μ L; acquisition time 2 min; Chip ESI: -0.85 kV; capillary exit: -30 V.

While NFC tissue expressed a high diversity of ganglioside structures, from short, monosialylated (GM) to large, polysialylated carbohydrate chains (GQ) and also ganglioside chains modified by Fuc, *O*-Ac and GalNAc peripheral attachments, ganglioside mixtures extracted from hemangioma tissue (HFC) are essentially dominated by species exhibiting short oligosaccharide chains with reduced sialic acid content. Thus, 12 from a total of 14 structures identified in hemangioma tissue are monosialotetraoses, GM1, GM2, GM3 and GM4, bearing ceramides of variable constitution. Additionally, one trisialo-GT1 (d18:1/18:0) detected as $[M-2H]^{2-}$ at m/z 1079.21, one asialo-GA2 with two possible ceramide configurations (d18:1/22:2) or (d18:0/22:3), detected as $[M-H]^{-}$ at m/z 1306.03 and two fucosylated GM2 (d18:0/21:0) and (d18:1/27:2) detected as $[M-H]^{-}$ at m/z 1555.98, respectively 1634.04, were also identified. These species are minor ganglioside components either low expressed or even absent in the normal human brain tissues. Their presence in hemangioma tissue is in correlation with dedifferentiation processes occurring in tumor cells vs. untransformed normal cells and constitutes a marker of aberrant tissue development arising in hemangioma.

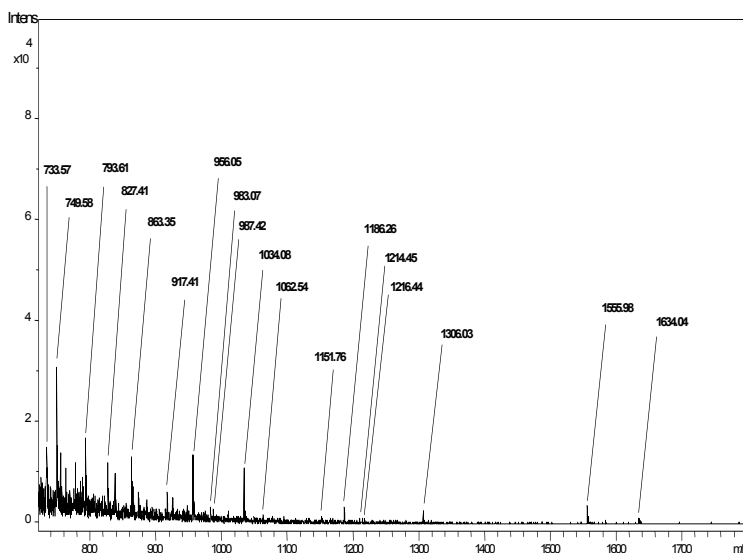


Fig. 3 Fully automated (-) nanoESI chip HCT MS¹ of the native ganglioside mixture extracted from frontal lobe hemangioma tissue. Solvent: MeOH; sample concentration 3 pmol/ μ L; acquisition time 2 min; Chip ESI: -0.85 kV; capillary exit: -30 V.

Table 1. Assignment of the molecular ions detected in the native ganglioside mixtures extracted from normal adult HFC

Type of Molecular Ion	<i>m/z</i> (monoisotopic)	Assigned structure
[M+2Na-4H] ²⁻ [M-H] ⁻	611.40 1179.70	GM3 (d18:1/18:0)
[M-H] ⁻	1382.68	GM2 (d18:1/18:0)
[M-2H] ²⁻ [M+Na-2H] ⁻	734.96 1492.78	GD3 (d18:1/18:0)
[M-2H] ²⁻ [M-H] ⁻	748.97 1518.51	GD3 (d18:1/20:0) GM1, nLM1 and /or LM1 (d18:0/16:0)
[M-2H] ²⁻ [M-H] ⁻	771.98 1544.80	GM1, nLM1 and /or LM1 (d18:1/18:0)
[M-2H] ²⁻ [M-H] ⁻	786.00 1572.80	GM1, nLM1 and /or LM1 (d18:1/20:0)
[M-2H] ²⁻	836.46	GD2 (d18:1/18:0)
[M-2H] ²⁻	850.47	GD2 (d18:1/20:0)
[M-2H] ²⁻ [M+Na-3H] ²⁻ [M-H] ⁻ [M+Na-2H] ⁻	917.44 928.45 1835.92 1858.00	GD1, nLD1 and /or LD1 (d18:1/18:0)
[M-2H] ²⁻	926.44	GD1, nLD1 and /or LD1 (t18:0/18:0)
[M-2H] ²⁻	924.44	GD1, nLD1 and /or LD1 (d18:1/19:0)
[M-2H] ²⁻ [M+Na-3H] ²⁻ [M-H] ⁻	931.46 942.44 1885.60	GD1, nLD1 and /or LD1 (d18:1/20:0)
[M-2H] ²⁻	940.49	GD1, nLD1 and /or LD1 (t18:0/20:0)
[M-2H] ²⁻	938.44	GD1, nLD1 and /or LD1 (d18:1/21:0)
[M-2H] ²⁻	945.47	GD1, nLD1 and /or LD1 (d18:1/22:0)
[M-2H] ²⁻	954.46	GD1, nLD1 and /or LD1 (t18:0/22:0)
[M-2H] ²⁻	952.47	GD1, nLD1 and /or LD1 (d18:1/23:0)
[M-2H] ²⁻	958.46*	GD1, nLD1 and /or LD1 (d18:1/24:1)

[M-2H] ²⁻	966.46	GD1, nLD1 and /or LD1 (d18:1/25:0) or (d20:1/23:0)
[M-2H] ²⁻	988.40	Fuc-GD1 (d18:1/18:2)
[M-2H] ²⁻	990.40	Fuc-GD1 (d18:1/18:0)
[M-2H] ²⁻	999.48*	Fuc-GD1 (t18:0/18:0)
[M-2H] ²⁻	1002.48	Fuc-GD1 (d18:1/20:2)
[M-2H] ²⁻	1004.49	Fuc-GD1 (d18:1/20:0)
[M-2H] ²⁻	1013.49*	Fuc-GD1 (t18:0/20:0)
[M-2H] ²⁻	1018.99	GalNAc-GD1 (d18:1/18:0)
[M-2H] ²⁻	1032.93*	GalNAc-GD1 (d18:1/20:0)
[M-3H] ³⁻	708.39	GT1 (d18:1/18:0)
[M-2H] ²⁻	1062.96	
[M+Na-3H] ²⁻	1073.92	
[M+2Na-4H] ²⁻	1084.93	
[M-3H] ³⁻	714.41	GT1 (t18:0/18:0)
[M+Na-3H] ²⁻	1082.92	
[M-3H] ³⁻	717.75	GT1 (d18:1/20:0)
[M-2H] ²⁻	1076.97	
[M+Na-3H] ²⁻	1087.95	
[M+2Na-4H] ²⁻	1098.92	
[M-3H] ³⁻	723.75	GT1 (t18:0/20:0)
[M+Na-3H] ²⁻	1096.93	
[M+Na-3H] ²⁻	1094.95*	GT1 (d18:1/21:0)
[M-3H] ³⁻	727.08	GT1 (d18:1/22:0)
[M+Na-3H] ²⁻	1101.92	
[M+Na-3H] ²⁻	1108.92*	GT1 (d18:1/23:0)
[M+Na-3H] ²⁻	1114.96	GT1 (d18:1/24:1)
[M-3H] ³⁻	722.39	O-Ac-GT1 (d18:1/18:0)
[M-3H] ³⁻	731.74	O-Ac-GT1 (d18:1/20:0)
[M-3H] ³⁻	805.40	GQ1 (d18:1/18:0)
[M+Na-4H] ³⁻	812.73	
[M+2Na-4H] ²⁻	1230.50	
[M+3Na-5H] ²⁻	1241.48	
[M-3H] ³⁻	814.74	GQ1 (d18:1/20:0)
[M+Na-4H] ³⁻	822.07	
[M+2Na-4H] ²⁻	1244.49	

d = dihydroxy sphingoid base; t = trihydroxy sphingoid base; * low intensity ions

Table 2. Assignment of the molecular ions detected in the native ganglioside mixtures extracted from hemangioma tissue extracted from HFC

Type of Molecular Ion	<i>m/z</i> (monoisotopic)	Assigned structure
[M-2H] ²⁻	733.57	GM2(d18:1/24:0) or GM2(d18:0/24:1)
[M-H] ⁻	983.07	GM4 (d18:1/16:4)
[M-H] ⁻	987.42	GM4 (d18:1/16:0) or GM4 (d18:0/16:1)
[M-H] ⁻	1034.08	GM4 (d18:0/19:0)
[M-H] ⁻	1062.54	GM4 (d18:0/21:0)
[M-2H] ²⁻	1079.21	GT1 (d18:0/20:0)
[M-H] ⁻	1151.76	GM3 (d18:0/16:1) or GM3 (d18:1/16:0)
[M-H] ⁻	1186.26	GM3 (d18:1/19:4)
[M+Cl-2H] ⁻	1214.45	GM3 (d18:0/18:1)
[M-H] ⁻	1216.44	GM3 (d18:1/21:3) or GM3 (d18:0/21:4)
[M-H] ⁻	1306.03	GA2 (d18:1/22:2) or GA2 (d18:0/22:3)
[M-H] ⁻	1555.98	Fuc-GM2 (d18:0/21:0)
[M-H] ⁻	1634.04	Fuc-GM2 (d18:1/27:2)
[M-H] ⁻	1634.94	GM1 (d18:1/27:2)

d = dihydroxy sphingoid base

Conclusions

Our present study is illustrating the performance of chip-based nanoESI HCT MS for the identification of human brain hemangioma-associated gangliosides. According to our knowledge this is the first systematic study of gangliosides in a histopathologically-defined hemangioma brain tumor and, certainly, the first utilizing the most advanced mass spectrometric methods available nowadays.

The ganglioside composition of hemangioma was found to be highly altered in comparison to the ganglioside expression in normal human brain (14 different ganglioside species in HFC vs. 40 in NFC). While in HFC short, monosialylated ganglioside components are predominant, in NFC mono- and polysialylated gangliosides as well as fucosylated and *O*-acetylated components could be identified; however the most abundant ion corresponds to GD1 (d18:1/18:0) detected as [M-2H]²⁻ at *m/z* 917.31.

We suppose that the marked reduction in the total ganglioside content (2.8x fold) and the altered pattern in hemangioma vs. healthy control tissue are the result of a lower overall biosynthetic rate, due to the change in expression of certain glycosyltransferases. Further

studies on glycosyltransferase expression are necessary to correlate their expression with our present MS screening results.

The obtained data indicate the benefits of ultra-sensitive mass spectrometric methods in determining an altered composition of brain hemangioma gangliosides as well as in discovery of new structures in various types of tumors in order to provide specific biochemical markers potentially useful in diagnosis, prognosis and therapy of benign and malignant brain proliferations.

Acknowledgements

This work was supported by Romanian National Authority for Scientific Research through the PN-II-41001/2007 project. Permission for experiments with human tissue for scientific purposes was obtained from the Ethical Commission of "Victor Babes" University of Medicine and Pharmacy Timisoara and Zagreb Medical School, under the Project no. 108120 granted by the Croatian Ministry of Science and Technology.

References

- [1] Siegel AM. Familial cavernous angioma: an unknown, known disease. *Acta Neurol Scand.* 98 (1998) 369-371
- [2] Pozzati E, Acciarri N, Tognetti F, Marliani F, Giangaspero F. Growth, subsequent bleeding, and de novo appearance of cerebral cavernous angiomas. *Neurosurgery.* 38 (1996) 662-670
- [3] Houtteville JP. Brain cavernoma: a dynamic lesion. *Surg Neurol.* 48 (1997) 610-614
- [4] Detweiler PW, Porter RW, Zabramski JM, Spetzler RF. De novo formation of a central nervous system cavernous malformation: implications for predicting risk of hemorrhage: case report and review of the literature. *J Neurosurg.* 87 (1997) 629-632
- [5] Martin NA, Wilson CB, Stein BM. Venous and cavernous malformations. In: Wilson CB, Stein MB, eds. *Intracranial Arteriovenous Malformations.* Baltimore, Md: Williams & Wilkins. (1984) 234-245
- [6] Lehnhardt FG, von Smekal U, Rückriem B, Stenzel W, Neveling M, Heiss WD, Jacobs AH. Value of Gradient-Echo Magnetic Resonance Imaging in the Diagnosis of Familial Cerebral Cavernous Malformation. *Arch Neurol.* 62 (2005) 653-658
- [7] LEDEEN RW, YU RK. GANGLIOSIDES: STRUCTURE, ISOLATION, AND ANALYSIS. *METHODS ENZYMOL.* 83 (1982) 139-191
- [8] Fishman PH and Brady RO. Biosynthesis and function of gangliosides. *Science.* 194 (1976) 906-915
- [9] Ledeen RW. Ganglioside structures and distribution: Are they localized at the nerve ending? *J. Supramol. Struct.* 8 (1978) 1-17
- [10] LEDEEN RW, YU RK. GANGLIOSIDES: STRUCTURE, ISOLATION, AND ANALYSIS. *METHODS ENZYMOL.* 83 (1982) 109-191
- [11] Yu RK, Macala LJ, Taki T, Weinfeld HM and Yu FS. Developmental changes in ganglioside composition and synthesis in embryonic rat brain. *J. Neurochem.* 50 (1988) 1825-1829

- [12] Yu RK. Developmental regulation of ganglioside metabolism. *Prog. Brain Res.* 101 (1994) 31–44
- [13] Hakomori S. Traveling for the glycosphingolipid path. *Glycoconj. J.* 17 (2000) 627–647
- [14] Ledeen RW, Wu G. Ganglioside functions in calcium homeostasis and signaling. *Neurochem. Res.* 27 (2002) 637–647
- [15] Ziche M, Alessandri G and Gullino PM. Gangliosides promote the angiogenic response. *Lab. Invest.* 61(1989) 629-634
- [16] ALESSANDRI G, KAJU KS AND GULLINO PM. INTERACTION OF GANGLIOSIDES WITH FIBRONECTIN IN THE MOBILIZATION OF CAPILLARY ENDOTHELIUM. POSSIBLE INFLUENCE ON THE GROWTH OF METASTASIS. *INV. METAST.* 6 (1986) 145-165
- [17] ALSSANDRI G, ILE CRISTAN G, ZICHE M, CAPP APM AND GULLINO PM. GROWTH AND MOTILITY OF MICROVASCULAR ENDOTHELIUM ARE MODULATED BY THE RELATIVE CONCENTRATION OF GANGLIOSIDES IN THE MEDIUM. *J. CELL. PHYSIOL.* 151 (1992) 23-28
- [18] Peter-Katalinić J and Egge H. Desorption mass spectrometry of glycosphingolipids. *Methods Enzymol.* 193 (1990) 713-733
- [19] Tai T, Kawashima I, Ozawa H, Kotani M, Ogura K. Cell type-specific expression of ganglioside antigens in the central nervous system. *Pure and Appl. Chem.* 69 (1997) 1903-1910
- [20] Kracun I, Rosner H, Drnovsek V, Heffer-Lauc M, Cosovic C, Lauc G. Human brain gangliosides in development, aging, and disease. *Int J Dev Biol.* 35 (1991) 289–295
- [21] Schnaar RL, Needham LK. Thin-layer chromatography of glycosphingolipids. *Methods Enzymol.* 230 (1994) 371-389
- [22] Muthing J. High-resolution thin-layer chromatography of gangliosides. *J. Chromatogr. A.* 720 (1996) 3-25
- [23] Almeida R, Mosoarca C, Chirita M, Udrescu V, Dinca N, Vukelić Z, Allen M, Zamfir AD. Coupling of fully automated chip-based electrospray ionization to high-capacity ion trap mass spectrometer for ganglioside analysis. *Anal. Biochem.* 378 (2008) 43-52
- [24] Serb A, Schiopu C, Flangea C, Vukelić Ž, Sisu E, Dinca N, Zagrean L and Zamfir AD. High-throughput analysis of gangliosides in defined regions of fetal brain by fully automated chip-based nanoelectrospray ionization multistage mass spectrometry. *J. Chromatogr. B.* (2008), in press
- [25] Svennerholm L and Fredman P. *Biochim. Biophys. Acta* 617 (1980) 97-109
- [26] Vukelić Ž, Metelmann W, Müthing J, Kos M and Peter-Katalinić J. *Biol. Chem.* 382 (2001) 259-274
- [27] Costello CE, Juhasz P, Perreault H. *Progr. Brain Res.* 101 (1994) 45-61
- [28] Domon B, Costello CE. *Glycoconjugate J.* 5 (1988) 397-409
- [29] Abad-Rodriguez J, Robotti A. *J. Neurochem.* 103 (2007) 47-55
- [30] Vukelić Z, Zamfir AD, Bindila L, Froesch M, Peter-Katalinić J, Usuki S, Yu RK. *J. Am. Soc. Mass Spectrom.* 16 (2005) 571-580

- [31] Zamfir AD, Vukelić Z, Schneider A, Sisu E, Dinca N, Ingendoh A. *J. Biomol. Tech.* 18 (2007) 188-193
- [32] Zamfir AD, *J. Chromatogr. A* 1159 (2007) 2–13
- [33] Zamfir AD, Vukelic Z, Bindila L, Peter-Katalinić J, Almeida R, Sterling A, Allen M, *J. Am. Soc. Mass Spectrom.* 15 (2004) 1649-1657
- [34] Zamfir AD, Lion N, Vukelić Z, Bindila L, Rossier J, Girault HH, Peter-Katalinić J, *Lab Chip* 5 (2005) 298-307

DETECTION OF A REACTIVE DYE USING A LACCASE MODIFIED BIOSENSOR

MUNTEANU Florentina-Daniela¹, CAVACO-PAULO Artur²

¹Department of Chemical and Biological Sciences, "Aurel Vlaicu" University of Arad, Elena Dragoi St, 2, 310330 Arad, Romania Phone: +40257219242, Fax: +40257219331, E-Mail: florentina.munteanu@uav.ro, <http://www.uav.ro>

²University of Minho, Department of Textile Engineering, 4800-058 Guimarães, Portugal

Abstract

In this paper the use of a laccase modified biosensor for detection of reactive dyes is presented.

The results obtained using a laccase biosensor for detection of a reactive dye, bezaktiv red S-3B, are presented and based on the calculated sensitivity in terms of $I_{\max}/K_m^{\text{app}}$ ratio it can be concluded that is possible to use a laccase biosensor for detection of reactive dyes that are used in textile industry.

Keywords: textile dye, laccase, electrochemistry, amperometric biosensor

Introduction

The textile effluents, usually highly colored, when discharged in open waters present an obvious aesthetic problem. Moreover, the dyes without an appropriate treatment can persist in the environment for extensive periods of time and are deleterious not only for the photosynthetic processes of the aquatic plants but also for all the living organisms since the degradation of these can lead to carcinogenic substances [1, 2]. The European community has not been indifferent to this problem and in September 2003 the European directive 2002/61/EC came into force. This directive forbids the use of some products, derivatives of a restricted number of dyes. However, these restriction measures are not enough to solve the problems due to the huge amount of dyes discharged in the environment every year.

Many studies on the biological degradation of dyes are focused on the identification and characterization of the enzymes that can degrade them [3-6]. One of these enzymes, laccase, was chosen for studying in detail the processes of oxidative degradation of dyes, keeping in mind the effluent recycling processes.

Laccase is an oxidoreductive ligninolytic enzyme used in various biotechnological and environmental applications. In the last years its capacity to degrade synthetic dyes has been extensively studied [7]. In comparison to other oxidoreductases, as for example the peroxidases that need H_2O_2 in its catalytic process, laccase only uses oxygen for the oxidation of its reduced state [8].

In this work are presented the results obtained using a laccase modified biosensor for determination of bezaktiv red S-3B.

Materials and methods

The salts were purchased from Sigma, St. Louis, MO. All chemicals were of high purity and used as received.

Laccase (EC 1.10.3.2) from *Trametes villosa* (5.3 mg protein/mL, 600 U/mL) was kindly provided by Novo Nordisk, Denmark.

Electrode preparation

The laccase modified electrodes were prepared using rods of solid spectroscopic graphite (SGL Carbon, Werke Ringsdorff, Bonn, Germany, type RW001, 3.05 mm diameter). The graphite rods were first polished on wet fine-structured emery paper (grit size: P1200) and then additionally polished on paper to obtain a mirror-like surface. The electrode rods were carefully rinsed with deionized water and allowed to dry at room temperature. A 5 μ l aliquot of the enzyme solution was added to each of the polished ends of the graphite rods and the electrodes were then placed at 4°C for 1 h in a glass beaker covered with sealing film, to allow the enzyme to adsorb slowly preventing rapid evaporation of the droplet of enzyme solution. The enzyme electrodes were then thoroughly rinsed with 0.1 M sodium citrate buffer, pH 5.0, and if not immediately used, they were stored in the same buffer at 4°C. Weakly adsorbed laccase was desorbed before measurements, by rotating the electrode in buffer for at least 30 min.

All the electrochemical experiments were performed using a Voltalab 30 Potentiostat (Radiometer Analytical, France), controlled by the Voltmaster 4 (version 5.6) electrochemical software. The working, counter and reference electrodes were respectively: glassy carbon electrode or the modified graphite electrode (0.07 cm²), coiled platinum wire (23 cm) and an Ag|AgCl electrode filled with a saturated solution of KCl (BAS, Bioanalytical Systems, West Lafayette, IN, USA). The supporting electrolyte used in the electrochemical cell was a solution of 0.1 M sodium-acetate buffer pH 5.0. All experiments were performed in bulk using amperometric detection (each experiment was repeated 5 times). The applied potential was -50 mV vs. Ag|AgCl. The experiments were performed using a laccase modified graphite electrode.

Results and discussion

The blue copper phenol oxidases, also known as laccases, represent one enzyme activity implicated in lignin degradation [9]. Laccase benzenediol: oxygen oxidoreductases, EC 1.10.3.2) catalyzes the oxidation of ortho- and paradiphenols, aminophenols, aryl diamines, polyphenols, polyamines, and lignin, as well as some inorganic ions coupled to the reduction of molecular dioxygen to water.

Laccase shows broad specificity in the process of oxidizing many compounds (mainly of phenolic type) and can be exploited for the oxidation/biodegradation of a number of aquatic and terrestrial xenobiotics, industrial wastewaters, as well as for biotechnological treatment of industrial products.

Laccase catalyzes the oxidation of organic substrates such as phenolic compounds by molecular oxygen in homogeneous solutions. When laccase is adsorbed on graphite,

bioelectrocatalytic reduction of oxygen occurs and is observed as a reduction current caused by direct (mediatorless) electron transfer (DET) from the electrode to the immobilized laccase and then further to molecular oxygen in solution. In the presence of soluble electron donors, laccase can be reduced in a mediated electron transfer (MET) mechanism (see Figure 1). In this mechanism the electron donor (substrate) penetrates the active site of the enzyme where it is oxidized in a single electron oxidation step often producing an electrochemically active compound (possibly a radical) that in turn can be re-reduced at the electrode surface in a mediated electron transfer (MET) step.

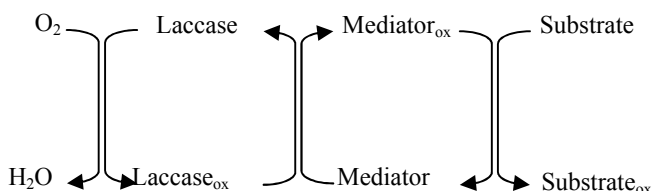


Fig. 1. Role of the mediator in the enzymatic activity

Initial experiment (applied potential -50mV versus Ag|AgCl) showed that these electrodes have low noise/background current while upon the injection of the solution of the dyes they generate a reduction current. Such a response is relatively well understood and it is usually ascribed to electrochemical reduction of laccase oxidation products [10].

The responses are dependent on the concentration of the dye in the solution of interest. At higher dye concentrations the current-concentration dependence gradually reached saturation (Figure 2). The apparent Michaelis–Menten constants (K_m^{app}) and maximal currents (I_{max}) have been calculated by fitting the variation of current–concentration dependencies of the analyzed compounds to the electrochemical Michaelis–Menten equation [11]. K_m^{app} is an indicator of the affinity that an enzyme has for a given substrate, and hence the stability of the enzyme-substrate complex.

$$I = \frac{I_{max} [S]}{[S] + K_M^{app}} \quad (1)$$

where S is the substrate concentration, I_{max} the maximum current and K_m^{app} the apparent Michaelis–Menten constant.

The calculated value of K_m^{app} (calculated from the equation (1)) and the catalytic efficiency are presented in Table 1.

The kinetics of laccase catalyzed reactions is firstly affected by the affinity between enzyme and the substrate. An estimation of this influence can be done by amperometric measurements in terms of I_{max}/K_m^{app} ratio. These parameters are often calculated in the design of enzymatic sensors to evaluate the sensitivity of the system proposed, which is related to the low or high affinity of the enzyme towards a specific substrate.

The results obtained using the laccase biosensor for detection of bezaktiv red S-3B are presented in Table 1 and are compared with the results obtained in [12].

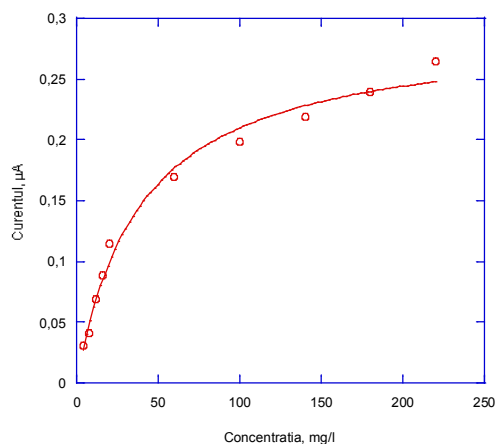


Fig. 2. Calibration graph for bezaktiv red S-3B obtained with a laccase modified graphite electrode in 0.1 M citrate buffer pH 5.0, at -50mV vs. Ag|AgCl electrode

Table 1 Results obtained using the laccase biosensor

	I_{max} (µA)	K_m^{app} (µM)	I_{max}/K_m^{app} (µA *µM ⁻¹)
Bezaktiv red S-3B	0.592±0.001	39.060±0.052	0.015±0.002
Methyl Orange*	0.793±0.002	31.497±0.075	0.025±0.003

* from reference [12]

As it can be observed from Table 1 the values obtained using the biosensor for determination of bezaktiv red S-3B are similar to the values obtained with the same type of biosensor for detection of Methyl Orange.

In terms of sensitivity the results presented in here are not much different from the one obtained with a laccase biosensor for detection of catechol (0,036 µA *µM⁻¹) in the absence of a mediator.

The reason of not using a mediator for this system is that the aim for which this kind of biosensor was tested is to be used in field. In this situations addition of another chemical to the tested effluent will further contribute to the environmental pollution.

Conclusions

This paper demonstrates that a laccase modified biosensor is appropriate for detection of a reactive dye. Moreover, the results are comparable to those obtained for detection of methyl orange. It can be concluded that laccase biosensor can be used for determination of reactive dyes that can be present in textile effluents.

Acknowledgments

This paper is part of the project CEEEX 77/2006 "Computerized filtration and separation systems activated by ultrasounds and controlled by biosensors for textile processes-FILTISOFTUS" and was supported by "Romanian Authority for Scientific Research/MATNANTECH".

References

- [1] Pinheiro H. M., Touraud E., and Thomas O., Aromatic amines from azo dye reduction: status review with emphasis on direct UV spectrophotometric detection in textile industry wastewaters, *Dyes and Pigments*, vol. 61, 2004, pp. 121-139.
- [2] Hao O. J., Kim H., and Chiang P. C., Decolorization of wastewater, *Crit. Rev. Env. Sci.*, vol. 30, 2000, pp. 449-505.
- [3] Abadulla E., Tzanov T., Costa S., Robra K. H., Cavaco-Paulo A., and Gübitz G. M., Decolourisation and detoxification of textile dyes with laccase from *Trametes hirsuta*, *Appl. Environ. Microbiol.*, vol. 66, 2000, pp. 3357-3362.
- [4] Blümel S. and Stolz A., Cloning and characterization of the gene coding for the aerobic azoreductase from *Pigmentiphaga kullae* K24, *Appl. Microbiol. Biotechnol.*, vol. 62, 2003, pp. 186-190.
- [5] Nyanhongo G. S., Gomes J., Gubitza G. M., Zvauya R., Read J., and Steiner W., Decolorization of textile dyes by laccases from a newly isolated strain of *Trametes modesta*, *Water Research*, vol. 36, 2002, pp. 1449-1456.
- [6] Nyanhongo G. S., Gomes J., Gübitz G. M., Zvauya R., Read J. S., and Steiner W., Production of laccase by a newly isolated strain of *Trametes modesta*, *Bioresource Technology*, vol. 84, 2002, pp. 259-263.
- [7] Mayer A. M. and Staples R. C., Laccase: new functions for an old enzyme, *Phytochemistry*, vol. 60, 2002, pp. 551-565.
- [8] Spadaro J. T. and Renganathan V., Peroxidase-Catalyzed Oxidation of Azo Dyes: Mechanism of Disperse Yellow 3 Degradation., *Arch. Biochem. Biophys.*, vol. 312, 1994, pp. 301-307.
- [9] Thurston C. F., *Microbiology*, vol. 140, 1994, pp. 19.
- [10] Haghighi B., Gorton L., Ruzgas T., and Jonsson L. J., Characterization of graphite electrodes modified with laccase from *Trametes versicolor* and their use for bioelectrochemical monitoring of phenolic compounds in flow injection analysis, *Analytica Chimica Acta*, vol. 487, 2003, pp. 3-14.
- [11] Shu R. and Wilson G. S., Rotating ring-disk enzyme electrode for surface catalysis studies, *Anal. Chem.*, vol. 48, 1976, pp. 1679-1686.

- [12] Zille A., Munteanu F. D., Gübitz G. M., and Cavaco-Paulo A., Laccase Kinetics of Degradation and Coupling Reactions, *Journal of Molecular Catalysis:B*, vol. 33, 2005, pp. 23-28.

REACTION KINETICS OF THERMALLY STABLE CONTACT METALLIZATION ON 6H-SiC

VOICAN Cristiana¹, STANESCU Constantin D.²

¹Electronics Technical College, e-mail: voicancristiana@yahoo.com

²University Politehnica of Bucharest, e-mail: voicancristiana@yahoo.com
e-mail: prof_cstanescu@yahoo.com

Abstract

The growth kinetics of thermally stable Ti(100nm)/TaSi₂ (200nm)/Pt (300nm) metallization on 6H-SiC was studied after heat treatment in air up to 700⁰ C. Scanning electron microscopy (SEM) of the contact surface morphology reveals a two-dimensional network of features that is attributed to non-uniform oxide growth associated with the multigrain structure of the platinum overlayer. Auger electron spectroscopy (AES) and high-resolution transmission electron microscopy (HRTEM) identified three important reaction zones after initial 30-minute anneal at 600⁰ C in nitrogen. One is the formation of a platinum silicide overlayer resulting from TaSi₂ decomposition. The second is titanium silicide formation adjacent to the decomposed TaSi₂.

Keywords: Kinetics, metallization, SEM

Introduction

There is a growing interest in the use of silicon carbide (SiC) as the wide bandgap (WBG) semiconductor of choice for electronics and sensors in high power and harsh environments. However, unresolved reliability issues, prominent among which is stable contact metallization, temper this growing interest in SiC. Thermal stability of electrical contacts is a fundamental requirement for reliable electronics and sensing devices operating in harsh environments. Aggressive packaging methodologies have been adopted that provide hermetic sealing against contact oxidation, but these suffer from the drawbacks of added complexity, cost, and new reliability issues. Also, in the course of testing SiC devices, the need to expand the research effort beyond the traditionally focused investigation of the immediate metal/SiC interface has become evident. The traditional approach will not guarantee long term contact stability because it ignores broader failure mechanisms that exist elsewhere.

Principal elements

6H-SiC, off-axis (3.5⁰) and (0001)-oriented, high resistivity p-type substrates with 0.5 μm thick type epilayer (Nd-Na = 2x10¹⁹cm⁻³) were purchased from Cree Research [1]. The wafers were inspected as received and surface features were mapped using a high-resolution Nomarski optical microscope. The samples were initially cleaned in 50:50 H₂SO₄ : H₂O₂ solution for 15 minutes, followed by a De-Ionized (DI)-water rinse. Dry

oxidation followed at 1150⁰C in 2 sccm of ULSI grade oxygen for three hours. The samples were then dipped in 49%HF to strip the oxide. Dry etching in NF₃ and argon was used to etch mesa strips in the n-type epilayer, thereby creating an n-p junction in a four-point probe configuration. A second 5-hour dry oxidation and oxide via etching was followed by metal deposition and patterned etching. A more detailed description of this process can be found elsewhere [2].

Results and Discussion

Accurate prediction of the dominant reaction mechanisms in a multilayer metallization system is generally an arduous task. Therefore, we identified surface oxidation of the platinum silicide and titanium silicide formation at the SiC interface zone as the two most critical reaction mechanisms for long-term electrical and mechanical stability of the contact. The theoretical analysis relied on the growth kinetics developed [3] for silicon oxidation [4] and for silicide formation.. The cross section HRTEM of the as-deposited sample is shown in Figs. 1(a-c). Figures 1a and c are magnified sections of Fig. 1b that highlight interface zones of Ti/SiC and Pt/TaSi₂, respectively. Measured lattice parameters confirmed epitaxial titanium ($a=0.295\text{ nm}$, $c=0.468\text{ nm}$) during sputter deposition as shown in Fig. 1a. In Fig. 1b, the platinum layer has columnar structures with a section magnified and shown in Figure 1c to reveal multigrain features.

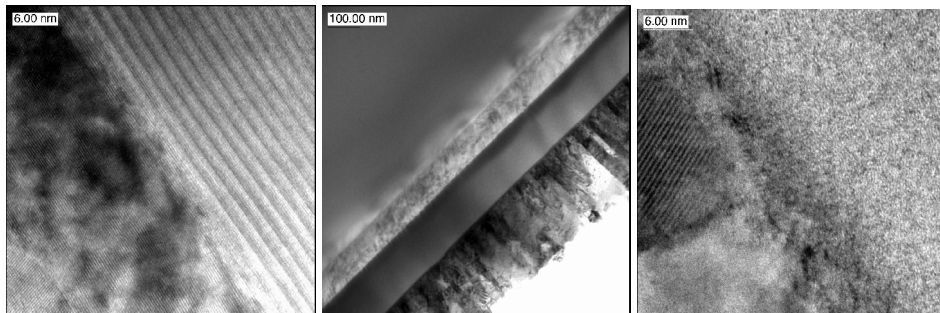


Fig. 1. Cross section HRTEM

- a) Magnified Ti/SiC interface. b) As-deposited metallization shows the columnar multigrain structure in platinum. c) Magnified Pt/TaSi₂ interface

The SEM figure in 2a depicts the smooth Pt surface morphology after deposition. However, after 50 hours at 600⁰C in air, microstructural changes on the surface can be observed as shown in Fig. 2b. It reveals surface roughness in obvious contrast with Fig. 2a.

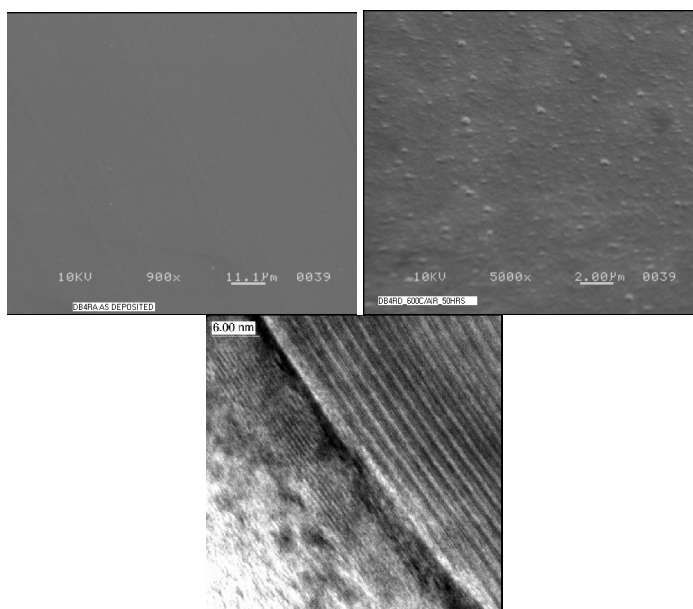


Fig. 2. a) SEM photomicrograph of platinum overlayer. b) Surface morphology of same sample after 600⁰C in air for 50 hours, revealing 2-D non-uniform oxide growth features. c) Cross-section HRTEM of SiC interface after 30-minute N₂ anneal at 600⁰C reveals an approximately 8nm quasi-epitaxial Ti₅Si₃ (*c* ≈ 0.55 nm)

This is believed to be the result of non-uniform surface oxidation of the platinum silicide, Pt₃Si [5], which is believed to form as a result of the decomposition of TaSi₂ during the initial 30-minute nitrogen anneal.

Oxidation of such a non-uniform surface will therefore result in uneven volume increase as was experimentally observed in Fig. 2b. Non-uniform volume increase during surface oxidation is believed to be due to the multigrain structure of the as-deposited platinum layer as observed in the HRTEM of Fig. 1c. The HRTEM of the Ti/SiC interface after half hour nitrogen anneal at 600⁰C shown in Fig. 2c reveals a quasi-epitaxial layer parallel to the 6H-SiC.

This layer has a periodicity of about 0.55 nm which, within limit of measurement error (7% higher), corresponds to the *c*-lattice parameter of hexagonal Ti₅Si₃ [6].

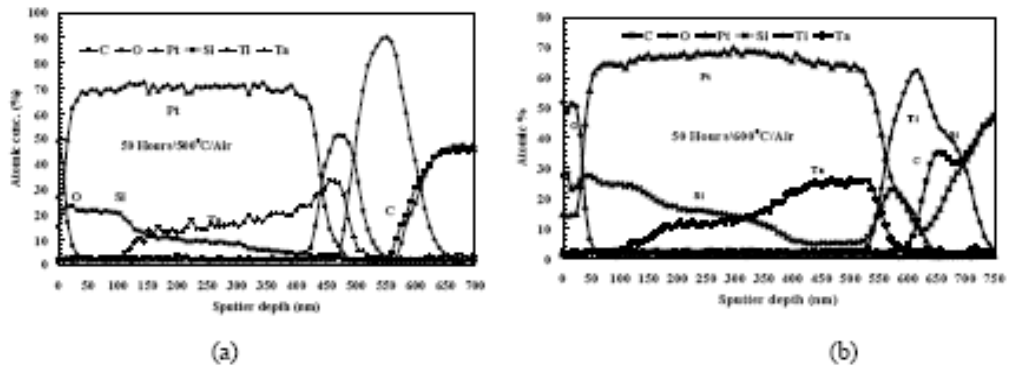


Fig. 3: AES depth profiles

a) 500⁰ C sample set treated in air for 50 hours, and b) 600⁰ C sample set treated in air for 50 hours. Oxygen containment is observed at the surface. TixCy formation appears to have been initiated during the 600⁰ C treatment

Representative AES depth profiles are shown in Figs. 3a and b for 50 hours treatment in air at 500⁰C and 600⁰C, respectively. After the 30-minute nitrogen anneal and subsequent treatment for 50 hours at 500⁰C (Fig. 3a), no strong evidence of TiC was observed. However, the AES depth profile shown in Fig. 3b of sample treated at 600⁰C in air indicated a distinct TixCy layer at about 650 nm depth, next to Ti5Si3. The values were substituted for *x* in (2a) and (2b), and together with the obtained *D* from equation 2b, were fitted into (1). The experimental results, together with a curve from calculation were plotted and shown in Fig. 4a for oxide growth in platinum silicide. [7] and [8] confirmed that the oxidation kinetics of TaSi₂ have a parabolic rate constant. Our result demonstrates the parabolic oxidation characteristics of Pt₃Si.

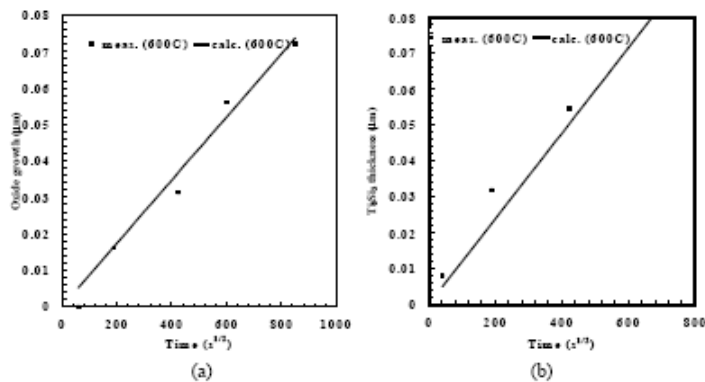


Fig. 4: Experimental and calculated growth at 600⁰ C in air of a) oxide in platinum silicide and b) titanium silicide

The growth thickness of Ti₅Si₃ is shown in Fig. 4b after 600⁰C for 50 hours in air. An attempt to obtain accurate growth rates beyond this time was inhibited by platinum migration toward the contact, which altered the reaction kinetics.

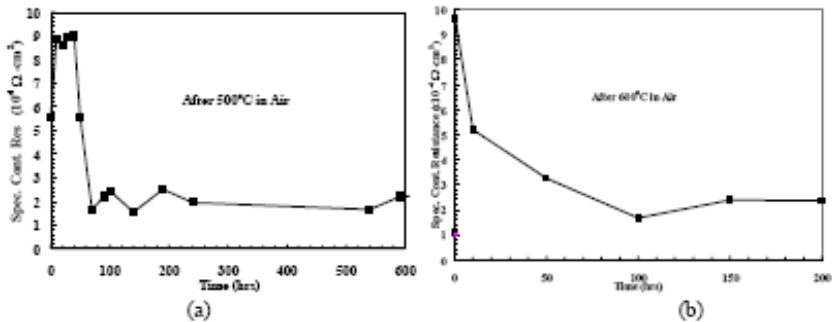


Fig. 5. Specific contact resistances after intermittent heat treatment in air at a) 500⁰C and b) 600⁰C

The specific contact resistance of samples treated at 500⁰C and 600⁰C in air is shown in Figs. 5a and b, respectively. The sample treated at 500⁰C exhibit high values in the first 40 hours before decreasing to near constant value of about 2x10⁻⁴ Ω·cm². The sample treated at 600⁰C exhibited a similar trend but the duration at high values was shorter. The phenomenon is attributed to temperature and time dependent product formation at the SiC interface, which, in this case will be accelerated at 600⁰C.

Conclusions

Studying the reaction kinetics of two critical interfacial zones revealed fundamental insights into the thermal stability of the Ti/TaSi₂/Pt ohmic contact on 6H-SiC. The oxidation of the platinum silicide overlayer exhibited parabolic rate dependence, demonstrated to inhibit the migration of oxygen to the SiC interface, thereby extending the life of the contact. We also demonstrated that thermodynamically stable, quasi-epitaxial Ti₅Si₃ forms at the SiC/metal interface, providing excellent electrical contact properties. Platinum is needed for the purpose of forming a protective silicide overlayer that is also wettable for wire bonding, but its potential deleterious effect on the long-term contact stability needs to be investigated. On the basis of this result, we have thus demonstrated thermally stable specific contact resistance after a long duration exposure in air ambient at 600⁰C.

References

1. CREE RESEARCH, Inc., Durham NC 27703 USA.
2. R. S. OKOJIE, D. SPRY, J. KROTINE, C. SALUPO, D. R. WHEELER, MRS Spring 2000, San Francisco, CA April
3. B.E. DEAL, A.S. GROVE, *J. Appl. Phys.*, **36**, p. 3770-3778, (1965).
4. M. NATHAN, S. W. DUNCAN, *Thin Solid Films*, **123** p. 69-84, (1985).
5. ASM Handbook of Alloy Phase Diagrams, Vol. 3, p. 2(347), (1992).
6. W. B. PEARSON, "A Handbook of Lattice Spacings and Structures of Metals and Alloys," Vol. 2, Pergamon,
7. L.N. LIE, W.A. TILLER, K.C. SARASWAT, *J. Appl. Phys.*, **56**, (7), p. 2127-2132, (1984).
8. R.R. RAZOUK, M.E. THOMAS, S.L. PRESSACO, *J. Appl. Phys.*, **53**, (7), p. 5342-5344, (1982).

ENERGY LEVELS CALCULATION FOR $\text{Eu}^{3+}:\text{ZnGa}_2\text{O}_4$ WITH EXCHANGE CHARGE MODEL

VASILE Mihaela^{1,2}, VLAZAN Paulina¹, AVRAM Nicolae M.²,
GROZESCU Ioan¹, RUSU Emil³

¹National Institute for Research and Development in Electrochemistry and Condensed Matter Timisoara, Romania; ²West University of Timisoara, Faculty of Physics, Timisoara, Romania; ³Institute of Applied Physics, Academy of Sciences of Moldova; E.mail: mihaela.vasile@icmct.uvt.ro

Abstract

The main goals of this work is theoretical calculation of the energy level scheme of transitions ${}^5\text{D}_0 - {}^7\text{F}_j$ ($j=0-6$) in the exchange charge model and explain, the experimental results of regarding structures spectra of $\text{ZnGa}_2\text{O}_4:\text{Eu}^{3+}$ in both nanocrystalline system. The obtained results suggest that Eu^{3+} ions can be doped into O_h Ga^{3+} sites for nanoparticles and prefers to occupy Td sites of Zn^{2+} in nano host materials.

Keywords: level, spinel, semiempirics

Introduction

Among many oxide phosphors, zinc gallate (ZnGa_2O_4) is a normal spinel crystal structure which crystallizes in the cubic space group $\text{Fd}\bar{3}\text{m}$ (O_h^7), with lattice constant $a=8.3358\text{\AA}$ [1], Zn^{2+} ions occupies octahedral sites and Ga^{3+} ions a tetrahedral sites or a trigonally distorted octahedral sites [2]. The energy band gap of this crystal is about 4.4eV [3] and ZnGa_2O_4 shows blue photoluminescence without doping via transition of a self-activated center. ZnGa_2O_4 shows various emission colors when doped with some transitional metal or rare earth ions, such as Cr^{3+} , Mn^{2+} , Eu^{3+} or Ce^{3+} [4-8].

ZnGa_2O_4 phosphor has been used for low-voltage cathode luminescence, vacuum fluorescent display and recently reported as promising candidate for field emission displays [9].

The main goal of this paper is theoretical calculation of energy levels scheme of $\text{ZnGa}_2\text{O}_4:\text{Eu}^{3+}$ in the frame of semiempirical model of the exchange charge model (ECM) [10]. To the best of our knowledge, this is the first attempt of the ECM calculations of energy levels for bulk crystals ZnGa_2O_4 doped with Eu^{3+} ions.

$\text{ZnGa}_2\text{O}_4:\text{Eu}^{3+}$ system

Due to the approximate validity of spin and parity selection rules, electric dipole transitions between the ${}^5\text{D}$ and ${}^7\text{F}$ levels of the Eu^{3+} impurity are forbidden in first approximation. The spin selection rule is lifted by the spin-orbit coupling. The magnetic dipole and quadrupole transitions are only forbidden by a spin coupling. To investigate the

effect of the symmetry of the surroundings, a series of compounds was studied, a compound in which the Eu^{3+} ion occupies a strict center of (O_h) symmetry, a compound in which small deviations from this symmetry occur, and a compound with no symmetry at all. The Eu^{3+} impurity occupies one of the Ga^{3+} sites with octahedral coordination. It is surrounded by six O^{2-} ions, forming an "[EuO_6] $^{9-}$ cluster".

The excitation spectra of Eu^{3+} for the 616 nm emission of ${}^5\text{D}_0$ - ${}^7\text{F}_2$ were obtained. The spectra of nano doped crystal consists of sharp lines ranging from 500 to 1000 nm, which are associated with the transitions from the excited ${}^5\text{D}_0$ level to ${}^7\text{F}_J$ ($J = 1; 2; 3; 4$) levels of Eu^{3+} activators. The Eu^{3+} ions of bulk sample prefer to occupy T_d sites or distended O_h sites with no inversion symmetry.

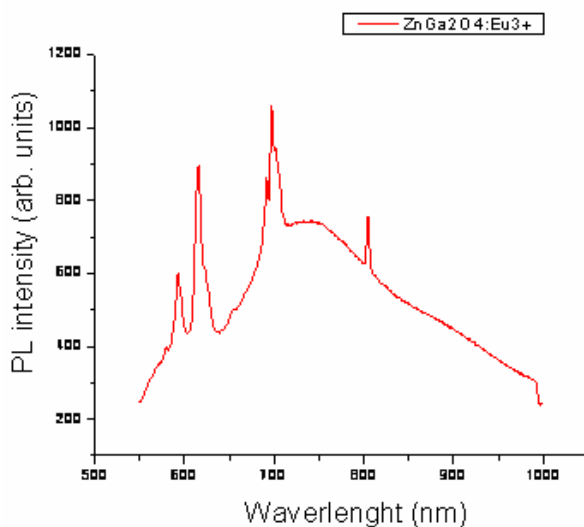


Fig. 1 Excited PL spectra of nanocrystalline $\text{ZnGa}_2\text{O}_4:\text{Eu}^{3+}$ phosphors

Calculation

The experimental support of our calculation are the results obtained in paper [11] for nano crystal ZnGa_2O_4 doped with europium trivalent ion. Eu^{3+} substitutes the Ga^{3+} ion and has an octahedral coordination of O^{2-} ions with local site symmetry.

Electrical charges of both substituted and substituting ions are the same no charge compensating addition is required to keep electrical neutrality of the crystals.

The measured energy spectrum of Eu^{3+} ions in ZnGa_2O_4 was analyzed using the Hamiltonian:

$$H = H_{FI} + H_{CF} \tag{1}$$

where H_{FI} is the effective free-ion Hamiltonian,

$$H_{FI} = \sum_{k=0,2,4,6} F^k f_k + \xi_{nl} A_{so}(nl) + \alpha L(L+1) + \beta G(G_2) + \gamma G(G_7) + \sum_{i=2,3,4,6,7,8} T^i t_i + \sum_{i=0,2,4} M^i m_i + \sum_{i=1,4,6} p_i P^i \tag{2}$$

The electrostatic interaction between 4f electrons determined by Racah parameters F^2 , F^4 , F^6 , spin-orbit interaction (with the coupling constant ζ), Trees' two-particle (α, β, γ parameters) and Judd' three-particle (parameters $T^2 - T^4$, $T^6 - T^8$) corrections to the electrostatic interaction were taken into account in the free-ion Hamiltonian For Eu^{3+} ions the parameters are: $F^1=83125$, $F^2=59268$, $F^3=42560$, $\alpha=20.16$, $\beta=-566.9$, $\gamma=1500$, $\zeta=1338$, $T^2=300$, $T^3=40$, $T^4=60$, $T^6=-300$, $T^7=370$, $T^8=320$, $M^0=2.1$, $M^2=118$, $M^4=65$, $P^2=360$, $P^4=180$, $P^6=36$, $\sigma_2=0.73$.

H_{CF} corresponds to the interaction of the Eu^{3+} ground $4f^6$ configuration with the crystal field.

The Hamiltonian of 4f electrons of the Eu^{3+} ions in a crystal field will be calculated using the following crystal field Hamiltonian [10]:

$$H_{CF} = \sum_{k,q,i} B_p^k C_p^{(k)}(i) \tag{3}$$

where $C_p^{(k)}$ are the linear combinations of spherical operators (which act on the angular parts of a 4f ion wave functions), and B_p^k are CFPs containing all information about geometrical structure of an impurity center. Salient feature of the ECM is that these parameters can be written as a sum of two terms [10]:

$$B_p^k = B_{p,q}^k + B_{p,S}^k \tag{4}$$

The first contribution arises from the electrostatic interaction between a 4f ion and ions of crystal lattice (treated as the point charges, without taking into account their electron structure), and the second one is proportional to the overlap of the wave functions of a central ion and ligands. This term accounts for all effects of the covalent bond formation and exchange interaction, and inclusion of these effects significantly improves agreement between the calculated and experimentally observed energy levels. Expressions for calculating both contributions to the CFPs in the case of 4f-ion are as follows [10]:

$$B_{p,q}^k = -K_p^k e^2 \langle r^p \rangle \sum_i q_i \frac{V_p^k(\theta(i), \varphi(i))}{R(i)^{p+1}} (1 - \sigma_p)$$

(5)

$$B_{p,S}^k = K_p^k e^2 \frac{2(2p+1)}{5} \sum_i (G_s S(s)_i^2 + G_\sigma S(\sigma)_i^2 + \gamma_p G_\pi S(\pi)_i^2) \frac{V_p^k(\theta_i, \varphi_i)}{R_i}$$

(6)

The sums are carried out over lattice ions denoted by i with charges q_i ; $R(i), \theta(i), \varphi(i)$ are the spherical coordinates of the i -th ion of crystal lattice in the system of reference centered at the central ion. The averaged values $\langle r^p \rangle$ of p -th power of the central ion electron radial coordinate can be found in the literature or calculated numerically. The values of the numerical factors K_p^k, γ_p and expressions for the polynomials V_p^k are given in [10]. $S(s), S(\sigma), S(\pi)$ correspond to the overlap integrals between f -functions of the central ion and p - and s -functions of the ligands: $S(s) = \langle 4f0|s0 \rangle, S(\sigma) = \langle 4f0|p0 \rangle, S(\pi) = \langle 4f1|p1 \rangle$. G_s, G_σ, G_π are dimensionless adjustable parameters of the model, whose values can be determined from the positions of the first three absorption bands. We assume that they can be approximated to a single value, i.e. $G_s = G_\sigma = G_\pi = G$, that can be estimated from only one (the lowest in energy) absorption band. This is usually a reasonable approximation. The strong advantage of the ECM is that if the G parameter is determined to fit the first absorption band, the other energy levels, located higher in energy, will also fit experimental spectra fairly well. Numerous applications of the ECM to the analysis of rare-earth and transition metal doped crystals show this model to be a powerful and reliable tool for analysis and interpretation of crystal field effects and optical absorption spectra.

Calculation of $\langle r^p \rangle$ was made using the wave function type Freeman and Watson [13].

$$|4f\rangle = r^4 \left(\begin{matrix} 1676.72e^{-12.095r} + 278.194e^{-6.800r} + \\ + 37.3965e^{-4.533r} + 1.23048e^{-2.489r} \end{matrix} \right)$$

(7)

The obtained values are (in a.u.):

$$\langle r^2 \rangle = 0.829, \langle r^4 \rangle = 1.678, \langle r^6 \rangle = 7.302$$

(8)

The overlap integrals are approximated as:

$$S_s = 1.41493e^{-1.0424R}$$

$$S_\sigma = 0.44560e^{-0.74525R}$$

$$S_\pi = 1.00458e^{-1.00814R}$$

(9)

Results of calculation

The CFPs were calculated using the ionic positions obtained from structural data [10]. To ensure convergence of CFPs (especially those ones of the second rank), a large cluster consisting of 12456 ions was taken into account. The overlap integrals between Eu^{3+} and O^{2-} ion (9) were calculated numerically using the wave functions from Refs. [12].

Obtained values of CFP_s were used to diagonalize the crystal field Hamiltonian (1) for Eu^{3+} doped ZnGa_2O_4 crystal.

Calculated energy levels for $G=7$ are shown in Table 1.

As seen from this Table, the calculated values are in good agreement with experimental data. Higher energy levels (though they also were obtained) are not shown here for the sake of brevity.

Table 1. Observed and calculated (this work) energy levels (in cm^{-1}) of Eu^{3+} ion in ZnGa_2O_4

Energy levels (O_h group notations)	This work	
	Experimental	Calculated
${}^5\text{D}_1$	18579	18562
${}^5\text{D}_0$	17354	17350
${}^7\text{F}_6$	5024	5007
${}^7\text{F}_5$	3873	3863
${}^7\text{F}_4$	2840	2809
${}^7\text{F}_3$	1890	1882
${}^7\text{F}_2$	1023	1019
${}^7\text{F}_1$	370	378
${}^7\text{F}_0$	0	0

Conclusions

Consistent calculations of the CFPs values and energy levels for Eu^{3+} ions in spinel crystal ZnGa_2O_4 were performed using the ECM of crystal field. For the first time, for the

considered crystal, the CFPs values were calculated from crystal structure data, with taking into account low symmetry component of crystal field. Calculated energy levels match well scarce available in the literature absorption spectra. Calculated complete energy level schemes can be used for analysis of the Eu^{3+} excited state absorption in the considered spinel, and the sets of CFPs can be used as initial (starting) sets for analysis of Eu^{3+} energy levels in other is structural crystals.

References

- [1] M. Wendschuh-Josties, H. S. C. O'Neill, K. Bente, G. Brey, *Neues Jahrbuch für Mineralogie Monatshefte*, 6, 273, (1995);
- [2] I. I. Krebs, G. H. Stauss and I. B. Milstei, *Phys. Rev. B* 20, 2586 (1979);
- [3] S. Itoh, H. Toki, Y. Sato, K. Morimoto and T. Kishino, *I. Electrochem. Soc.*, 138, 1509 (1991);
- [4] J. S. Kim, J. S. Kim H. L. Park, *Solid State Commun* 131, 735 (2004);
- [5] M. Yu, Y. H. Zhon, S. B. Wang, *Mater. Lett.* 56, 1007 (2002)
- [6] J. S. Kim, I. S. Kim, T. W. Kim, S. M. Kim, H. L. Park, *Appl. Phys. Lett.* 86, 091912 (2005);
- [7] T. Ohtake, N. Sonoyama, T. Sakata, *Chem. Phys. Lett.*, 318, 577 (2000);
- [8] P. D. Rack, I. I. Peterson, M. D. Potter, W. Park, *I. Mater. Res.* 16, 1429 (2001);
- [9] T. Minami, Y. Kuroi, T. Maeno, T. Miyata, *I. Appl. Phys. Jpn.*, 34, L 684 (1995);
- [10] B. Malkin, in: A. A. Kaplyanskii and RM Macfarlane (Eds), *Spectroscopy of Solids Containing Rare-Earth Ions*, North-Holland, Amsterdam, pp. 33 (1987);
- [11] J. S. Kim, A. K. Kwon, I. S. Kim, H. L. Park, G. C. Kim and S. do Han, *J. Lumin.*, 122-123, 851 (2007);
- [12] A. J. Freeman and R. E. Watson, *Phys. Rev.* 127, 2058 (1962).

MATHEMATICAL MODELLING OF THE FLAX FIBRES ENZYMATIC COTTONISATION PROCESS IN ULTRASOUND CONDITIONS WITH PECTINASES

PUSTIANU Monica¹, SIRGHIE Cecilia²

University "Aurel Vlaicu" of Arad, ¹Faculty of Engineering Textile Departement, ²Faculty of Food Engineering, Tourism and Environmental Protection, 2 Elena Drăgoi, Str., 310330, Arad, Romania, E-mail: e-mail pustianumonica@yahoo.com, cecilias1369@yahoo.com, tel.0257/ 369091

Abstract

In order to describe the random phenomena occurred into ultrasonic- enzymatic treatments, a rotating center composed program with two variables were used for mathematical modeling of the flax fibers cottonisation process. The treatments parameters have been varied according to the statistic plan of two variables and the regression equations for certain parameters of the flax fibers cottonization process, are discussed in this study.

Keywords: mathematical modeling, ultrasonic-enzymatic cottonisation,

Introduction

The flax fibers belong to the bast fibers category. The main particularity is the presence of medium lamella that includes in her structure the elementary cells. The lamella material is glue formed from macromolecular compounds more or less cross-linked, rigid that offer mechanical strength to the flax plant stem. The most significant compounds in this glue are: lignin, pectin and hemicelluloses.

The pectin (a skeleton like polysaccharide) are present in all vegetable cells walls, and are mainly form from pectin acid which have α -D-galacturonic acid units formed in 1,4- β -glucozidic bounders. The pectin is non-soluble in water but the sodium salts of the pectin acid are soluble. By hydrolysis is able to offer a soluble compound- D-galacturonic acid. The delignification process of flax fibers is based on these phenomena [1].

The complete removal of the glue leads to the liberation of the elementary fibers (individualization) and this process is called „ cottonisation”. The cotonisation could be done by mechanical, chemical and enzymatic methods. The ultrasonic-enzymatic cottonisation is the newest one [9]. The enzymes are bio-catalysts produced by microorganisms, able to act on a very well defined substrate, accelerating the reaction velocity. The pectinases are one of the enzymes class largely used for pectin removal based on their ability to hydrolyze the pectin and the D-galacturonic acid is resulted thus.

The hydrolysis degree could be measured by potassium permanganate method. The method is based on the measuring the discoloration time of a known quantity of potassium permanganate from a very weak sulfuric acid solution. In this case, the potassium permanganate will quantify the content of D-galacturonic acid from the reaction liquid, in

the presence of sulfuric acid and therefore, a direct correlation between the discoloration time and the quantity of pectin solved during enzymatic reaction could be established, thus.

The usage of ultrasounds in wet textile processing showed a series of advantages such as: shortening the process time, reducing the energy and chemicals, improving the products characteristics [4, 7, and 8]. The usage of enzymes for the flax cottonising purposes has been intensively studied [5, 6]. Recently, a new ultrasonic-enzymatic-cottonisation method [9] which showed that the ultrasounds favorable the pectin disorder and the hydrolysis degree could be increased till a certain concentration of enzymes, were registered. Combined usage of ultrasounds and enzymes has been intensively studied in the last years, proving significant benefits for cottonising process.

In order to obtain the optimal treatment conditions (enzymes concentration) for which the ultrasound could have significant influences, the mathematical modeling of the ultrasonic-enzymatic cottonisation process for flax fibers is studied in this paper.

Experimental

The kinetics of pectin's enzymatic hydrolysis from flax fibers in ultrasound conditions is studied. For these experiments have been used flax fibers and pectin's –Biopreparation 3000 (from Novozyme). The working parameters were: pH 9, 2 realized with a buffer borax/boric acid; liquid ratio 1:25; temperature 50°C; time 60 min. The fibers were treated in a thermostat ultrasound bath (Cole Palmer) to a frequency of 47 kHz with a temperature precision of $\pm 0,1^{\circ}$ C. Each 10 minutes, from the reaction bath, known quantities of reaction liquid have been extracted for analyses. The enzyme activity was stopped by adding known quantities of sulfuric acid solution (0,1N) in an ice bath. The samples were maintained to this temperature and soon after analyzed using potassium permanganate method. The analyses were done to the ambience temperature. Initially, an etalon curve that allows the transformation of discoloration time to equivalent of galacturonic acid milligrams was established. The etalon curve which shows a multiple correlation coefficient of 99, 7% have been used for measuring the hydrolysis degree, too and shown in fig.1. The experimental results are shown in table 1 and the reaction kinetics is shown in fig 2.

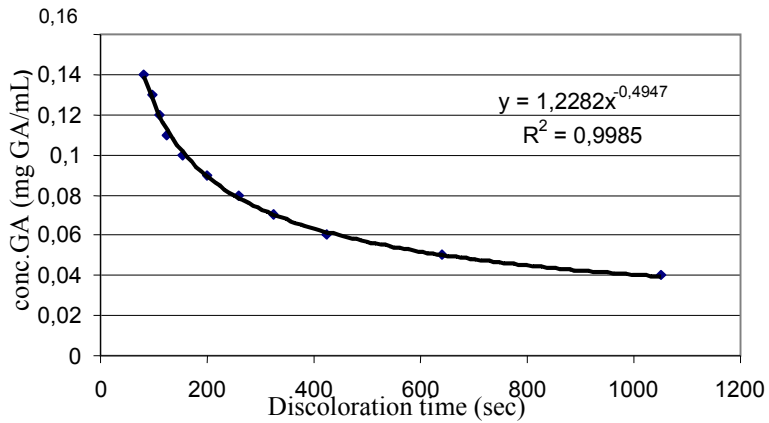


Fig.1 Etalon curve for potassium permanganate method.

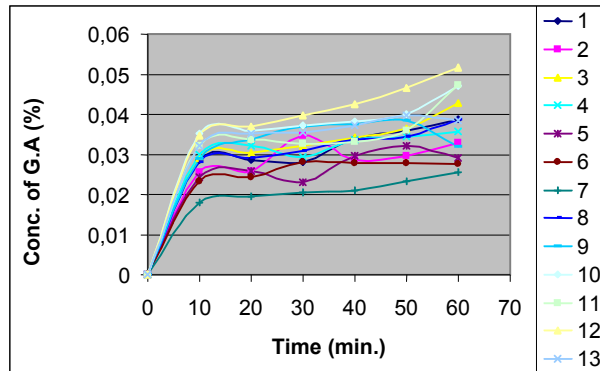


Fig. 2 Kinetics curve for variation of galacturonic acid concentration.

Previous to this experimental set, preliminary experiments for setting the minimum number of tests were made. The number of tests was established according to a center-routable-experimental program of two independent variables. The variation limits and experimental plan are shown in table 2 and 3.

The center-routable- experimental program of two independent variables has the following mathematical expression:

$$Y = b_0 x_0 + b_1 x_1 + b_2 x_2 + b_{12} x_1 x_2 + b_{11} x_1^2 + b_{22} x_2^2 \tag{1}$$

Table 1. Experimental results

Nr.	Discoloration time 10min (s)	Conc. of galacturonic acid (%)	Discoloration time 20min (s)	Conc. of galacturonic acid (%)	Discoloration time 30min (s)	Conc. of galacturonic acid (%)	Discoloration time 40min (s)	Conc. of galacturonic acid (%)	Discoloration time 50min (s)	Conc. of galacturonic acid (%)	Discoloration time 60min (s)	Conc. of galacturonic acid (%)
1.	215	0,029	216	0,029	226	0,028	153	0,034	136	0,036	118	0,039
2.	391	0,026	389	0,026	213	0,035	313	0,029	294	0,030	236	0,033
3.	210	0,029	193	0,030	172	0,032	151	0,034	132	0,037	96	0,043
4.	198	0,030	171	0,032	205	0,029	156	0,034	150	0,034	138	0,036
5.	301	0,024	266	0,026	339	0,023	201	0,030	172	0,032	209	0,029
6.	328	0,023	302	0,024	225	0,028	230	0,028	231	0,028	234	0,028
7.	198	0,018	169	0,019	150	0,021	144	0,021	118	0,023	97	0,026
8.	224	0,028	209	0,029	186	0,031	155	0,034	150	0,034	117	0,039
9.	212	0,029	156	0,034	129	0,037	125	0,038	119	0,038	175	0,032
10.	325	0,035	308	0,036	291	0,037	275	0,038	251	0,040	180	0,047
11.	170	0,032	156	0,034	166	0,033	162	0,033	136	0,036	78	0,047
12.	147	0,035	129	0,037	112	0,040	97	0,043	81	0,047	66	0,052
13.	170	0,032	143	0,035	141	0,035	127	0,037	112	0,040	119	0,038

For a model with two variables, the program contains experiments equal distributed on a circle circumference, in the x_1 x_2 plane, with the center (0,0) plus one or more experiments in the center of the circle. The points located on the circle forms a regular polygon inside the circle. These points represent the program codification [10, 11].

Table 2. The variation limits of the independent variables.

Val. cod. Val. real	-1,414	-1	0	1	+1,414
x_1 (g fiber)	1	1,29	1,5	1,78	2
x_2 (pectin's ml)	0,004	0,012	0,032	0,051	0,06

Table3. Experimental plan (two independent variables).

Nr. experimnts	x_1	x_2
1.	-1	-1
2.	1	-1
3.	-1	1
4.	1	1
5.	-1,414	0
6.	1,414	0
7.	0	-1,414
8.	0	1,414
9.	0	0
10.	0	0
11.	0	0
12.	0	0
13.	0	0

The cottonising ability of flax fibers have been appreciated through the concentration of the galacturonic acid result from the pectin enzymatic hydrolysis with pectinases in the presence of ultrasounds.

Results and Discussions

The experiments matrix and the measured values for the responses functions are shown in table 4. The experimental results have been processed using MAT-CAD software.

Mathematical model statistic interpretation.

The center-routable-experimental program of two independent variables have been considered to be more appropriate for the mathematical modeling of the ultrasonic-enzymatic cottonisation process of flax fibers. This program was used for a better evaluation of precise influence of some parameters in the presence of ultrasounds on the galacturonic acid concentration obtained after hydrolysis. More exactly we refer to the fiber weight (g) and enzymes consumption (pectinase in ml) that were chosen as independent variables thus:

x_1 – fiber weight (g);

x_2 – enzyme concentration (pectinase in ml).

The concentration of galacturonic acid was chosen as purpose function (Y).

The fiber weight is established between 1-2g and enzymes consumption between 0,004 and 0, 6 ml.

Table 4. The experiments matrix and the measured values for the responses functions.

Nr. exp.	Independent variables				Responses						
	X1		X2		F (x,y)						
	cod.	real	cod.	real	Concentration of galacturonic acid (%)						
					10 min	20 min	30 min	40 min	50 min	60 min	The curve slope at 10 min
1	-1	1,29	-1	0,303	0,029	0,029	0,028	0,034	0,036	0,039	0,0029
2	1	1,78	-1	0.303	0,026	0,026	0,035	0,029	0,030	0,033	0,0026
3	-1	1,29	1	1,297	0,029	0,030	0,032	0,034	0,037	0,043	0,0029
4	1	1,78	1	1,297	0,030	0,032	0,029	0,034	0,034	0,036	0,0030
5	-	1	0	0,8							0,0024
	1.414				0,024	0,026	0,023	0,030	0,032	0,029	
6	1.414	2	0	0,8	0,023	0,024	0,028	0,028	0,028	0,028	0,0023
7	0	1,5	-	0,1							0,0018
			1.414		0,018	0,019	0,021	0,021	0,023	0,026	
8	0	1,5	1.414	1,5	0,028	0,029	0,031	0,034	0,034	0,039	0,0028
9	0	1,5	0	0,8	0,029	0,034	0,037	0,038	0,038	0,032	0,0029
10	0	1,5	0	0,8	0,035	0,036	0,037	0,038	0,040	0,047	0,0035
11	0	1,5	0	0,8	0,032	0,034	0,033	0,033	0,036	0,047	0,0032
12	0	1,5	0	0,8	0,035	0,037	0,040	0,043	0,047	0,052	0,0035
13	0	1,5	0	0,8	0,032	0,035	0,035	0,037	0,040	0,038	0,0032

For establishing the experiments according with these two independent variables, a professional programme in MathCAD and Excel programme have been used. For the expressions of the purpose functions, which represents the concentration of galacturonic acid after 10 min. up to 60 min., were founded the following equations:

Y10

$$f(x,y) = 0,033 + (-4,268 * 10^{-4}) * x + (2.268 * 10^{-3}) * y + (-3,237 * 10^{-3}) * x^2 + (-3,488 * 10^{-3}) * y^2 + (1 * 10^{-3}) * x * y \quad (2)$$

Y20

$$f(x,y) = 0,035 + (-4,786 * 10^{-4}) * x + (2.643 * 10^{-3}) * y + (-3,913 * 10^{-3}) * x^2 + (-4,413 * 10^{-3}) * y^2 + (1,25 * 10^{-3}) * x * y \quad (3)$$

Y30

$$f(x,y) = 0,035 + (-4,786 * 10^{-4}) * x + (2.643 * 10^{-3}) * y + (-3,913 * 10^{-3}) * x^2 + (-4,413 * 10^{-3}) * y^2 + (1,25 * 10^{-3}) * x * y \quad (4)$$

Y40

$$f(x,y) = 0,038 + (-9,786 * 10^{-4}) * x + (2.923 * 10^{-3}) * y + (-3,275 * 10^{-3}) * x^2 + (-4,025 * 10^{-3}) * y^2 + (1,25 * 10^{-3}) * x * y \quad (5)$$

Y50

$$f(x,y) = 0,035 + (-4,786 * 10^{-3}) * x + (2.57 * 10^{-3}) * y + (-3,85 * 10^{-3}) * x^2 + (-4,6 * 10^{-3}) * y^2 + (7,5 * 10^{-4}) * x * y \quad (6)$$

Y60

$$f(x,y) = 0,043 + (-1,802 * 10^{-3}) * x + (3,173 * 10^{-3}) * y + (-5,538 * 10^{-3}) * x^2 + (-3,537 * 10^{-3}) * y^2 + (2,5 * 10^{-4}) * x * y \quad (7)$$

The purpose function Y_{10} , given by the expression (2) which means the concentration of galacturonic acid after 10 min., is made by statistical analysis of the obtained data's.

The coefficient of multiple correlations was determined in order to establish the links between independent and dependent variables. The coefficient had appropriate value to 1 which means that is a high influence of independent variables upon dependent ones. In order to verify the significance of the multiple correlation coefficients was used the Fisher Test. It was found that, $F = 9,8$ which is higher than $F_c = 3,97$ it means that all independent variables have a significant influence upon dependent variables.

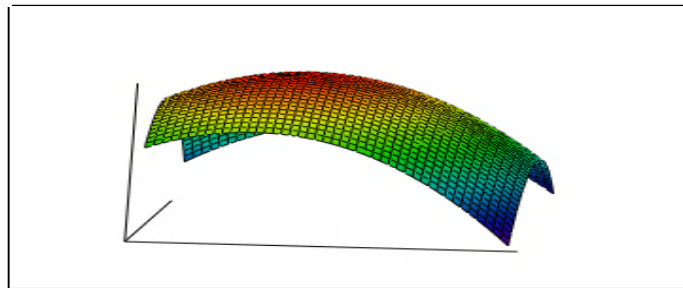
The coefficients of the regression equation have been statistically verified using Student Test by comparing also with table value of Student test =2,132 and the following values have been obtained: $\alpha = 0,95$, $\nu = 4$ and for all terms analyzed: $tb_0 = 25877,47$; $tb_1 = -541,905$; $tb_2 = 2879,365$; $tb_{11} = -3555,76$; $tb_{22} = -3831,85$; $tb_{12} = 317,4603$ the significance level was proved. For the model adequacy, respectively for the model ability to express the studied phenomena mathematically, the deviation A of the calculated values comparatively with the experimental values, were also determinate. Each individual deviation is inside of the imposed limits of $\pm 10\%$, which indicate a very good adequacy of the obtained model. It was found that: $F=2,96 > F_{tab} = 2,69$ which means that the model is adequate. In the last step of the statistical data's interpretation was verified the model adequacy using Fisher Test. All the evaluation criteria confirmed the model adequacy.

Mathematical model technological interpretation

Analyzing the expression (2) we conclude that independent variables have a significant influence upon dependent variables (concentration of galacturonic acid).

$$f(x,y) = 0,033 + (-4,268 * 10^{-4}) * x + (2,268 * 10^{-3}) * y + (-3,237 * 10^{-3}) * x^2 + (-3,488 * 10^{-3}) * y^2 + (1 * 10^{-3}) * x * y \quad (2)$$

The quarter coefficients from the regression equation have negative values and determine the curve shape of the response surface. The interaction term, being positive, determines a direct influence upon the size of the dependent variables. At high enzymes concentrations a negative effect, indicated by the negative value of B_{22} , could be observed. It is supposed that the positive effect of B_2 could lead to constantly over certain enzyme concentrations. The dependence of the purpose function of the two independent variables and the response surface in 3D view (elliptic hill) is shown in fig.3.



M
Fig.3 The dependence of purpose function of the dependent variables. x_1 – fiber weight (g); x_2 – enzyme concentration (pectinase in ml).

Some sections (after different planes) in this 3D view of the response surfaces named - „contour curves” are projected in the XY plane. These „contour curves” for different values of the galacturonic acid concentration between 0,018 and 0,035, are shown in fig.4.

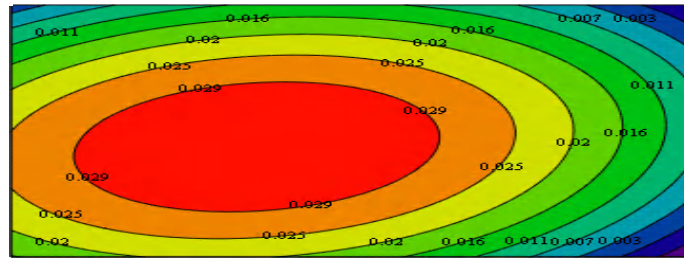


Fig.4 Contur curves for different values of the galacturonic acid concentration.

The center of the response surface (which is an elliptic one) is prolonged to the x_2 direction because the coefficients b_{11} and b_{22} are negatives and also because $b_{11} > b_{22}$. This dependence has a stationary point which is considered a maximum point. The cod coordinates of this point are: $X_1 = 0$ and $X_2 = 0$. To these cod coordinates corresponds 0,8 % pectinases concentration and 1,5 g fiber weight. The value of the purpose function in this point is: $Y = 0,029$. The dependencies of the purpose function of one (y) from the two variables(x, y), for all significant parameters values, when the second variable(x) is constant zero, are shown in fig.5.

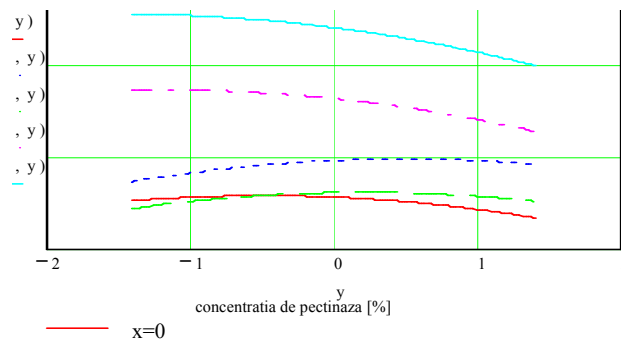


Fig.5 The dependency of the purpose function for all significant values of the parameter y when parameter x = constant.

From this figure we could see that, for a constant value of the fibers weight, the concentration of the galacturonic acid according with the enzymes concentration shown that, for the interval $[-1,414, 0]$, the maximum point is corresponding 0,8%, enzyme concentration which means a stronger influence of this parameter upon galacturonic acid concentration. For the interval $[1, +1,414]$ the galacturonic acid concentration decrease when the enzymes concentration is increased.

The dependencies of the purpose function of one (x) from the two variables (x,y), for all significant parameters values, when the second variable (y) is constant zero, are shown in fig.6.

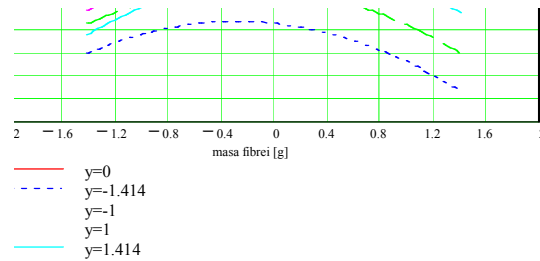


Fig.6 The dependency of the purpose function for all significant values of the parameter x when parameter y = constant.

When the enzyme concentration is constant, the evolution of the galacturonic acid concentration shown a stronger dependency of this parameter from the fiber weight. The maximum value registered for the galacturonic acid concentration is corresponding to 1,5 g fibers. Increasing the fibers weight over 1,5g the galacturonic acid concentration will decrease.

Conclusions

The routable composed program with two variables, used in this study, is suitable for describing the random phenomena occurred into ultrasonic-enzymatic process. The factorial experimental method has the advantage of selection and reducing the number of experiments being a good evaluation method for practical applications of enzymes in several biotechnologies. The experimental dates are processed using the regression equations method. All graphics shows stronger dependencies between galacturonic acid concentration, enzymes concentration and fibers weight, respectively. The maximum value for the concentration of the galacturonic acid (0,029%) was registered when the fibers weight was 1,5g and the enzymes concentration was 0, 8%.

References

1. Dăescu, C., Materiale fibroase naturale, Editura Helicon, Timișoara, 1996
2. A.G.I.R., S.I.T.R., Manualul inginerului textilist, Editura AGIR, 2003
3. Militky, J., Bajzic, V., Cottonised flax Geometrical and Mechanical Properties, Tecnitex 2001, AUTEX Conference, 150-157
4. Thakore, K.A., Smith, C.B., Application of ultrasounds to textile wet processing, American Dystuff Reporter, 1990, october, 30-38
5. Sedelnik, N., Biotechnology to assist cottonising of flax fibres Ist Nordic Conference on Flax and Hemp Processing, Tampere, Finland, august, 1998, 267
6. Sedelnik, N., Enzymes based modification of the properties of flax hackling noil, Bast Plants in the New Millenium, Borovets, Bulgaria, june, 2001, 362-365
7. Moholkar, V.S., Warmoeskerken, M.C., Intensification of mass transfer in textiles materials by ultrasound waves, Tecnitex, 2001, AUTEX Conference, 204-213
8. Moholkar, V.S., Warmoeskerken, M.C., investigation in mass transfer enhancenment in textiles with ultrasound, Chemical Engineer Science, 59, (2004), 299-311
9. Sirghie, C., Bucur, M.S., Dincă, N., L.van Langenhove, Popa. M., Ultrasound application in enzymatic treatment of bast fibres, COST 847 Action, Conference, 26-28 februarie, 2004, Maribor, Slovenia, p.31
10. Mihail, R., Intoducere în strategia experimentală cu aplicații din tehnologia chimică, Editura Științifică și Enciclopedică, București, 1976.
11. Cojocar, N., s.a., Metode statistice aplicate în industria textilă, Editura Tehnică, Bucuresti, 1986

FOOD SCIENCE

SUSTAINABLE FOOD PRODUCT PRODUCTION AND CONSUME

Oana Brînzan, Dana Radu, Eugenia Țigan

¹ "Aurel Vlaicu" University of Arad, 3 Elena Dragoi Str, RO-310330 Arad, Romania
oana.brinzan@uav.ro, poianarusca@yahoo.com,

Abstract

This paper emphasizes the importance of sustainability concept concerning the production and consume of food, in the context of European and global policys. The growing demand for safer, healthier, higher quality food products and for sustainable use and production of renewable bio-resources became nowadays social, environmental and economic challenges. That is why, education towards sustainable consumption which takes into accounts both economic efficiency and the greater social and environmental good, is vital.

Keywords: sustainability, food products, production, consume.

Introduction

The way we consume in modern society squanders resources and often makes us spend large amounts on unsustainable products that are less than beneficial to us and society at large. We need to create sustainable consumption which takes into account both economic efficiency and the greater social and environmental good.

Overconsumption of resources was first pointed out in 1949 at International Scientific Conference on the Conservation and Use of Resources, conference that was held with the occasion of new formed United Nation. In the same year the Club of Rome published for the first time the most important document that brought the attention upon the scarcity of resources and environment degradation.

Agenda 21, a very important instrument of United Nation, impose the terminology of "sustainable development", and during the Earth Summit held in Rio de Janeiro in 1992. There was underlined for the first time the necessity to change the consumption patterns in order to change our life standards and not exhausting the environment resource.

Results and discussions

Food losses begin on the farm and continue through the retail chain to the consumer. Also, considerable quantities of edible food available for human consumption are lost due to spoilage by retailers, the food service industry and consumers. Food service and consumer food loss accounted for nearly all of the waste. Food waste is the wettest and most dense component of domestic waste streams; composting is underdeveloped.

The trend toward increased packaging for household goods, including pre-packaged foods and food service packaging has helped reduce food waste from spoilage, transportation and storage. However, it has also significantly increased the amount of non-organic wastes entering the waste stream from household food consumption and diversified the materials. Although recycling rates for many packaging materials have increased, wastes from household food consumption are among the least affected by these trends.

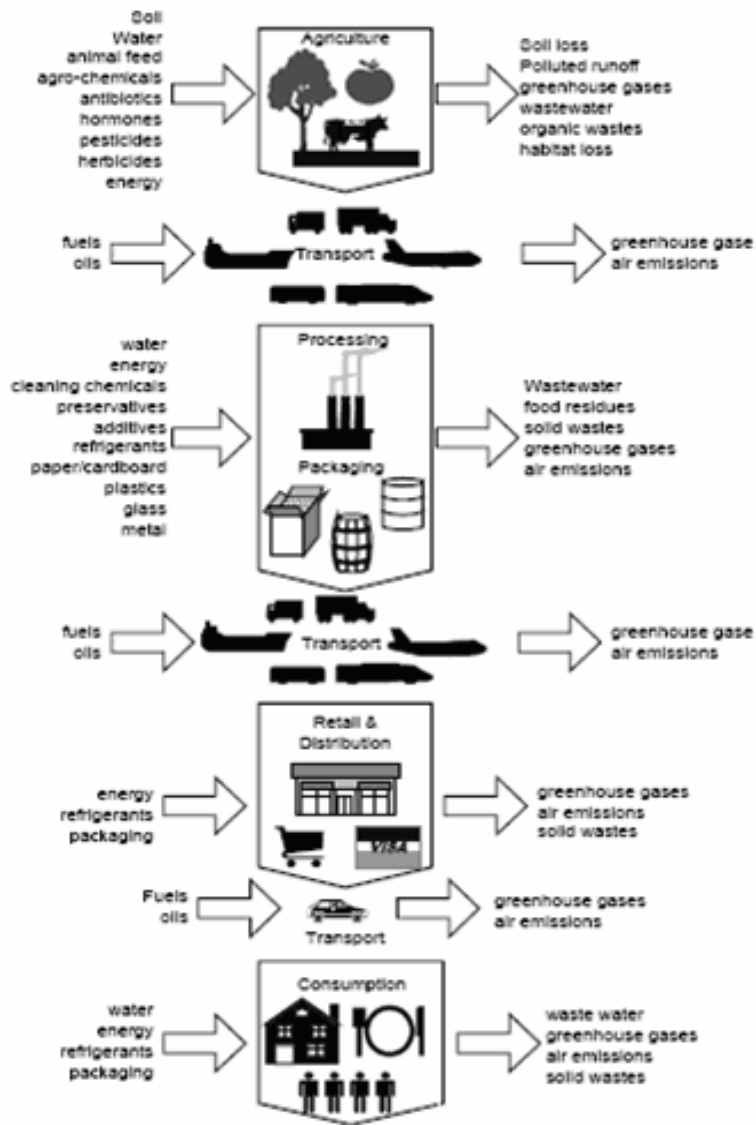


Figure 1. Environmental impacts from food sector (Jedvall, 2000)

Impacts from food produced by intensive agriculture can be greater than food produced using organic methods. Meat and vegetables from organic and intensive production were evaluated according to a set of environmental factors. Meat from intensive agriculture was found to have twice the environmental pressure score as organic meat, while the difference between vegetables from intensive agriculture and organic agriculture differed by a factor of more than three (European Commission, 2007). Other studies have shown that organic milk production is almost five times more energy efficient on a per animal basis and three- and- a- half times more energy efficient per litre of milk than intensive milk production (ADAS Consulting, 2001).

Studies carried out in areas mostly based on intensive agriculture in Western Europe and North America, have consistently found that meat and dairy products require considerably higher inputs of energy, water and land and lead to greater environmental pressures than equivalent amounts of vegetables, cereals and other crops (European Commission, 2006). This is particularly true where animals are fed with processed vegetable feeds rather than put to pasture. On average, 10 g of vegetable protein are needed to generate 1 g of animal protein (European Commission, 2007).

Food products vary widely in terms of the environmental pressures they create along their full production chain. The full production chain for beef, for example, includes all inputs invested in the growing of grain for animal feed, energy used in producing artificial fertilisers and pesticides which are applied to the grain during its growth, energy used for transporting animal feed to the livestock farms, fertiliser and water inputs into pastures, and energy and water used in farms and during the slaughter and processing of the cows.

Achieving sustainable consumption and production involves changing the way we produce, buy and throw away. The EU has identified key targets to make our consumption and production patterns less harmful:

- Put an end to the destructive link between economic growth and damage to the environment
- Encourage businesses and the general public to use objects that have been produced responsibly
- Aim to get public authorities across Europe to buy products and services that do not damage the environment
- Increase the market in technologies and innovations that are environmentally-friendly
- Improve the welfare of animals both within the EU and beyond

Agriculture and fisheries have seen many recent changes; the Common Fisheries Policy has been reformed and in farming the Common Agricultural Policy has shifted its focus away from support for production of agricultural products to general support for farmers. New laws concerning animal welfare and organic food production, hygiene and food quality, deal with concerns that more intensive farming was to blame for 'mad cow disease', dioxin in milk, artificial hormones in meat and other food-related health scares.

Some key principles and challenges include:

- i) improving the quality of life of populations without increasing environmental degradation, and without compromising the resource needs of future generations;
- ii) decoupling the link between economic growth and environmental degradation, by
 - reducing the material intensity and energy intensity of current economic activities and reducing generation of emissions and waste during extraction, production, consumption and disposal
 - encouraging a shift of consumption patterns towards groups of goods and services with lower energy and material intensity without compromising quality of life;
- iii) applying life- cycle thinking, which considers the impacts from all life- cycle stages of the production and consumption process and guards against unforeseen shifting of impacts from one life- cycle stage to another, from one geographical area to another, or from one environmental medium to another;
- iv) guarding against the rebound effect, where technological efficiency gains are cancelled out by resulting increases in consumption.

We need to build a European knowledge-based bio-economy by bringing together science, industry and other stakeholders, to exploit new and emerging research opportunities that address social, environmental and economic challenges:

- the growing demand for safer, healthier, higher quality food and for sustainable use and production of renewable bio-resources;

- the increasing risk of epizootic and zoonotic diseases and food related disorders;
- threats to the sustainability and security of agricultural, aquaculture and fisheries production;
- the increasing demand for high quality food, taking into account animal welfare and rural and coastal contexts and response to specific dietary needs of consumers.

Bringing together all relevant actors (research and food industry, farmers, consumers, etc.) to develop the basis for new, sustainable, safer, affordable, eco-efficient and competitive food products is in line with the European strategy on life sciences and biotechnology and the Lisbon objectives, and will help increase the competitiveness of European agriculture, biotechnology and food companies.

By 2050, with current trends, the global energy demand could double as populations rise and developing countries expand their economies, we urgently need to develop products and services that use fewer resources, to prevent needless waste of resources and to consume more responsibly.

These are objectives that will take considerable effort to achieve, and represent a common task for all: international organisations, public authorities, producers, retailers, consumers and people educating the new generation and the public.

Cross-cutting in character, sustainability of consume and production needs the active involvement of all stakeholders and a wide range of locally-adapted policy responses. These can range from introduction of more eco-efficient technologies, holistic policy approaches which combine regulatory frameworks, the use of economic instruments, dissemination of environmental information, development of physical and social infrastructure and improved education and public awareness.

References

- ADAS Consulting, (2001), *Energy use in organic farming systems*, UK Ministry of Agriculture, Food and Fisheries Project OF0182, London.
- JEDVALL, I. (2000), *The consumption of food: a Swedish case study* (Paper for the OECD Environment Directorate, Programme on Sustainable Consumption, September 2000)
- European Commission, 2006. *Environmental Impact of Products (EIPRO) — Analysis of the life cycle environmental impacts related to the final consumption of the EU - 25*. European Communities
- EEA Report, (2007), *Sustainable consumption and production in South East Europe and Eastern Europe, Caucasus and Central Asia*, No 3/2007, p.90

PRELIMINARY STUDY ON THE USE OF VACUUM IMPREGNATION IN VEGETABLE PRODUCT PROCESSING

URSACHI Claudiu¹, SEGAL Rodica²

¹ "Aurel Vlaicu" University of Arad, Romania

² "Dunarea de Jos" University of Galati, Romania

Abstract

Vegetal products are generally characterized through a high level of sensitivity due to environmental factors and to the operations they are submitted to during their preparation. This leads to meaningful changes regarding vegetal products nutritional and sensorial characteristics. The prevention of such drawbacks can be made by introducing active compounds in their structure in order to protect them from unwanted alterations. The introduction of compounds can be achieved through classical infusion, through the immersion of the products in hypertonic solutions of the respective compound, or through a new technology, vacuum impregnation. In this paper, we present the data obtained during the experiments regarding impregnation with sucrose, through classical infusion, at atmospheric pressure and infusion under a 500 mbarr vacuum of some vegetables, evaluated through weight alterations varying with the duration of the processing.

Keywords: vacuum impregnation, apples, infusion, sucrose

Introduction

The current tendency in feeding is to consume products that are minimally processed, in order to prevent the alteration of their quality, their nutritional and sensorial value, the result being fresh-like products, which are very similar to natural ones. Another tendency is to consume fortified food, with beneficial effects upon one's health (Artes and colab. 2007).

As we know, vegetable products are characterized through a high level of perishable and great sensitivity towards environmental factors and towards the technological operations to which they are exposed during the processing. This leads to important changes of sensory and nutritional features (Banu and colab. 2004).

Due to this fact, one of the main directions in the alimentary industry is focused upon obtaining vegetable products with a minimum degree of preparation, that can save as much as possible of their natural characteristics or to obtain food with active physiological compounds, like prebiotics, probiotics (Betoret, Puente, Diaz ,2002), vitamins, minerals, fibers, antioxidants etc. (Zhang, 2007). This can be achieved through the infusion of these compounds in vegetable products.

The classical infusion implies the immersion of products in a hyper tonic solution that contains impregnation substance where, based on osmosis and diffusion phenomena, it gets inside the vegetable cell. This method leads to the elimination of water from the cell, but along with it, it loses some soluble compounds from the product: sucrose, vitamins, mineral salts (Park and Zhao, 2005).

Another possibility is to introduce the compounds in the structure of vegetable products by using a new technology, vacuum impregnation (Xie and Zhao, 2003).

Vacuum impregnation consists in the immersion of vegetable products, characterized through high porosity, in solutions which contain dissolved substances meant to impregnate the product, followed by their storage in a place, under a certain void pressure (Xie and Zhao, 2003). This technology can be applied in order to better the texture of the product (Banjongsinsiri, Kenney and Wicker, 2004), to reduce its level of oxidation and its exudates at

defrosting, to maintain its color, and to strengthen the different vegetable products with all kinds of nutrients (Cattaneo, Leva Avitabile and Toreggiani, 2002).

Materials and methods

The aim of this paper is to observe the difference between the impregnation with a sucrose solution of some vegetable products with pores, such as apples, at atmospheric pressure and impregnation under void. The evaluation will emphasize the direct influence exercised by the duration of the process upon the products' mass.

The sorts of apples that have been used are called Jonathan. The healthiest products have been chosen for the experiments, they were washed, their seeds and the seed home were removed with an inoxidable tubular knife and afterwards they were peeled off and cut in round shapes with the help of an inoxidable knife. The round circles had between 7 and 10 mm and a mass between 11 and 13.5 g. The samples were immersed in a solution in order to avoid their contact with the the air, apples sensitivity towards oxidation being a well known feature.

For impregnation we used sucrose solution, with a 20% concentration, obtained through the mixture of distillate water and sucrose.

The following instrumentation has been used: installation for impregnation under void which consists in a RL-2 void pump and a vacuumeter - manufactured by REFCO Manufacturing Ltd. from Switzerland- linked to a void exicator. For the weighting, an analytical Kern scale was used.

Working method

For impregnation at atmospheric pressure, the apple slices were weighted in the analytical scale(m1), they were introduced in sucrose solution, immersed with the help of a watch glass and kept in the solution for a different amount of time, from 10 to 220 minutes. When the time expired, the apples have been removed from the solution, they were put on a filter paper in order to obviate excessive water and afterwords they were weighted.

We calculated the quantity of impregnated solution (ΔM): $\Delta m = m_2 - m_1$

The quantity of impregnated solution (ΔM) was expressed in percentage:

$$\Delta M = \frac{\Delta m}{m_1} * 100$$

The results can be seen in Table 1.

Table 1 Impregnation with sucrose solution at atmospheric pressure

t [min]	m ₁ [g]	m ₂ [g]	Δm [g]	ΔM [%]
10	12,298	12,675	0,377	3,06
20	11,463	11,894	0,431	3,76
40	12,119	12,773	0,611	5,04
60	12,755	13,441	0,686	5,38
100	13,124	0,738	1,862	5,63
140	13,507	14,302	0,795	5,89
180	11,864	12,591	0,727	6,13
220	12,396	13,157	0,761	6,14

For vacuum impregnation, the apple slices were weighted in the analytical scale(m1), they were introduced in sucrose solution, immersed with the help of a watch glass and kept at a

500 mbar void pressure for a different amount of time, from 4 to 16 minutes. When the time expired, the apples have been removed from the solution, they were put on a filter paper in order to obviate excessive water and afterwards they were weighted.

We calculated the quantity of impregnated solution and expressed it in percentage. The maximum amount of time to maintain the apple slices in the solution was established in order to obtain identical percentage of impregnated solution.

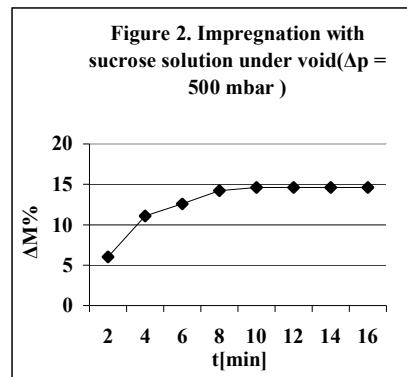
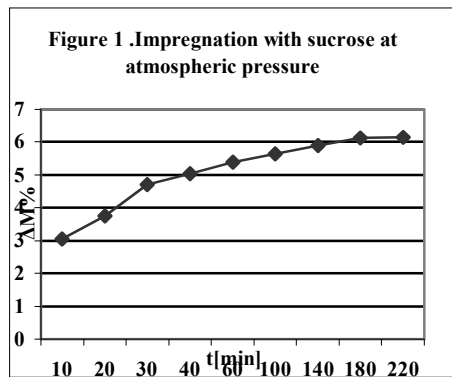
The results appear in Table 2.

Table 2 Impregnation with sucrose solution under void ($\Delta p = 500$ mbar)

t [min]	m ₁ [g]	m ₂ [g]	Δm [g]	ΔM [%]
2	12,163	12,891	0,728	5,985
4	13,146	14,602	1,456	11,07
6	12,409	13,97	1,561	12,58
8	11,482	13,113	1,631	14,21
10	12,424	14,332	1,908	14,63
12	13,06	14,968	1,908	14,61
14	12,833	14,71	1,877	14,62
16	11,658	13,363	1,705	14,63

Results and discussions

The results were presented graphically in Figure 1 for the impregnation realized under atmospheric pressure, while in figure 2 for the impregnation realized under vacuum.



Based on these results, we can observe the growth of apples' impregnation capacity under void, from 6, 14% to 14, and 63%. In the same time, the duration of the process is reduced 13.7 times, from 220 min to 16 min, therefore the advantages of this method are proven. The quantity of impregnated solution after 140 min at atmospheric pressure is close to the quantity impregnated after only two min under void.

In the case of vacuum impregnation, the percentage of mass augmentation (ΔM) is significant in the first six minutes due to the fact that in the first phase of the process, the air from the vegetal tissues is replaced with the solution that is to be impregnated.

Conclusions

Vacuum impregnation allows compounds that are nutritionally and technologically useful to be incorporated in vegetal products' structure. The impregnation duration is very short in comparison to classical infusion. The process doesn't lead to the loss of product compounds by making them soluble. Through vacuum impregnation, the air from the product's structure is replaced, therefore the air, a potential starter of oxidizing processes is removed.

References

1. Artes, F., Gomez, P., Aguayo, E. and Escalona, V. 2007. Improved strategies for keeping overall quality of fresh cut produce. *ISHS Acta Horticulturae* 746, Bangkok, Thailand.
2. Banjongsiniri, P., Kenney, J. and Wicker, L. 2004. Detection of vacuum infusion of Pectinmethylesterase in strawberry by activity staining. *Journal of Food Science*, Volume 69, Number 3, 179-183.
3. Banu, C. și colaboratorii. 2004, Principiile conservării produselor alimentare, 411, Editura AGIR, București.
4. Betoret, N., Puente, L. and Diaz M.J. 2002. Development of probiotic-enriched dried fruits by vacuum impregnation. *Journal of Food Engineering*, Volume 56, 273-277.
5. Cattaneo, T.M.P., Leva Avitabile, A. and Toreggiani, D. 2002. Improvement of strawberry ingredients using vacuum infusion: influence on the quality characteristics of strawberry yoghurt. *ISHS Acta Horticulturae* 587, Tampere, Finland
6. Park, S. and Zhao, Y. 2005. Vitamin E and mineral fortification in fresh-cut apples (Fuji) using vacuum impregnation. *Nutrition and Food Science*, Volume 35, Number 6, 393-402.
7. Rocha A. and Morais A. M. 2007. Role of minimally processed fruit and vegetables on the diet of the consumers in the XXXST century. *ISHS Acta Horticulturae* 746, Bangkok, Thailand.
8. Xie, J. and Zhao, Y. 2003. Nutritional enrichment of fresh apple (Royal Gala) by vacuum impregnation. *International Journal of Food Science and Nutrition*, Volume 54 Number 5, 387-398.
9. Xie, J. and Zhao, Y. 2004. Practice application of vacuum impregnation technology in fruit and vegetable processing. *Trends in Food Science and Technology*, Volume 15, Number 9, 434-451.
10. Zhang, X. 2007. New approaches on improving the quality and safety of fresh fruits and vegetable, *ISHS Acta Horticulturae* 746, Bangkok, Thailand.

PECTINASES FOR IMPROVING RASPBERRY AND BLACKBERRY JUICE PRODUCTION

RADU Dana Gina, GAVRILAȘ Simona, STĂNESCU Michaela Dina

"Aurel Vlaicu" University of Arad, 3 Elena Dragoi Str, RO-310330 Arad, Romania

Abstract

This paper presents a study concerning the technological effects of different commercial pectinases in the raspberry and blackberry juice production. Among different commercial pectinases proposed for juice extraction and clarification steps, the Biozym range could be successfully utilised for blackberry and raspberry juices from frozen berries, resulting in a higher yield and a better clarification. The vivid and appealing color, an important feature of the fruit juices and an enhanced fresh fruit flavor are achieved.

Keywords: commercial pectinases, raspberry juice, blackberry juice, clarification.

Introduction

The European Technology Platform on Food for Life Strategic Research Agenda 2007-2020 stated as a major research challenge – “To identify bioactive food constituents from plant, animal and microbial sources, and beneficial microorganisms and their mechanisms of action”; and as deliverables – “new product functions arising from new ingredients or from processing via biotechnology, separation technology or nanotechnology, understanding and predicting a) impact of bioactive compounds in food and beneficial microorganisms on human health, b) effect of food matrix formulation (structure, components) on the activity, delivery and transfer of bioactive compounds and beneficial microorganisms”¹.

The natural fruit juices are more and more part of a healthy diet due to their nutritional properties. These juices contain vitamins and anti-oxidants having improving the health state of the consumers.

Thus there is of interest to find new products with an improved quality. Raspberries and blackberries are good sources for fruit juices having a high content of vitamin C and also antioxidative properties, destroying free radicals which generate cancer and other diseases. Pectinases play an important role in the juice production due to the following actions: better yields in juice manufacture; preparation of pulp type juices; clarification of the juices; increasing the juice content in useful compounds; flavone derivatives hydrolysis with taste improvement^{2,3}.

A study of the technological effects of different commercial pectinases in the raspberry and blackberry juice preparation is presented. The improvement of the fabrication is explained based on the mechanism of enzyme interaction with the substrates.

Materials and methods

1. **Biozym® p. rossi** (Valley Research) is a granular pectolytic enzyme derived from a selected strain of *A. niger*, which has an overall activity of 140,000 AJDU/g, stabilized at a pH of 3.5, which is exempt from anthocyanasic activity. It is specific for maceration of

- red grapes: its high pectolytic activity accelerates extraction of colour; the hemicellulasic and arabanasic activities favor the freeing of tannins bond to the vacuole membrane and cell wall, with an increase in the overall extraction of all of the phenolic and aromatic compounds contained in the skin. It is stabile at extreme pH and temperature values. Biozym® p. rossi is active up to a temperature of 65°C; therefore it can be used in warm maceration for short periods of time. Advised dosages: 1-2 g/hl. ⁴
2. **Biozym® XP** (Valley Research) is a specific granular pectolytic enzyme for skin contact maceration of white grapes; the product is stabilised at low pH and purified by cinnamyl esterase activity (FCE). The equilibrium between the pectolytic and secondary activities (hemicellulasic and arabanasic) favors the disaggregation of the skin wall structure and extraction of the aromatic substances. Specific for skin maceration of white grapes in the press, it favours clarification, increases aromatic precursors in the must and free run juice yield, improving filterability. Advised dosages: skin maceration, 2– 3 g/q; must clarification, 1 – 2 g/hl. ⁴
 3. **BioPrep® 3000L** (Novo Nordisk) - a bacterial pectinase enzyme usually applied for bio-scouring of cotton fabrics.
 4. **Biozym® p. bianchi** is a granular pectolytic enzyme derived from a selected strain of *A. niger*, with a pectolytic activity of 150,000 AJDU/g, stabilized at pH 3.5. This enzyme hydrolyzes and depolymerises the pectin at low pH and temperatures. It is purified by cinnamyl esterase activity (FCE). Biozym® p. bianchi is the ideal product for the must clarification, even in extreme conditions, facilitating decanting, increasing the free-run juice yield, improving performance in filtering and favoring the extraction of the precursors of aromatic substances (thanks to specific secondary activities). Advised dosage: 0.5– 2 g/hl. ⁴
 5. Fresh ripe blackberries (*Rubus hirtus W.&K.*) and raspberries (*Rubus idaeus*) were carefully harvested, inspected for cleanliness and freezed at -21°C. Thawed berries were directly crush, and the first three different commercial pectolytic enzymes were added to the weighted pulp in amounts as producers recommended, for enzymatic maceration. A blank sample for raspberries and another one for blackberries with no enzyme added were manipulated identically. After three hour maceration at 30°C, all samples were pressed and the 4th pectolytic enzyme was added to the obtained juice, for clarification (at 30°C).

Results and discussion

After maceration, both raspberry and blackberry samples with Biozym® p. rossi and Biozym® XP proved to have better yields in juice than blank samples. Samples with BioPrep® 3000L didn't improve their yields in juice comparing to blanks, because the bacterial pectinases are active in an alkaline environment and the berry juices pH is 3,0 for blackberries and 3,47 for raspberries.

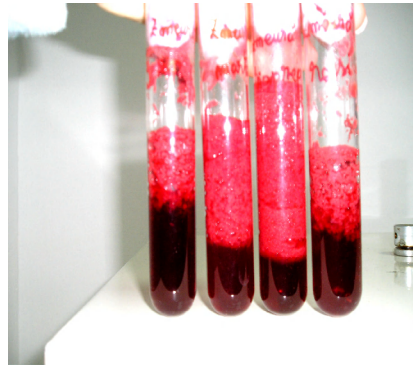


Fig. 1. Comparing raspberry juice sample yield and clarity

After only two hours, raspberry juice sample I (Biozym® Xp + Biozym® p. bianchi) was clarified, sample II (Biozym® p. rossi+ Biozym® p. bianchi) was a little less clarified and sample III (BioPrep® 3000L+ Biozym® p. bianchi) even less clarified. After 7 hours all raspberry samples tend to clarify (figure 1).

For the blackberry juice samples the clarification process was a little bit slower, but samples clarified in the same order. Remarkable was that even after 4 days at 4°C the blank was still cloudy (figure 2).

The fact that the average pectin content, expressed as (%w/w) calcium pectate was found to be 0.40 for raspberry, and 0.93 for blackberries, it justifies the slower clarification of blackberry juice samples.



Fig. 2. Comparing blackberry juice sample yield and clarity

CONCLUSIONS

In order to efficiently extract the juice from the cells of the skin and pulp of the berries, it is necessary to break up the cell wall, which has a protective function and maintains the consistency of the fruit, being made up of pectic acids and neutral substances, cellulose,

hemicelluloses and protein substances. Pressing the berries makes the juice rich in soluble pectin, which forms a colloid structure capable of holding solid parts in suspension and impurity, which does not favour sedimentation. The pectolytic enzymes used for clarification have various activities (poly-galacturonases, pectinliases, and pectinmethylesterases) capable of breaking the soluble chains of pectin and reducing the viscosity of the musts, thereby facilitating flocculation and separation of the solid parts. The Biozym range proposed for clarification of musts could be successfully utilised for blackberry and raspberry juices from frozen berries, resulting in a higher yield and a better clarification. The vivid and appealing color, an important feature of the fruit juices and an enhanced fresh fruit flavor are achieved.

References

1. European Technology Platform on Food for Life Strategic Research Agenda 2007-2020, http://etp.ciaa.be/documents/CIAA-ETP%20broch_LR.pdf
2. R.P. Bates, J.R. Morris and P.G. Crandall, Principles and practices of small - and medium - scale fruit juice processing, Food Science & Human Nutrition Department, University of Florida USA
3. A. R. Vicente, C. Ortugno, A. L. T. Powell, L. C. Greve, & J. M. Labavitch, Temporal Sequence of Cell Wall Disassembly Events in Developing Fruits. 1. Analysis of Raspberry (*Rubus idaeus*) *J. Agric. Food Chem.* **2007**, *55*, 4119-4124
4. www.intecwine.com/

WAYS TO IMPROVE BREAD QUALITY BY ENZYME USE

DIACONESCU Daniela , CHAMBRE Dorina

"Aurel Vlaicu" University of Arad, Revolutiei Bd., no. 77, Arad, zip 310130, Romania

Abstract

The aim of this study was to demonstrate that some enzymes can substitute the chemical additives in bread quality improving. Glucose oxidase, hemicellulase, xylanase, α -amylase, cellulase, amyloglucosidase and mixtures of them were used. Enzyme preparations were added in dough and then, the quality of dough and bread were analyzed in terms of stickiness of dough, bread volume, crumb porosity and elasticity and staling rate. All added enzymes act as improvers; they increase the bread volume, they improve the crumb properties and some of them prolong the freshness of bread. Taking all the quality properties of bread into account, the best improver seem to be xylanase-cellulase mixture.

Introduction

To fulfil the consumer request, baking industry must offer also products without chemical additives and to do that there are many ways by enzymes use. Exogenous enzymes are used in baking for improving the quality of baked products with aim to increase loaf volume, to improve crumb structure and crust colour and also to delay the bread staling. In this experimental work we used glucose oxidase, hemicellulase, xylanase, α -amylase, cellulase, amyloglucosidase and mixtures of theme.

Glucose oxidase is an oxidizing enzyme that has an effect similar to that of chemical oxidants: the improving of dough by increasing the resistance and decreasing the extensibility of the dough, the increasing of bread volume and the improving of crumb grain of bread. It appears that oxidation of water-soluble SH groups and the oxidative gelation of pentosans is the mechanism by which glucose oxidase improves the rheological properties of the dough [1], [2].

The hemicellulases are hydrolases which catalyze the hydrolysis of hemicelluloses, which are found in cell walls from both endosperm and grain cover. They are wall-degrading enzymes. The effect of hemicellulases on bread volume improvement results from the redistribution of water from the pentosan phase to the gluten phase. The increase in gluten volume fraction gives the gluten more extensibility, which results in a better oven spring [3].

The xylanase catalyses the hydrolysis of soluble and insoluble xylans and depending of its origin, it acts differently on dough and bread properties. Positive action of xylanase in dough can be explained by the diminution of insoluble xylans content and by the fact that the liberated water from hydrolyzed xylanase becomes available to gluten formation and as a result, bread volume is increased and crumb bread is softer [4].

To improve its effects, xylanase was added in mixture with α -amylase or cellulase. α -Amylase increases the bread volume and reduces the staling rate. Maat *et al* (1992) [5] reported that α -amylase added together with xylanase brings better baking results than individual enzymes. The cellulase catalyzes the hydrolysis of cellulose. Kulp, 1993 [6] reported that part of the pentosans are in a cellulose matrix and therefore also requires cellulase in addition to xylanase.

We added amyloglucosidase in dough because, by glucose forming, the fermentative activity of yeast was intensified and that had as result a bigger bread volume obtaining.

All this enzymes were added in dough and their effects on bread quality were analysed.

Experimental Part

Materials

It had been used a commercial white flour with normal breadmaking properties (12.75% proteins, water absorption 56.25%).

The enzyme preparations used were:

Fermizyme GO1500 (G) – enzyme preparation extracted from *Aspergillus niger* which comprised glucose oxidase with 1500 SARRET UNIT enzymatic activity/g (Overseas Bakery & Ingredients Romania SRL București);

Fermizyme I (H) – enzyme preparation extracted from *Trichoderma viride*, which comprised hemicellulase with 4100 XTU enzymatic activity/g (Overseas Bakery & Ingredients Romania SRL București);

***Bel`Ase C* - a pure diluted bacterial xylanase (Beldem Food Ingredients Romania).**

X503 (X+αA) – standard mixture of α-amylase and xylanase (Puratos Romania);

Fermizyme HE 400 (X+C) – standard mixture of xylanase and cellulase with 4000 LYX/g, 400 XVU/g enzymatic activity (Overseas Bakery & Ingredients Romania SRL București);

Fermizyme AG 800 (Ag) – enzyme preparation extracted from *Aspergillus niger* which comprised amyloglucosidase with 65000 AGI/g enzymatic activity (Overseas Bakery & Ingredients Romania SRL București).

Baking test

The recipe for bread was: 800g of flour, 13g of yeast, 13g of salt and 450g water according to the water absorption determined by farinograph. The dough was mixed into a laboratory mixer for 3 min. After the fermentation time – 60 min. at 25-30°C – dough pieces at 1000g were shaped in a long shape by hand and they were allowed to stay in the leavening chamber – 60 min. at 25-30°C. The breads were baked at 35 min. at 250°C. The enzyme preparations using limits were founded by attempts and only the levels which had maximum effects were elected.

The flour quality analysis were made according to STAS 90-77 and bread quality analysis were made according to STAS 91-83 [7].

Results and Discussion

The results of bread and dough quality analysis with different enzyme preparations are given in table 1.

Table 1. Dough and bread quality parameters

Enzyme preparation	G	H	X	X+αA	X+C	Ag
Level of preparation [g/100kgflour]	22	11	15	9	25	7
Stickiness of dough*	0	2	0	2	1	0
Specific volume [cm ³ /100g]	272	328	295	312	320	328
Volume increase [%]	4.2	26.1	13.0	20.9	30.6	31.5
Crumb porosity increase [%]	1,9	8.6	2,9	3.7	11.2	10.6
Crumb elasticity increase [%]	1	1	0	1	1	1
Staling rate	-	↓	-	↓	↓	-

*Sensory stickiness evaluation reported to corespondent control dough: 0 – not stickier; 1 – slightly stickier; 2 – sticky; 3 – very sticky.

Quality of dough

By adding the glucose oxidase, more elastic, drier and no sticky dough was obtained, with better mixing, fermentation and shaping tolerance.

The addition of hemicellulase from *Trichoderma viride* in dough caused significant increase of dough stickiness. Fermizyme I is an enzyme preparation which does not contain α -amylase, so the increase of dough stickiness is due to the increased solubility of cell walls.

The use of xylanase in breadmaking has positive effects like increasing of water absorption in dough (meaning better freshness for bread and increased yield), improving of dough stability and its mixing tolerance. No sticky dough was obtained.

The xylanase- α -amylase mixture brought a significant increase of dough stickiness and xylanase-cellulase mixture slightly increased the stickiness of dough.

Dough containing amyloglucosidase had not presented differences in report to correspondent control dough, regarding the stickiness.

Generally, the dough stickiness increases concomitantly with the intensity increase of positive effects in bread quality brought by added enzymes. In this way, we must try to find the proper dosage of enzyme preparation and the proper enzyme mixtures to improve the bread quality without simultaneous impairing of dough handling properties.

Quality of bread

All added enzymes act as improvers, as we see in tabel no.1.

The samples with glucose oxidase had better definite forms and they were higher than no enzyme sample. The maximum increase of specific volume (4.2%) appears to 22g level of *Fermizyme GO1500*/100kg flour. The crumb porosity increases very little without reaching 80%. The crumb elasticity had a good increase. Regarding the oxidizing degree, bread with glucose oxidase had a crumb structure, with a large number of elongated cells, with a distinct slip plane. It has not been detected any difference between samples and control regarding the staling rate up to 72 hours yet.

Addition of hemicellulase extracted from *Trichoderma viride* in bread results in larger loaf volume - a great volume increase (26.1%) -, softer crumb - a great crumb porosity increase (8.6%) and a good increase of crumb elasticity - and retarded staling - the staling rate of bread with enzyme preparation is lower than that of corresponding control bread. The optimum dose of enzyme preparation is 11g *Fermizyme I*/100kg flour.

All the samples with xylanase had better specific volumes and better crumb porosity than control bread (without xylanase), but the crumb elasticity was not modified. The maximum bread volume increase was 13% over bread control specific volume. All the samples had a delicate crumb texture, but regarding the staling rate it has not been observed any differences. The optimum dose of enzyme preparation is 15g *Bel Ase C*/100kg flour.

The maximum volume increase given by xylanase- α -amylase mixture in bread was 20.9%. The xylanase- α -amylase mixture increases crumb porosity (3.7%) and crumb elasticity and it reduces bread staling rate. The optimum dose of enzyme preparation is 9g *X503*/100kg flour.

The xylanase-cellulase mixture gave a very good volume increase (30,6%) and the best crumb porosity increases (11.2). It also increases crumb elasticity and reduces bread staling rate. The optimum dose of enzyme preparation is 25g *Fermizyme HE 400*/100kg flour.

The amyloglucosidase has the capacity to generate glucose from dextrans which results in improving the volume, taste and colour of bread. So, it gave the greater increase of volume (31.5%), a very good crumb porosity increase (10.6%) and a good crumb elasticity increase. Regarding the staling rate it has not been observed any differences in samples with amyloglucosidase in comparison with control sample. The optimum dose of enzyme preparation is 7g *Fermizyme AG 800*/100kg flour.

Conclusion

Glucose oxidase, xylanase and amyloglucosidase do not increase the stickiness of dough, but the rest of the enzyme preparations do, especially hemicellulase extracted from *Trichoderma viridae* and xylanase- α -amylase mixture.

All added enzymes act as improvers: they increase the bread volume, improve the crumb properties and some of them prolongs the freshness of bread. The best result was obtained with amyloglucosidase, regarding bread volume. It was also very efficient in increasing the crumb porosity, but not staling rate. If we want to prolong the freshness of bread we can use hemicellulase or mixtures like xylanase- α -amylase and xylanase-cellulase. Regarding the crumb porosity, the best result was obtained with xylanase-cellulase mixture. Taking all the quality properties of bread into account, the best improver seems to be xylanase-cellulase mixture.

So, we can use just enzyme preparations to improve the bread quality obtaining in same time a product with a good quality and without chemical additives.

References

- [1]. Vemulapalli, V., Miller, K.A., and Hosoney, R.C. 1998. Glucose oxidase in breadmaking systems. *Cereal Chem.* 75:439-442.
- [2]. Diaconescu, D., Popa, A. 2003. The effects of glucose-oxidase in bread. *Scientifical Researches Agroalimentary Processes and Technologies*, vol. IX. Ed. Agroprint Timisoara Romania. pg. 66-79.
- [3]. Laurikainen, T., Härkönen, H., Autio, K., and Poutanen, K. 1998. Effects of enzymes in fibre-enriched baking. *J. Sci. Agric.* 76:239-249.
- [4]. Diaconescu, D. 2004. Rezults of pure diluted, bacterial xylanase addition in bread. VI International Conference of Food University of Szeged. ISBN 9634826768.
- [5]. Maat, J., Verbakel, J., Stam, H., Santos de Silva, M.J., Bosse, M., Egmond, M.R., Hagemans, M.L.D., Gorcom, R.F.M., Hessing, J.G.M.1992. Xylanases and their application in bakery. In: *Xylans and Xylanases*. Eds. Elsevier Science Publishers, Amsterdam. The Netherlands, pp. 349-360.
- [6]. Kulp, K. 1993. Enzymes as dough improvers. In: *Advances in Baking Technology*, eds. Kamel B S & Stauffer C E. Blackie, Glasgow, UK, pp. 153-178.
- [7]. ***Romanian Professional Standards Collection: *Millng – Breadmaking*.

EVALUATION OF THE ANTIOXIDANT EFFECT OF *JUGLANDIS FOLIUM* EXTRACTS USING THE CHEMILUMINESCENCE TECHNIQUEDICU Anca¹, SEGAL Rodica²

¹University "Aurel Vlaicu" of Arad, Faculty of Food Engineering, Tourism and Environmental Protection, 2 Elena Drăgoi, Str., 310330, Arad, Romania, E-mail: anca1474@yahoo.com

²University „Dunărea de Jos”, 4 Domnească Str., 800008, Galați, Romania

Abstract

Antioxidants are natural or synthetic substances that have the capacity to warn free radicals formation. Antioxidant activity of natural produce reflected the activity of all antioxidants which are in their composition. Out of all classes of compounds with antioxidant activity a great attention is paid to phenolic compounds which have antioxidant properties (flavones, catequine, fenols, isoflavones) that are found in vegetal products, and which have antioxidant properties.

In this work were used aqueous and alcoholic extracts of *Juglandis folium*. These plants have in their composition different compounds with antioxidants properties and the obtained extracts have hypoglycemic and astringent effects. The antioxidant activity was measured using chemiluminescence technique. The results are presented in comparison to the activity of ascorbic acid.

Keywords: antioxidants, phenolic compounds, extracts, chemiluminescence technique

Introduction

The biogenesis of the uncombined radicals (UR) is of great interest and is one of the most important theoretically and applicative problems in this field. The formed URs are capable to degrade in oxidation reactions biological molecules, and their accumulation to cellular level and to entire organism releases oxidative stress.

As the growth of the knowledge about the UR and the oxidative stress aspects became more extensive, the interest for the studies on antioxidants grew, becoming a debated subject in biochemistry as well as in nourishment, pharmacology and medicine. Antioxidants are natural or synthetic substances with the capability of preventing the formation of URs.

The intensity of metabolic redox processes are conditioned by the nature and the existing nutrient content in food and can be limited by a few antioxidants: micronutrients from the vitamins A,C,E groups, minerals and biological active substances (bioflavons, proteic sulphur compounds).

Based on these considerations there is huge interest regarding the consumption of food and drinks prepared from plants rich in flavonols, flavons, catequines that are known to have active biological action against uncombined radicals accumulation. The efficiency of antioxidants consists in the synergy of their action, each of them functioning by similar or different mechanisms and at various levels of the UR evolution chain in the organism.[9]

In the present study aqueous and alcoholic extracts of walnut leaves that have antioxidant properties are used. Due to the presence of the antioxidant compounds present in the walnut leaves the obtained extracts have astringent and hypoglycemic activities. The obtained results have been related to ascorbic acid, a well known antioxidant. Various determination methods of antioxidant capacity are based on chemiluminescence and different fluorescence substances

are used in order to detect uncombined radicals and to measure the activity of antioxidants against oxygen' uncombined radicals.[3,5]

Experimental

Walnut leaves were collected from Banat region, Romania. Operational parameters, respectively the plants' mincing level, the plant/solvent relation, the extraction type and the extraction time were identical, the only difference was the type of solvent that was used: double distilled water and ethanol of different concentrations (50%, 70%,96%).

The aqueous vegetable extracts and the alcoholic ones have been obtained by the classic way: solid-liquid extraction, with reflux boiling for 2 minutes.

The resulted extracts are nominated as follows:

-aqueous extract -EA

-ethanol alcoholic extract 50%-EtOH50

-ethanol alcoholic extract 70%-EtOH70

-ethanol alcoholic extract 96%-EtOH96

For the antioxidant activity determination through chemiluminescence were used:

generator couple chemiluminescence luminol +H₂O₂, [LH₂] = 10⁻⁵ M, [H₂O₂] = 0,2 M buffer-HCL, la pH = 8,6;chemiluminometer TD20/20 (turner design, USA) ; aqueous and alcoholic plant extracts (96%,70%,50%) obtained as it follows:0,6 g of plant is boiled with 25 ml solvent, for 2 minutes, the extract is cooled down and filtered; ascorbic acid solution 0,4·10⁻³M.

The antioxidant activity was determined with CL using: (i) the system: luminol and hydrogen peroxider with pH=8,6 in the presence of the buffer TRIS+HCl, according to an adapted process [2]. The luminol was dissolved in DMSO (MERCK, GERMANY); (ii) chemiluminometer TD 20/20 (Turner Design, USA)

CL is a natural or provoked phenomenon,based on a physical mechanism, within which the resulting energy absorption in a chemical reaction determines the formation of some excited substances. The appearance of CL chemiluminescence emissions during some chemical reactions is known for a long time and it is connected to the intermediate uncombined radical formation.[4]. The antioxidant activity AA of vegetable extracts, in percentage, was calculated with the relation:

$$AA\% = \frac{I_0 - I_p}{I_0} \cdot 100$$

I_0 – the initial chemiluminescence emission of the blank sample

I_p - extract's chemiluminescence emission

Results and Discussion

Using the CL generator system composed by luminol (LH₂) and hydrogen peroxide, in a basic environment, it is distinguished a reduction in the intensity of chemiluminescence emission. The decrease of the chemiluminescence emission in time, exemplified for the alcoholic extract 70%,EtOH 70, is presented in Figure 1.

It is noticed that, in the first minute, the decrease of CL intensity for all extracts is the most important, and further to be slower, to the end of the reaction they reach a bearing.

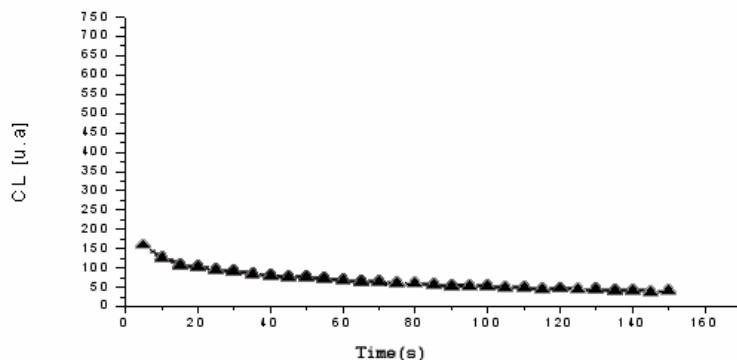


Fig. 1 CL intensity diminution for walnut extract

The calculated values for antioxidant activity for each extract, compared with the antioxidant activity of ascorbic acid (Asc) are presented in table 1:

Table 1 The total antioxidant activity values for vegetable extracts

Extracts	AA%				
	EA	EtOH 50	EtOH70	EtOH96	Asc
	90,04	97,83	98,1	95,14	98,2

Transposing the charted values to a graphic presentation, the antioxidant activities of walnuts extracts, related to the ascorbic acid activity is presented as shown:

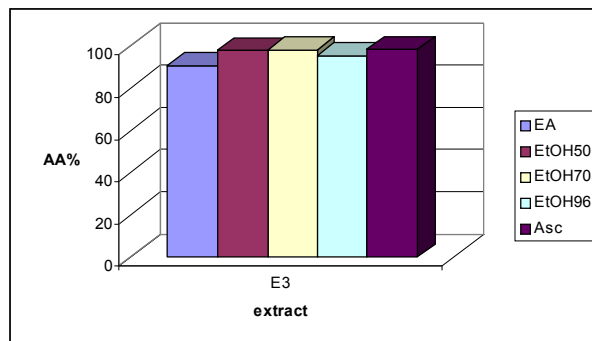


Fig. 2 Antioxidant activities for walnut extracts

One can notice that from all four types of extracts, the aqueous extract has the smallest values of antioxidant activities (with 8,16% smaller than the values obtained for ascorbic acid). The EtOH96 extract has the lowest activity, lower even then the ascorbic acid's (with 3,06%) and in comparison with the other two types of alcoholic extracts (EtOH50 - 2,69%, EtOH70 - 2,96%).

Conclusions

All analyzed extracts, aqueous and alcoholic, present antioxidant activity comparable to the ascorbic acid, but a strong dependence is observed and this is a function of the type of the solvent that is used for the preparation of extracts. In comparison to the aqueous extracts, in

most cases, a high antioxidant activity is observed for the alcoholic extracts, and among them EtOH70 has the highest value. The results obtained by chemiluminescence indicates that antioxidant activity of extracts can be assigned to flavonoid compounds present in the studied material, and to other structures as well (tanins, vitamins, complex compounds that contain rutoside)

References

1. Costin, G.M., Segal R., 1999, Functional food, Academica Publishing House, Galați,
2. Dicu, A., Rodica Segal, 2006, Spectral and Chemiluminescence characteristics of some plants with antidiabetic role, *Rev. Chim. (Bucharest)*, 57(1), 45-48
3. Desmarchelier, C., and colab., 1998, Antioxidant free radical scavenging effects in extracts of medicinal herb *Achyrocline satureioides*, *Braz. J. Med.Biol.Res.*, vol 31(9), 1163-1170
4. Olinescu, R., Greabu, Maria, 1987, Chemiluminescence and bioluminescence , Tehnică Publishing House, Bucharest
5. Pineda A., and colab., 1999, Capacidad antioxidante y potencial de sinergismo entre los principales constituyentes antioxidantes de algunos alimentos, *Rev. Cubana Aliment*, vol. 13, (2), 104-111;
6. Safta, M., 2002. Natural Super-Antioxidants n nourishment and medicine, Sudura Publishing House, Timișoara

**THE ACTION OF SOME CHEMICAL FERTILIZERS WITH MICROELEMENTS
BY UNIVERSOL AND FERTICARE I TYPE AND THEIR ACTION ON THIAMINE,
RIBOFLAVIN AND PYRIDOXINE CONTENT AT PISUM SATIVUM**

PALCU Sergiu E.¹

¹University "Aurel Vlaicu" of Arad, Faculty of Food Engineering, Tourism and
Environmental Protection, 2 Elena Drăgoi, Str., 310330, Arad, Romania, E-mail:
palcusergiu@yahoo.com

Abstract

Chemical fertilizers containing microelements are characterized by their permeability and excellent solubility, which make them highly efficient when used on any type of cultures regardless of the application method: at soil level or on the leaves, and for all irrigation methods. For experimentation we used the Börđi peas variety which is a semi-early maturing variety with wrinkled beans. Fertilization of experimental plots cultivated with pea was realised using two different microelements fertilizers: Universol Blue and Ferticare I, radically applied in the same time with irrigation water (fertirrigation). The use of Universol Blue and Ferticare I complex microelements fertilizers during vegetation period produces an increasing of hydrosoluble vitamins B₁, B₂ and B₆ content in peas. Appliance of Ferticare I fertilizer causes an important increase of vitamin B₆ quantity in green pea.

Keywords: pea, fertilizers with microelements, hydrosoluble vitamins, experimental parcels

Introduction

Fertilizers are mineral or organic substances applied on the soil or on the plants and are intended to replenish the necessary of nutritional substances of the plants in order to obtain horticultural products (vegetables) with a high content of hydro-soluble vitamins (B₁, B₂ and B₆) and to improve the growth and development conditions of the plants [1].

Together with enzymes and hormones, vitamins belong to catalyse category, substances which participate to regulation and stimulation of metabolically processes [6]. Among vegetables cultivated for green beans excels pea (fam. Papilionaceae). Experimental researches had been carried out during 2005-2007 period in Munar locality, Arad County, a favorable area for pea cultivation from pedoclimatical viewpoint.

Experiments aimed the following scientifically objectives: pea crop foundation Börđi variety, appliance of some complex chemical fertilizers with microelements during vegetation period, in order to stimulate and increase content of hydrosoluble vitamins B₁, B₂ and B₆ from peas, extraction, identification and dosing hydrosoluble vitamins B₁, B₂ and B₆ from peas through physico-chemical methods [4]. Due to the fact that microelements have a catalytic role and which are needed only in small quantities, their role is very complex and for this reason it is necessary to fertilize the crops with fertilizers containing microelements [2].

Experimental

For the experimentation we had used the Börđi peas variety which is a semi-early maturing variety with wrinkled beans [5]. Physical factors had been had in view and entered as part of an experiment which included 18 plots - 6 variants and 3 repetitions. As far as the field location and the dimensions of the experimental plots are concerned we took into

consideration that there was only one type of peas and two types of fertilization compared with the control plot.

All these experiments are characterized by the fact that, together with *fertilization* factor it had been also had in view the usage of fixed nitrogen from atmosphere by means of nitrogen fixing bacterium (bacterization). Used bacterial product for seeds treatment was Biotrofin biofertilizer [3].

Each experimental parcel has a rectangular surface, 1.5 m wide x 2.5 m long, this making a total surface of 3.75 square meters. The distances between the parcels of one repetitions is 0.3 m and respectively 0.5 meters. The experimental parcels were protected by cultivating a continuous protective strip at 0.5 meters from the parcels. All parcels including the protective strip were cultivated with pea [7].

The fertilization was made with two types of soluble fertilizers containing microelements. The doses of fertilizers used and presented in table 1.

Table 1. – Fertilization with Universol and Feticare I for the pea experimentation cultures

Plot / Variant	Specie	Fertilizer used	Recommended dose g/m ² /week	Dose applied per each variant g/(3,75 m ²)	Total dose per variant g/3 weeks
	Cultivated variety Pea				
Control (Mt)	Bördi	-	-	-	-
V ₂	Bördi	Universol	10	37,5	337,5
V ₃	Bördi	Universol	12,5	46,875	421,875
V ₄	Bördi	Universol	15	56,25	506,25
V ₅	Bördi	Feticare I	16	60,0	540
V ₆	Bördi	Feticare I	18	67,5	607,5

Results and Discussions

At the harvest of the 18 plots cultivated with pea, after 65 days of vegetation the results from table 2 were obtained.

As a conclusion for determinations that were effectuated on experimental field, cultivated with Bördi variety pea during 2005-2007, from pedoclimatical viewpoint, 2007 was the most favourable year because of the registered soil's temperatures and pH at experimental plots' foundation moment

Table 2. – Phonological observations on the experimentation fields cultivated with pea

Cultivated specie	Variants	Weight of pea shells with peas per variant (g)	Weight of pea shells with peas per each variant (3 × V)	Total number of pea-shells per variant
Pea: Bördi	Control (Mt)	5.200	14.700	815
	V ₂	6.220	16.940	996
	V ₃	6.480	16.190	1100
	V ₄	6.160	17.540	952
	V ₅	6.100	18.380	939
	V ₆	6.230	18.330	1011

Experimental results for quantitative determination of B₁, B₂ and B₆ vitamins from raw peas (Bördi variety), by means of chemical methods, are showed in Table 3 and 4.

Table 3. – Content of B₁ vitamins from peas (Bördi variety) obtained as part of fertilized experimental plots (2005-2007)

Experimental plot (variant)	Thiamin hydrochlorate mg/100 r.s. (method 1)			Thiamin hydrochlorate mg/100 g r.s. (method 2)		
	2005	2006	2007	2005	2006	2007
1 - Control	0,46	0,47	0,45	0,33	0,32	0,30
2 – Universol	0,63	0,60	0,62	0,48	0,41	0,44
3 – Universol	0,59	0,62	0,57	0,51	0,54	0,52
4 – Universol	0,54	0,55	0,53	0,42	0,43	0,42
5 – Ferticare	0,54	0,59	0,61	0,45	0,49	0,48
6 – Ferticare	0,65	0,65	0,64	0,57	0,58	0,59

Table 4. – Content of B₂ and B₆ vitamins from peas (Bördi variety) obtained as part of fertilized experimental plots (2005-2007)

Experimental plot (variant)	Riboflavin phosphate mg/100 g r.s.			Pyridoxine hydrochlorate mg/100 g r.s.		
	2005	2006	2007	2005	2006	2007
1 - Control	0,12	0,12	0,09	0,15	0,14	0,15
2 – Universol	0,16	0,16	0,14	0,24	0,27	0,26
3 – Universol	0,15	0,17	0,15	0,42	0,42	0,41
4 – Universol	0,14	0,15	0,16	0,30	0,34	0,32
5 – Ferticare	0,18	0,16	0,18	0,39	0,38	0,41
6 – Ferticare	0,19	0,18	0,19	0,51	0,53	0,54

In accordance with data from Table 3 and 4, values of vitamin concentrations established for control plots in 2005 show minor variations related to vitamin concentrations established for control plots in 2006 (ex. 0,14 mg pyridoxine hydrochlorate/100 g r.s. for 2006 related to 0,15 mg pyridoxine hydrochlorate/100 g r.s. for 2005).

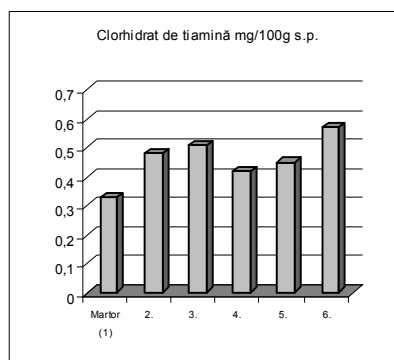


Figure 1 - Concentration values of B₁ vitamin in green pea beans obtained on the experimental plots (year 2005)

On the other hand, for fertilized plots there are registered significant differences (ex. 0,48 mg thiamin hydrochlorate/100 g r.s. in 2005 comparative with 0,41 mg thiamin hydrochlorate/100 g r.s. in 2006).

Referring to control variants (unfertilized plots), it can be observed that the concentrations of hydrosoluble vitamins B₁, B₂ and B₆ for 2007 show insignificant differences comparative to the values registered in 2005 and 2006 (ex. the quantities of vitamin B₁ of peas proceeded from control plots are: 0,33, 0,32 and 0,30 mg thiamin hydrochlorate/100 g r.s.– Method 2).

Significant increases were obtained for both years 2006 and 2007. For example, experimental results of the year 2005 by means of chemical methods are showed in figure 1, 2 and 3.

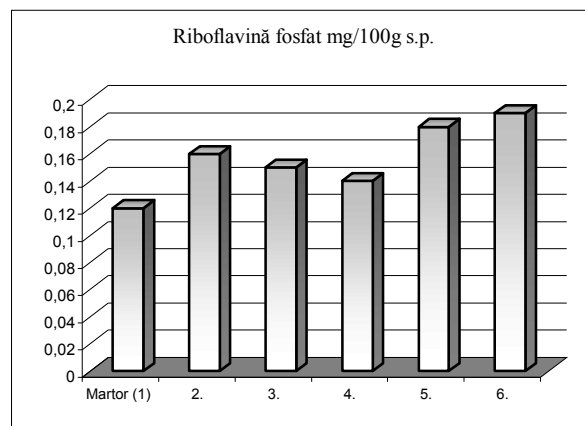


Figure 2 - Concentration values of B₂ vitamin in green pea beans obtained on the experimental plots (year 2005)

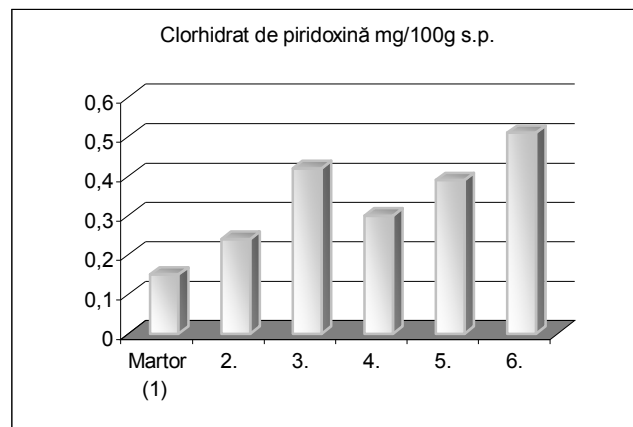


Figure 3 - Concentration values of B₆ vitamin in green pea beans obtained on the experimental plots (year 2005)

Conclusions

In agreement with data from Table 3, values of vitamin concentrations established for control plots in 2005 show minor variations related to vitamin concentrations established for control plots in 2006 (ex. 0,14 mg pyridoxine hydrochlorate/100 g r.s. for 2006 related to 0,15 mg pyridoxine hydrochlorate/100 g r.s. for 2005). On the other hand, for fertilized plots there are registered significant differences (ex. 0,48 mg thiamin hydrochlorate/100 g r.s. in 2005 comparative with 0,41 mg thiamin hydrochlorate/100 g r.s. in 2006).

Performed researches demonstrate that the best results when microelements chemical fertilizers were used at pea, were obtained when Universol Blue is given with a dose of 15 g/m² cultivated surface and when Feticare I is given with a dose of 16 g/m² cultivated surface. Concerning 2005, the highest quantities of thiamin, riboflavin and pyridoxine were registered at samples of peas proceeded from plots number 6, fertilized with Feticare I in doses of 180 kg/ha for 3 times.

For 2006, by applying Feticare I fertilizer, in peas can be observed an increasing of thiamin quantity for 1,2-1,5 times, riboflavin quantity for 1,3-1,5 times and pyridoxine quantity for 2,5-3,5 times.

In 2007, by using Feticare I fertilizer with a dose of 180 kg/ha in three different moments, can be noticed a significant increase of vitamin B₆ quantity in peas, for 3,6 times higher than the control.

The use of Universol Blue and Feticare I complex microelements fertilizers during vegetation period produces an increasing of hydrosoluble vitamins B₁, B₂ and B₆ content in peas. Also, appliance of Feticare I fertilizer causes an important increase of vitamin B₆ quantity, comparative with vitamins B₁ and B₂.

It can be also noticed that from toxicological viewpoint, doses of microelements fertilizers applied during vegetation period doesn't cause problems concerning consumers' health, as a consequence of peas consumption.

References

1. Andrews M., Sprent J.I., Raven J.A., Eady P.E., 1999 – Relationships between shoot to root ratio, growth and leaf soluble protein concentration of *Pisum sativum*, *Phaseolus vulgaris* and *Triticum aestivum* under different nutrient deficiencies, *Plant, Cell and Environment*, 22, 949-958
2. Gherghi A., Burzo I., Bibicu Miruna, Mărgineanu Liana, Bădulescu Liliana, 2001 – Fruits and vegetable biochemistry and physiology, Editura Academiei Române, București
3. Indrea D., Apahidean S.A.I., Apahidean Maria, Măniuțiu D.N., Sima Rodica, 2007 – Vegetable cultivation, Editura Ceres, București
4. Palcu S.E., 2008 – Researches concerning extraction technology of hydrosoluble B complex vitamins by using some garden and agricultural crop plants as raw material, Teză de doctorat
5. Popescu V., Atanasiu N., 2001 – Vegetable cultivation, vol.3, Editura Ceres, București
6. Neamțu G., 1996 – Natural substances with biological activity, vol.I, Vitamine, Editura Ceres, București, pp.201 – 220
7. Official catalogue for plants used in cultures in Romania, ediția 2004, Editura Printexim, București, ISTIS

INFLUENCE OF VACUUM PACKAGING ON THE SENSORY CHARACTERISTICS OF MEAT

POP Gabriela, BUCULEI Amelia

“Stefan cel Mare” University of Suceava, Food Engineering Faculty, Universitatii str., nr.13, Suceva, cod 720246, gabriela.pop@usv.ro, ameliab@usv.ro

Abstract

The evolution of the sensory characteristics is influenced by the preservation technology used in strong connection with the changes of physical, chemical, biochemical and microbiological nature that take place during the processing and preservation of the food product. In our experiments, we compare the sensory characteristics of meat in various conditions of packaging, storage time and temperatures. Comparatively with the meat preserved in classic refrigeration conditions the vacuum packaging presented more advantages regarding the sensory qualities. During the entire storage in refrigerating conditions the vacuum packed meat maintained its faded-pink color, a fresh smell and an acceptable appearance and consistence.

Keywords: vacuum packaging, meat, sensory characteristics

Introduction

The preservation of food was initially manifested empirically. In time there have appeared and imposed preservation techniques conditioned by the social evolution and the industrial development. The preservation techniques of foods developed and mingled the purpose being just one: ensuring the stability of food products for a longer period of time, without affecting their initial quality. Food preservation is in fact a stage in the technical circuit of merchandize (from supplier to beneficiary) that depends on a series of influential factors both internal (agregation state, structure, density, humidity, chemical composition, resistance to the action of the corrosion agents, behaviours regarding acids, basis and oxygen) and external factors (biological, mechanical, the type of package and nature of manufacture, the storage conditions). The existence of on equilibrium between the internal and external factors determines the optimum conditions that ensure the preservation of products for a longer period of time.

Materials and Methods

In our study as raw material we used pork muscles in a refrigerating state (from 0 to 24 hours after the slaughter). The samples was prepared like in figure 1, according to the following stages: i) Pork muscle; ii) Slicing; iii) Weighting; iv) Vacuum packing; v) Storage; vi) Sensory Examination



Fig.1 Pork muscle before slicing



Fig..2 – Pork muscle vacuum packed

Like packaging materials we used plastic with characteristic shown in table 1.

Table 1 Characteristic of the plastic package used for the vacuum package

Package	Package traits (at 23 ^o C and 0% U.R.)		
	Permeability at O ₂ (cm ³ /m ² 24 h atm)	Permeability at CO ₂ (cm ³ /m ² 24 h atm)	Permeability at H ₂ O vapors (cm ³ /m ² 24 h atm)
Zepter	< 30	150-200	unspecified

The packing was realized in vacuum at atmospheric pressure, using home type equipment Vacsy System produced by Zepter International.

The appreciations of meat quality is done by sensory methods the using of these methods represent an compulsory stage in the sensory quality appreciation of a food product and alones the establishing of the general clear characteristics that differ the fresh products from the one touched by time storing and the underlining of the particular traits of individual or mixed compounds that give the taste and the flavors of a specific food product. Usually no equipment or instrument can perceive the complex sensation as those perceived by the consumer through his perception organs. Due to the fact that the measure instrument is represented by the human perception organs (with their specificity and physic or variation the sensory methods have a subjective character). The sensory examination consists in the registration of the olfactory (smell) gustative (taste), tactile and optical (appearance, color) sensations, determined in the process of sample examination. The establishing of the sensory characteristics of meat is done in a certain order being underlined the appearance, the color, the consistency, the smell.

Results and discussion

In order to appreciate the sensory qualities of meat the following characteristics must be taken into account: the color, the flavor (smell and taste), freshness consistence, texture The evolution of the sensory characteristics is influenced by the preservation technology used in strong connection with the changes of physical, chemical, biochemical and microbiological nature that take place during the processing and preservation of the food product. The intensity of the changes that can be induced by a preservation technology at the level of the sensory characteristics of a product it is considered to be criteria of appreciation of its efficiency. On the other hand, the changes of the sensory characteristics signal both the possible appearance of some defects as well as the reason for the altering of the product. In order to exam the influence of vacuum packaging on meat quality, we compare the samples which were storage unpacked and vacuum packed at 0-4^oC (table 2).

Comparing the evolution of the sensory characteristics for unpacked and packed meat depending on the storage conditions (0-4C) and storage time we can draw the following conclusions: the vacuum packed meat does not suffer significant color changes during the storage time, unlike the unpacked meat kept in the same storage condition. The color of the unpacked meat gradually transforms negatively along with the growing period of storage time.

Immediately after the packaging the meat presented different color characteristics against the fresh meat the cause of them being probably the partial reduction of oxygen. During the entire storage in refrigerating conditions the vacuum packed meat maintained its color being noticed a certain degree of discoloration on its surface against the inner areas of the muscular tissue. The causes of discoloration of the outer layer of muscular tissue are generated by the pH of the meat and loss of juice. The pH maintenance at low values determines a "closed" meat structure as well as the modification of water distribution in the extra and intra cellular spaces so that percentage of light reflected increases and the color of the meat becomes brighter

Table 2 The sensory characteristics of meat depending on the storage condition (0- 4°C) and the storage time

Characteristic	Storage time	Vacuum packed meat	Unpacked meat
Appearance	Initially	At the surface the meat is slightly humid in the section it is slightly humid; at finger pressure it give a sensation of cold without being sticky; the fat is white, pink – white, soft and when touching it gives a grease sensation.	At the surface the meat has a dry covering; in the section it is slightly humid; when pressing with the finger it gives a coldness sensation without being sticky; the fat is white or pink-white colored, soft and when touching it is gives a grease sensation.
	2 days	At the surface it is partially covered by a sticky mucus, the fat has an opaque color; in the section it is slightly humid	At the surface it is partially covered with a sticky mucus in small quantity; the fat has an opaque color and in section is slightly humid
	4 days	At the surface the meat has a humid coverage and also sticky due to the mucus formed; in the section it is slightly humid; the fat is opaque.	At the surface the meat has a humid and sticky cover due to the formed mucus; in the section is slightly humid; the fat has an opaque color
	6 days	The surface of the meat is humid and sticky; the section is very humid and sticky.	The surface of the meat is humid and sticky the section is humid and very sticky.
Color	Initially	At the surface there is a normal pink faded color; in the section the characteristic color is pink – red.	At the surface it has a normal pink faded color; in the section the characteristic color is pink-red; the muscle juice is hardly obtained but it is clear.
	2 days	At the surface the color is pink faded in	At the surface the color is

		the section the color is opaque pink the muscle juice is not very clear.	opaque, pink-reddish; in the section it is opaque pink; the muscle juice is not so clear
	4 days	At the surface the color is pink but it can be observed a discoloration against the initial color.	At the surface the color is pink but it can be observed a discoloration against the initial color.
	6 days	At the surface the color is pink but different from that of the initial meat	At the surface the color is pink- slightly greenish.
Consistency	Initially	Both compact and flexible at the surface as well as in the section; there are no finger prints left after pressing.	Both compact and flexible at the surface as well as in the section, there are no finger prints left after pressing.
	2 days	The meat is both flexible and soft at the surface as well as in the section; the finger prints left after pressing easily disappear.	The meat is flexible and soft both at the surface as well as in the section; the traits left after finger pressing easily disappear.
	4 days	Diminished consistency; both at the surface as well as in the section the finger prints left after pressing persist longer.	Diminished consistency at the surface and in the section, the traits left after finger pressing persist longer.
	6 days	Diminished consistency; both at the surface as well in the section remains a finger print after pressing	Diminished consistency at the surface and in the section, the traits persist for a very long time.
Smell	Initially	Pleasant characteristic for fresh meat; after cooking the smell of the meat was appreciated as very pleasant specific for steak in general.	Pleasant, characteristic to the species, after cooking the smell of the meat was appreciated as very pleasant specific for steak in general.
	2 days	The smell is a little bit different from that of the initial meat and it is a little bit sour.	The smell is a little bit different from that of the initial meat it is a little bit sour.
	4 days	At the surface it is perceived a sour/acid smell.	At the surface it is perceived a sour acid smell and a little bit as the one of un fresh meat.
	6 days	Sour/Acid smells and a little bit of unfreshness.	Sour/acid smell and a little bit rancid; in the inner layers it can be perceived a stronger rancid smell.

The smell of vacuum packed meat has a series of particularities due to the microbiological and biochemical modifications that take place during the storage. The smell profile established after the sensory experiment has the following basic components: the sour/ acid smell and the smell of unfreshness. The presence of other odors characteristic to the altered meat wasn't noticed. Generally the smell of vacuum packed meat was appreciated as pleasant, characteristic for a fresh meat. During the storage, due to the modifications that take place in the proteic system there was also identified the unfresh smell whose intensity was less strong against the unpacked meat.

Comparatively with the unpacked meat the consistency of the vacuum packed samples was stronger. Starting with the 6th day of storage after finger pressing a finger print remains

because the tissue has lost from it flexibility. Unlike the unpacked meat, the vacuum packed meat didn't show any visible modifications the appearance of the muscular tissue being unmodified from the beginning.

Conclusions

After the experimental studies performed in order to identify the particular traits that the vacuum packaging as a preservation method has, we can draw the following conclusions regarding the evolution of the sensory characteristic as a result of the biochemical processes: 1. Immediately after the packaging the meat presented different color traits against the fresh meat the cause of these modifications being probably the reduction of the partial oxygen pressure; 2. Comparatively with the meat preserved in classic refrigeration conditions the vacuum packaging presented more advantages from the color maintenance point of view. Also, during the entire storage in refrigerating conditions the vacuum packed meat maintained its faded-pink color being observed a certain degree of surface discoloration against the inner layers of the muscular tissue; 3. The smell of vacuum packed meat presents a series of features due to the microbiological and biochemical modifications that take place during the storage.

References

1. Banu, C., *Calitatea si controlul calitatii produselor alimentare*, Editura AGIR, Bucuresti, 2002;
2. Daraba, A., *Conservarea carnii sub vid*, Editura Didactica si Pedagogica, Bucuresti, 2007;
3. Daraba, A., *Evaluarea calitatii carnii*, Editura Didactică si Pedagogică, Bucuresti, 2007;

ASPECTS OF LIFE IN ROMANIAN RURAL COMMUNITIES

MATEOC Teodor¹, MATEOC-SÎRB Nicoleta¹, ȘEULEAN Victoria², MĂNESCU Camelia¹

¹University of Agricultural Sciences and Veterinary Medicine of Banat, Timișoara,
Calea Aradului, Nr. 119, mateocnicol@yahoo.com

²West University of Timișoara, Blvd. V. Pârvan, nr. 4, 300223

Abstract

Though in the developed economies there is a trend to remove differences between rural and urban from the points of view of accommodation, infrastructure development, and ensuring services necessary for the population, which has resulted in a loss of significance of the traditional perception of the rural area as underdeveloped area, in Romania there is still a major discrepancy between rural and urban which is not beneficial for the Romanian rural area. Starting from these premises, we think that an analysis of the life quality in the Romanian rural area is opportune, taking into account that in the 12,946 villages of present Romania live over 45% (about 9.7 million inhabitants) of Romania's population in conditions unbelievable for the 21st century and for the 3rd millennium when science and technology are very advanced worldwide in all the fields of activity; this is also the time in which globalisation as a phenomenon resulted in economic integration both regionally and worldwide as a result of the large-scale promotion of information technologies (e.g. the Internet), of the removal of artificial barriers from the circulation of goods, services, capital, knowledge, and people.

Keywords: rural infrastructure, unsatisfactory service, low income, implications, access to education, poverty, inequality

Introduction

In order to capture a most exact situation of life quality, i.e. of life conditions in the rural area, we have structured the main aspects aiming at the studied issue, in three important parts: (i) infrastructure and services in the rural area; (ii) economic growth and income as factors of development; (iii) rural population and access to education.

Materials and methods

As working material, we have used partial results from our research in the field due to a grant over the period 2006-2007, by researchers of the USAMVB Timișoara in partnership with other 7 institutions in the country.

We have carried out field surveys at household level and a monographic study of the commune per localities, in the following counties: Timiș, Arad, Bihor, and Caraș-Severin.

As for the field surveys, at household level we monitored random samples establishing 50-60 households per commune. The households have been chosen after a certain numbering step of the total household number, on the ground of the household list and of the house number.

The method we have used, named "pole survey", focused on the achievement of representativity on the ground of a questionnaire whose answers and observations were collected and mentioned by the operators. At the level of each locality, the team operating the questionnaire was made up of 6-10 operators guided by teaching staff.

Presentation and analysis of the localities covered by the survey were done with the help of a commune monographic study, using a guide containing the following chapters: name of the locality, short history, physical and geographical presentation of the locality (space and natural conditions, morphological structure of the locality), infrastructure of the locality (present and future state), habitat (houses, yards, households, dwellings), demographic structures (population, labour force, migration and commutism), and commune economics.

Results and discussion

Infrastructure and services in the rural area

Romania is facing at present a major discrepancy between the rural and urban areas from the point of view of the social and physical infrastructure. We analyse below a few indicators considered important to ensure life quality in the rural area.

In the rural area, the most important access ways are the roads, but the present road network covers only 60% of the needs of the rural population and, moreover, over 25% of the communes cannot use their roads when it rains (World Bank Study, 2004).

The analysis carried out shows that the worst road state is in the Caraş-Severin County, followed by the Bihor, Arad, and Timiș counties. There are localities which, from a tourism point of view, could develop economically but the road state prevents it.

In Romania, of the total public roads, 80% are county roads and communal roads. According to the Statistic Year Book for 2006, only 10.6% of these roads have been modernised, of which 30.7% have been asphalted. In 2005, public roads in Romania covered 79,904 km; through the SAPARD Program, they have developed and modernised only 2,058 km, which represents very little of the necessary infrastructure. As for the drinking water supply, only 33% of the rural population has access to the public water network; when speaking of the warm water network, the situation is even more critical. About 70% of the rural households use wells to get their necessary amounts of water. For example, in most wells in the Bihor County, nitrite and nitrate content is above maximum admitted limit and yet the inhabitants keep drinking the water in these wells. The public sewage network assist only 10% of the total rural population, determining a major risk of polluting the water table, particularly where the sewage network has not been developed together with the water supply networks. Lack of sewing systems contributes mostly to soil and water table pollution.

Thermal energy is very little used in the rural area: only 0.5% of the total thermal energy is distributed in the rural area, compared to the urban area where the percentage reaches 58%.

Rural infrastructure in the field of communications is very poor from all the points of view: there are 138 Internet users per 1000 inhabitants and 92 computers per 1000 inhabitants.

Population's access to medical services is hindered by the deficit transport services, and the quality of medical services is hindered by the very old or even absent medical equipment, by the low number of doctors, and by the professional skill level of the medical staff. In most communes, there are only basic medical services. In order to benefit from specialised services, inhabitants of rural areas have to go to town.

Economic growth and income as factors of development

Development, as a complex factor, is, economically, the capacity of a national economy of generating and supporting annual growth through the prism of macro-economic indicators. Economic development is often seen as a continuous growth Gross Domestic Product phenomenon per both economy on the whole and inhabitant.

This approach does not, unfortunately, solve such particular issues as poverty, unemployment, and uneven income distribution. These issues, if left unsolved, expand and aggravate.

Poverty rate in Romania increased from 4% in 1989 to 20% in 1993 reaching in 2000 the highest level ever – 35.9% of the country’s population.

Between 2000 and 2006, as a result of economic growth (the Gross Domestic Product increased with 5-6% yearly), poverty rate diminished with 13.8%, i.e. there were still 3 million people in absolute poverty in 2006.

Rural areas are marked by vulnerability since incomes are based mainly on incomes from subsistence agriculture, which means that in unfavourable agricultural years poverty rate risks to increase considerably and have a bad impact on rural area children’s access to education and training.

Income inequality has had an evolution in strict opposition to poverty rate. Income inequality decreased during periods of economic regression and started to increase with economic growth, so that the gap between the poorest and the richest has been larger and larger particularly after 2000.

Compared to other European nations, income inequality in Romania has had among the highest values in the European Union.

As for the unemployment rate in Romania, it has had an ascending trend after 2000 (Table 1).

Table 1. Unemployment rate evolution in Romania (2001-2006)

Year	2001	2002	2003	2004	2005	2006
Unemployment rate (%)	8.8	8.4	7.4	6.3	5.9	5.2

Source: Romania’s Statistic Yearbook

The number of unemployed people in the rural area represents 33% of the total number of unemployed people in Romania, with ‘masked unemployment’ as a basic phenomenon.

Per age groups, the highest unemployment rate was at the level of young rural population, with ages between 15 and 24 years (13.9%).

The precarious situation of the incomes from the rural area pleads in favour of the necessity for developing a diversified rural economy, with emphasis on the developing potential in the non-agricultural sector as a sustainable source for the living conditions of the communities in the rural area and for the development of rural economy.

In rural areas, the average income per capita is about 95€, while in the urban area it reaches 135€. At the level of rural households, the income comes particularly from agricultural production, ensuring 43.4% of the total income. The average of the income from non-agricultural activities at the level of households was in 2005 about 12€ per month, i.e. 4.1% of the net income.

At present, rural economy is characterized by a low degree of diversification and by a dependence on agricultural activities that determines the maintenance of low income levels for the populations live in rural area.

Rural population and access to education

The issue of labor occupancy is directly linked to that of ensuring incomes and to the issue of life quality at individual and social levels.

In rural areas, because of the low density of population (45.1 inhabitants per km²), there is low interest in investors. A proper infrastructure and quality services could contribute to the development of jobs and better living conditions for the rural population.

The banking sector is not interested in financing rural business since they are perceived as risky; this is why there is a trend for the banking sector to diminish its activity in the rural area

because of the low profitability rate. This aggravates the financial situation of economic agents in the rural area and, as a consequence, they hinder rural economic development.

The diversification of rural economy also depends on the level of education, knowledge and professional skills. Though infrastructure is an important element in the social and economic development of the rural area, professional training and primary education are the main instruments of good development through the conversion of the agricultural labour force into non-agricultural labor force. The number of educational institutions in the rural area decreased as a result of restructuring the educational system and of the lack of trained teachers.

Though rural population represents 45.1% of the total Romanian population, the degree of participation in the rural area in the academic year 2005-2006 was 31.5% of the total population enrolled in education. In the rural area, over 30% of the population aged 15 has not graduated from school or only graduated from primary school.

In 2007, only 24.54% of the students in the rural area managed to attend high school courses, in decline from the year 2005 when the percentage was 36,0%. The share of students in the rural area attending high school decreases from one year to another, which is rather worrying.

The share of rural population with a high level of education represents 1.8% of the total population ages over 15 as a consequence of low incomes. There is a direct relation between the educational level and poverty; this is why stability of incomes in a family has considerable impacts on the participation to the educational acts.

Children from families with low incomes are twice more exposed to school abandonment, compared to children from families with a stable income source.

Conclusions

The present situation of roads, running water, and sewage network affects considerably the life quality of the rural population and is an impediment in the development of economic activities in rural areas. The access of rural population to basic education and to health services is hindered by the transportation services and by the lack of incomes. Deficit infrastructure results in a low interest in investments and hinders the development of rural economy. The banking sector is not interested in financing rural business, they are considerate is not efficient. The low level of instruction and education is reflected by the quality of labour force in the rural area, a restrictive factor for the perspectives of diversification of economic activities. Population occupancy rate in the rural area from the total active population in the rural area is as follows: 64.2% in the primary sector, 18.7% in the secondary sector, and 17.1% in the tertiary sector. The precarious situation of incomes in the rural area pleads for the necessity of developing a diversified rural economy. The general objectives of the national strategy for rural development over the period 2007-2013 are: (i) increasing the economic dynamics of rural areas in Romania, including sustainable development of the agricultural and forestry sectors; (ii) preserving and improving the environment; (iii) increasing social and life quality dynamics in the rural areas.

These objectives correlate with the EC Regulation No. 1698/2005 as well as with the strategic directions of development of the EEC.

All these aspects characterize the Romanian rural area. Each rural community has its own specific problems that need special approach. Solving these specific problems is the task of local authorities and of the local mayor that should very well know the needs of the inhabitants of the community in which he/she lives.

References

I.Man, T. E., Nicoleta Mateoc-Sîrb, 2008, Dezvoltarea rurală și regională durabilă a satului românesc, Editura Politehnica, Timișoara

2. Otiman, P. I. et al., 2006, Dezvoltarea rurală și regională durabilă a satului românesc, Editura Academiei, București
3. ***Anuarul Statistic al României colecție
4. ***Barometrul Opiniei Publice (BOP) 1998-2007, realizat de Fundația Soros
5. ***INS - Tendințe Sociale 2006
6. ***Planul Național Strategic pentru Dezvoltare Rurală 2007-2013

DEVELOPMENT OF AGRICULTURAL INSURANCE MARKET IN ROMANIAMATEOC Teodor¹, ŞEULEAN Victoria², MATEOC-SÎRB Nicoleta¹¹ University of Agricultural Sciences and Veterinary Medicine of Banat, Timișoara, Calea Aradului, Nr. 119; ² West University of Timișoara, Blvd. V. Pârvan, nr. 4, 300223
victoriaseulean@yahoo.com**Abstract**

Maintaining a certain degree of certainty among agricultural producers about the possibility of obtaining stable and efficient results makes it necessary to have protection through insurance and re-insurance in the field. In this respect, in this paper we intend to make an analysis of the degree of penetration of agricultural crop insurance in Romania as well as of the involvement of the state as an insurer. The conclusion of the authors is that of the 43 insurance companies operating on the Romanian market, only 11 offer agricultural insurance policies. The degree of coverage by insurance of agricultural areas in the year 2006-2007 is only 17%, i.e. only 1.8 million ha are insured out of 10.5 million ha. Insured areas have only increased with about 20-25% compared to the agricultural year 2005-2006. In order to reach the level of industrially developed nations in the European Union, where the degree of coverage by agricultural insurance is, on the average, 65-70%, Romania still has a segment of 48-53% that should be insured of the total insurable agricultural areas.

Keywords: agricultural crop insurance, subscribed raw premiums, damage rate, insurance coverage

Introduction

Natural calamities and other highly dangerous situations existing in agriculture are the factors that can overturn the results of the agricultural process. That is why maintaining a certain degree of certitude in what concerns stable and efficient results implies the protection through insurance and reinsurance in this field.

Materials and Methods

As a working material the authors have used information and statistics data published in different papers or specialty books and as a working method we have used observation, analysis, selection, comparison, and statistics interpretation.

Results and discussion*Recent developments of agricultural insurance in Romania*

Agricultural insurance practiced at present in Romania aim at achieving the compensation function of the damage by natural calamities and by different accidents and diseases as well as the prevention function of damages. In this respect, the main categories of specific insurance practiced in the field aim at the following: (i) insuring agricultural crops and vineyard and orchard produce; (ii) insuring the livestock.

Risks such insurances protect from are, in a non-exhaustive order, as follows: excessive, time-persisting drought that affects non-irrigated lands; floods caused by rivers or other water courses or from dam break; abundant and long-lasting rainfalls; excessively low temperatures, below plants' biological resistance limit; thick layer of snow that damages vegetal and animal sectors; sudden melting of the snows that cause floods from rivers and marshing; hurricanes and other disasters and catastrophes caused over extended areas. *Largo sensu*, they consider natural calamities quantitative and qualitative crop losses, mortality and/or necessity slaughtering of the livestock caused by the destructive power of natural phenomena and

diseases over wide areas.

Naming and grouping within diseases categories causing natural calamities in plants and animals is done by the Ministry of Agriculture, Food and Forests and is acknowledged by Government's Decision. At present, in Romania agricultural insurance are practiced by a limited number of insurers, among which: FATA Asigurări, ASIROM S.A., OMNIASIG S.A., ALLIANZ ȚIRIAC S.A., and others.

Optional insurance in agriculture has been relatively low. In the agricultural year 2006-2007 they insured only 1.8 million ha of a potential of about 10.5 million ha, i.e. a coverage degree of only 17%. Insured areas increased with only about 20-25% compared to the agricultural year 2006-2006. In order to reach the level of European Union nations, where the coverage degree is, on the average, 65-70%, Romania still has a segment of 48-53% of the total agricultural areas that needs to be insured.

To ensure the degree of development of agricultural insurance, we focussed on the analysis of this field over the period 2007-2008.

As for the first half of the year 2008, the value of raw premiums on the market of agricultural insurance reached 41.40 million RON, i.e. 11.3 million Euros (Table 1)¹.

The total value, representing below 1% of the total subscriptions of the insurance companies in Romania represent the cost paid by agriculturists to cover spring crops in 2008. In the entire year 2007, raw premiums subscribed for agricultural insurance reached 54.76 million RON (16.41 Euro). At the same time, the volume of damage paid for agricultural damage total 5.31 million RON (1.45 million Euro) of which the highest payment obligations belonged to the following insurance companies: ALLIANZ-TIRIAC (1.88 million RON), ASIROM (0.92 million RON) and FATA Asigurări (0.66 million RON).

Table 1 Raw premiums subscribed in agricultural insurance in 2007-2008

No.	Insurance company	Share of agricultural insurance of the total portfolio of 2008	Raw premiums subscribed				Market share in 2008
			Semester I 2008		Year 2007		
			Million Euro	Million RON	Million Euro	Million RON	
1.	FATA Asigurări	47.58%	3.32	12.18	2.63	8.77	29.41
2.	ASIROM	1.89%	2.07	7.59	5.10	17.00	18.34
3.	OMNIASIG	0.94%	1.57	5.76	0.28	0.95	13.92
4.	ALLIANZ-TIRIAC	0.65%	1.23	4.53	4.52	15.08	10.94
5.	ARDAF	1.54%	0.92	3.37	1.72	5.76	8.13
6.	GENERALI	1.17%	0.67	2.48	1.31	4.39	5.98
7.	ASTRA-UNIQA	0.65%	0.46	1.70	0.23	0.77	4.10
8.	ASIBAN	0.52%	0.43	1.57	0.33	1.11	3.80
9.	EUROINS	2.21%	0.41	1.49	0.00	0.00	3.60
10.	B.C.R. ASIGURARI	0.24%	0.17	0.62	0.24	0.82	1.50
11.	CARPATICA ASIGURARI	0.27%	0.03	0.11	0.04	0.12	0.27
	TOTAL	0.98%	11.28	41.40	16.41	54.76	100.00

Source: www.lasig.ro.

Among insurers practicing agricultural insurance at present, Societatea FATA Asigurări is the leader, with a volume of raw premium of 12.18 million RON in the 1st semester of 2008 (rank 3 in 2007, with a value of raw premium subscribed of 8.77 million RON), with a market share of 29.41%. This share represents 47.6% of the total portfolio of the Societatea FATA Asigurări.

The following positions in the top list of the first five agricultural insurers ran the following: ASIROM, with 7.59 million RON subscriptions and a market share of 18.34% (rank 1 in 2007 with a value of raw premium subscribed of 17.00 million RON), and OMNIASIG, with 5.76

million RON and 13.92% of the market (rank 6 in 2007 with a value of raw premium subscribed of 0.95 million RON). They are followed by ALLIANZ-TIRIAC, with 10.94% of the market, with a value of raw premium subscribed of 4.53 million RON (rank 2 in 2007 with a value of raw premium subscribed of 15.08 million RON), and ARDAF, with a value of raw premium subscribed of 3.37 million RON, and 8.13% of the market (rank 4 in 2007 with a value of raw premium subscribed of 5.76 million RON).

The classification presented above – raw premiums subscribed and agricultural insurance market share – can still be completed. Thus, an interesting evolution can be relevant also from the point of view of the damage coverage of the insured agriculturists who faced calamity crops. This type of activity can be characterised, on one hand, on the ground of the volume of payments for damage in insured crops and, on the other hand, on the ground of the damage rate calculated as a ratio between raw premiums subscribed and cashed in for agricultural insurance and the value of payments for damage in agricultural crops.

But before we do so, we need to present natural phenomena having had an impact on agricultural production and having damaged crops during the period under study. From an agro-meteorological point of view, the agricultural year 2006-2007 can be characterised as atypical. There were late spring frosts (at the beginning of May) that greatly damaged particularly vineyards, orchards, and vegetable crops, and in May-September 2007 there violent meteorological phenomena such as ht days resulting in drought followed by torrential rainfalls accompanied by hail stones and storms, and even by floods. The events described above resulted in losses (crops on large areas were destroyed).

The damage recorded were extremely high, so that insurance companies paid for the agricultural year 2006-2007 a volume of damage of about 48.3 million RON for a value of insurance premiums of about 53.7 million RON. In this case, the rate of calculated damage was 89.94%, as shown above¹.

In the first semester of the year 2008, damage paid by insurance companies reached 5.31 million RON (1.45 million Euro), and in the financial year 2007 they paid 32.26 million RON (9.7 million Euro) agricultural insurance. Analysing damage rate per insured at the level of the year 2007, we can see there are great differences between insurers (Table 2).

For example, Societatea ALLIANZ-TIRIAC paid damage for 20.16 million RON for a volume of cashed in premiums of 15.08 million RON, with a damage rate of 133.6%, i.e. a clear loss over this segment. This led to a loss of the interest of the insurance company for agricultural insurance which went down in the top list of agricultural insurers from the 2nd to the 4th position. A high damage rate in 2007 was that of the insurance companies ASTRA-UNIQA S.A. and GENERALI S.A. – 79.2%-67.6%. The other insurance companies recorded small damage rates within the group of agricultural insurance – 0-30%.

Table 2 Agricultural insurance damage paid in 2007-2008

No.	Insurance company	DAMAGE PAID				Damage rate and rank in the top of damage payers in 2007
		Semester I 2008		Year 2007		
		Million Euro	Million RON	Million Euro	Million RON	
1.	FATA Asigurări	0.18	0.66	0.60	2.01	22.9% (4)
2.	ASIROM	0.25	0.92	1.51	5.02	29.5% (2)
3.	OMNIASIG	0.08	0.29	0.04	0.12	12.6% (8)
4.	ALLIANZ-TIRIAC	0.51	1.88	6.04	20.16	133.6%(1)
5.	ARDAF	0.07	0.27	0.36	1.21	21.0% (5)
6.	GENERALI	0.11	0.42	0.89	2.97	67.6% (3)
7.	ASTRA-UNIQA	0.00	0.00	0.18	0.61	79.2% (6)
8.	ASIBAN	0.11	0.40	0.01	0.04	3.6% (9)
9.	EUROINS	-	-	-	-	-
10.	B.C.R. ASIGURARI	0.10	0.38	0.06	0.22	26.8%(7)
11.	CARPATICA ASIGURARI	0.02	0.08	-	-	-

	TOTAL	1.45	5.31	9.70	32.36
--	-------	------	------	------	-------

Source: www.lasig.ro.

State involvement in agricultural insurance

The low degree of coverage in contract insurance of agricultural crops in Romania corroborated with the fact that catastrophe risks have known a continuous increase these years resulted in the state involvement as agricultural insurer. In this sense, in 2002, Romania's Government issued the Law 381 concerning damage payment in case of calamity in agriculture.

In fact, state involvement in agricultural insurance is manifest in two directions. The first has in view state support of some of the insurance premium for risk factors insured for agricultural crops, livestock, poultry, bee families, and fish as listed by Ministry's Order.

In the years 2007 and 2008 state subvention reached 50%. This measure aimed at enhancing the demand for agricultural insurance among Romanian agricultural producers.

Secondly, the state grants damage to agricultural producers that suffered damage from natural phenomena and diseases (zoonoses) that generate natural calamity. The payment of damage by agricultural producers – physical or legal people – for natural calamity produced by natural phenomena and disease generating calamity is only done for agricultural crops, livestock, and poultry that were insured by insurance companies.

Administering, using, managing the amounts for agricultural damage payments are done by the Ministry of Agriculture. Damage payment is granted to agricultural producers in the following conditions: (i) for agricultural crops and plantations affected by natural calamity, only for damage above 30% of the production, the maximum level of the damage payment being 70% of the expenses until the time the insured phenomenon occurred; (ii) for livestock, poultry, bee families, and fish, the damage represents maximum 80% of the insurance value, diminished by the value of the by-products resulted, and that can be valorised according to legal stipulations.

Conclusions

The first conclusion to be dawn from this study is that the coverage degree in agricultural crop insurance is very low compared to the agricultural potential and to the level of European Union developed nations. As we showed based on data, Romania still has a segment of 48-53% agricultural land of the total insurable agricultural area that should be insured. On one hand, this gap is difficult to recuperate, but on the other hand, it represents a considerable potential in the evolution of agricultural insurance group in Romania.

A second conclusion we could draw from the present study is related to the state's role of insure. Protection offered by the state is limited to a relatively low number of risks, and damage payment is conditioned by the existence of optional insurance contracts for calamity crops. In our opinion, this conditioning has the role of protecting agricultural producers in case of natural calamity resulting in material damages. State's involvement in agricultural insurance will increase in the years to come, in our opinion. The state will be the basic insurer for catastrophe risks while common risks, i.e. those events acting on smaller areas and having a random unpredictable distribution, protection will be done by commercial insurance companies.

The third conclusion is that agricultural insurance have a low incidence because of the high costs. Covering crop damage is, as we have shown above, rather risky for many insurers because of the increasing frequency and intensity of risks, resulting, in some cases, in an insurance premium of 6-8% of the insurance value.

As a corollary of our findings and conclusions, we claim the necessity of agricultural insurance. More than that, we suggest an integrated complex system of insurance that include,

together with agricultural crop and livestock insurance, a complex household insurance (buildings, their content, and household inventory).

References

- 1.*** 381/2002 Law, regarding indemnity in case of natural calamities in agriculture
- 2.*** 136/1995 Law, completed and modified regarding the activity of insurance-reinsurance
- 3.*** The Report of the Commission of Insurance Surveillance during the years 2002-2006
According to www.lasig.ro

PRODUCTION OF MEDICINAL PLANTS IN ASIA DOCUMENTAR STUDY

ȘIMONAȚI Claudiu-Nicolae¹, HĂLMĂGEAN Lucian², PANCAN Bujor²

¹ Germisara Hotel Resort&SPA , Str.Germisara.No.1B,Geoagiu-Bai, Hunedoara,Romania

E-mail: claudiu.simonati@yahoo.com;

² Aurel Vlaicu University of Arad, Faculty of Food Industry, Tourism and Environment Protection, Arad, Romania

Abstract

Medicinal plants (MP) have played a significant role in many ancient traditional systems of medication and still do today in both developed and developing countries in Asia. They generate incomes via sale of collected, wild products or cultivated products. Collection of naturally-occurring MP has been practiced in Asia since prehistoric time for use in traditional medicine or for processing into pharmaceutical products. Cultivation of MP in Asia is characterized by (i) subsistence cropping systems, (ii) scattered farming areas, (iii) poor quality, and (iv) lack of integration. Compared to other economic crops, MP received much less attention in their genetic and cultural improvement. Cultivation techniques are quite primitive, resulting in poor yield and quality of the materials. Due to higher demand of raw material for industrial processing, coupled with the loss of natural habitats of most MP, large-scale cultivation of promising species has recently been attempted in several countries.

Keywords: *naturally-occurring medicinal plants*

Introduction

Medicinal plants (MP) had a significant role in various ancient traditional systems of medication such as Ayurvedic and Unanic (India), Chinese traditional medicine and their derivatives. Today, MP still play an important role in developing countries in Asia, both in preventive and curative treatments, despite advances in modern western medicine. People of many Asian countries earn a living from selling collected materials from the forest, or from cultivation on their lands.

The development of modern medicine with the introduction of modern drugs produced by pharmaceutical companies, has dealt harshly with traditional medicine which was accused of being inefficient, laborious in preparation and unavailable due to scarcity of raw material. This is exacerbated by the lack of traditional doctors who cannot earn a living without basic material (MP) and demand (customers).

The high cost of modern drugs (mostly imported), their unavailability in remote areas, and most importantly the serious side effects of certain drugs, have resulted in a significant return to traditional medicine. The importance and value of traditional and indigenous herbal medicine were the subject of WHO's campaign during the 70s in an appeal to all member countries to preserve their national heritage of ethno-medicine and ethno-pharmacology and to re-include the use of known and tested MP and derivatives into their primary health care in rural areas and as an alternative when modern medicine was not available. Since a large portion of pharmaceutical drugs are derived from MP, the demand for these raw materials is steadily rising. Such demand is met by obtaining naturally-occurring plants through indiscriminate collecting or by cultivating them.

Medicinal plants available in Asia

The vast number of species known to Asian people makes listing all MP found in Asia difficult and impracticable. Thus, in order to provide a meaningful list of MP, we have

categorised promising species in the following groups.

Medicinal plants that are collected from the wild habitat

It has been estimated that four out of five MP used by man are collected from the wild (Srivastana et al., 1995). See Table 1.

Table 1. List of medicinal plants collected from the wild Asian habitat

Species	Family	Country of collection
<i>Aesculus indica</i>	Sapindaceae	PAK
<i>Alocasia macrorrhiza</i>	Araceae	LAO, VIE
<i>Alstonia scholaris</i>	Apocynaceae	LAO, VIE
<i>Amomum</i>	Zingiberaceae	LAO, VIE
<i>Amorphophallus rivieri</i>	Araceae	LAO, VIE
<i>Artemisia maritima</i>	Compositae	PAK, VIE
<i>Artocarpus lakoocha</i>	Moraceae	LAO, VIE
<i>Blumea balsamifera</i>	Compositae	LAO, VIE
<i>Catharanthus roseus</i>	Apocynaceae	LAO, VIE
<i>Cassia alata</i>	Leguminosae	PHI, VIE
<i>Cinchona ledgeriana</i>	Rubiaceae	LAO, VIE
<i>Coscinium usitatum</i>	Menispermaceae	LAO, VIE
<i>Costus speciosus</i>	Zingiberaceae	LAO, VIE
<i>Dioscorea deltoidea</i>	Dioscoraceae	PAK, VIE
<i>Drymaria fortunei</i>	Caryophyllaceae	LAO, VIE
<i>Embelia ribes</i>	Euphorbiaceae	LAO, VIE
<i>Ephedra Gerardiana</i>	Gnetaceae	PAK
<i>Glycyrrhiza glabra</i>	Leguminosae	PAK, CPR
<i>Kaempferia galanga</i>	Zingiberaceae	LAO, VIE
<i>Lagerstroemia speciosa</i>	Lythraceae	PHI, VIE
<i>Leonurus heterophyllus</i>	Labiatae	LAO, VIE
<i>Moringa oleifera</i>	Moringaceae	PHI, VIE
<i>Rauvolfia serpentina</i>	Apocynaceae	IND, NEP, LAO, HA, VIE
<i>Schefflera elliptica</i>	Araliaceae	LAO, VIE
<i>Smilax glabra</i>	Liliaceae	LAO, VIE
<i>Stephania rotunda</i>	Minispermaceae	LAO, VIE
<i>Sterculia lygnophora</i>	Sterculiaceae	LAO
<i>Styrax tonkinensis</i>	Styracaceae	LAO, VIE
<i>Swietenia macrophylla</i>	Meliaceae	PHI
<i>Vitex negundo</i>	Verbenaceae	PHI, VIE
<i>Xanthium strumarium</i>	Compositae	LAO, VIE

Cultivated medicinal plants

Due to higher demand of raw materials for drug manufacture and to meet other requirements such as standard quality, reliable supply, reasonable price, many MP are now being cultivated. See Table 2.

Countries of production of major medicinal plants in Asia

Although most countries are capable of acquiring MP for their traditional uses, only China, India, Indonesia, and Nepal produce them in commercial quantity. A few countries are able to produce MP on a commercial scale, but the quantity produced is still quite small, and mainly used domestically.

Collecting naturally-occurring medicinal plants

As the result of population explosion and forest clearing for food production, most Asian countries, which until recently collected MP from the wild, have almost completely ceased such practice as MP are quite scarce or non-existent. Nepal, Bhutan and Lao PDR and to a lesser extent, Bangladesh, China, India, Indonesia and Pakistan, maintain considerable natural forest cover are still able to collect MP from the wild (Table 1).

Objectives of collecting

1. For use in traditional medicine. For native people in remote areas and those who cannot afford to buy expensive western drugs, traditional medication, e.g., Ayurvedic, Unanic, Jamu, are the only means to cure illness. Such systems depend almost exclusively on MP with about 90% being collected from the forest.

2. For processing into pharmaceutical products. Due to the scarcity of MP occurring naturally, transportation costs, the variability and irregular supply of collected material, very few countries are able maintain the practice. Nepal is the exception to this predicament and processes and exports wild MP.

Measures to conserve naturally-occurring medicinal plants

Realizing that naturally occurring MP are threatened, several conservation measures have been undertaken by various approaches or agencies.

1. Systematic and reasonable collecting. Sustainable collecting can be achieved if it is done appropriately as in Nepal where proper harvesting techniques and appropriate methods of post-harvest treatment (Rawal 1996) mutually benefit the collector and local processor providing incentives for conservation of species for future collection.

2. Reduction of pressure on collecting. Cultivation, whether small or large scale, backyard garden or subsistence can reduce the pressure on collecting MP in the wild.

3. National Legislations. A few countries have formulated legislation to conserve MP - (i) administrative regulation for "Protection of Wild Medicinal Plant Resources", in China since 1987 (Chen, 1996); (ii) an "Action Plan for Conservation of Biodiversity", in Sri Lanka including conservation of MP as a project (Arambewela, 1996); (iii) all wild MP have been banned for export from India since 1993 (Uniyal, 1993).

4. International Regulations. It is a common practice of international conferences to come up with a "Declaration" or "Resolution", within which measures to conserve MP are included. Examples can be seen in: (i) "Washington Convention - 1973" which includes a statement, "The trade and use of some of the MP collected from wild sources are restricted" (Hussain, 1996); and (ii) the "Chiang Mai Declaration" exhorted governments and the public to pay attention to the potential inherent in MP (Henle, 1996).

Cultivation of medicinal plants in Asia. Characteristics of medicinal plant cultivation

At present, cultivation of MP is characterized by the following traits:

1. Subsistence cropping systems. As cultivation is new for MP, most are grown by small-holders in subsistence or mixed cropping systems with low yield and quality.

2. Scattered farming areas. With few exceptions, most growing areas are widely scattered resulting in difficulty in collecting harvested raw materials by the middlemen.

3. Poor quality. This is due to various factors including the use of unimproved cultivars, poor cultural techniques, and poor post-harvest handling.

4. Lack of integration. In some areas, MP are grown commercially as inter-crops. There is no systematic integration between primary crops and MP. Even in China, where total production of MP is high, monoculture (usually by industrial enterprises) is very small.

Advantages of commercial cultivation of medicinal plants

Commercial cultivation may become increasingly popular among farmers as naturally-occurring MP diminish and demand increases. Cultivation advantages are:

1. Conserves endangered species in their natural habitat. Many species are listed as endangered due to indiscriminate collecting for the pharmaceutical industry.

2. Permits production of uniform material. Commercial cultivation of selected clones or improved cultivars should produce uniform material resulting in consistent, standard MP of high quality, a pre-requisite for successful pharmaceutical industrial use.

3. Provides good income to farmers. MP are high-valued crops and should bring higher

income to the growers if improved, high-yielding clones or cultivars are used.

4. Provides opportunities for value-adding through processing. Processing technology is available in many developing countries. Commercial cultivation would provide raw material for local processing where cultivation takes place.

5. Provides a better environment; utilize waste and unproductive land. As MP yield high incomes to the growers, costly inputs can be used for their cultivation.

6. Provides continuity of supply. Cultivation is less risky for supply of raw material allowing manufacturers to set production targets well in advance.

Table 2. List of some Medicinal Plants cultivated on commercial scale in Asia

Species	Family	Country of cultivation
<i>Aconitum napellus</i>	Ranunculaceae	NEP
<i>Adhatoda vasica</i>	Acanthaceae	NEP, VIE
<i>Alisma orientale</i>	Alismataceae	CPR
<i>Allium domesticum</i>	Liliaceae	THA
<i>Aloe barbadense</i>	Liliaceae	THA
<i>Ammi majus</i>	Umbelliferae	NEP, VIE
<i>Andrographis paniculata</i>	Acanthaceae	THA, INS, VIE
<i>Angelica gigas</i>	Umbelliferae	ROK
<i>Artemisia annua</i>	Compositae	CPR, THA, VIE
<i>Atropa belladonna</i>	Acanthaceae	IND, NEP, VIE
<i>Baleriana lupulina</i>	Acanthaceae	THA, VIE
<i>Cassia angustifolia</i>	Leguminosae	IND, THA, VIE
<i>Catharanthus roseus</i>	Apocynaceae	IND, VIE, PHI
<i>Cephaelis ipecacuanha</i>	Rubiaceae	IND
<i>Cinnamomum camphora</i>	Lauraceae	CPR, THA, VIE
<i>Clinacanthus nutans</i>	Acanthaceae	THA, VIE
<i>Coptis chinensis</i>	Ranunculaceae	CPR, VIE
<i>Cornus officinalis</i>	Cornaceae	CPR
<i>Corydalis yanhusua</i>	Papaveraceae	CPR
<i>Costus speciosus</i>	Zingiberaceae	NEP
<i>Croton sublyratus</i>	Euphorbiaceae	THA
<i>Curcuma domestica</i>	Zingiberaceae	IND, INS, PAK, SRL, HA, VIE
<i>Dioscorea deltoidea</i>	Dioscoreaceae	IND
<i>Hibiscus sabdariffa</i>	Malvaceae	THA, VIE
<i>Isatis indigotica</i>	Cruciferaeae	CPR
<i>Kaempferia galanga</i>	Zingiberaceae	INS, VIE
<i>Lonicera japonica</i>	Caprifoliaceae	CPR
<i>Lycium barbarum</i>	Solanaceae	CPR
<i>Magnolia officinalis</i>	Magnoliaceae	CPR
<i>Matricaria chamomile</i>	Compositae	NEP
<i>Mentha arvensis var. piperascens</i>	Labiatae	CPR, IND, NEP, PAK, THA, VIE
<i>Morinda officinalis</i>	Rubiaceae	CPR, VIE
<i>Ophiopogon japonicum</i>	Liliaceae	CPR, VIE
<i>Paeonia lactiflora</i>	Ranunculaceae	ROK, VIE
<i>Panax ginseng</i>	Araliaceae	CPR, ROK
<i>Papaver somniferum</i>	Papaveraceae	IND
<i>Philodendron chinense</i>	Rutaceae	CPR, VIE
<i>Piper betel</i>	Piperaceae	SRL, THA, VIE
<i>Piper retrofractum</i>	Peperaceae	IND, INS, SRL, THA
<i>Plantago ovata</i>	Plantaginaceae	IND
<i>Platycodon grandiflorum</i>	Campanulaceae	ROK
<i>Rauwolfia serpentina</i>	Apocynaceae	IND, NEP, VIE
<i>Solanum khasianum</i>	Solanaceae	NEP
<i>Sophora japonica</i>	Leguminosae	VIE
<i>Swertia chirata</i>	Gentianaceae	NEP, PAK
<i>Syzygium aromaticum</i>	Myrtaceae	IND, INS, MAL, SRL

Species	Family	Country of cultivation
<i>Tinospora crispa</i>	<i>Menispermaceae</i>	IND, PHI
<i>Trichosanthes bracteata</i>	<i>Cucurbitaceae</i>	NEP
<i>Valeriana jatamansi</i>	<i>Valerianaceae</i>	IND, NEP
<i>Vitex negundo</i>	<i>Verbenaceae</i>	PHI
<i>Withania somnifera</i>	<i>Solanaceae</i>	IND
<i>Zingiber officinalis</i>	<i>Zingiberaceae</i>	CPR, IND, INS, ROK, SRL, THA

Conclusions

MP are man's best friend in time of need. As technology and development advance, the need for them is much higher and the chance to collect them from the forest is receding. Rural property and constant demand for cultivated land are threatening the forests homes of uncountable numbers of species of valuable MP. The only solution to save this inheritance is to cultivate them systematically providing socio-economic benefits to rural people and satisfying the need of urban people who want to go 'back-to-nature' with the use of MP as raw material for pharmaceutical manufacture.

MP continue to play a significant role in the peoples' welfare as they have been for several millennia. Due to higher demand of raw material for industrial processing and the loss of natural habitats of most MP, large-scale cultivation of promising species has been attempted in several countries. Collecting in the wild will cease due to over-exploitation, unless the campaign to conserve biodiversity is successful. MP have not been subjected to intensive breeding programs so yield and quality are quite low. To start any breeding program, germplasm collection and conservation are most essential. As most natural habitats are on the verge of being destroyed, there is an urgent need to collect and conserve valuable germplasm of MP before they become extinct and many breeding programs initiated. They should be supplemented with R&D on agro-technology to obtain optimum yield and quality of the source raw materials for pharmaceutical products.

References

- Ali, A.M., Kadir, A.A. and Lajis, N.H. 1996. Production, processing and utilization of medicinal and aromatic plants in Malaysia.
- Arambewela, L.S.R. 1996. Production of medicinal plants in Sri Lanka.
- Chan, N.G. 1996. Production, processing and utilization of medicinal plants in Vietnam.
- Chi, H.Y. and Park, S.K. 1996. Production of medicinal plants in the Republic of Korea.
- Chowdhury, S.A. 1996. Production, processing and utilization of medicinal and aromatic Plants in Bangladesh.
- De Padua, L.S. 1996. Production, processing and utilization of medicinal and aromatic plants in the Philippines.
- Henle, H.V. 1996. Socio-economic aspects of medicinal and aromatic plant production in Asia.
- Xiao, P.G. and Yong, P. 1996. Production and processing of medicinal and aromatic plants in China.

PREPARATION OF STANDARD *PUNICA GRANATUM* FRUIT PEEL EXTRACTȘIMONAȚI Claudiu-Nicolae¹, MUREȘAN Claudia²

¹ Germisara Hotel Resort&SPA , Str.Germisara.No.1B,Geoagiu-Bai, Hunedoara, Romania
e-mail: claudiu.simonati@yahoo.com;

² Aurel Vlaicu University of Arad, Faculty of Food Industry, Tourism and Environment
Protection, Arad, Romania e-mail: muresanclaudette@yahoo.com

Abstract

In this paper, presented process of extraction of natural coloring, the peel fruit *Punica granatum* and pharmacology affects this one. In this study, *Punica granatum* fruit peel was further studied suitable extraction and evaluated antioxidant activity. The extraction methods used in the paper showed a high antioxidant activities at compounds from pomegranate fruit peel. In order to increase the value of *Punica granatum* fruit peel, we are interested in preparing of the extract for a topical cosmetic product and nutraceutical applications.

Keywords: *Punica granatum*, extraction, antioxidant activity

Introduction

The fruit peel of *Punica granatum* L. (or pomegranate in English) has long been used in folk medicine as astringent for treatment of diarrhea and dysentery. Several biological activities of *P. granatum* fruit, including antibacterial (Alanis et al., 2005), antiviral (Caballero et al., 2001), antioxidant (Lansky and Newman, 2007), anti-inflammatory (Ahmed et al., 2005) and immunomodulatory (Ross et al., 2001) have been reported.

Experimental*Solvents for extraction*

Dried material of *P. granatum* fruit peel was ground into powder and extracted consecutively with chloroform (CHCl₃), EtOAc, MeOH and 70%acetone using maceration method (x3). The extracts were evaporated to dryness *in vacuo* and were evaluated antioxidant activity.

Pre-purification of the extract

The methanolic extract was partitioned consecutively between EtOAc and water, n-butanol (n-BuOH) and water, n-BuOH:EtOAc and water. The organic fractions were evaporated to dryness in vacuum. The organic fractions were then evaluated antioxidant activity.

Extraction method

Methods of extraction including maceration and reflux examined for the suitable method of extraction. The antioxidant activity (ED₅₀) of the extracts obtained from these methods was compared.

Maceration method

Dried powder was macerated in methanol for 3 day (x3) and the extract was evaporated to dryness in vacuum. The methanolic extract was then partitioned between EtOAc and water, and the EtOAc fraction was evaporated to dryness *in vacuo*. The EtOAc fraction was then evaluated antioxidant activity.

Reflux method

Dried powder was refluxed in methanol for 1 hour (x2) and the extract was evaporated to dryness in vacuum. The methanolic extract was then partitioned between EtOAc and water,

and the EtOAc fraction was evaporated to dryness *in vacuum*. The EtOAc fraction was then evaluated antioxidant activity.

Evaluation of antioxidant activity by DPPH radical scavenging assay

The scavenging effects of samples for DPPH radical were monitored according to the method of the previous report (Duan et al., 2006). Briefly, a 500 µl sample (in ethanol) was added 500 µl of 6×10^{-5} M DPPH ethanolic solution. The mixture was vortexed for 1 min and then left to stand at room temperature for 30 min in the dark, and its absorbance was read at 520 nm. The ability to scavenge the DPPH radical was calculated using the following equation:

$$(\%) \text{ Inhibition} = [(OD_{\text{control}} - OD_{\text{sample}}) / OD_{\text{control}}] \times 100$$

Where OD_{control} is the absorbance of the control (DPPH solution without sample), OD_{sample} is the absorbance of the test sample (DPPH solution plus test sample). Quercetin (Qu) was used as positive control.

Results and discussion

Antioxidant activity of CHCl_3 , EtOAc, MeOH, and 70% acetone extracts were determined by using DPPH radical scavenging assay and found that all extracts exhibited antioxidant activity (Table 1). The result indicated that MeOH extract possessed the highest antioxidant activity. Thus, MeOH was suitable for extraction of antioxidative compounds from pomegranate fruit peel.

Metanolic extract was pre-purified by partitioning between EtOAc and water, n-BuOH and water and n-BuOH:EtOAc (1:1) and water. It was found that all fractions exhibited antioxidant activity (Table 2). The EtOAc fraction showed the highest antioxidant activity. Thus, partitioning between EtOAc and water was suitable for isolation of antioxidative compounds from methanolic extract.

Methods of extraction including maceration and reflux were examined for the suitable method of extraction. The reflux method used extraction time less than maceration method (Table 3). Antioxidant activities of the obtained from both methods showed the same high ED_{50} value. Thus, the reflux method was suitable for extraction of antioxidative compounds from pomegranate fruit peel.

Table 1. Antioxidant activity of the extracts and quercetin evaluated by DPPH radical scavenging assay ($\mu\text{g/ml}$)^a

Extract	ED_{50} ($\mu\text{g/ml}$)
Quercetin	3.07±0.05
CHCl_3	180.93±1.36
EtOAc	91.16±1.18
MeOH	68.99±1.40
70%Acetone	76.16±1.54

^a Values expressed are mean S.D. of three experiments.

Table 2

Antioxidant activity of the fractions and quercetin evaluated by DPPH radical scavenging assay

Extract	ED_{50} ($\mu\text{g/ml}$)
Quercetin	3.65±0.02
EtOAc fraction	6.33±0.13
n-BuOH fraction	32.23±2.37
n-BuOH:EtOAc fraction	24.53±1.39

Table 3

Comparison of extraction time and ED₅₀ of the extracts obtained from two methods of extraction

Methods	Times (hour)	ED ₅₀ (µg/ml)	
		MeOH ext.	EtOAc fraction
Maceration	240	65.92±0.04	6.33±0.13
Reflux	3.5	67.88±0.70*	7.36±0.32

*Not significantly different (P < 0.05)

Table 4

Antioxidant activity and %yield of the extract

Extract	%yield	ED ₅₀ (µg/ml)
Quercetin	-	3.05±0.87
EtOAc fraction	6.75	10.03±1.10

Conclusions

In the present study, suitable extraction of *P. granatum* fruit peel showed high antioxidant activity. Thus, *P. granatum* fruit peel was refluxed in methanol and was then fractionated by partitioning between EtOAc and water to obtain high antioxidant. These data further implicate *P. granatum* fruit peel extract as potential antioxidant for cosmetic and nutraceutical applications.

References

- Ahmed, S. Wang, N. Hafeez, B.B. Cheruvu, V.K. Haqqi, T.M. 2005. *Punica granatum* L. extract inhibits IL-1 β -induced expression of matrix metalloproteinases by inhibiting the activation of MAP kinases and NF-KB in human chondrocytes *in vitro*. Journal of Nutrition. 135, 2096-2102.
- Alanis, A.D. Calzada, F. Cervantes, J.A. Torres, J. Ceballos, G.M. 2005. Antibacterial properties of some plants used in Mexican traditional medicine for the treatment of gastrointestinal disorders. Journal of Ethnopharmacology. 100, 153-157.
- Caballero, O. Pena, B.R. Zurcher, J. Martinez, T. 2001. Actividad inhibitory de extractos del fruto de *Punica granatum* sobre cepas del virus de la gripe. Rev. Cubana Quimica. XIII, 106.
- Duan, X.J. Zhang, W.W. Li, X.M. Wang, B.G. 2006. Evaluation of antioxidant property of extract and fractions obtained from a red alga, *Polysiphonia urceolata*. Food Chemistry. 95, 37-43.
- Lansky, E.P. and Newman, R.A. 2007. *Punica granatum* (pomegranate) and its potential for prevention and treatment of inflammation and cancer. Journal of Ethnopharmacology. 109, 177-206.
- Ross, R.G. Selvasubramanian, S. Jayasundar, S. 2001. Immunomodulatory activity of *Punica granatum* in rabbits-a preliminary study. Journal of Ethnopharmacology. 78, 85-87.

ENGINEERING

EXTREME METEOROLOGICAL PHENOMENON RECORDED IN ARAD AS EFFECT OF GLOBAL WARMING

CIUTINA Virgil, MUREȘAN Claudia

"Aurel Vlaicu" University of Arad, Faculty of Food Engineering, Tourism and Environmental Protection, 2 Elena Drăgoi, Str., 310330, Arad, Romania, E-mail:virgilciutina@yahoo.com

Abstract

The climate has a very important role for life on Earth and a major influence on providing food for population, protecting life and property and also the hydrographic network and the sources of drinkable water and not last over spending free time and social development. It is also know to a certain extent the influence that the climate has upon our mood, character as well as on the way of thinking and culture of people.

Keywords: global warming, extreme temperatures, climate elements

Introduction

The phenomenon of our planet's heating in the result of the growth of the concentration of greenhouse gases in the atmosphere, is one of the major, contemporary problem of humankind. The purpose of the ecological era is to explain to people the effects of the global warming and the consequences for the whole world in general and our country in particular. Moreover, ecological era has to present also the actions to be taken in order to diminish the negative impact of global heating on nature and society.

The most important change takes place in the atmosphere. The industry, transport, and agriculture produce the so called „greenhouse gases” as the carbon dioxide (CO₂), methane (CH₄), nitrous oxide (N₂O), tropospheric ozone (O₃), chloroflouorocarbon (CFC), watery vapours and other gases.

Excess of greenhouse gases increase the quantity of the absorbed radiation in the atmosphere and gradually the overheating of the planet occurs. Starting with the 1850's, the average temperature has increased by half degree. For the next one hundred years it is forecasted a global warming of 1- 3.5 degrees.

Although the most recent projections take in sight the next 100 years, the scientists' concerns are directed towards the next centuries as well, sustained by the fears according to which, the global warming induced by the antropic activity could last for a long time due to the long life of the greenhouse gases, especially the carbon dioxide, even if its emission is drastically reduced.

The measurement of the climate elements have been carried out by the aid of an automatic meteorological station.

An automatic meteorological station (AMS) is defined as a meteorological station where the measurements are automatically recorded and transmitted.

AMS has the option to accept the observations made by the human observer for the dimensions that are too difficult, expensive or impossible to be measured automatically such as the types of clouds, the state of the surface, the type of the rainfalls etc.

Why the automation of meteorological measurements is a necessity?

The reason for which the automatization of the meteorological measurements is compulsory, is the growing necessity for homogenous data, uniform in time, with an increased temporal resolution available in due time. A temporal resolution of 10 minutes has

become a basic requirement to forecast a severe meteorological phenomenon and to generate the appropriate warning.

An AMS is a structure easy to configure, so that it can be used at the same time for synoptic applications, climatic, agro meteorological, aeronautical and for pollution. AMS can work in different ways according to the demands of the application; the changing of the way of working can be produced automatically or at demand.

The advantages of automation

- improvement of the observation's homogeneity (from one location to another, from one day to another);
- improvement of the unity and objectivity of the measurements;
- increasing of the frequency of the measurements;
- increasing of the precision and quality of the dates;
- better temporal uniformity and availability of the data;
- more frequent special observations;
- superior density of the observations available in due time;
- permanent measurements of atmospheric parameters;
- = SMA data can be easily integrated with the dates produces by other systems (radar, satellites, etc.);
- SMA data can be easily archived;
- lower costs of individual measurement.

Results and Discussion

Increasing of the air temperature

In our country it has already been registered a tendency of temperature increasing strengthened by the effects of the pollution in industrial areas.

The growth of the average temperature in the air is obvious in Arad as well; the growth is slow, but certain in the last 53 years.

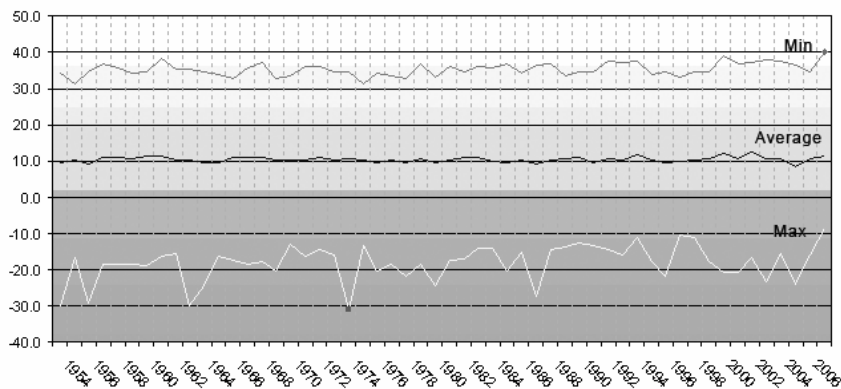


Figure 1. Variation of the air temperature in Arad between 1954-2007

a) Average annual temperatures

- The multiannual average temperature in Arad is 10.5°C.
- The lowest annual average was 8.4°C in 2005 and the highest annual average was 12.4°C in 2002.

- The multiannual average amplitude of the air temperature is of 4.0°C, which makes evident the framing of Arad in the area of the temperate continental moderate climate (figure 1).

b) Extreme temperatures

The maximum absolute temperature in Arad in the last 53 years was 40.2°C and was registered in 2007. Analyzing the evolution of the maximum temperatures in the air during the last years, a tendency of growth from one year to another can be observed. The value of the minimum temperatures in the air have a definite tendency of growth in the last 53 years, the minimum absolute value being -31,0 °C on the 21st of December 1974 (figure 2).

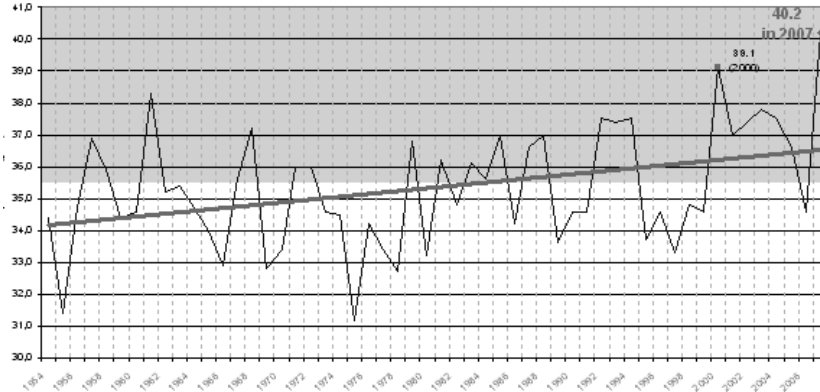


Figure. 2. Variation of maximum air temperatures in Arad between 1954-2007

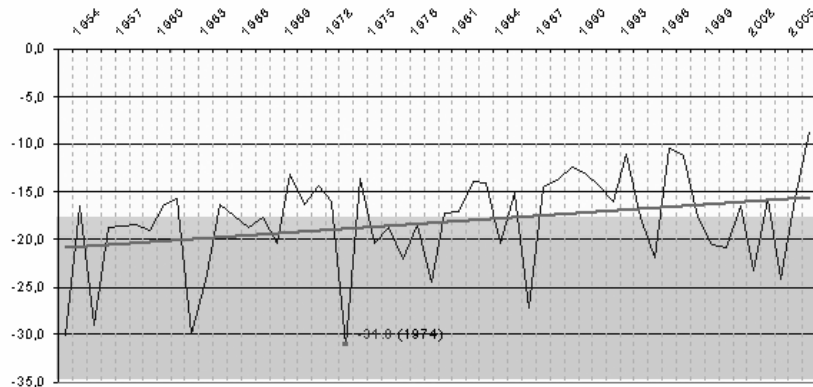


Figure 3. Variation of minimum air temperatures in Arad between 1954-2007

Analyzing the plot of monthly thermic deviations over the years (figure 3), it can be observed that the deviations from February to April are negative (the average temperature for February to April are below the normal monthly temperature), and the deviations from May to January are positive with the exception of September (the average temperatures from May to January are situated over the normal monthly temperature).

In other words, the months from February to April have become colder than normal, and the summer and autumn months warmer, which confirms the theory of global warming.

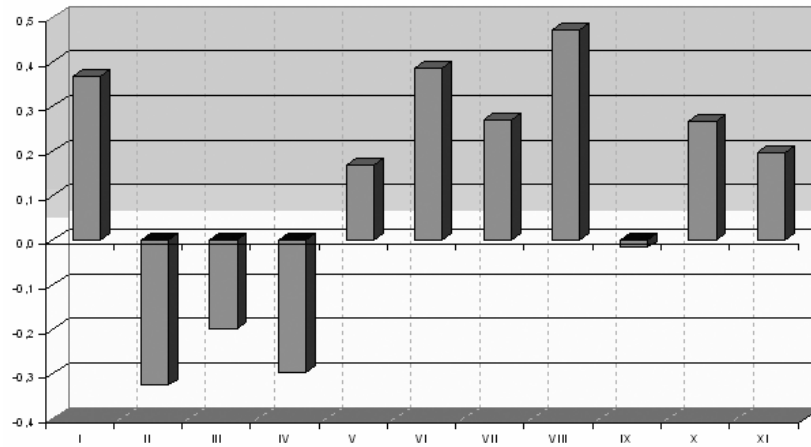


Figure 4. Monthly thermic deviation in Arad between 1954 - 2007

Analyzing the graphic of the monthly thermic deviations over the years (figure 4) it can be observed that the thermic deviations are prevalent positive starting with 1970, and as value they gradually grow in time, the maximum of the deviation being +2.0°C in 2002.

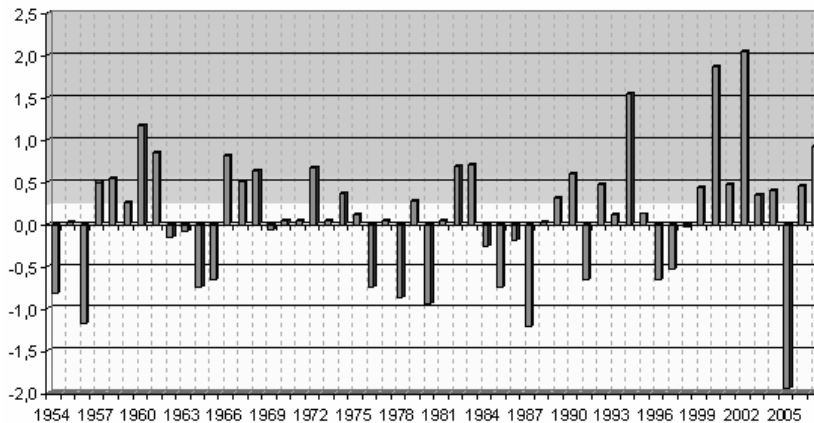


Figure 5. Annual thermic deviation in Arad between 1954 – 2007

The negative thermic deviations grow (as value) in time, the minimum of the deviation being -1.9°C in 2005 (figure 5).

As an extreme meteorological phenomenon from the point of view of annual thermic deviations, it can be observed the recording of the maximum and minimum thermic deviation in a very short interval of time (three years) and, moreover, in the last 6 years.

In the last years as well, another anomaly is represented by the variation of extreme temperatures, positive and negative ones, during the same year. In the years 2000 and 2003 (droughty years) maximum temperatures in the air of 39,1°C respective 37,8° C have been registered during summer and during winter time the minimum temperatures in the air have dropped to -20,6°C respective -23,3 ° C (figure 6). These years were hit by warmth and drought during summer and harsh frost during winter.

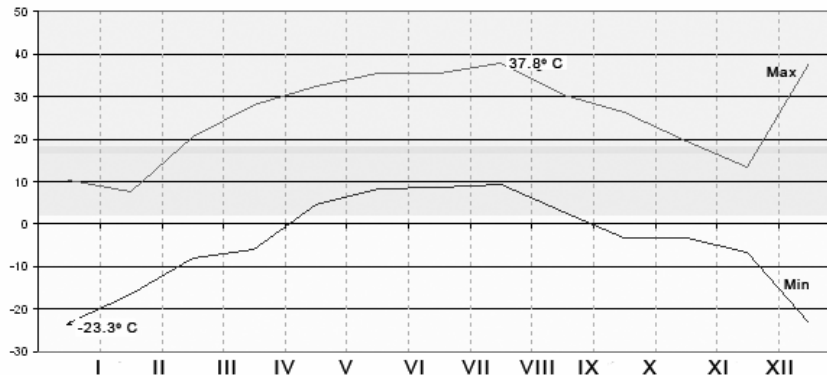


Figure. 6. Variation of maximum and minimum temperatures in Arad during 2003

Conclusions

As a follow up of the study concerning the extreme meteorological phenomena and their direct impact over global warming in Arad, we summarize the following conclusions:

Besides the territorial geographical diversity of Arad district, with its characteristics, it can add the pollutant factors emitted on the surface of the district, which lead to major climatic transformations.

From the measurements performed at the meteorological station in Arad between 1954-2007 we can draw the following conclusions:

- The average air temperature in Arad has had values between 8.4°C respective 12.4°C having a clear tendency of growth in the last 53 years, its maximum value being registered in 2002.

- The maximum and minimum air temperatures have also had a tendency of progressive growth from one year to another, the maximum registered value being 40.2°C in the year 2007 and the minimum one -31.0°C in the year 1974.

- As an extreme meteorological phenomenon from the point of view of annual thermic deviations it can be noticed the recording of the maximum and minimum thermic deviations in a very short interval of time (three years), this phenomenon being produced in the last 6 years.

In the last years as well another anomaly is the variation of extreme temperatures, positive and negative ones, during the same year. In the years 2000 and 2003 have been recorded maximum air temperatures during summer of 39,1°C respective 37,8°C, and in wintertime minimum air temperatures have dropped to -20,6°C respective -23,3°C. These years were hit by warmth and drought during summer and harsh frost during winter.

References

- Ciulache S., Ionac Nicoleta – Esential in meteorologie si climatologie, Edit. Universitara, Bucuresti, 2006
- Ciulache S., Ionac Nicoleta – Fenomene atmosferice de risc – Edit. Stiintifica, Bucuresti, 1995
- • ***, 1992, Geografia României, vol IV – Regiunile pericarpatiche: Dealurile și Câmpia Banatului și Crișanei, , Ed. Acad., pg. 90 – 160, 179 – 345, 421 – 559;

SUSTAINABLE DEVELOPMENT via BIOTECHNOLOGY

STANESCU Michaela Dina

"Aurel Vlaicu" University, Revolutiei Blvd. 77, 310130 Arad, Romania

Abstract

Climate changes and energy crisis modified the perception about industrial development. New processes with high yield, diminished consumptions of energy and raw materials are in agreement with today development strategy. The *sustainable development* became the focus of research activity, leading to actions that ensure long-term industry competitiveness. Biotechnology is one of the ways for such development by replacing pollutant and less efficient chemical processes with green solutions by using one of the most efficient catalysts, enzymes. The paper introduces such bio-solutions with application in textile and food industries. The results obtained in biotechnology application, developed by our research group, are presented.

Introduction

The concept of *sustainable development* was introduced in 1987, by the World Commission on Environment and Development in the report "*Our Common Future*", known also as Bruntland Report. According the definition such development means:

"A development that meets the needs of the present, without compromising the ability of the future generations to meet their own needs. A development that provides economic, social, and environmental benefits in the long term, having regards to the needs of living of future generations" [1].

Biotechnology represents a good solution for making a *sustainable development* [2-4]. The processes catalyzed by enzymes are characterized by: (i) high yields; (ii) high *regio*- and *stereo*-selectivity leading to almost no secondary products; (iii) mild reaction conditions with reduced energy consumption.

Enzymes and enzymatic processes for textile and food industries

The enzymes used are mostly oxido-reductases and hydrolyses [5]. Some of the enzymes used by our research group, and their applications are described.

Laccases belong to a family of enzymes catalyzing the oxidation of phenols, aromatic amines, etc, with the concomitant reduction of molecular oxygen to water. A Laccase is a metallo-enzyme, having four copper atoms at the catalytic site [6]:



Fig.1. X-ray structure of *Trametes versicolor laccase* [7]

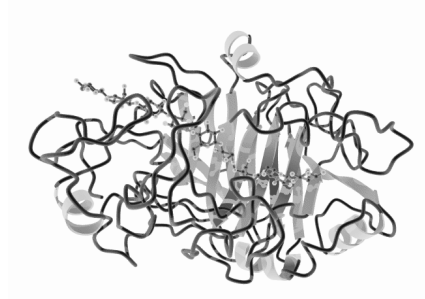
Preliminary researches performed by us, on laccases capacity of dye bio-degradation have been presented at national and international meetings [8-10]. The obtained results depend on

the reaction conditions and also of the structure of dye used as substrate [10]. The biotechnology may replace classical procedures for dye elimination which need energy and polluting reagents [8]

Laccases may be used also successfully for food quality improvement [11-13]. Researches on this topic are in progress.

One of the disadvantages of enzymatic degradation of dyes is the large quantity of enzyme needed leading to high costs of the process. Thus, new attempts have been done by using a new procedure with immobilized *Laccase* on/in cryogel type matrix [14].

Cellulases are hydrolytic enzymes. The complex structure of cellulose, which is mostly a crystalline material, demands a diversity of enzymes for its bio-degradation [15]. The cellulolytic enzyme system contains a mixture of cellobiohydrolases, endoglucanases and β -glucosidase, working together synergistically [16].



F.1. X-ray structure of an endoglucanase [15]

Some applications of enzymatic reactions, using commercial cellulases, have been performed for cotton finishing processes, improving the material surface quality and its dye fixation properties using mild conditions and eliminating polluting reagents [17-20].

Cellulases could be used also for textile waste biodegradation, replacing the strong acids usually used for such purpose [21]. The importance of the pre-treatment of the material in the case of the enzymatic biodegradation was evidenced by us [22].

Other process using cellulases for cellulose bio-degradation is the wool carbonization. Performed researches gave some results in the application of a biotechnological solution, showing a prospect for elimination of the concentrated sulphuric acid used in the classical procedure [23].

Pectinases are a mixture of depolymerising and demethoxylating enzymes [24]. As depolymerising enzymes, there are polygalacturonases breaking the polycarbohydrate chain by hydrolysis, and Pectinlyases which depolymerise the pectin chain by elimination reactions. Hydrolysis of methyl ester groups is performed by pectinesterases.



Fig.3. X-ray structure of an endopolygalacturonase [25]

Commercial pectinases have been used with good results, for improvement of fruit juice quality [26]. In cotton treatment [27] the enzymatic procedure may replace with success the classical strong alkaline procedure used for eliminating the pectins.

Proteases are enzymes used for proteins hydrolysis. Proteases have been used for wool [28] and also polyester [29] finishing.

For wool, problems are generated by its complex, mostly amorphous structure, as well as the low molecular mass of the proteolytic enzymes, which may enter inside the fibre leading to a possible advanced destruction of it. Thus, an entrapped protease, in a silicate matrix, have been synthesised by the sol-gel procedure [30].

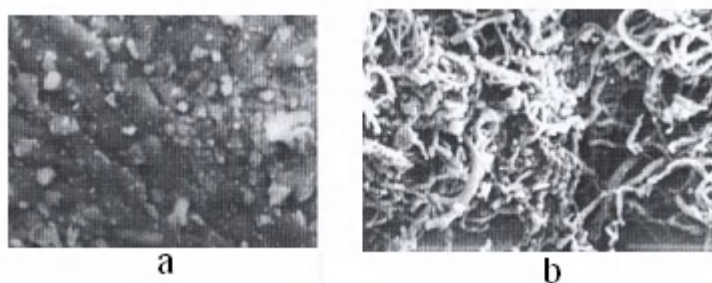


Fig.4. SEM analyses of a) matrix, b) immobilized protease [30]

The new bio-catalysts have been used for wool anti-shrinking treatment [31-33]. The proposed biotechnological process may replace the classical, high polluting, procedure based on chlorine oxidation [28].

An important aspect to take in account for bio-processes is the accurate monitoring of the reaction. The easiest, non-destructive way of doing it is by different type of spectral measurements. Some applications of UV-Vis method for monitoring the enzymatic processes have been presented before and proved to be a success [34].

Conclusions

The use of biotechnology is recommended for realizing a sustainable development in textile or food industry. Enzymes replace successfully pollutant reagents and lead to the development of green procedures with less consumption of raw materials and energy. Immobilized enzymes represent a better solution due to enhanced stability of enzymes, easy separation from reaction mixture and possible reuse of it in a number of cycles. Future researches will be focus on the synthesis and application of new bio-catalysts prepared by enzyme immobilization.

References

1. Gilpin, A. "Dictionary of Environment and Sustainable Development", J.Wiley & Sons, New York, 1996, p.206.
2. Puscas, E., Stanescu, M.D., Fogorasi, M., Dale, V.: *Dezvoltarea durabila prin protectia mediului si biotehnologii textile*, Ed. Aurel Vlaicu, Arad, 2003, pp. 250-320.
3. Stanescu, M.D.: Enzymes in textile finishing an Overview, *Proceedings of World Textile Conference "Textile Engineering at the dawn of a new millennium"*, Bruges-Belgium, 1-3 July 2002, pp. 446-453.

4. Stanescu, M.D., Fogorasi, M., Bucur, M, Textile Biotechnologies an Ecological Approach, *Proceedings of the 3rd International Meeting of Textile Chemists and TheColorists*, Budapest-Hungary, 12-13 June 2001, pp. 42-47.
5. Stanescu, M.D., *Scientific Study & Research*, 2006, 7, 223-232.
6. Solomon, E. I., Sundaram, U. M., and Machonkin, T. E., *Chem. Rev*, 1996, 96, 2563-2605.
7. Piontek, K., Antorini, M., Choinwski, T, *J. Biol. Chem.*, 2002, 277, 37663-37669.
8. Stanescu, M.D., *Scien. and Techn. Bull.* Chemistry, Food Science & Engineering 2003, 9(8), 81-86
9. Stanescu, M.D., A. Sanislav, V. Kokol, A. Kresal, Lacaza o enzima pentru biodegradarea colorantilor, *Book of Abstracts XXIXth Romanian Chemistry Conference*, Calimanesti-Caciulata-Romania, 4-6 October 2006, p.64.
10. Stanescu, M.D., Influence of the chemical structure on the interaction enzyme-textile substrate, *Proceedings of the 1st Aachen-Dresden International Textile Conference*, Aachen-Germany, 29-30 November 2007, pp. 131-136.
11. De Stefano, G., Piacquaido, P., Sciancalepore, V., *Biotechn. Techn.*, 1996, 10, 857-860.
12. Piacquaido, P., De Stefano, G., Sammartino, M., Sciancalepore, V., *Biotechn. Techn.*, 1997, 11, 515-517.
13. Riva, S., *Trends.Biotechnol.*, 2006, 24, 219-226.
14. Stanescu, M.D., Fogorasi M., Ivanov R.V., Lozinsky V.I. , Immobilized Laccase for dye biodegradation, *Proceedings of the 2nd European Chemistry Congress*, Torino-Italy, 16-20 September 2008.
15. Nevalainen, H., Penttila, M., Molecular biology of cellulolytic fungi in "*The Mycota II. Genetics and Biotechnology*", U.Kuck editor, Springer Verlag, Berlin, 1995, pp. 303-319.
16. Flachner, B., Reczey, K., *Chem.Biochem.Eng. Q.*, 2004, 18, 303-307.
17. Stanescu, M.D., Fogorasi, M., Preda, C., *Scien. and Techn. Bull.* 1999, 5, 23-24.
18. Stanescu, M.D., Fogorasi, M., *Ind. Textila*, 2000, 51, 184-188.
19. Fogorasi, M., Puscas, E., Stanescu, M.D., Grigoriu, A., *DWI Reports*, 2003, 127, 63-67.
20. Fogorasi, M.S., Stanescu, M.D., Dochia, M., *Scien. and Techn. Bull.* Chemistry, Food Sciences & Engineering, 2004, 9, 53-57.
21. Stanescu, M.D., Mihuta, S., Bibe, M., *DWI Reports*, 2005 129, P18, pp.1-5
22. Stanescu, M.D. Fogorasi, M. Dochia, M., Mihuta, S., Lozinsky, V.I., *Rev.Chimie*, 2009, 000.
23. Bucur, M.S., Stanescu, M.D., Enzymatic Treatment of Cotton: a Model for Wool Carbonization, *Proceedings of 10th International Wool Textile Research Conference*, Aachen-Germany, 29 November- 2 December 2000, EN-P4, 1-5
24. Soares, M.M.C.N., da Silva, R., Gomes, E., *Rev. Microbiol.*, 1999, 30, 299-303.
25. van Santen, Y., Benen, J.A.E., Schroter, K.-H., Halk, K.H., Armand, S., Visser, J., Dijkstra, B.W., *J.Biol.Chem.*, 1999, 274, 30474-30480.
26. Radu, D., Stanescu, M.D., Pectinases for improving fruit juice production, *Book of Abstracts COST928 meeting*, Wien-Austria, 4-6 September 2007, P 18.
27. Stanescu, M.D., Fogorasi, M., Bucur, M.S., Pustianu, M., M. Dochia, M., Enzymes in Cotton Bioscouring, *Proceedings of the 13th Romanian International Conference Chemistry and Chemical Engineering* , Bucharest-Romania, 13-15 September 2003, Vol 3, pp. 43-48.
28. Cegara, J., Riva, A., Gacen, J., Naik, A., *Boletin Intexter*, 1993, 104, 35-41.

29. Stanescu, M.D., Mihuta, S., Noel, I., Nonconventional Catalysis in PET Finishing, *Proceedings of Sustainability and Recycling of Textile Materials*, Guimaraes-Portugal, May 17-19 2000, pp. 173-174.
30. Raileanu, M., Stanciu, L., Parlog, C., Bordeianu, I., Stanescu, M.D., Badea M., *Rev Roum.Chim.*, 2002, 47, 535-538.
31. Stanescu, M.D., Mihuta, S., Bucur, M.S., Raileanu, M., Popovici, D., Wool Finishing with Enzymes in Advances in "Biotechnology for Textile Processing", Hardin, R., Akin D.E., Wilson, S.J., editors, University of Georgia, Athens, 2002, pp. 109-116.
32. Raileanu M., Stanciu, L., Badea M., Stanescu, M.D., Bordeianu, I., *UPB.Sci.Bull.Series B*, 2002, 64, 55-62.
33. Stanescu, M.D., Bucur, M.S., Pustianu, M., Mihuta, S., Raileanu, M., *Textile Asia*, 2003, 34(5), 29-30.
34. Stanescu, M.D., Fogorasi, M., Chiraleu, M., Dochia M., Heine, E., *DWI Reports*, 2004 128, 39-43.

METHODS OF OBTAINING OXIDE CRYSTALS**Mirela F. Nicolov* and Cornelis F. Woensdregt****

* Faculty of Engineering, University "Aurel Vlaicu" of Arad, Department of Physics, Bd. Revolutiei no.77, 310130 Arad, Romania;** Faculty of Earth Sciences, Utrecht University, P.O. Box 80.021, NL-3508 TA Utrecht, The Netherlands

ABSTRACT

The mineral quartz (α -SiO₂) is also known as a technologically important material. were realized an hydrothermal experiment for obtaining quartz. Was realized SEM and AFM analysis to make a complete analysis from theory to experiment.

1. INTRODUCTION

Quartz is not only an important rockforming mineral but also a commercially important material due to its interesting physical properties (piezoelectric).

Many studies in experimental petrology and allied branches of geology depend on having starting compositions from which small amounts can be taken and used in experiments. The essential properties of such starting materials are homogeneity and accurately known chemical composition. J.F. Schairer of the Geophysical Laboratory is well known for his excellent ground-glass starting materials, these have been used and tested by many people and have been found to fill these two requirements admirably.

This dried, decomposed and fired material will in future be referred to as a "GEL".

A "GEL" when used in hydrothermal heating experiments is very reactive and quickly produces a crystalline assemblage, but not necessarily the one of having the lowest free energy. In certain experiments, therefore a ground glass starting material being a little reactive, might be preferred. This may be made from the "gel" by a single fusion followed by crushing. In more volatile systems it has been found possible to fuse a "gel" in a closed platinum (gold) and thus retain all the volatile constituents. In systems involving silicate crystal-liquid equilibrium we have found no appreciable difference in the assemblages produced starting with "gel" or ground glass.

2. CHEMICAL ANALYSIS OF "GELS"

If the "gel" analysis agrees closely with the calculated composition, then the "gel" is presumably homogeneous and can be said to be on composition. However, analytical results can be equivocal and our main reservations concerning the meaning of an analysis are first, that "gels" are particularly hygroscopic and difficult to completely dehydrate (even above 1000°C); it is difficult to be sure of the absolute weight (water free) of a portion of "gel" taken for analysis. And secondly, if the replicate analysis of a "gel" for a particular element showed good precision but were consistently high or low as compared with the part of the analyst or analytical method, or, if results are consistently low, to the "gel" being hydrous; if the results are accurate reflection of the bulk composition the "gel" would be *off* composition.

We feel, therefore that it is better to analyze "gels" to test their homogeneity rather than to determine their absolute composition. The method of "gel" preparation described below employs only weighing of pure chemicals and neglecting any accidents, the bulk chemical compositions depends only on the accuracy of weighing and purity of the chemicals and reagents used in the preparation. We think that weight yield of a "gel" is a good indication of its reliability and we find that compositions made up and fired in the same

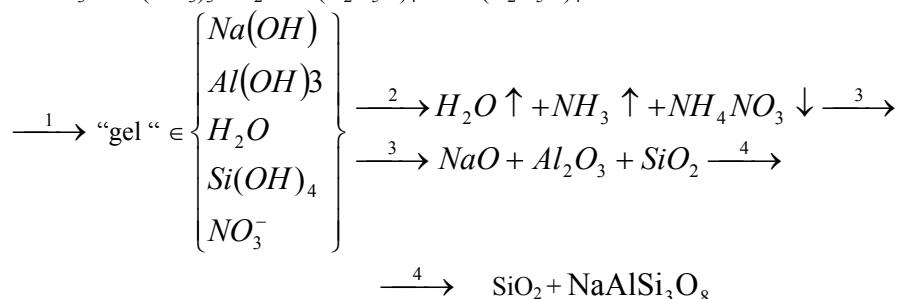
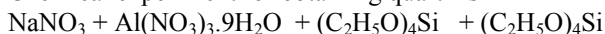
platinum container give yields in the range 100.0-100.5%. The small extra weight is probably due to absorbed water. Thus we know accurately what we have added and if the "gels" are shown to be homogeneous then they must be on composition.

Materials used

The choice to used in preparing a "gel" is critical. Ideally only the highest purity chemicals available should be used but if a large number of "gels" are to be made a compromise between expense and purity has to be made. For "gels" in which purity is of the utmost importance (e.g. for those to be as standards in microprobe and X-ray fluorescence analysis or trace-element distribution studies) Johnson – Matthey Grade I high – purity chemicals are recommended ; ; the purity of these are normally near to 99.999% . For less exacting work Johnson Matthey Grade II chemicals are advised , these are normally near 99.99% purity and much less expensive. ANALAR grade chemicals that have been used and found to be satisfactory . Two sources of SiO₂ are available. One is Tetraethyl Orthosilicate (T.E.O.S.) and other is an ammonia-stabilized colloidal solution (Ludox) . Either are satisfactory but we prefer TEOS for the next reason: although it is volatile it loses SiO₂ stoichiometrically and thus loss before gelling can be allowed for in the initial weighing; if allowed to stand for a long time it will absorb water and hydrolyse but experiments have shown that TEOS weighed and allowed standard for three hours before being reweighed and gelled gives an identical yield to that gelled directly; Ludox contains some Na₂O and this amount varies considerably from batch to batch , thus in soda – bearing systems a correction should be made for the Na₂O contributed by Ludox and soda free system Ludox should not be used as a source of SiO₂ . Evaporation of water from Ludox will concentrate the SiO₂ and Na₂O and must be kept in a tightly stoppered bottle; yields of SiO₂ and Na₂O should therefore be determined frequently.

3. chemical experiment for obtaining quartz (SiO₂)

Chemical experiment for obtaining quartz is



where :

- 1 : gellation process by adding excess of NH₄OH (15 ml of solution 25%)
- 2 : drying process to 110 °C
- 3 : heating process to 800 °C in Ar/H₂ atmosphere
- 4 : HPT experiment at a pressure of p=3 kbar, temperature of t=700°C and for different period for example T = 7 days .

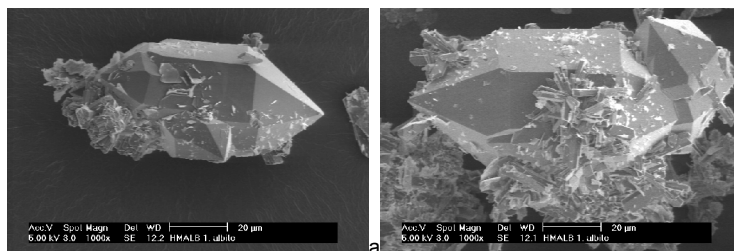
4. HYDROTHERMAL EXPERIMENT

The gold capsule with material inside (gel with water in a well known liquid-solid ratio) is put inside of a TUTTLE vessel. The volume which is not use from the vessel is filled with a steel rod. The vessel in mounted inside of a safety cabinet .

We connect the water cooling system at the bottom part of the vessel , the thermocouple (Type K till 1200 °C), pressure and close the valves and leave the system 12 hours to check for leakage. If everything is OK we can switch on the heating in the furnace. After 1 hour we can put down the furnace , on top of the vessel and using these we can increase the temperature . IN the same time we have pressure in the vessel (furnace) . The temperature in the vessel increase and for this reason pressure increase too and we have to decrease the pressure manually to avoid excess pressure in the system. Hydrothermal experiment can be made for different pressure , temperature times and different liquid – solid ratio (ml/mS calculated already. The experiment ends by taking up the furnace and cooling the system with air and after that released the pressure again.

After opening the vessel and then the gold capsule we start the experimental part of recognition of the material obtained in the experiment . First the material is took out using water First we can have an optical observation on a normal optical microscope to see there are crystals inside of he material or not. When we looked at the microscope using polarized light we can see very well the anisotropic crystals We can still recognize the morphology of the crystals by using 1 polarized filter.

5. SEM analysis of quartz



b)

Figure 1 : quartz crystals and most of them are twins after the hydrothermal experiment ;a) twins quartz crystals ;b) quartz crystals and albite crystals ;

In figure 1 we can see the SEM image of flat faces of quartz obtained in a hydrothermal experiment .

6. AFM analysis of quartz

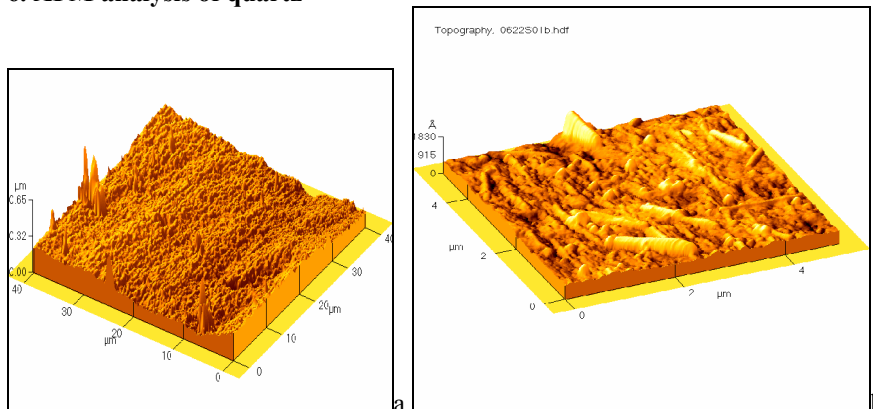


Figure 2 AFM image of quartz surface

In figure 2 we can see the AFM mage of flat faces of quartz obtained in a hydrothermal experiment . In figure 3 we can observe the AFM analysis of steps and faces for quartz.

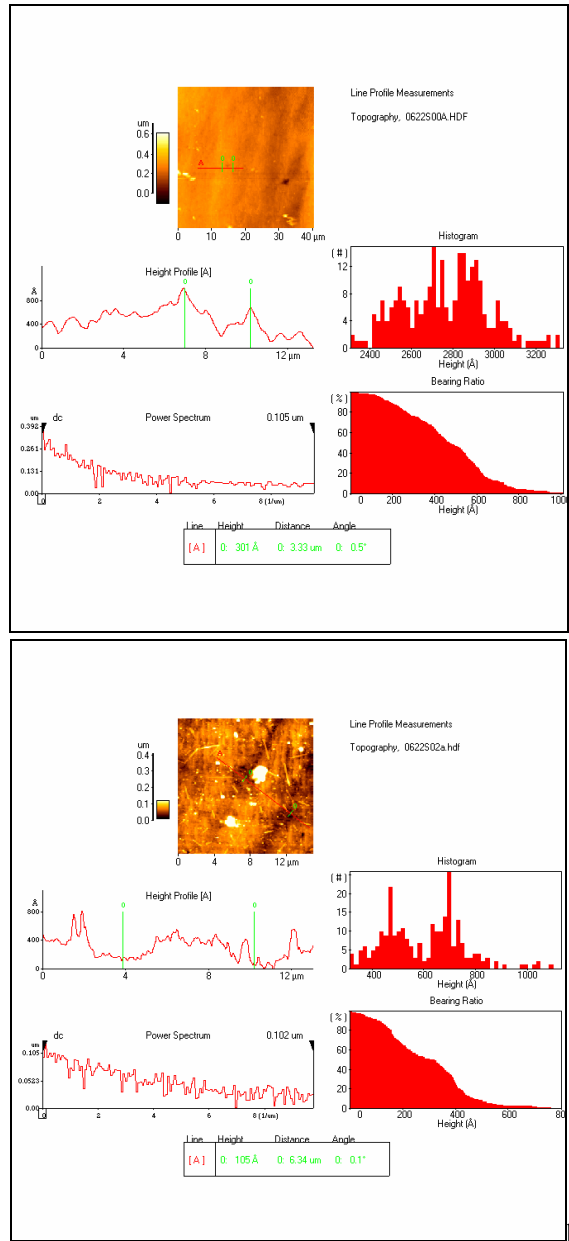


Figure 3 AFM analysis of quartz surface

7. CONCLUSIONS

We can see that quartz crystals obtained in a hydrothermal experiment is according to theory . SEM and AFM analysis show the same faces as in the theory.

Quartz is very good example that has faces which are parallel to at least 2 PBCs and are not always F faces. A very good example is {11-21} which is parallel to two PBC and the base is parallel to three PBCs . None is an F face because of the strong bonds which have not the direction parallel to this face [3]

8. REFERENCES

18. Andrew Putnis, Introduction to Mineral Sciences ,Cambridge University press, 1992.
19. International Tables for Crystallography, vol.A space group Symmetry , D.Reidel Publishing Company, Dordrecht Holland, 1983.
20. Ichiro Sunagawa, Morphology of Crystals, PartA, Terra Scientific Publishing Company/Tokyo, 1989.(from the book:Chapter4:" Modern PBC Theory ", P. Hartman, 269)
21. F.C. Phyllips , An Introduction to crystallography , Bristol, Longmas Publishing House, 1955
22. Duncan MaKie, Christine McKie , Essentials of Crystallography, Blackwell Scientific Publications, London Oxford , 1986
23. Joseph I. Goldstein et als ., Scanning Electron Microscopy and X-ray Microanalysis , Plenum Press New York and London , 1981.
24. Handbook of Chemistry and Physics , 62 -th edition , 1982.